Identification and Dead-Beat Control of a Heat Diffusion Process

Leden, Bo

1975

Document Version:
Publisher's PDF, also known as Version of record

Bo Leden

Identification and Dead-Beat Control of a Heat Diffusion Process

REPORT 7508
APRIL 1975

Identification and Dead-Beat Control of a Heat Diffusion Process

B. LEDEN

LTH

Department of Automatic Control · Lund Institute of Technology

IDENTIFICATION AND DEAD-BEAT CONTROL OF A HEAT DIFFUSION PROCESS

Bo Leden
tekn.lic., Mlm

Akademisk avhandling som för avläggande av teknisk doktorsexamen vid tekniska fakulteten vid universitetet i Lund kommer att offentligen försvaras i sal M:A, Maskinhuset, Lunds Tekniska Högskola, måndagen den 26 maj 1975 kl 10^{15}.

Bo Leden

Identification and Dead-beat Control of a Heat Diffusion Process

Lund 1975

To Agneta

Printed in Sweden
σ-tryck
Lund 1975

To Agneta

Printed in Sweden
σ-tryck
Lund 1975

TABLE OF CONTENTS

CHAPTER 5 - ESTIMATION OF THERMAL DIFFUSIVITY

CHAPTER 6 - MULTIVARIABLE DEAD-BEAT CONTROLLERS

CHAPTER 7 - OPTIMAL FILTERING AND PROFILE CONTROL

CHAPTER 1

1. INTRODUCTION

Heating of solids is an important engineering problem. A typical example is heating of ingots and slabs in the steel industry. Other examples are found in precision instruments like frequency oscillators and micro calorimeters, where it is desired to keep certain components at a constant temperature.

The purpose of this thesis is to explore some control problems associated with the heating of solids. A characteristic feature of the problem is that the controlled object can be described by a parabolic partial differential equation. An important problem is to find suitable lumped models, which can be used for analysis and synthesis of control strategies. Techniques for control system design is another crucial problem.

The thesis is partly analytical and partly experimental. The experiments were performed using a simple pilot plant. An overview of the main results are given below.

Apparatus

The apparatus consists of a rod and a concentric guard tube. These are thermally connected to heat sources at their end surfaces. The guard reduces the heat loss rate from the rod considerably. In fact, the employed configuration makes it possible to obtain a very accurate realization of a one-dimensional heat diffusion process without using vacuum equipments. The temperature along the rod is measured using thermistor sensors. The heat sources consist of Peltier elements. In some experiments the process is connected to a

process computer using A/D- and D/A-converters.

Model building

Mathematical models of the rod and its environment are required for analysis and design. In this thesis input-output models are obtained using system identification techniques and state-space models are obtained from basic physical laws.

Input-output models - Clustering

The rod is a linear infinite dimensional system. The transfer function, relating the temperature at a point z on the rod to one end point temperature, has the series expansion

$$G(z,s) = \sum_{k=1}^{\infty} \frac{K_k(z)}{1 + T_k s} \qquad (1.1)$$

The transfer function is estimated from measurements, using system identification techniques [2]. Statistical tests indicate that the appropriate orders of the obtained models are relatively low. This is explained by the fact that the models are estimated from sampled data. Furthermore, it is found empirically that successive terms in the expansion (1.1), having gain factors of the same sign, are identified as a single term K/(1+sT), where K is approximately equal to the sum of the gain factors and T is some average value of the time constants of the clustered terms.

State-space models

It is straightforward to obtain a model using physical laws. This leads to partial differential equations. Lumped state-space models of the rod have been derived using finite-difference techniques. It is found that the accuracy of these models is essentially deter-

mined by the number of intervals used and that a refinement of the approximation to the partial derivatives only improves the accuracy to a certain extent.

Determination of thermal diffusivity

To obtain models based on physical equations it is necessary to know the thermal diffusivity. A method to determine this quantity was given by the Swedish physicist Ångström [1] in 1861. This method is still considered as one of the most accurate methods for determining thermal diffusivity. In this thesis Ångström's method and a maximum likelihood method are used to determine the thermal diffusivity of the rod.

Errors in measuring the thermal diffusivity of the rod mainly originate from systematic errors in the sensor position and the characteristics of the temperature transducers. Compared to the Ångström's method the maximum likelihood method has the distinct advantage of allowing a larger sensor separation. It is also possible to estimate the characteristics of the temperature transducers. The relative errors in the thermal diffusivity can thereby be reduced. The conclusion is that the thermal diffusivity of the rod can be determined approximately three times more accurate using the maximum likelihood method instead of the Ångström's method.

Control design

The nature of the heat equation implies that it takes considerable time for a solid to reach a steady state temperature profile. The purpose of many control systems is therefore to speed up the time required to reach equilibrium. This means that it is quite reasonable to consider dead-beat control strategies.

A multivariable dead-beat theory for sampled-data control has been developed. The following types of controllers are derived

- state dead-beat controllers
- output dead-beat controllers
- constrained output dead-beat controllers
- minimum gain dead-beat controllers

The dead-beat controllers drive the state or the output of a discrete-time system to zero in a minimum number of time steps. The output dead-beat controllers may give an unstable closed loop system and, therefore,it is important to consider constrained output dead-beat controllers which always give a stable closed loop system. Computational aspects of the algorithms for computing the dead-beat controllers are presented. The approach used is basically geometric and much inspiration comes from Wonham [3].

Experimental results show that the lumped models proposed may be used to estimate the profile of the rod accurately using Kalman filtering techniques. Moreover, these models well predict the performance of the closed loop system, obtained with dead-beat control. The experiments also show that the dead-beat control strategies are very relevant for controlling the diffusion process.

Organization of material

In Chapter 2 the apparatus is described in detail. Physical models of the rod are also derived. Particular attention is given to the modelling of the heat loss rate from the rod. The lumped state-space models of the rod are given in Chapter 3. In Chapter 4 the input-output models of the process are found. The clustering effect is accounted for in detail here. The Ångström's method and the maximum likelihood method are described in Chapter 5. A discussion on the systematic errors of the two methods is also given. The multivariable dead-beat control theory is developed in Chapter 6. Several engineering aspects of the controllers are given here. Finally the optimal filtering and profile control experiments are presented in Chapter 7.

Acknowledgements

It is a pleasure to express my sincere appreciation to Professor Karl Johan Åström for his encouragement and invaluable help throughout this work.

I am indepted to all my colleagues at the Division of Automatic Control, who form a group with an open and stimulating atmosphere. Many improvements have resulted from our frequent discussions. In particular, I whish to express my gratitude to Gunnar Bengtsson, Per Hagander and Sture Lindahl for several valuable discussions of the subjects. I would also like to thank Jan Holst, Ivar Gustavsson and Per Hagander for detailed comments and suggested improvements on the final manuscript.

I am grateful to Anette Bansjö and Gudrun Christensson, who typed the manuscript and to Britt-Marie Carlson, who prepared the figures. Thanks also to Hans Libelius, who did the mechanical work.

References

[1]: Ångström, A.J.: "Neue Methode das Wärmeleitungsvermögen den Körpen zu bestimmen", Ann. der Phys u. Chem., Poggendorff's Annal. Vol. 114, 513-530, 1861.

[2]: Åström, K.J. and Bohlin, T.: "Numerical identification of linear dynamic systems from normal operating records", Paper IFAC Symp. on Theory of Self-Adaptive Control Systems, Teddington, Engl. In Theory of Self-Adaptive Control Systems (Ed. Hammond P.H.), Plenum Press, New York, 1966.

[3]: Wonham, W.M.: "Linear multivariable control - A geometric approach", Berlin, Springer-Verlag, 1974.

CHAPTER 2

DIFFUSION PROCESS, MODELLING AND MEASUREMENTS

1. INTRODUCTION

The process is a laboratory pilot plant. It consists of a long copper rod. A guard tube is used to reduce the heat loss from the rod. The rod and the tube form a concentric cylindrical annulus. Silver plates thermally connect the end surfaces of the rod and the tube. The heat sources consist of Peltier elements which uniformly heat or cool the silver plates. Thermistor sensors are used to measure the temperature along the rod. The input and output variables of the process are the end point temperatures of the rod and the temperature in seven equidistant points along the rod respectively. The process operates in the temperature range 20 ^{o}C - 30 ^{o}C.

The process has been designed in such a way that it should well be described by a simple model. To reduce the heat loss completely, it would be necessary to evacuate the space between the rod and the guard. The complication of vacuum equipment is avoided by accepting a small heat loss. A static and a dynamical model are used to describe the conduction of heat in the rod. The static model is primarily used for design purposes. The heat loss rate from the rod is assumed to be proportional to the temperature difference between the rod and the tube in this model. The dynamical model is used for parameter estimation and control. In this model, the heat loss rate from the rod is supposed to be proportional to the temperature of the rod only. Although this model is less accurate than the static model, it describes the dynamics of heat conduction in the rod very well.

2. APPARATUS

A photograph of the pilot plant is shown in Fig. 2.1. This plant consists of a heat process, a temperature transducer and control unit, a computer interface, a power control unit, a power amplifier and a fan unit.

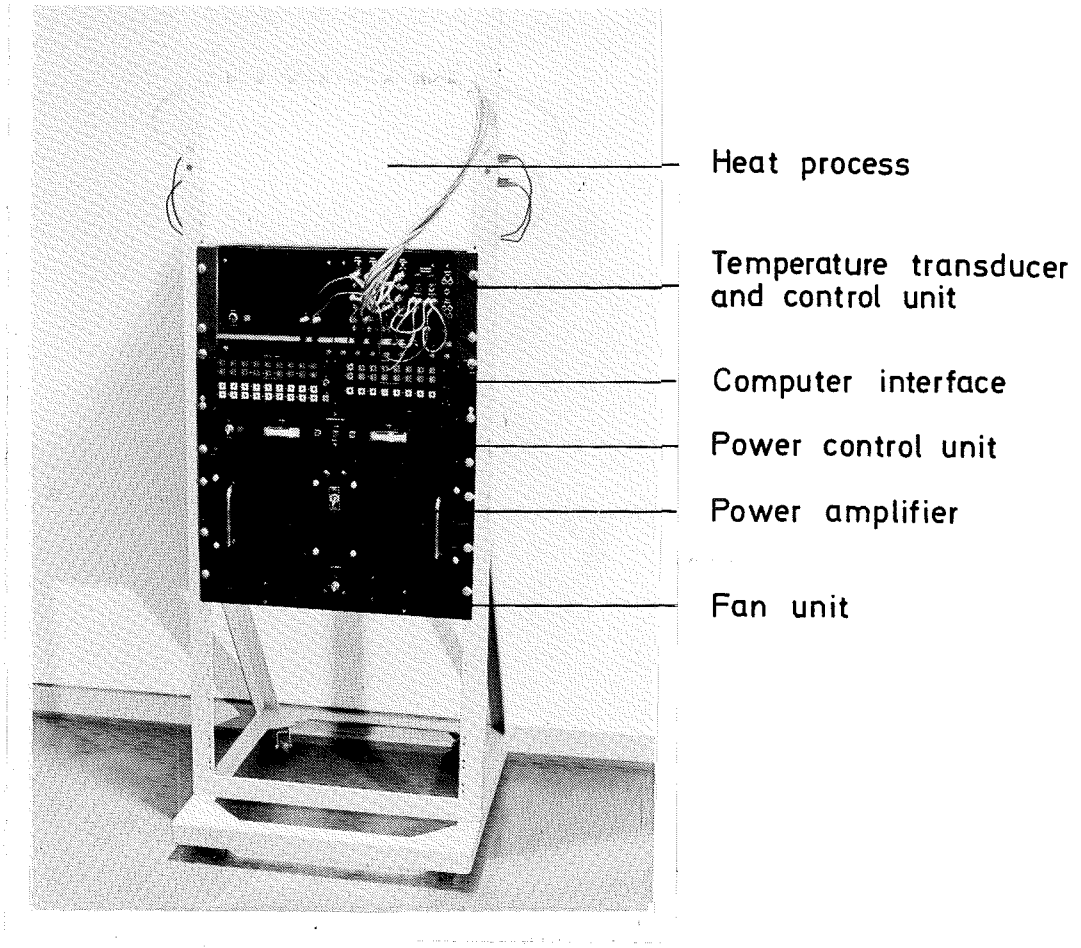

Fig. 2.1 - The pilot plant.

Heat process

The experimental process is shown schematically in Fig. 2.2. The rod is 14 mm in diameter and 450 mm long. Nine 0.06" Veco 32A129

glas probe thermistors are placed into 3 mm deep equidistant holes along the rod. The spaces between the thermistors and the rod are filled with silicon paste. Two of the nine thermistors are situated at the ends of the rod. The holes are drilled with a 1.2 mm drill. All diameters are less than 1.27 mm. The separation of the centers of the holes is ± 0.1 mm. The nine thermistors are selected from 20 units. They have diameters of 1.22 ± 0.05 mm and off-center distances of the beads less than 0.05 mm. Therefore, the sensor separation and its maximal error become

$$d = 0.05625 \pm 0.0003 \text{ m} \qquad (2.1)$$

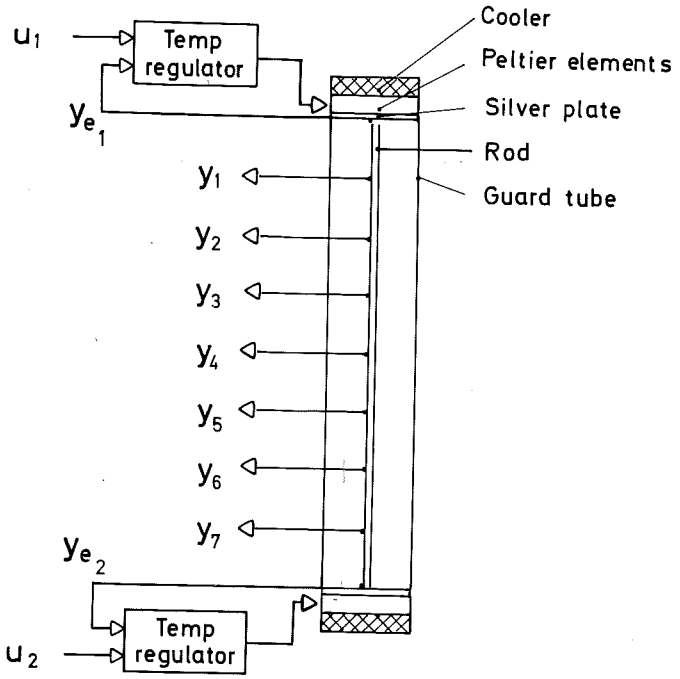

Fig. 2.2 - A schematic diagram of the experimental process.

A guard tube, made of the same material as the rod, is used to reduce the heat loss from the rod. The rod and the tube form a concentric cylindrical annulus. Silver plates thermally connect the end surfaces of the rod and the tube. The heat sources con-

sist of Peltier elements. One side of the Peltier elements is kept at constant temperature by water cooling (see Fig. 2.3). A heat insulation, made of small polystyren balls enclosed in a box, surrounds the guard tube.

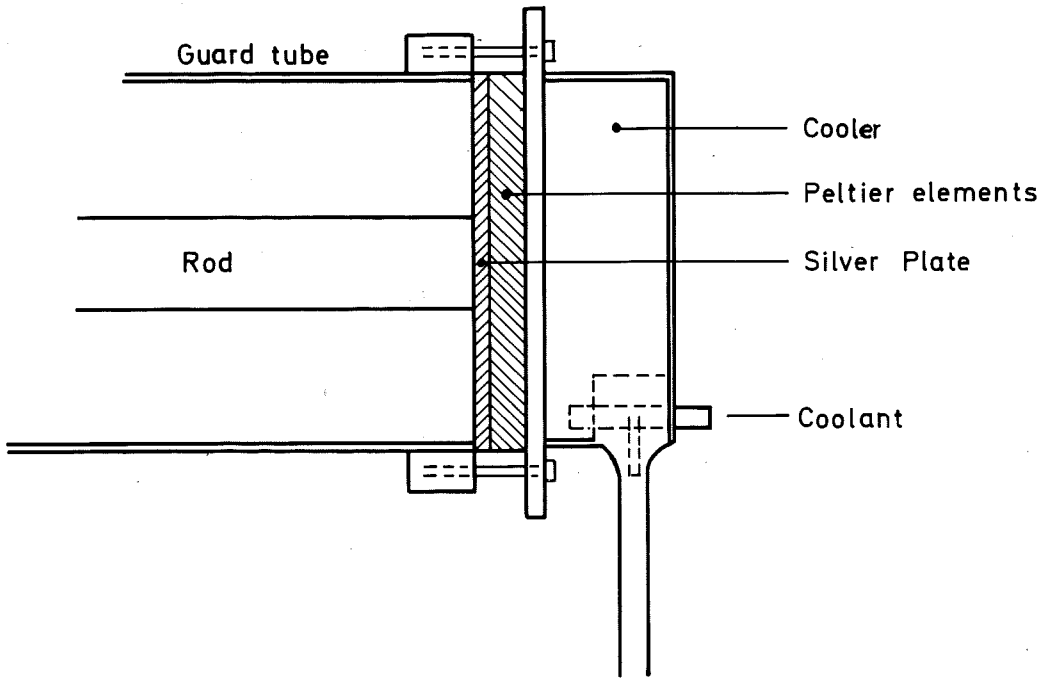

Fig. 2.3 - A figure, on a reduced scale, showing the connection of the cooler, the Peltier elements, the silver plate, the guard tube and the rod.

The rod and the tube are made of commercial, pure, oxygen free and high conductivity copper. Chemical analyses show that the rod and the tube consist of 99.7 ± 0.2 % and 99.8 ± 0.2 % copper respectively, where the percentage deviations are the 3σ-limits. The amounts of arsenic in these materials are less than 0.1 %.

The Siemens PKE 36E 0260 Peltier element is made of a semiconductor material and consists of 36 pairs of small bars. Each pair

is made of one n-doped and one p-doped bar. The bars are joined with copper bridges. The pairs are connected in series electrically, but in parallell thermally. The current through the element causes heat to flow from one side of the element to the other. The direction of the heat flow is altered by a reversed current. For small currents, the power transferred through the element is proportional to the magnitude of the current. However, for large currents, the Joule heating of the elements is appreciable. The maximum cooling power of a Peltier element is 23 W and is obtained at a current of 10 A and zero temperature difference across the element. Each servo contains two Peltier elements, which give a maximum cooling power of 46 W.

Temperature transducers

The temperature transducer consists of a resistive Wheatstone bridge and a differential amplifier (see Fig. 2.4). The Veco 32A129 thermistor is placed in one leg of the bridge circuit. This thermistor has a nominal resistance R_0 = 2000 Ω at 25°C. Under the laboratory conditions, the maximal yearly change in the resistance R_0 is 0.05% or 1 Ω. At 25°C, the time constant of the thermistor, in still oil, is 0.5 s and the temperature coefficient is -0.039 1/°C

The resistance versus temperature characteristic of a thermistor is non-linear. In [6], it is shown that by a proper choice of the Thevenin resistance R_{th}, with respect to the thermistor terminals, the transducer can be designed to give an almost linear voltage versus temperature characteristic over a fairly large temperature range. For proper choices of R_{th}, the maximal theoretical linearity errors of the thermistor used are 0.003 % and 0.06 % in the temperature ranges 24 °C - 26 °C and 20 °C - 30 °C respectively. It also follows from [6] that the linearity is not sensitive to variations of the resistance R_{th}.

A circuit diagram of the transducer is given in Fig. 2.4. In this

figure, the thermistor resistance is denoted by R_T and the Thevenin resistance is denoted by R_{th}. The potentiometers R_{1_p} and R_{f_p} are used to adjust the zero level and the voltage swing of the transducer. The bridge voltage is E= 0.306 V. This value was chosen so that the self-heating would be much smaller than 0.01 °C. Assume that the amplifier has infinite gain and that its input current can be neglected. With the notation in Fig. 2.4, the output of the transducer then becomes

$$e_T = \left(\frac{R_{th}}{R_{th}+R_T} - \frac{R_1}{R_1+R_2} - \frac{1}{K} \frac{R_2}{R_1+R_2} \right) KE \qquad (2.2)$$

where

$$R_1 = R_{1_0}+R_{1_p}$$
$$R_f = R_{f_0}+R_{f_p}$$
$$R_{in} = R_s+R_1R_2/(R_1+R_2) \qquad (2.3)$$

and

$$R_1/(R_1+R_2) = 0.42$$
$$K = 1+R_f/R_{in} = 686 \qquad (2.4)$$

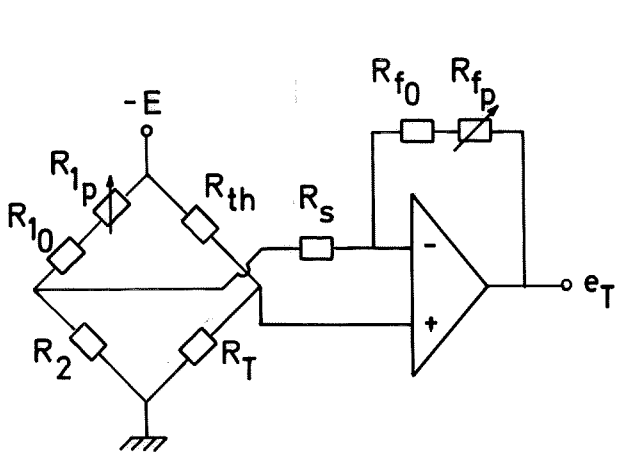

Fig. 2.4 - A schematic circuit diagram of the transducer.
Resistances: R_{1_0}=300 Ω, R_2=R_s= 500 Ω, R_{f_0}=450 kΩ
Potentiometers: R_{1_p}= 150 Ω, R_{f_p}= 200 kΩ

Calibration

The transducers are calibrated against a mercury-in-glass thermometer in the temperature range 20 ^{o}C - 30 ^{o}C. For calibration, the thermistors and the thermometer are immersed in a well stirred temperature bath with a long term stability of 0.01 ^{o}C. If stem-exposure corrections are made, the accuracy of the thermometer is 0.01 ^{o}C. In [6] it is found that the maximal linearity error and the slope error of the transducers both are 0.01 ^{o}C in the temperature range 20 ^{o}C - 30 ^{o}C. Moreover, it follows from [6] that the zero adjustment error δ_0 of the transducers is less than 0.01 ^{o}C in this temperature range. Neglecting the linearity error of the transducers, the relation between the body temperature T [^{o}C] of a thermistor and the output y [V] of the corresponding transducer is given by

$$y = (1+\delta_s)(T-25)+\delta_0, \quad 20<T<30$$
$$|\delta_s| < 0.002, \quad |\delta_0| < 0.01 \qquad (2.5)$$

The 12 hours drift of the transducers is 0.001 ^{o}C.

Temperature servo

The open loop system consists of the Peltier elements (see Fig. 2.2). The Bode diagram of the transfer function, relating the voltage across the Peltier elements to the end point temperature of the rod, is shown in Fig. 2.5. The temperature regulator consists of a PID-regulator followed by a power amplifier. This regulator also has nonlinear compensators, to eliminate the influence of the nonlinearites of the Peltier elements, due to Joule heating.

The PID-regulator is implemented as a cascade of a PI-network and a lead compensator. The circuit diagram is given in Fig. 2.6. Assume that the amplifiers have infinite gains, that their input currents can be neglected and that $R_3 >> R_5R_6/(R_5+R_6)$. Provided that no zenerdiod is active, the transfer funcion of the PID-regulator

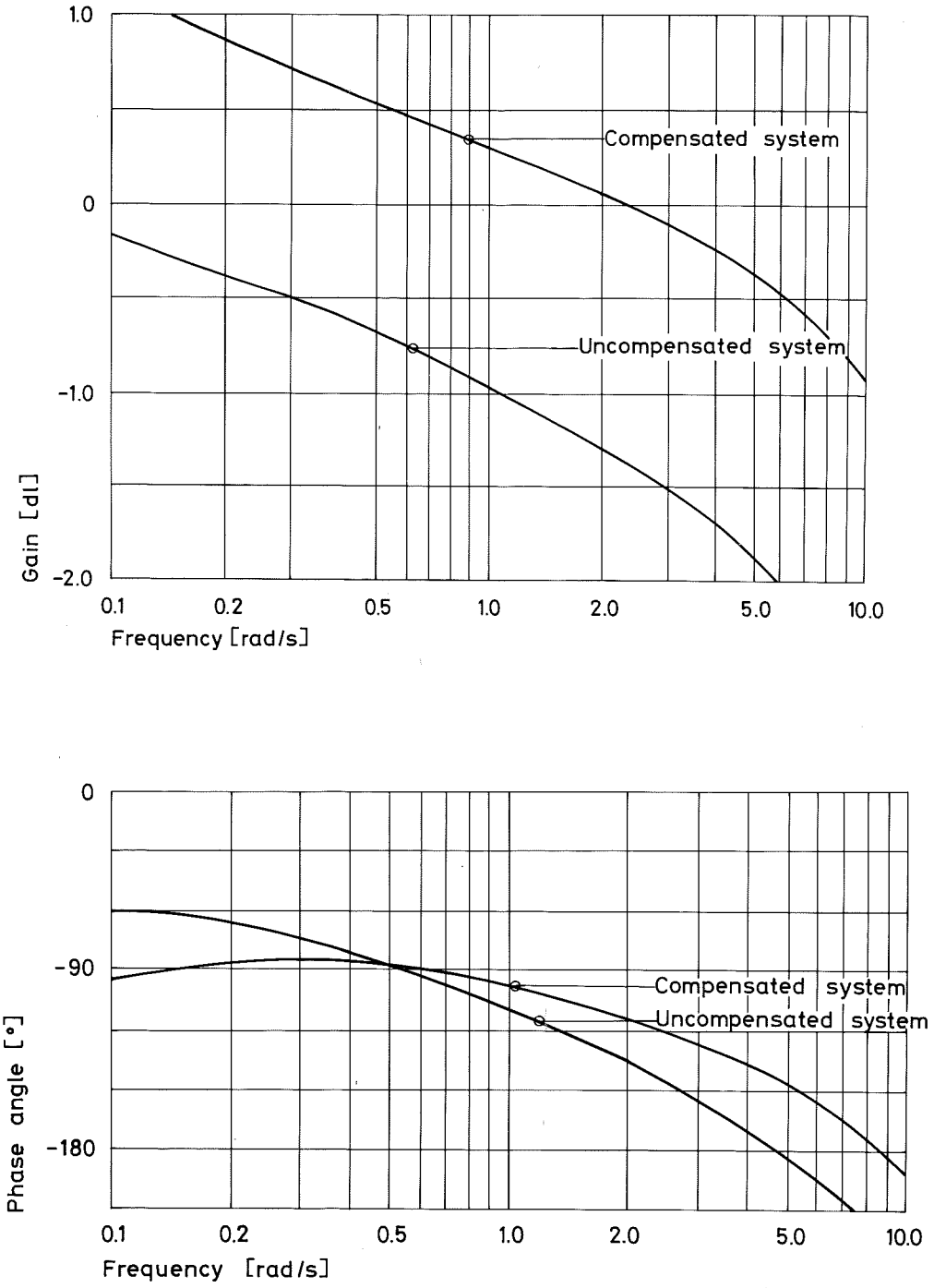

Fig. 2.5 - Bode diagram of uncompensated and compensated Peltier elements.

is given by

$$G_{PID}(s) = K\left(1+\frac{1}{Ts}\right)\frac{s+b}{s/N+b} \tag{2.6}$$

where

$$\begin{aligned} R_{f1} &= R_{f1_0}+R_{f1_p} \\ R_{f2} &= R_{f2_0}+R_{f2_p} \end{aligned} \tag{2.7}$$

and

$$K = \frac{R_8}{R_8+R_9}\;\frac{1+Rf_1/R_3}{1+R_4/R_{g1}}\;\frac{R_{f2}}{R_6+R_7} = 1.4$$

$$\frac{1}{T} = \frac{R_p}{R_5+R_p}\;\frac{1+R_4/R_{g1}}{1+R_3/R_{f1}}\;\frac{1}{R_2C_1} = 0.082$$

$$b = \frac{1}{R_7C_2} = 3.1$$

$$N = 1+ R_7/R_6 = 11 \tag{2.8}$$

In order to increase the corner frequency T of the PI-network, the integrator is connected to the differential amplifier via a voltage divider. The corner frequency of this network may be adjusted with the potentiometer R_p. By means of the potentiometer R_{f2_p}, the gain K of the PID-regulator is varied. The output swing of the lead compensator is matched to the input swing of the power amplifier by inserting a voltage divider between these two circuits.

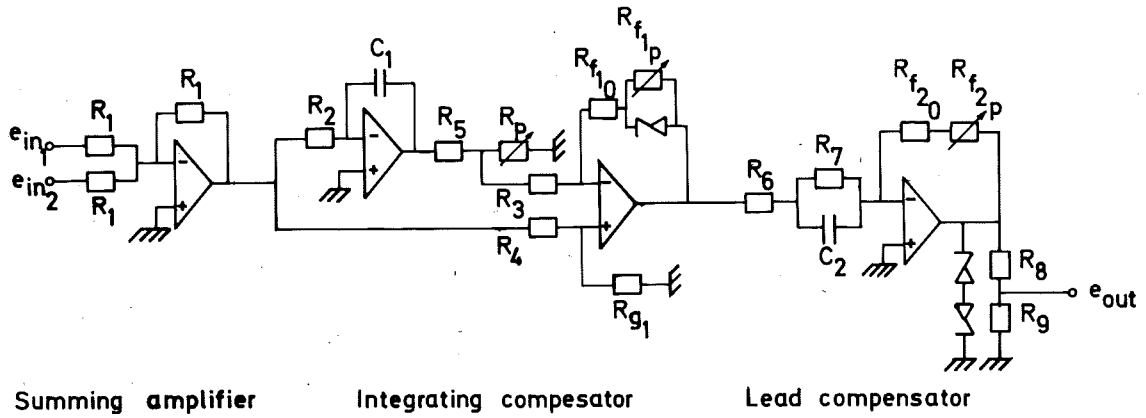

Fig. 2.6 - A schematic diagram of the PID-regulator
Resistances: $R_1=R_7=R_{f2_0}=100$ kΩ, $R_2=390$ kΩ, $R_3=R_4=R_{g_1}=R_{f1_0}=39$ kΩ, $R_5=8.2$ kΩ, $R_6=R_8=10$ kΩ, $R_9=1$ kΩ
Potentiometers: $R_p=2$ kΩ, $R_{f1_p}=R_{f2_p}=500$ kΩ

The power amplifier supplies a maximum direct power of 130 W at a resistive load of 1 Ω. The gain of this amplifier is 10. The input and output impedances of the amplifier are 500 kΩ and 25 mΩ respectively. Moreover, the bandwidth of the amplifier is 110 rad/s. The transfer function of the temperature regulator becomes

$$G_k(s)= 10\ G_{PID}(s) \qquad (2.9)$$

The Peltier elements require a maximum power of 80 W at a current of 10 A.

The Bode diagram of the compensated open loop system is given in Fig. 2.5. For high frequencies, (2.8) and (2.9) indicate that the measured phase angle curve of the compensated system should go

somewhat higher. The phase angle decrease of the PID-regulator is caused by a filtering capacitor in the regulator [7]. The integrating compensator introduces a phase shift of -2.2^{o} at the crossover frequency $\omega_c = 2.2$ rad/s of the compensated system. The lead compensator gives a maximum positive phase angle of 57^{o} at the frequency $\omega_{max} = b\sqrt{N} = 10.3$ rad/s. As a rule of thumb, the maximum phase lead angle should occur at a frequency close to ω_c. From practical experiences, it was found that by choosing ω_{max} considerably larger than ω_c, the creeping tendency in the step response of the compensated closed loop system could be eliminated. Since the uncompensated open loop system is not sensitive to high frequency noise, it is possible to use a relative large value of N. The parameter K is adjusted so that the compensated closed loop system obtains an overshoot of 4 % at reference temperature changes of ± 1 ^{o}C. The bandwidth of the compensated closed loop system is $\omega_B = 4.4$ rad/s.

The PID-regulator contains two non-linear compensators for the Joule heating of the Peltier elements. The first compensator, consisting of a single zenerdiode, is inserted across one of the feedback resistances of the differential amplifier in Fig. 2.6. This compensator gives the amplifier a voltage dependent gain. The gain may be adjusted with the potentiometer R_{flp}. During a heat cycle of the rod, the gain of the amplifier is reduced.

The second non-linear compensator is a limiter and consists of two different zenerdiodes, connected in series. The bounds of the limiter are chosen so that the same maximal heating and cooling power is obtained in the Peltier elements. The zenerdiodes used have steep forward characteristics, which give sharply defined bounds of the limiter.

The step responses of the temperature servo are shown in Fig. 2.7 for changes in the reference temperature of ±0.5 ^{o}C, ±1 ^{o}C and ±2 ^{o}C. From this figure, it is seen that the solution time (5 % of final value) of the servo increases somewhat with increasing step sizes. It also follows from Fig. 2.7 that the solution time

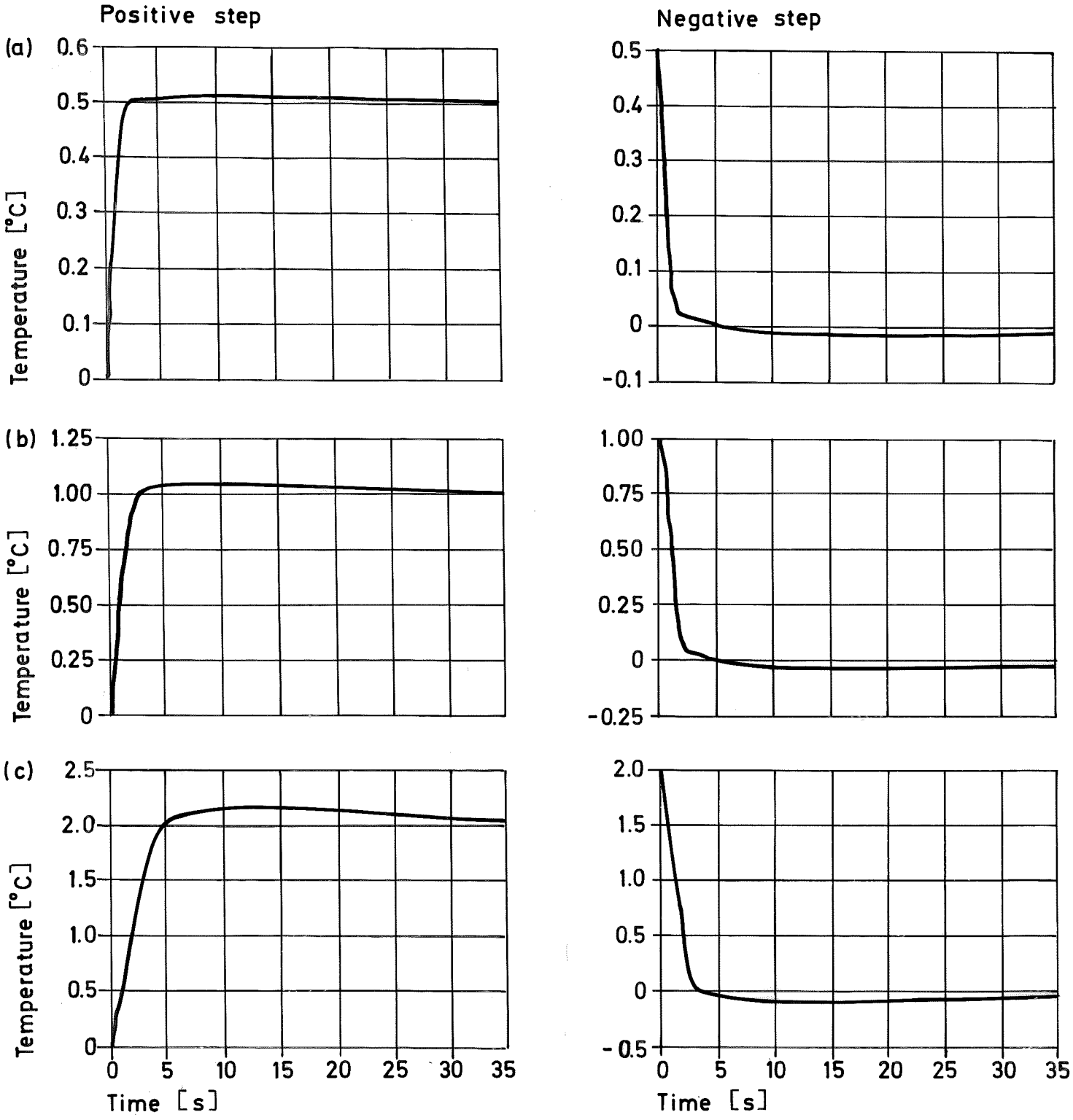

Fig. 2.7 - Step responses of the temperature servo for the following values of the reference temperature changes

(a) ±0.5 °C

(b) ±1 °C

(c) ±2 °C

of the servo is 2 s for reference temperature changes of ±1 ^{o}C.

It is found in [7] that the stationary error δ_0 of the servos is less than 0.01 ^{o}C in the temperature range 20 ^{o}C - 30 ^{o}C. Therefore, the output u [V] of a servo and the corresponding end point temperature T [^{o}C] of the rod are statically related by (2.5). The 12 hours stability of the temperature servo is 0.001 ^{o}C.

3. MATHEMATICAL MODELS

A static and a dynamical model for the process are derived in this section. The static model is primarily used for process design. Ideally, there would be no radial heat loss from the rod, if the rod and the tube always had the same temperature distribution. The temperature errors due to the temperature drops in the silver plates and the heat losses from the rod and the tube may be calculated from the static model. Since the temperature drops decrease with the thickness of the plates whereas the rise time of the servos increases with the thickness of the plates, this model is useful for the trade-off between the servo responses and the temperature errors in the rod.

The dynamical model is primarily used for parameter estimation and control design. Although, the heat loss rate from the rod is modelled less accurate in this model than in the static model, it describes the conduction of heat in the rod very well. In Chapters 4 and 7 it is shown that the model is adequate for parameter estimation and control purposes.

Nomenclature

The following notations are used:

z, r, φ	space coordinates in cylindrical system	
r	radius	m
s	length	m
ℓ	length of rod	m
p	perimeter	m
A	area	m^2
t	time	s
$\tau = t/(\ell^2/a)$	dimensionless time	-
T	time constant	s
Θ	temperature	K
Θ_a	ambient temperature	K
$\theta = \Theta - \Theta_a$	temperature difference	K (^oC)
$\Theta_0, \Theta_\ell, \theta_0, \theta_\ell$	boundary temperatures at z=0 and z=ℓ	K (^oC)
Φ	heat-transfer rate	W
Q	heat-transfer rate per unit volume	W/m^3
Φ_{loss}	heat-transfer rate loss	W
Φ_0, Φ_ℓ	heat-transfer rates at z=0 and z=ℓ	W
ρ	density	kg/m^3
c_p	specific heat at constant pressure	J/kg K
λ	thermal conductivity	W/m K
λ_e	effective thermal conductivity	W/m K
$a = \frac{\lambda}{\rho c_p}$	thermal diffusivity	m^2/s
υ	kinematic visconsity	m^2/s
β	volume coefficient of expansion	1/K
ε	emissitivity	-
α_c	convection heat-transfer coefficient	W/m^2 K
α_r	radiation heat-transfer coefficient	W/m^2 K
$\alpha = \alpha_c + \alpha_r$	surface heat-transfer coefficient	W/m^2 K

$\eta = \frac{\alpha p}{\rho c_p A}$	coefficient of surface heat loss	1/s
R	thermal resistance	W/K
g	acceleration of gravity	9.81 m^2/s
σ	Stefan-Boltzmann constant	5.70 $10^{-8} W/m^2K^4$

Dimensionless groups:

$Bi = \alpha s/\lambda$	Biot number
$Fo = at/s^2$	Fourier number
$Pr = \nu/a$	Prandtl number
$Gr = g\beta(\theta_o - \theta_i)s^3/\nu^2$	Grashof number
$Ra = Pr \cdot Gr$	Rayleigh number

Subscripts:

1,2,3,4	refer to medium 1,2,3,4
i	refer to inside cylinder surface
o	refer to outside cylinder surface
s	based on length s

Preliminaries - Conduction of heat in a rod with linear heat losses

Consider a long rod with linear loss of heat from its surface. Assume that the temperature in all points of a cross-section of the rod may be taken to be the same. Then, the temperature $\theta = \theta(z,t)$ is a function of the time t and the distance z measured along the rod. The constant thermal properties of the rod are ρ, c_p and λ. The thermal diffusivity is then $a = \lambda/(\rho c_p)$. Moreover, the length of the rod is ℓ.

The rate at which heat is dissipated from each surface element of the rod is supposed to be proportional to the temperature difference between the element and its environment. The latter is assumed to have the constant temperature θ_a. Therefore, the rate Q at which heat is lost at the surface per unit volume become

$$Q = \frac{\alpha p(\theta-\theta_a)}{A} \tag{3.1}$$

where α denotes the surface heat-transfer coefficient, p denotes the perimeter and A denotes the area of the cross-section of the rod.

Since the thermal properties of the rod are assumed to be constant, an energy balance for a volume element of the rod gives:

$$\rho c_p \frac{\partial\theta}{\partial t} = \lambda \frac{\partial^2\theta}{\partial z^2} - \frac{\alpha p}{A}(\theta-\theta_a) \tag{3.2}$$

By taking θ_a as the zero of the temperature scale, (3.2) can be written

$$\frac{\partial^2\theta}{\partial z^2} = \frac{1}{a}\frac{\partial\theta}{\partial t} + \xi^2\theta \tag{3.3}$$

where

$$\xi^2 = \frac{\alpha p}{\lambda A} \tag{3.4}$$

has been introduced. The steady-state solution of (3.3), subject to the boundary conditions

$$\begin{aligned}\theta(0) &= \theta_1 = \theta_1-\theta_a \\ \theta(\ell) &= \theta_1 = \theta_1-\theta_a\end{aligned} \tag{3.5}$$

is given by, [2]

$$\theta(z) = \frac{\sinh\xi(\ell-z)+\sinh\xi z}{\sinh\xi\ell}\,\theta_1 \tag{3.6}$$

As ξ tends to zero, it follows from (3.6) that $\theta(z)$ tends to θ_1 for all $z\in[0,\ell]$. If

$$q_1(z) = \frac{z}{\ell} - \left(\frac{z}{\ell}\right)^2$$

$$q_2(z) = \frac{z}{\ell} - 2\left(\frac{z}{\ell}\right)^2 + 2\left(\frac{z}{\ell}\right)^3 - \left(\frac{z}{\ell}\right)^4 - 2q_1(z) \qquad (3.7)$$

then a series expansion of $\Delta\theta(z) = \theta(z) - \theta_1$ gives

$$\Delta\theta(z) = -\frac{\xi^2\ell^2}{2} q_1(z)\theta_1 - \frac{\xi^4\ell^2}{24} q_2(z)\theta_1 + O((\xi\ell)^6) \qquad (3.8)$$

It follows from Fourier's law of heat conduction that the steady-state heat-transfer rate at the end points of the rod is given by

$$\Phi_0 = -\lambda A \left.\frac{d\theta}{dz}\right|_{z=0} = -\Phi_\ell = \lambda A \left.\frac{d\theta}{dz}\right|_{z=\ell} \qquad (3.9)$$

By an energy balance, it follows from (3.6) that the radial heat loss rate from the rod between z=0 and z=ℓ is given by

$$\Phi_{loss} = \Phi_0 - \Phi_\ell = 2\lambda A \frac{\xi(\cosh\xi\ell - 1)}{\sinh\xi\ell}\theta_1 \qquad (3.10)$$

A series expansion of (3.10) gives

$$\Phi_{loss} = \frac{\lambda A}{\ell}\left(\xi^2\ell^2 - \frac{\xi^4\ell^4}{12}\right)\theta_1 + O((\xi\ell)^6) \qquad (3.11)$$

Preliminaries - Natural convection in horizontal concentric cylindrical annuli

Natural convection in a horizontal annulus, formed by two concentric cylinders, has been experimentally studied in [1], [5] and [8]. The axial temperature variations in all experiments were neglectable. For small inner radius, it was found that the fluid circulated in a twin kidney-shaped pattern with the centers of rotation located above the horizontal axis. The velocity was low near the centers of rotation and at the bottom of the annulus. Pro-

vided that $Pr \cdot Ra/(1.36+Pr) < 10^3$, then it follows from [8] that the heat is essentially only transferred by conduction in the annulus, i.e.

$$\lambda_e/\lambda = 1, \qquad Pr \cdot Ra/(1.36+Pr) < 10^3 \tag{3.12}$$

where λ_e is the effective thermal conductivity and λ is the thermal conductivity of the fluid.

Construction and material data

A cross-section of the diffusion process is shown in Fig. 3.1.

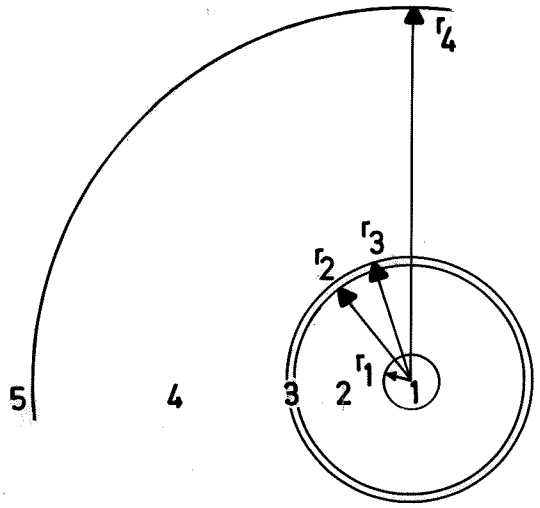

Fig. 3.1 - A cross-section of the diffusion process.

Media : 1 = rod
2 = air gap
3 = guard tube
4 = thermal insulation
5 = environment

The construction and material data relevant for the diffusion process at 25 °C are given by

$$
\begin{aligned}
r_1 &= 0.007 \text{ m} \\
r_2 &= 0.027 \text{ m} \\
r_3 &= 0.0285 \text{ m} \\
r_4 &= 0.13 \text{ m} \\
\ell &= 0.45 \text{ m}
\end{aligned}
$$

$$
\begin{aligned}
\lambda_1 &= \lambda_3 = 3.8 \cdot 10^{2} \text{ W/mK} \\
\lambda_2 &= 2.6 \cdot 10^{-2} \text{ W/mK} \\
\lambda_4 &= 4 \cdot 10^{-2} \text{ W/mK}
\end{aligned}
$$

$$
\begin{aligned}
a_1 &= a_3 = 1.16 \cdot 10^{-4} \text{ m}^2/\text{s} \\
a_2 &= 2.3 \cdot 10^{-5} \text{ m}^2/\text{s} \\
a_4 &= 3 \cdot 10^{-6} \text{ m}^2/\text{s}
\end{aligned}
$$

$$
\begin{aligned}
\beta_2 &= 3.6 \cdot 10^{-3} \text{ 1/K} \\
\nu_2 &= 1.6 \cdot 10^{-5} \text{ m}^2/\text{s} \\
\varepsilon_1 &= \varepsilon_3 = 0.03
\end{aligned}
\qquad (3.13)
$$

The material data are taken from [9] and [12]. The values of ε_1 and ε_3 apply to polished emeried commercial copper.

From experiments, it is known that the modulus of the temperature difference between the rod and the tube is less than 1 °C in the temperature range 20 °C - 30 °C. Therefore, by (3.13), the following bounds on the Prandtl number, the Grashof number and the Rayleigh number are obtained

$$
\begin{aligned}
Pr_2 &= 0.70 \\
Gr_2 &< 1.10 \cdot 10^{3} \\
Ra_2 &< 7.7 \cdot 10^{2}
\end{aligned}
\qquad (3.14)
$$

The Grashof number is evaluated at the mean temperature 25 °C.

When modelling the diffusion process, it is of great value to know the orders of magnitude of the Biot numbers and the Fourier numbers

of the different media of the heat process. Taking $\alpha = 10\ W/m^2K$ as an upper bound for the surface heat-transfer coefficients of the rod and the tube, (3.13) gives the following limits on the Biot numbers of these objects

$$(Bi_{r_1})_1 < 1.8 \cdot 10^{-4}$$
$$(Bi_{r_3})_3 < 7.1 \cdot 10^{-4} \qquad (3.15)$$

Assuming that the surface temperatures of the rod and the tube are equal to the boundary temperatures of the air gap for $r = r_1$ and $r = r_2$ respectively, it follows that the Biot numbers of the air gap are

$$(Bi_{r_2-r_1})_2 = \infty \qquad (3.16)$$

Moreover, on the assumption that the surface temperature of the tube and the boundary temperature of the thermal insulation for $r = r_4$ are equal, the Biot number of the insulation becomes

$$(Bi_{r_3})_4 = \infty \qquad (3.17)$$

The dominant time constant of the rod is T = 176 seconds. For this given time, (3.13) implies that the Fourier numbers of the air gap and the heat insulation are

$$(Fo_{r_2-r_1})_2 = 10.1$$
$$(Fo_{r_4})_4 = 0.65 \qquad (3.18)$$

All dimensionless groups are calculated at 25 ^{o}C.

Heat-transfer mechanisms in the air gap

The transition from conduction to convection heat-transfer in the air gap is determined by (3.12). It follows from (3.14) that

$Pr_2 \cdot Ra_2/(1.36 + Pr_2) < 2.6 \cdot 10^2 < 10^3$. Therefore, by (3.12), the heat in the air gap is mainly transferred by conduction and the effective thermal conductivity is

$$\lambda_{e_2}/\lambda_2 = 1 \tag{3.19}$$

Then, using [10], it is clear from (3.16) and (3.18) that the heat transfer mechanism in the air gap can be considered as stationary for all end point temperature variations.

For the steady-state heat transfer in the air gap, it is convenient to define a convection heat-transfer coefficient α_{c_1} by

$$\Phi_2 = \alpha_{c_1} A_1 (\Theta_1 - \Theta_3) \tag{3.20}$$

If this formula is used with the conventional relation for radial steady-state conduction in a cylinder

$$\Phi_2 = \frac{\Theta_1 - \Theta_3}{\frac{\ln(r_2/r_1)}{2\pi\lambda_2 \ell}} \tag{3.21}$$

it follows that α_{c_1} is given by

$$\alpha_{c_1} = \frac{\lambda_{e_2}}{r_1 \ln(r_2/r_1)} = 2.7 \text{ W/m}^2\text{K} \tag{3.22}$$

where (3.19) and the numerical values in (3.13) have been used.

The heat is also transferred by radiation in the air gap. It follows from [4] that the radiative heat-transfer coefficient is given by

$$\alpha_{r_2} = \frac{\sigma(\Theta_1^2 + \Theta_3^2)(\Theta_1 + \Theta_3)}{\frac{1}{\varepsilon_1} + \frac{A_1}{A_3}\left(\frac{1}{\varepsilon_3} - 1\right)} = 0.14 \text{ W/m}^2\text{K} \tag{3.23}$$

where the data in (3.13) are employed. The total heat transfer in the air gap

$$\alpha_1 = \alpha_{c_1} + \alpha_{r_1} = 2.8 \text{ W/m}^2\text{K} \tag{3.24}$$

is thus dominated by conduction ($\alpha_{c_1} = 2.7$ W/m^{2}K)

Heat-transfer mechanisms in the thermal insulation

The heat is mainly transferred by conduction in the heat insulation. Employing [2], the temperature wave penetration depth for persistently varying end point temperatures can be calculated from (3.17) and (3.18). It follows that this penetration depth is 0.09 m. This result should be compared with the radius of the insulation which is $r_4 = 0.13$ m.

For steady-state heat transfer in the insulation, it is convenient to define a convective heat transfer coefficient by $\Phi_4 = \alpha_{c3} A_3 \cdot (\theta_3 - \theta_5)$. If this formulae is used with the relation (3.21) for steady-state conduction in a cylinder, it follows that

$$\alpha_{c_3} = \frac{\lambda_4}{r_3 \ln(r_4/r_3)} = 0.92 \text{ W/m}^2\text{K} \tag{3.25}$$

where the numerical values in (3.13) are used.

Temperature drops in the silver plates

Experimental studies show that thermal resistances between the two end surfaces of the rod and the tube are not negligible. Moreover, it is found that the temperature drops in the silver plates can be modelled by

$$\theta_{0_3} = (1-\gamma)\ \theta_{0_1}$$
$$\theta_{\ell_3} = (1-\gamma)\ \theta_{\ell_3}$$
$$\gamma = 0.04 \qquad (3.26)$$

where γ is a correction factor.

A static model of the rod

A static model for the process will now be derived. Some assumptions will first be made which will simplify the calculations. These assumptions will then be verified by experiments. Assume that the heat loss rates from the rod and the tube are proportional to the temperature difference between these objects and their environments. Also, assume that the heat flow rate from the rod to the tube is negligible compared to the heat flow rate from the tube to the thermal insulation. By this assumption, the heat conduction equation for the tube is decoupled from the one of the rod, but not vice versa. The Biot numbers of the rod and the tube are very small, according to (3.15). Therefore, it follows from [10] that the temperature in all points of a cross section of the rod or the tube may be taken to be the same.

Putting

$$\xi_1^2 = \frac{\alpha_1 p_1}{\lambda_1 A_1}$$
$$\xi_3^2 = \frac{\alpha_3 p_3}{\lambda_3 A_3} \qquad (3.27)$$

it now follows from (3.3) that the steady-state heat conduction in the rod and the tube is governed by

$$\frac{d^2\theta_1}{dz^2} - \xi_1^2(\theta_1-\theta_3) = 0 \tag{3.28}$$

and

$$\frac{d^2\theta_3}{dz^2} - \xi_3^2\theta_3 = 0 \tag{3.29}$$

respectively. Let the boundary conditions of (3.28) and (3.29) be

$$\begin{aligned}\theta_1(0) &= \theta_1^c \\ \theta_1(\ell) &= \theta_1^c\end{aligned} \tag{3.30}$$

and

$$\begin{aligned}\theta_3(0) &= \theta_3^c \\ \theta_3(\ell) &= \theta_3^c\end{aligned} \tag{3.31}$$

respectively. From (3.5), it follows that the solution of (3.29), subject to the boundary conditions (3.31), is given by

$$\theta_3(z) = \frac{\sinh\xi_3(\ell-z) + \sinh\xi_3 z}{\sinh\xi_3\ell}\ \theta_3^c \tag{3.32}$$

A substitution of (3.32) into (3.28) gives

$$\frac{d^2\theta_1}{dz^2} - \xi_1^2\theta_1 = -\xi_1^2\ \frac{\sinh\xi_3(\ell-z) + \sinh\xi_3 z}{\sinh\xi_3\ell}\ \theta_3^c \tag{3.33}$$

The solution of (3.33), subject to the boundary conditions (3.30), is

$$\theta_1(z) = \frac{\sinh\xi_1(\ell-z) + \sinh\xi_1 z}{\sinh\xi_1\ell}\,\theta_1^c + \frac{\xi_1^2}{\xi_1^2-\xi_3^2}\left(\frac{\sinh\xi_3(\ell-z) + \sinh\xi_3 z}{\sinh\xi_3\ell} - \right.$$

$$\left. - \frac{\sinh\xi_1(\ell-z)+\sinh\xi_1 z}{\sinh\xi_1\ell}\right)\theta_3^c \qquad (3.34)$$

As ξ_1 tends to zero, it follows from (3.34) that $\theta_1(z)$ tends to θ_1^c, for all $z\in[0,\ell]$. The steady-state temperature error $\Delta\theta_1(z) = \theta_1(z)-\theta_1^c$ can be expanded in the following series

$$\Delta\theta_1(z) = -\frac{\xi_1^2\ell^2}{2}\,q_1(z)\,(\theta_1^c-\theta_3^c) - \frac{\xi_1^4\ell^4}{24}\,q_2(z)\,(\theta_1^c-\theta_3^c)$$

$$+ \frac{\xi_1^2\xi_3^2\ell^4}{24}\,q_2(z)\,\theta_3^c + O((\xi_1+\xi_3)^6\ell^6) \qquad (3.35)$$

This equation is very valuable for design purposes. The first two terms in (3.35) represent the temperature error in the rod due to the temperature drops in the silver plates whereas the third term represents the temperature error in the rod due to heat losses from the rod and the tube.

By an energy balance, it follows from (3.34) that the radial heat loss rate from the rod is given by

$$\Phi_{loss_1} = \Phi_{0_1} - \Phi_{\ell_1} = 2\lambda A\left(\frac{\xi_1(\cosh\xi_1\ell-1)}{\sinh\xi_1\ell}\,\theta_1^c + \frac{\xi_1^2}{\xi_1^2-\xi_3^2}\left(\frac{\xi_3(\cosh\xi_3\ell-1,}{\sinh\xi_3\ell} - \right.\right.$$

$$\left.\left. - \frac{\xi_1(\cosh\xi_1\ell-1)}{\sinh\xi_1\ell}\right)\theta_3^c\right) \qquad (3.36)$$

A series expansion of (3.36) shows

$$\Phi_{loss_1} = \frac{\lambda A}{\ell}\left(\xi_1^2\ell^2(\theta_1^c-\theta_3^c) - \frac{\xi_1^4\ell^4}{24}\,(\theta_1^c-\theta_3^c) + \frac{\xi_1^2\xi_3^2\ell^4}{12}\,\theta_3^c\right) +$$

$$+ O((\xi_1+\xi_3)^6\ell^6) \qquad (3.37)$$

Remembering that the area of the cross-section of the tube is $A_3 = \pi(r_3^2 - r_2^2)$, it follows from (3.13), (3.24), (3.25) and (3.27) that

$$\xi_1 \ell = 0.66$$
$$\xi_3 \ell = 0.57 \qquad (3.38)$$

Assume that $\theta_{0_1} = \theta_{\ell_1} = 30\ ^{o}C$ and $\theta_a = 25\ ^{o}C$. On this assumption (3.11), (3.13), (3.26), (3.37) and (3.38) yield that the heat loss rates from the surfaces of the rod and the tube are

$$\Phi_{loss_1} = 0.02\ W$$
$$\Phi_{loss_3} = 0.34\ W \qquad (3.39)$$

Moreover, on this assumption (3.7), (3.8), (3.13), (3.26), (3.35) and (3.38) imply that the steady-state temperature errors in the mid-points of the rod and the tube become

$$\Delta\theta_1(\ell/2) = -\ 0.02\ ^{o}C$$
$$\Delta\theta_3(\ell/2) = -\ 0.19\ ^{o}C \qquad (3.40)$$

The calculated temperature error in the mid-point of the rod is in agreement with the measurement results in Table 4.1. According to this table, the maximum absolute value of the temperature errors is $0.02\ ^{o}C$. From Table 4.2, it can be seen that approximately the same temperature errors are obtained when a temperature gradient is introduced in the rod. This is in fact a simple consequence of the principle of superposition.

It follows from (3.35) that the temperature drops in the silver plates and the heat losses from the rod and the tube give equal contributions to the temperature error in the mid-point of the rod. This shows that the trade-off between the servo responses and the temperature drops in the silver plates is well made. On the assumption $\theta_{0_1} = \theta_{\ell_1} = 30\ ^{o}C$ and $\theta_a = 25\ ^{o}C$, (3.26) and (3.40) imply that

$$\theta_3(\ell/2) - \theta_1(\ell/2) = \theta_3^c + \Delta\theta_3(\ell/2) - (\theta_1^c + \Delta\theta_1(\ell/2)) = \\ = -0.37\ ^oC \qquad (3.41)$$

This temperature difference should be compared with the value -0.4 ^oC, obtained from measurements. The error in this measured value might be relatively large, since the influence of the room temperature on the result is not known.

In a dynamical model the heat loss rate from the rod is modelled by the term $\xi_1^2\theta_1$, instead of the term $\xi_1^2(\theta_1-\theta_3)$. The ratio between the terms, used to describe the heat loss rates from the rod is

$$c(z) = \frac{\xi_1^2(\theta_1(z)-\theta_3(z))}{\xi_1^2\theta_1(z)} \qquad (3.42)$$

Assume that the constant end temperatures of the rod and the tube are θ_1^c and θ_3^c respectively. Neglecting the steady-state temperature error in the rod, it then follows from (3.8), (3.26) and (3.42) that

$$c(z) = \frac{-\Delta\theta_3(z)+\gamma\theta_1^c}{\theta_1^c} = \frac{\xi_3^2\ell^2}{2} q_1(z)\ (1-\gamma) + \gamma + O((\xi_3\ell)^4) \qquad (3.43)$$

In particular, it is found that

$$c(\ell/2) = 0.079 \qquad (3.44)$$

where (3.7), (3.26), (3.38) and (3.43) have been used.

A dynamical model of the rod

The main problem, which arises when setting up a dynamical model of the rod, is to adequately model the heat flow rate from the surface of the tube. It follows from (3.15) and (3.18) that this rate,

in general, is not proportional to the temperature difference between the tube and its environment. This means that the complete system, describing the conduction of heat in the rod, involves three coupled partial differential equations. The problem of simplifying this system of partial differential equations therefore naturally arises.

Since the heat flow rates from the surfaces of the rod and the tube are very small and since the conduction of heat in the air gap can be considered as stationary, the heat loss rate from a surface element on the rod may as a first approximation be taken to be proportional to the temperature of the surface element. On this assumption, it follows from (3.3) that the conduction of heat in the rod is described by

$$a_1 \frac{\partial^2 \theta_1}{\partial z^2} = \frac{\partial \theta_1}{\partial t} + \eta_1 \theta_1 \qquad (3.45)$$

where η_1 is the coefficient of surface-heat loss

For given variations of the end point temperatures of the rod, η_1 is a measure of the mean heat loss rate from the rod. If the frequency content in these variations is increased then the heat loss rate from the tube is increased and, consequently, η_1 is increased. Therefore, the static consideration (3.42) yields an estimate of the lower bound of η_1, valid for a case where the end point temperatures of the rod are perturbed very slowly. A comparison of (3.28) and (3.45), together with (3.13) and (3.38), gives that this lower bound is

$$\eta_1 = c(\ell/2)\xi_1^2 a_1 = 2.0 \cdot 10^{-5} \text{ 1/s} \qquad (3.46)$$

The value of η_1, estimated by means of a maximum likelihood experiment in Section 3 of Chapter 5, is $\eta_1 = 3.6 \cdot 10^{-5}$ 1/s. In this specific experiment, it is found that the heat loss rate from the rod is increased only by a factor 1.8, compared to the static case.

To calculate the transfer function and the step response of the rod, it is convenient to introduce the dimensionless time

$$\tau = t/T$$
$$T = \ell^2/a_1 \tag{3.47}$$

Equation (3.45) then becomes

$$\frac{\partial^2\theta_1}{\partial z^2} = \frac{1}{\ell^2}\frac{\partial\theta_1}{\partial\tau} + \frac{\eta_1}{a_1}\theta_1 \tag{3.48}$$

with the boundary conditions

$$\theta_1(0,\tau) = \theta_{0_1}(\tau)$$
$$\theta_1(\ell,\tau) = \theta_{\ell_1}(\tau) \tag{3.49}$$

and initial condition

$$\theta(z,0) = \theta_{i_1}(z) \tag{3.50}$$

Introduce the laplacetransforms

$$\psi_1(z,s) = \int_0^\infty e^{-s\tau}\theta_1(z,\tau)d\tau$$
$$\psi_{0_1}(s) = \int_0^\infty e^{-s\tau}\theta_{0_1}(\tau)d\tau$$
$$\psi_{\ell_1}(s) = \int_0^\infty e^{-s\tau}\theta_{\ell_1}(\tau)d\tau \tag{3.51}$$

If $\theta_i(z) = 0$, for all $z \in [0,\ell]$, then a Laplace transformation of (3.48), subject to the boundary conditions (3.49), gives

$$\frac{d^2\psi_1}{dz^2} - \frac{s+\frac{\eta_1}{a_1}\ell^2}{\ell^2}\psi_1 = 0$$

$$\psi_1(0,s) = \psi_{0_1}(s)$$

$$\psi_1(\ell,s) = \psi_{\ell_1}(s) \tag{3.52}$$

Putting

$$b = \eta_1\ell^2/a_1 \tag{3.53}$$

The solution of (3.52) is

$$\psi_1(z,s) = \frac{\sinh \frac{\ell-z}{\ell}\sqrt{s+b}}{\sinh \sqrt{s+b}}\psi_{0_1}(s) + \frac{\sinh \frac{z}{\ell}\sqrt{s+b}}{\sinh \sqrt{s+b}}\psi_{\ell_1}(s) \tag{3.54}$$

The transfer function from the end point temperatures of the rod to the temperature at a point z on the rod thus becomes

$$G(z,s) = \left[\frac{\sinh \frac{\ell-z}{\ell}\sqrt{s+b}}{\sinh \sqrt{s+b}}, \frac{\sinh \frac{z}{\ell}\sqrt{s+b}}{\sinh \sqrt{s+b}}\right] \tag{3.55}$$

If the time scale of the temperatures θ_{0_1}, θ_{ℓ_1}, θ_1 is changed from τ to t, then G(z,s) becomes

$$H(z,s) = \left[\frac{\sinh \frac{\ell-z}{\ell}\sqrt{s\tau+b}}{\sinh \sqrt{s\tau+b}}, \frac{\sinh \frac{z}{\ell}\sqrt{s\tau+b}}{\sinh \sqrt{s\tau+b}}\right] \tag{3.56}$$

A modal analysis shows that this transfer function may be written

$$H(z,s) = \left[2\pi \sum_{k=1}^{\infty}(-1)^{k+1}k \frac{\sin \frac{\ell-z}{\ell}\pi k}{s\tau+b+\pi^2k^2}, 2\pi \sum_{k=1}^{\infty}(-1)^{k+1}k \frac{\sin \frac{z}{\ell}\pi k}{s\tau+b+\pi^2k^2}\right] \tag{3.57}$$

The transfer function $H(z,s)$ has an infinite number of poles

$$s_k = -(b+\pi^2 k^2)/T \qquad k = 1,2,... \tag{3.58}$$

These poles are negative and real. If z/ℓ is a rational number, then pole-zero cancellations occur in the transfer function $H(z,s)$. The cancelled modes are unobservable from measurement of the temperature in the point z. This is discussed in detail in Section 5 of Chapter 4. The response of the rod to a temperature step change θ_1^c in the end point temperature θ_{01} is

$$\theta(z,t) = \frac{\sinh\xi_1(\ell-z)}{\sinh\xi_1\ell}\,\theta_1^c - 2\pi\sum_{k=1}^{\infty}(-1)^{k+1}k\,\frac{\sin\frac{\ell-z}{\ell}\pi k}{b+\pi^2k^2}\,e^{-(b+\pi^2k^2)/T}\,\theta_1^c \tag{3.59}$$

4. MEASUREMENTS

Steady-state measurements

The steady-state temperature distribution of the rod was measured in two different cases. The measurements were performed with a Tekelec, model 350, digital voltmeter, with a long term accuracy of 0.01 % of full scale and 0.02 % of readings. The ambient temperature was 25 °C. In the first case, the end point temperatures of the rod were equal and varied from 20 °C to 30 °C, with a temperature increment of 1 °C. The measurement results are given in Table 4.1. The modulus of the temperature errors is largest at 20 °C and 30 °C. The maximum absolute value of the temperature errors in the table is 0.02 °C, which is just noticable relative to the transducer errors 0.01 °C.

In the second case a temperature gradient was introduced in the rod. The different values of the employed end point temperatures are found in Table 4.2. In this table, there is no longer a strong cor-

relation between the sign of the temperature errors and the sign of the corresponding temperatures (relative to 25 ^{o}C). This is due to the slope and linearity errors of the transducers. The maximum absolute value of the temperature errors in Table 4.2 is 0.02 ^{o}C. Notice that the temperature errors in Table 4.1 and 4.2 are calculated on the assumption that the temperature transducers are ideal.

Dynamical measurements

To verify the dynamical model of the rod experiments were performed by perturbing one end point temperature of the rod and measuring the temperature along the rod. A Dynamco, series 6000, data logger was used in these experiments. The input channels of the logger were scanned sequentially. The time elapsed between the readings of two consecutive channels was 0.18 s. Aitken´s scheme for Lagrange interpolation was used to synchronize the readings of the different channels of the logger, within the same sampling interval, to the readings of the input of the process. The long term accuracy of the DM 2006 digital voltmeter of the logger was 0.01 % of full scale and 0.02 % of readings.

The input signal of the process was a pseudo random binary signal (PRBS), generated by a special signal generator. This signal had a mean level of 25 ^{o}C and a temperature swing of 1.8 ^{o}C. The readings of the input channels of the data logger were synchronized to the shifts of the PRBS-signal.

In all experiments, the input u_1 was manipulated and the input u_2 was kept constant at 25 ^{o}C. The initial temperature profiles of the rod were stationary, but the temperature gradient was nonzero. The room temperature changed several degrees centigrade during the experiments. The variation of the sampling period was kept within 0.1 %.

In Table 4.3 the three series used for identification of the dynamics of the rod are specified. The input-output samples of these

Steady-state temperature profile of the rod									Temperature errors: $e_i = y_i - (\frac{\ell - z_i}{\ell} y_{e1} + \frac{z_i}{\ell} y_{e2})$, i = 1,2...7						
y_{e1} °C	y_{e2} °C	y_1 °C	y_2 °C	y_3 °C	y_4 °C	y_5 °C	y_6 °C	y_7 °C	e_1 °C	e_2 °C	e_3 °C	e_4 °C	e_5 °C	e_6 °C	e_7 °C
-5.00	-5.00	-4.99	-4.99	-4.99	-4.99	-4.98	-4.98	-4.98	0.01	0.01	0.01	0.01	0.02	0.02	0.02
-4.00	-4.00	-4.00	-3.99	-3.99	-3.99	-3.98	-3.99	-3.99	0.01	0.01	0.01	0.01	0.02	0.01	0.01
-3.00	-3.00	-3.00	-3.00	-3.00	-2.99	-2.99	-2.99	-2.99	0.00	0.00	0.00	0.01	0.01	0.01	0.01
-2.00	-2.00	-2.00	-2.00	-2.00	-2.00	-1.99	-2.00	-1.99	0.00	0.00	0.00	0.00	0.01	0.00	0.01
-1.00	-1.00	-1.00	-1.01	-1.01	-1.01	-1.00	-1.00	-1.00	0.00	-0.01	-0.01	-0.01	0.00	0.00	0.00
0.00	0.00	0.00	-0.01	0.00	0.00	0.00	0.00	-0.01	0.00	-0.01	0.00	0.00	0.00	0.00	-0.01
1.00	1.00	1.00	1.00	1.01	1.00	1.00	1.00	1.00	0.00	0.00	0.01	0.00	0.00	0.00	0.00
2.00	2.00	1.99	1.99	1.99	1.99	2.00	2.00	1.99	-0.01	-0.01	-0.01	-0.01	0.00	0.00	-0.01
3.00	3.00	2.99	2.99	2.99	2.99	3.00	2.99	2.99	-0.01	-0.01	-0.01	-0.01	-0.00	-0.01	-0.01
4.00	4.00	3.99	3.99	3.99	3.99	3.99	3.99	3.99	-0.01	-0.01	-0.01	-0.01	-0.01	-0.01	-0.01
5.00	5.00	4.99	4.98	4.99	4.99	4.99	4.99	4.98	-0.01	-0.02	-0.01	-0.01	-0.01	-0.01	-0.02

Table 4.1 - Steady-state temperature distribution of the rod for different values of the end point temperatures. The temperature errors are calculated on the assumption, that the transducers are ideal. The ambient temperature is $\Theta_a = 25$ °C

Steady-state temperature profile of the rod									Temperature errors: $e_i = y_i - (\frac{\ell - z_i}{\ell} y_{e1} + \frac{z_i}{\ell} y_{e2})$, i = 1,2...7						
y_{e1} °C	y_{e2} °C	y_1 °C	y_2 °C	y_3 °C	y_4 °C	y_5 °C	y_6 °C	y_7 °C	e_1 °C	e_2 °C	e_3 °C	e_4 °C	e_5 °C	e_6 °C	e_7 °C
1.00	-5.00	0.25	-0.50	-1.26	-2.01	-2.76	-3.51	-4.24	0.00	0.00	-0.01	-0.01	-0.01	-0.01	0.00
3.00	-5.00	2.00	1.00	-0.01	-1.01	-2.02	-3.01	-4.00	0.00	0.00	-0.01	-0.01	-0.02	-0.01	-0.00
5.00	-5.00	3.75	2.50	1.25	-0.01	-1.27	-3.52	-3.76	0.00	0.00	0.00	-0.01	-0.02	-0.02	-0.01
-5.00	1.00	-4.25	-3.51	-2.76	-2.00	-1.24	-0.50	0.25	0.00	-0.01	-0.01	0.00	0.01	0.00	0.00
-5.00	3.00	-4.01	-3.02	-2.01	-1.01	0.01	1.00	2.00	-0.01	-0.02	-0.01	-0.01	0.01	0.00	0.00
-5.00	5.00	-3.76	-2.52	-1.26	-0.01	1.26	2.50	3.75	-0.01	-0.02	-0.01	-0.01	0.01	0.00	0.00
-1.00	5.00	-0.26	0.48	1.24	1.99	2.75	3.50	4.24	-0.01	-0.02	-0.01	-0.01	0.00	0.00	-0.01
-3.00	5.00	-2.01	-1.02	-0.01	0.99	2.01	3.01	3.99	-0.01	-0.02	-0.01	-0.01	0.01	0.01	-0.01
-5.00	5.00	-3.76	-2.52	-1.26	-0.01	1.26	2.50	3.75	-0.01	-0.02	-0.01	-0.01	0.01	0.00	0.00
5.00	-1.00	4.25	3.49	2.74	1.99	1.24	0.49	-0.26	0.00	-0.01	-0.01	-0.01	-0.01	-0.01	-0.01
5.00	-3.00	4.00	3.00	1.99	1.00	-0.01	-1.01	-2.00	0.00	0.00	-0.01	0.00	-0.01	-0.01	0.00
5.00	-5.00	3.75	2.50	1.25	-0.01	-1.27	-2.52	-3.76	0.00	0.00	0.00	-0.01	-0.02	-0.02	-0.01
-5.00	0.00	-4.38	-3.76	-3.13	-2.50	-1.86	-1.24	-0.62	0.00	-0.01	0.00	0.00	+0.02	+0.01	+0.01
0.00	0.00	0.00	-0.01	0.00	0.00	0.00	0.00	-0.01	0.00	0.00	0.00	0.00	0.00	0.00	-0.01
5.00	0.00	4.37	3.75	3.12	2.50	1.87	1.25	0.62	-0.01	0.00	-0.01	0.00	-0.01	0.00	-0.01
0.00	-5.00	-0.63	-1.25	-1.88	-2.50	-3.13	-3.75	-4.37	0.00	0.00	-0.00	0.00	0.00	0.00	0.01
0.00	0.00	0.00	-0.01	0.00	0.00	0.00	0.00	-0.01	0.00	-0.01	0.0	0.00	0.00	0.00	-0.01
0.00	5.00	0.62	1.24	1.87	2.50	3.13	3.75	4.37	-0.01	-0.01	-0.01	0.00	0.00	0.00	-0.01

Table 4.2 - Steady-state temperature distribution of the rod for different values of the end point temperatures. The temperature errors are calculated on the assumption, that the transducers are ideal. The ambient temperature is Θ_a = 25 °C.

series are believed to be useful test examples for comparing different identification algorithms. In [11] such a comparison is performed between the generalized least squares method and the maximum likelihood method for the series S1. The choice of the sampling interval for the diffusion process has been discussed briefly in [3].

Series	Sampling period s	Number of sampling events	PRBS-signal minimum puls length s	PRBS-signal period s	Measured signals
S1	10	862	60	4095	$u_1, y_1, y_2, \ldots, y_7, ye_1, ye_2$
S2	4	920	60	255	$u_1, y_1, y_2, \ldots, y_7, ye_1, ye_2$
S3	2	1828	20	1023	$u_1, y_1, y_2, ye_1, ye_2$

Table 4.3 - Series used for maximum likelihood identification of the rod.

5. REFERENCES

[1]: Beckman, W.: "Die Warmeübertragung in zylindrischen Gasschichten bei natürlicher Konvektion", Forsch. Gebiete Ingenieurswesen, Vol. 2, 165-178, 1931.

[2]: Carslaw, H.S. and Jaeger, J.G.: "Conduction of heat in solids", 2nd ed., Clarendon Press, Oxford, 1959.

[3]; Gustavsson, I: "Choice of sampling interval for parametric identification", Report 7103, Lund Inst. of Techn., Div. of Automatic Control, 1971.

[4]: Holman, J.P.: "Heat transfer", 2nd ed., McGraw-Hill, New York, 1968.

[5]: Kraussold, H.: "Wärmeabgabe von zylindrischen Flüssigkeitsschichten bei natürlicher Konvektion", Forsch. Gebiete Ingenieurswesen, Vol. 5, 186-188, 1934.

[6]: Leden, B.: "Linear temperature scales from one thermistor reciprocal networks", Report 7009, Lund Inst. of Techn., Div. of Automatic Control, 1970.

[7]: Leden, B.: "The design of a one dimensional heat diffusion process", Report 7010, Lund Inst. of Techn., Div. of Automatic Control, 1970.

[8]: Liu, C.Y., Mueller, W.K. and Landis, F.: "Natural convection heat transfer on long horizontal cylindrical annuli", Int. Development in Heat Transfer, paper 117, Boulder, Colorado, 1961.

[9]: McAdams, W.H.: "Heat transmission", 3rd ed., McGraw-Hill, New York, 1954.

[10]: Schneider, P.J.: "Temperature response charts", John Wiley, New York, 1963.

[11]: Söderström, T.: "Convergence properties of the generalized least squares identification method", Preprint 3rd IFAC Symp. on Identification and Parameter Estimation, the Hague, Part 2, 691-700, 1973.

[12]: Touloukain, Y.S., Powell, R.W., Ho, C.Y. and Nicolau, M.C.: "Thermal Diffusivity", Thermophysical properties of matters, Vol. 10, IFI/Plenum Data Corporation, New York, 1973.

CHAPTER 3

LUMPED STATE-SPACE MODELS

1. INTRODUCTION

In the previous chapter the rod was modelled as a linear distributed parameter system. To obtain numerical solutions to filter and control problems for such a system, it is, in general, necessary to make approximations. These approximations can either be done, at the beginning, by approximating the infinite dimensional system by a finite dimensional system or, at the end, when the partial differential equation, yielding the solution to the problem, is obtained. Approximation at the beginning has the advantage, in most cases, of simplifying the mathematical manipulations whereas approximation at the end probably gives better accuracy.

This chapter deals with the problem of obtaining lumped state-space models of the rod. The finite-difference method described in [6] and [7] is used. Filter and control strategies, based on the lumped models, are derived in Chapter 7. In that chapter it is shown that these strategies, obtained by the approximations, can be used to, online, estimate and control the profile of the rod satisfactorily.

2. FINITE-DIFFERENCE STATE-SPACE MODELS

In Section 3 of Chapter 2 it was found that the rod could be modelled by the distributed parameter system

$$a \frac{\partial^2 \theta}{\partial z^2} = \frac{\partial \theta}{\partial t} + \eta\theta \tag{2.1}$$

subject to the boundary conditions

$$\theta(0,t) = \theta_0(t)$$
$$\theta(\ell,t) = \theta_\ell(t) \tag{2.2}$$

To obtain a lumped state-space model of the system (2.1), the rod is divided into a number of intervals and the partial derivative $\partial^2\theta/\partial z^2$ is approximated in the nodal points using finite-difference formulae. The accuracy of this approximation can be improved by increasing the number of nodes, by using higher order difference formulae or by choosing smaller intervals where the temperature gradient can be expected to be large.

Preliminaries

If v is a continuous function in one variable with continuous derivatives then [1] gives

$$\frac{d^2v}{dz^2}\Bigg|_{z=z_0} = \frac{1}{h_z^2}\left(\delta^2 - \frac{1}{12}\delta^4 + \frac{1}{90}\delta^6\right)v\Bigg|_{z=z_0} + O(h_z^6) \tag{2.3}$$

where h_z is the interval size and δ is the central difference operator. This operator is defined by

$$(\delta v)(z) = v\left(z + \frac{h_z}{2}\right) - v\left(z - \frac{h_z}{2}\right) \tag{2.4}$$

Let the value of v at $z_i = z_0 + ih_z$ be v_i. Then (2.3) and (2.4)

give the following approximations to d^2v/dz^2

$$\left.\frac{d^2v}{dz^2}\right|_i = \frac{1}{h_z^2}(v_{i-1} - 2v_i + v_{i+1}) + O(h_z^2) \tag{2.5a}$$

$$\left.\frac{d^2v}{dz^2}\right|_i = \frac{1}{12h_z^2}(-v_{i-2} + 16v_{i-1} - 30v_i + 16v_{i+1} - v_{i+2}) + O(h_z^4) \tag{2.5b}$$

$$\left.\frac{d^2v}{dz^2}\right|_i = \frac{1}{180h_z^2}(2v_{i-3} - 27v_{i-2} + 270v_{i-1} - 490v_i + 270v_{i+1} - 27v_{i+2} + 2v_{i+3}) + O(h_z^6) \tag{2.5c}$$

where $O(h_z^k)$ denotes terms containing k:th and higher power of h_z. The approximations (2.5a), (2.5b) and (2.5c) require knowledge of v in 3, 5 and 7 equidistant points.

ROD1

Assume that the rod is divided into n_z intervals. Let the temperature in the i:th nodal point of the rod, at time t, be $\theta_i(t)$ for $i = 0,1, \ldots, n_z$. Choose as the state-vector of the lumped model the temperature in the n_z-1 internal nodal points of the rod, i.e.

$$x = \begin{bmatrix} \theta_1 \\ \theta_2 \\ \vdots \\ \theta_{n_z-1} \end{bmatrix} \tag{2.6}$$

and choose as the input vector of this model the temperature in the two end nodal points of the rod, i.e.

$$u = \begin{bmatrix} \theta_0 \\ \theta_{n_z} \end{bmatrix} \tag{2.7}$$

Then it is possible to set up a set of lumped state-space models of the system (2.1).

If all intervals have the size h_z and if the approximation (2.5a) to $\partial^2\theta/\partial z^2$ is used for all internal nodal points, this model becomes

$$\dot{x} = \begin{bmatrix} -a_1 & a_2 & & & 0 \\ a_2 & -a_1 & a_2 & & \\ & \ddots & \ddots & \ddots & \\ & & a_2 & -a_1 & a_2 \\ 0 & & & a_2 & -a_1 \end{bmatrix} x + \begin{bmatrix} a_2 & 0 \\ 0 & 0 \\ \vdots & \vdots \\ 0 & 0 \\ 0 & a_2 \end{bmatrix} u \triangleq A_1 x + B_1 u \tag{2.8}$$

where

$$\begin{aligned} a_1 &= 2a/h_z^2 + \eta \\ a_2 &= a/h_z^2 \end{aligned} \tag{2.9}$$

This model is called ROD1.

ROD2

Let all the intervals have the size h_z and let the approximations (2.5a) and (2.5b) to $\partial^2\theta/\partial z^2$ be used for the nodal points i = 1, n_z-1 and i = 2, 3, ..., n_z-2 respectively. Then the lumped model of the system (2.1) is

$$\dot{x} = \begin{bmatrix} -a_1 & a_2 & & & & & & \\ b_2 & -b_1 & b_2 & -b_3 & & & & \\ -b_3 & b_2 & -b_1 & b_2 & -b_3 & & & \\ & & & & & & & \\ & & & & & & & \\ & & & & & & & \\ & & & & -b_3 & b_2 & -b_1 & b_2 & -b_3 \\ & & & & & -b_3 & b_2 & -b_1 & b_2 \\ & & & & & & & a_2 & -a_1 \end{bmatrix} x + \begin{bmatrix} a_2 & 0 \\ -b_3 & 0 \\ 0 & 0 \\ \vdots & \vdots \\ 0 & 0 \\ 0 & -b_3 \\ 0 & a_2 \end{bmatrix} u \triangleq A_2 x + B_2 u \qquad (2.10)$$

where

$$a_1 = 2a/h_z^2 + \eta$$
$$a_2 = a/h_z^2$$

$$b_1 = 30a/(12h_z^2) + \eta$$
$$b_2 = 16a/(12h_z^2)$$
$$b_3 = a/(12h_z^2) \qquad (2.11)$$

This model is called ROD2.

ROD3

Provided that all intervals have the size h_z and provided that the approximations (2.5a), (2.5b) and (2.5c) to $\partial^2\theta/\partial z^2$ are used for the nodal points i = 1, n_z-1; i = 2, n_z-2 and i = 3, 4, ..., n_z-3, respectively the lumped model of the system (2.1) becomes

$$
\dot{x} = \begin{bmatrix}
-a_1 & a_2 & 0 & 0 & & & & & & & \\
b_2 & -b_1 & b_2 & -b_3 & 0 & & & \mathbf{0} & & & \\
-c_3 & c_2 & -c_1 & c_2 & -c_3 & c_4 & & & & & \\
c_4 & -c_3 & c_2 & -c_1 & c_2 & -c_3 & c_4 & & & & \\
 & \ddots & \ddots & \ddots & \ddots & \ddots & \ddots & \ddots & & & \\
 & & & & c_4 & -c_3 & c_2 & -c_1 & c_2 & -c_3 & c_4 \\
 & & & & & c_4 & -c_3 & c_2 & -c_1 & c_2 & -c_3 \\
 & & \mathbf{0} & & & & 0 & -b_3 & b_2 & -b_1 & b_2 \\
 & & & & & & & 0 & 0 & a_2 & -a_1
\end{bmatrix} x + \begin{bmatrix}
a_2 & 0 \\
-b_3 & 0 \\
c_4 & 0 \\
0 & 0 \\
\vdots & \vdots \\
0 & 0 \\
0 & c_4 \\
0 & -b_3 \\
0 & a_2
\end{bmatrix} u \triangleq
$$

$$\triangleq A_3 x + B_3 u \tag{2.12}$$

where

$$a_1 = 2a/h_z^2 + \eta$$
$$a_2 = a/h_z^2$$

$$b_1 = 30a/(12h_z^2) + \eta$$
$$b_2 = 16a/(12h_z^2)$$
$$b_3 = a/(12h_z^2)$$

$$c_1 = 490a/(180h_z^2) + \eta$$
$$c_2 = 270a/(180h_z^2)$$
$$c_3 = 27a/(180h_z^2)$$
$$c_4 = 2a/(180h_z^2) \tag{2.13}$$

This model is called ROD3.

ROD4

Assume that the interval sizes are chosen according to Fig. 2.1.

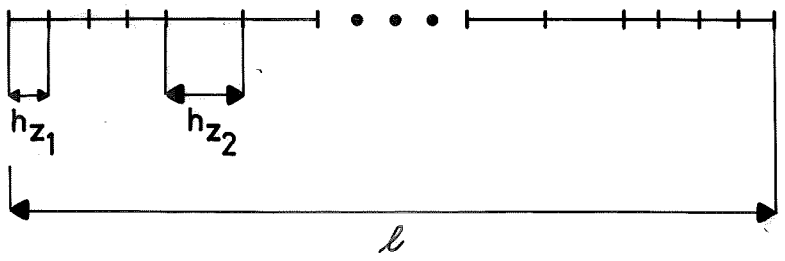

Fig. 2.1 - Choice of the interval sizes for the model ROD4.

In this figure the interval sizes are chosen smaller near the end points of the rod since the temperature gradients are expected to be large here. Let the approximations (2.5a), (2.5b) and (2.5c) to $\partial^2\theta/\partial z^2$ be used for the nodal points i = 1, 3, n_z-3, n_z-1; i = 2, 4, n_z-4, n_z-2 and i = 5, 6, ..., n_z-5 respectively. Then the lumped model of the system (2.1) is

$$\dot{x} = \begin{bmatrix}
-a_1 & a_2 & 0 & 0 & & & & & & & & & \\
b_2 & -b_1 & b_2 & -b_3 & 0 & & & & & & & & \\
0 & a_2 & -a_1 & a_2 & 0 & 0 & & & & & & & \\
0 & c_2 & 0 & -c_1 & c_2 & -c_3 & 0 & & & & & & \\
0 & -d_3 & 0 & d_2 & -d_1 & d_2 & -d_3 & d_4 & & & & & \\
 & d_4 & 0 & -d_3 & d_2 & -d_1 & d_2 & -d_3 & d_4 & & & & \\
 & & 0 & d_4 & -d_3 & d_2 & -d_1 & d_2 & -d_3 & d_4 & & & \\
 & & & & & & & & & & & & \\
 & & & & & & & & & & & & \\
 & & & & & & & & & & & & \\
 & & & & & & & & & & & & \\
 & & & & & & & & & & & & \\
 & & & & & & & & & & & & \\
 & & & & & & & & & & & &
\end{bmatrix} x +$$

$$\begin{bmatrix}
 & & & & & & & & & & & & \\
 & & & & & & & & & & & & \\
 & & & & & & & & & & & & \\
 & & & & & & & & & & & & \\
 & & & & & & & & & & & & \\
 & & & & & & & & & & & & \\
 & & & & & & & & & & & & \\
d_4 & -d_3 & d_2 & -d_1 & d_2 & -d_3 & d_4 & 0 & & & & & \\
 & d_4 & -d_3 & d_2 & -d_1 & d_2 & -d_3 & 0 & d_4 & & & & \\
 & & d_4 & -d_3 & d_2 & -d_1 & d_2 & 0 & -d_3 & 0 & & & \\
 & & & & 0 & -c_3 & c_2 & -c_1 & 0 & c_2 & 0 & & \\
 & & & & & 0 & 0 & a_2 & $-a_1$ & a_2 & 0 & & \\
 & & & & & & & 0 & $-b_3$ & b_2 & $-b_1$ & b_2 & \\
 & & & & & & & & 0 & 0 & a_2 & $-a_1$
\end{bmatrix}$$

$$+\begin{bmatrix} a_2 & 0 \\ -b_3 & 0 \\ 0 & 0 \\ -c_3 & 0 \\ d_4 & 0 \\ 0 & 0 \\ 0 & 0 \\ | & | \\ 0 & 0 \\ 0 & 0 \\ 0 & d_4 \\ 0 & -c_3 \\ 0 & 0 \\ 0 & -b_3 \\ 0 & a_2 \end{bmatrix} u \triangleq A_4 x + B_4 u \qquad (2.14)$$

where

$$h_{z_1} = \ell/n_z$$

$$h_{z_2} = \ell/(2n_z)$$

and

$$a_1 = 2a/h_{z_2}^2 + \eta$$

$$a_2 = a/h_{z_2}^2$$

$$b_1 = 30a/\left(12h_{z_2}^2\right) + \eta$$

$$b_2 = 16a/\left(12h_{z_2}^2\right)$$

$$b_3 = a/\left(12h_{z_2}^2\right)$$

$$c_1 = 30a/\left(12h_{z_1}^2\right) + \eta$$

$$c_2 = 16a/\left(12h_{z_1}^2\right)$$

$$c_3 = a/\left(12h_{z_1}^2\right)$$

$$d_1 = 490a/\left(180h_{z_1}^2\right) + \eta$$

$$d_2 = 270a/\left(180h_{z_1}^2\right)$$

$$d_3 = 27a/\left(180h_{z_1}^2\right)$$

$$d_4 = 2a/\left(180h_{z_1}^2\right) \qquad (2.15)$$

This model is called ROD4.

The order of the models ROD1, ROD2, ..., ROD4 is given by

$$n = n_z - 1 \qquad (2.16)$$

It should be noticed that the approximation among (2.5a) and among (2.5a), (2.5b) which has the highest possible order is chosen in each node for the models ROD1 and ROD2 respectively. Similar the approximation, among (2.5a), (2.5b) and (2.5c), that has the highest possible order is chosen in each of the nodal points for the models ROD3 and ROD4. Also notice that for each of the models ROD1, ROD2 ..., ROD4 there exist choices of n such that the measurable signals of the rod are contained among the state variables of the considered model.

3. SIMULATION STUDIES

In this section the eigenvalues and the step responses of the lumped models are calculated. These values and responses are com-

pared with the eigenvalues and step responses of the infinite dimensional system (2.1). From this comparison some conclusions are drawn about the accuracy of the different finite-difference techniques used to lump the system (2.1). It is not claimed that all aspects of the approximations can be judged from the eigenvalues and the step responses.

The eigenvalues of the models ROD1, ROD2, ..., ROD4 are given for different values of n in Table 3.1. This table also contains the eigenvalues of the infinite dimensional system, given by (3.58) in Chapter 2. The step responses of the models ROD1, ROD2, ..., ROD4 are given in Tables A.1, A.2, ..., A.6 for $z = \ell/8$, $3\ell/8$, ..., $7\ell/8$ and for different values of n. In these tables the differences between the approximated step responses and the step responses of the infinite dimensional system, given by (3.59) in Chapter 2, are also presented. All calculations are based on the parameter values $a = 1.159 \cdot 10^{-4}$ m^2/s and $\eta = 3.6 \cdot 10^{-5}$ $1/s$ (see Section 3 of Chapter 5).

The main conclusion to be drawn from Table 3.1 and Tables A.1, A.2, ..., A.6 is that the accuracy of the lumped models is primarily determined by the number of intervals. The refinement of the difference approximation to $\partial^2\theta/\partial z^2$ improves the accuracy to a certain extent. However, such a refinement improves the accuracy of the eigenvalues considerably more than the accuracy of the step responses. These conclusions are obtained by comparing, for example, the eigenvalues and the step responses of the models ROD1, ROD2 and ROD3 for n = 7, given in Table 3.1 and Tables A.1, A.2 and A.3 respectively, and the corresponding values and responses of the models ROD2 and ROD3 for n = 15, given in Table 3.1 and Tables A.5 and A.6 respectively. It should be observed that it is not possible to increase the order of the approximation to $\partial^2\theta/\partial z^2$ near the end points of the rod where the temperature gradients are large.

It is important to use smaller intervals near the ends of the rod where the temperature gradients can be expected to be large. This means that the temperature in the mid-section of the rod, for fixed but arbitrary t, is well described by low order polynomials in z.

Model / Order of model		ROD1 7	ROD2 7	ROD3 7	ROD4 11	ROD2 15	ROD3 15	Theoretical eigenvalues
	λ_1	-0.005613	-0.005677	-0.005678	-0.005684	-0.005685	-0.005687	-0.005685
	λ_2	-0.021493	-0.022229	-0.022249	-0.022539	-0.022613	-0.022618	-0.022631
E	λ_3	-0.045261	-0.047569	-0.047764	-0.050207	-0.050682	-0.050727	-0.050875
I	λ_4	-0.073296	-0.078694	-0.079760	-0.088207	-0.089421	-0.089618	-0.090417
G	λ_5	-0.101332	-0.114556	-0.116207	-0.130972	-0.137863	-0.138510	-0.141257
E	λ_6	-0.125099	-0.152543	-0.157156	-0.169853	-0.194613	-0.196412	-0.203394
N	λ_7	-0.140980	-0.183380	-0.200255	-0.204496	-0.258203	-0.262380	-0.276929
V	λ_8				-0.293077	-0.327460	-0.355298	-0.361561
A	λ_9				-0.293077	-0.401325	-0.413632	-0.457591
L	λ_{10}				-0.564665	-0.478100	-0.496098	-0.564919
U	λ_{11}				-0.564684	-0.554796	-0.582031	-0.683544
E	λ_{12}					-0.627171	-0.669446	-0.813467
S	λ_{13}					-0.690333	-0.752616	-0.954688
	λ_{14}					-0.734514	-0.822432	-1.107206
	λ_{15}					-0.770761	-0.869196	-1.271022

Table 3.1 - Eigenvalues of the lumped models ROD1, ROD2, ..., ROD4 of the infinite dimensional system (2.1) for different values of n. The eigenvalues of the system (2.1), calculated from (3.58) in Chapter 2, are also given. The calculations are based on the parameter values $a = 1.159 \cdot 10^{-4}$ m^2/s and $\eta = 3.6 \cdot 10^{-5}$ $1/s$.

This is, however, not the case near the end points of the rod. The conclusion above is obtained by comparing the eigenvalues and the step responses, for example, of the model ROD4 for n = 11 and the model ROD3 for n = 15, given in Table 3.1 and Tables A.4 and A.6 respectively. In particular, it is found that the modulus of the maximal temperature errors of the step responses of the model ROD4 for n = 11 is less than 0.002 ^{o}C for all t at z = $\ell/8$, $3\ell/8$, ..., $7\ell/8$. Hence, the lumped models are very accurate even for relatively small values of n.

Since the eigenvalues and the step responses are very accurate, it has not been considered necessary to use more accurate weighted residuals models [2] and [3]. Moreover, on the basis of simulation studies in [4] and [5], it should be expected that the performance of the system (2.1) only is decreased slightly if filter and control strategies are based upon lumped models of (2.1), instead of (2.1) itself.

4. REFERENCES

[1]: Comrie, L.J.: "Chamber's shorter six-figure mathematical tables", Chambers, London, 1961.

[2]: Finlayson, B.A. and Scriven, L.E.: "The method of weighted residuals - A review", Appl. Mech. Rev., Vol. 19, 735-748, 1966.

[3]: Frazer, R.A., Jones, W.P. and Skan, S.W.: "Approximations to functions and to the solution of differential equations", Gt. Brit. Aero. Res. Council Rept. and Memo., No. 1799, 1937.

[4]: Prabhu, S.S. and McCausland, I.: "Time-optimal control of linear diffusion process using Galerkin's method", Proc. I.E.E., 1398-1404, 1970.

[5]: Prabhu, S.S. and McCausland, I.: "Optimal control of linear diffusion processes with quadratic error criteria", Automatica, Vol. 8, 299-305, 1972.

[6]: Smith, G.P.: "Numerical solutions of partial differential equations", Oxford University Press, London, 1969.

[7]: Zienkiewicz, O.C.: "The finite element method in engineering science", 2nd ed., McGraw-Hill, London, 1971.

Time	Step responses				Errors: $e_i = y_i - y_{th_i}$, i = 1, 3, ..., 7			
t	y_1	y_3	y_5	y_7	e_1	e_3	e_5	e_7
s	°C	°C	°C	°C	°C	°C	°C	°C
0	0.000000	0.000000	0.000000	0.000000	0.000000	0.000000	0.000000	0.000000
10	0.264468	0.004868	0.000030	0.000000	0.021845	0.004412	0.000030	0.000000
20	0.408270	0.024447	0.000563	0.000007	-0.000321	0.011258	0.000527	0.000007
30	0.496188	0.054371	0.002565	0.000064	-0.003565	0.011395	0.001821	0.000061
40	0.555268	0.088591	0.006718	0.000277	-0.003550	0.008984	0.003231	0.000234
50	0.597924	0.123348	0.013165	0.000784	-0.003044	0.006487	0.004189	0.000533
60	0.630410	0.156761	0.021669	0.001712	-0.002552	0.004516	0.004612	0.000890
70	0.656155	0.188040	0.031824	0.003139	-0.002151	0.003078	0.004630	0.001220
80	0.677185	0.216956	0.043196	0.005090	-0.001835	0.002054	0.004395	0.001466
90	0.694774	0.243548	0.055391	0.007544	-0.001584	0.001327	0.004023	0.001608
100	0.709761	0.267967	0.068078	0.010446	-0.001383	0.000807	0.003590	0.001652
110	0.722729	0.290406	0.080997	0.013724	-0.001221	0.000430	0.003139	0.001616
120	0.734090	0.311061	0.093946	0.017297	-0.001088	0.000152	0.002697	0.001521
130	0.744150	0.330116	0.106772	0.021088	-0.000978	-0.000057	0.002278	0.001388
140	0.753137	0.347737	0.119362	0.025025	-0.000887	-0.000217	0.001887	0.001233
150	0.761228	0.364072	0.131636	0.029046	-0.000811	-0.000343	0.001529	0.001069
160	0.768559	0.379248	0.143535	0.033095	-0.000747	-0.000445	0.001204	0.000906
170	0.775239	0.393377	0.155020	0.037130	-0.000694	-0.000530	0.000910	0.000748
180	0.781358	0.406558	0.166068	0.041114	-0.000650	-0.000602	0.000648	0.000601
190	0.786985	0.418875	0.176665	0.045021	-0.000613	-0.000664	0.000414	0.000465
200	0.792180	0.430403	0.186804	0.048828	-0.000583	-0.000719	0.000207	0.000342
210	0.796992	0.441207	0.196489	0.052520	-0.000559	-0.000767	0.000024	0.000232
220	0.801461	0.451344	0.205723	0.056086	-0.000539	-0.000810	-0.000137	0.000134
230	0.805622	0.460866	0.214517	0.059518	-0.000522	-0.000848	-0.000277	0.000049
240	0.809504	0.469818	0.222881	0.062813	-0.000509	-0.000881	-0.000398	-0.000026
250	0.813134	0.478241	0.230830	0.065968	-0.000498	-0.000911	-0.000503	-0.000091
260	0.816531	0.486171	0.238378	0.068984	-0.000489	-0.000937	-0.000593	-0.000146
270	0.819717	0.493642	0.245541	0.071861	-0.000482	-0.000958	-0.000670	-0.000194
280	0.822707	0.500685	0.252335	0.074603	-0.000476	-0.000977	-0.000735	-0.000234
290	0.825516	0.507325	0.258775	0.077212	-0.000470	-0.000991	-0.000789	-0.000268
300	0.828159	0.513589	0.264877	0.079692	-0.000465	-0.001003	-0.000834	-0.000296

Table A.1 - Unit step responses of the lumped model ROD1, for n = 7, in the points z = $\ell/8$, $3\ell/8$, ..., $7\ell/8$. The step responses y_{th_i} of the infinite dimensional system (2.1) are obtained from (3.59) in Chapter 2. The calculations are based on the parameter values a = $1.159 \cdot 10^{-4}$ m^2/s and $\eta = 3.6 \cdot 10^{-5}$ 1/s.

Time	Step responses				Errors: $e_i = y_i - y_{th_i}$, i = 1, 3, ..., 7			
t	y_1	y_3	y_5	y_7	e_1	e_3	e_5	e_7
s	°C	°C	°C	°C	°C	°C	°C	°C
0	0.000000	0.000000	0.000000	0.000000	0.000000	0.000000	0.000000	0.000000
10	0.262409	0.000235	-0.000048	0.000000	0.019786	-0.000222	-0.000048	0.000000
20	0.404990	0.017191	-0.000201	-0.000006	-0.003601	0.004001	-0.000237	-0.000005
30	0.493028	0.047342	0.000708	-0.000023	-0.006725	0.004366	-0.000035	-0.000025
40	0.552699	0.082723	0.003892	0.000025	-0.006119	0.003116	0.000405	-0.000018
50	0.595980	0.118707	0.009723	0.000303	-0.004987	0.001846	0.000748	0.000051
60	0.628990	0.153160	0.017964	0.000987	-0.003972	0.000915	0.000907	0.000165
70	0.655139	0.185265	0.028120	0.002203	-0.003168	0.000303	0.000926	0.000284
80	0.676471	0.214825	0.039665	0.004002	-0.002549	-0.000077	0.000864	0.000377
90	0.694282	0.241917	0.052132	0.006368	-0.002076	-0.000303	0.000765	0.000432
100	0.709435	0.266731	0.065143	0.009243	-0.001710	-0.000429	0.000655	0.000449
110	0.722525	0.289485	0.078405	0.012543	-0.001425	-0.000492	0.000546	0.000435
120	0.733978	0.310394	0.091695	0.016176	-0.001200	-0.000515	0.000446	0.000400
130	0.744109	0.329659	0.104850	0.020053	-0.001020	-0.000514	0.000356	0.000353
140	0.753150	0.347455	0.117751	0.024091	-0.000874	-0.000499	0.000276	0.000299
150	0.761283	0.363938	0.130312	0.028220	-0.000755	-0.000477	0.000205	0.000244
160	0.768649	0.379241	0.142475	0.032381	-0.000656	-0.000451	0.000144	0.000191
170	0.775359	0.393482	0.154201	0.036525	-0.000575	-0.000425	0.000091	0.000143
180	0.781502	0.406761	0.165465	0.040613	-0.000506	-0.000399	0.000045	0.000099
190	0.787150	0.419165	0.176257	0.044617	-0.000448	-0.000374	0.000006	0.000061
200	0.792364	0.430770	0.186570	0.048514	-0.000400	-0.000352	-0.000028	0.000027
210	0.797193	0.441642	0.196409	0.052288	-0.000358	-0.000331	-0.000056	-0.000001
220	0.801677	0.451841	0.205780	0.055927	-0.000323	-0.000312	-0.000080	-0.000024
230	0.805852	0.461418	0.214694	0.059426	-0.000293	-0.000295	-0.000099	-0.000043
240	0.809747	0.470419	0.223164	0.062780	-0.000267	-0.000280	-0.000115	-0.000059
250	0.813388	0.478885	0.231205	0.065987	-0.000244	-0.000267	-0.000129	-0.000072
260	0.816796	0.486853	0.238833	0.069049	-0.000225	-0.000255	-0.000139	-0.000082
270	0.819991	0.494357	0.246064	0.071966	-0.000208	-0.000244	-0.000147	-0.000089
280	0.822990	0.501427	0.252916	0.074742	-0.000193	-0.000234	-0.000154	-0.000095
290	0.825807	0.508091	0.259406	0.077381	-0.000180	-0.000225	-0.000158	-0.000099
300	0.828455	0.514375	0.265550	0.079887	-0.000168	-0.000217	-0.000161	-0.000101

Table A.2 - Unit step responses of the lumped model ROD2, for n = 7, in the points z = $\ell/8$, $3\ell/8$, ..., $7\ell/8$. The step responses y_{th_i} of the infinite dimensional system (2.1) are obtained from (3.59) in Chapter 2. The calculations are based on the parameter values a = $1.159 \cdot 10^{-4}$ m^2/s and η = $3.6 \cdot 10^{-5}$ 1/s.

Time	Step responses				Errors: $e_i = y_i - y_{th_i}$, i = 1, 3, ..., 7			
t	y_1	y_3	y_5	y_7	e_1	e_3	e_5	e_7
s	°C	°C	°C	°C	°C	°C	°C	°C
0	0.000000	0.000000	0.000000	0.000000	0.000000	0.000000	0.000000	0.000000
10	0.262441	0.000847	0.000064	0.000000	0.019818	0.000391	0.000064	0.000001
20	0.405062	0.017277	0.000078	0.000004	-0.003529	0.004088	0.000042	0.000004
30	0.493095	0.047231	0.000969	0.000007	-0.006659	0.004255	0.000225	0.000005
40	0.552739	0.082575	0.004046	0.000072	-0.006079	0.002967	0.000559	0.000029
50	0.595994	0.118568	0.009773	0.000354	-0.004974	0.001707	0.000798	0.000102
60	0.628984	0.153041	0.017941	0.001031	-0.003978	0.000796	0.000884	0.000209
70	0.655122	0.185164	0.028055	0.002234	-0.003185	0.000202	0.000860	0.000315
80	0.676448	0.214738	0.039578	0.004018	-0.002572	-0.000163	0.000777	0.000394
90	0.694257	0.241843	0.052037	0.006371	-0.002101	-0.000377	0.000670	0.000435
100	0.709409	0.266667	0.065048	0.009235	-0.001736	-0.000493	0.000560	0.000441
110	0.722500	0.289428	0.078314	0.012528	-0.001450	-0.000548	0.000456	0.000420
120	0.733956	0.310344	0.091610	0.016156	-0.001223	-0.000565	0.000361	0.000380
130	0.744088	0.329614	0.104772	0.020030	-0.001041	-0.000558	0.000278	0.000329
140	0.753131	0.347415	0.117680	0.024067	-0.000893	-0.000539	0.000205	0.000274
150	0.761266	0.363902	0.130249	0.028196	-0.000772	-0.000512	0.000142	0.000219
160	0.768634	0.379210	0.142418	0.032357	-0.000672	-0.000483	0.000088	0.000167
170	0.775345	0.393454	0.154151	0.036502	-0.000588	-0.000453	0.000041	0.000120
180	0.781489	0.406736	0.165421	0.040592	-0.000519	-0.000424	0.000001	0.000078
190	0.787139	0.419143	0.176218	0.044597	-0.000460	-0.000396	-0.000033	0.000041
200	0.792354	0.430750	0.186536	0.048496	-0.000410	-0.000371	-0.000062	0.000010
210	0.797184	0.441625	0.196379	0.052272	-0.000367	-0.000348	-0.000086	-0.000016
220	0.801669	0.451826	0.205754	0.055913	-0.000331	-0.000327	-0.000105	-0.000038
230	0.805845	0.461405	0.214672	0.059414	-0.000300	-0.000309	-0.000121	-0.000056
240	0.809741	0.470408	0.223145	0.062769	-0.000273	-0.000292	-0.000134	-0.000070
250	0.813382	0.478875	0.231189	0.065978	-0.000250	-0.000277	-0.000144	-0.000081
260	0.816791	0.486845	0.238819	0.069040	-0.000229	-0.000263	-0.000152	-0.000090
270	0.819987	0.494350	0.246053	0.071959	-0.000212	-0.000250	-0.000158	-0.000096
280	0.822986	0.501422	0.252907	0.074736	-0.000196	-0.000239	-0.000162	-0.000101
290	0.825804	0.508087	0.259399	0.077376	-0.000183	-0.000229	-0.000165	-0.000104
300	0.828453	0.514372	0.265545	0.079882	-0.000171	-0.000220	-0.000166	-0.000106

Table A.3 - Unit step responses of the lumped model ROD3, for n = 7, in the points $z = \ell/8, 3\ell/8, \ldots, 7\ell/8$. The step responses y_{th_i} of the infinite dimensional system (2.1) are obtained from (3.59) in Chapter 2. The calculations are based on the parameter values $a = 1.159 \cdot 10^{-4}$ m^2/s and $\eta = 3.6 \cdot 10^{-5}$ 1/s.

Time	Step responses				Errors: $e_i = y_i - y_{th_i}$, i = 1, 3, ..., 7			
t	y_1	y_3	y_5	y_7	e_1	e_3	e_5	e_7
s	°C	°C	°C	°C	°C	°C	°C	°C
0	0.000000	0.000000	0.000000	0.000000	0.000000	0.000000	0.000000	0.000000
10	0.243744	-0.000774	0.000076	0.000000	0.001121	-0.001230	0.000076	0.000000
20	0.407355	0.013537	0.000035	0.000005	-0.001236	0.000348	-0.000001	0.000005
30	0.498914	0.043874	0.000642	0.000006	-0.000839	0.000899	-0.000101	0.000004
40	0.558226	0.080335	0.003432	0.000033	-0.000592	0.000727	-0.000055	-0.000010
50	0.600496	0.117331	0.009002	0.000235	-0.000472	0.000470	0.000026	-0.000017
60	0.632564	0.152517	0.017140	0.000815	-0.000398	0.000272	0.000083	-0.000007
70	0.657965	0.185100	0.027306	0.001932	-0.000341	0.000138	0.000112	0.000013
80	0.678725	0.214953	0.038921	0.003659	-0.000295	0.000052	0.000120	0.000034
90	0.696103	0.242218	0.051484	0.005987	-0.000254	-0.000002	0.000117	0.000051
100	0.710924	0.267124	0.064597	0.008855	-0.000220	-0.000036	0.000108	0.000061
110	0.723758	0.289921	0.077955	0.012173	-0.000192	-0.000055	0.000097	0.000065
120	0.735011	0.310844	0.091334	0.015840	-0.000168	-0.000065	0.000085	0.000064
130	0.744982	0.330103	0.104567	0.019760	-0.000146	-0.000069	0.000073	0.000060
140	0.753896	0.347884	0.117536	0.023846	-0.000128	-0.000070	0.000061	0.000054
150	0.761925	0.364346	0.130157	0.028023	-0.000113	-0.000069	0.000050	0.000046
160	0.769206	0.379627	0.142371	0.032228	-0.000099	-0.000066	0.000040	0.000039
170	0.775846	0.393844	0.154141	0.036413	-0.000088	-0.000063	0.000031	0.000031
180	0.781930	0.407101	0.165443	0.040538	-0.000078	-0.000058	0.000023	0.000024
190	0.787529	0.419484	0.176266	0.044574	-0.000070	-0.000055	0.000015	0.000018
200	0.792702	0.431069	0.186607	0.048498	-0.000062	-0.000052	0.000009	0.000012
210	0.797495	0.441925	0.196467	0.052295	-0.000056	-0.000048	0.000004	0.000007
220	0.801950	0.452108	0.205858	0.055954	-0.000050	-0.000045	-0.000002	0.000003
230	0.806099	0.461670	0.214788	0.059469	-0.000046	-0.000044	-0.000005	0.000000
240	0.809972	0.470658	0.223271	0.062836	-0.000042	-0.000041	-0.000008	-0.000003
250	0.813594	0.479113	0.231322	0.066053	-0.000038	-0.000038	-0.000011	-0.000006
260	0.816986	0.487071	0.238958	0.069122	-0.000035	-0.000036	-0.000014	-0.000008
270	0.820167	0.494566	0.246195	0.072045	-0.000032	-0.000035	-0.000017	-0.000010
280	0.823153	0.501627	0.253052	0.074826	-0.000029	-0.000034	-0.000017	-0.000011
290	0.825959	0.508284	0.259545	0.077467	-0.000027	-0.000032	-0.000019	-0.000012
300	0.828598	0.514561	0.265691	0.079975	-0.000025	-0.000031	-0.000020	-0.000013

Table A.4 - Unit step responses of the lumped model ROD4, for n = 11, in the points $z = \ell/8, 3\ell/8, \ldots, 7\ell/8$. The step responses y_{th_i} of the infinite dimensional system (2.1) are obtained from (3.59) in Chapter 2. The calculations are based on the parameter values $a = 1.159 \cdot 10^{-4}$ m^2/s and $\eta = 3.6 \cdot 10^{-5}$ 1/s.

Time t s	Step responses y_1 °C	y_3 °C	y_5 °C	y_7 °C	Errors: $e_i = y_i - y_{th_i}$, i = 1, 3, ..., 7 e_1 °C	e_3 °C	e_5 °C	e_7 °C
0	0.000000	0.000000	0.000000	0.000000	0.000000	0.000000	0.000000	0.000000
10	0.242918	0.000401	-0.000000	-0.000000	0.000295	-0.000055	0.000000	0.000000
20	0.406965	0.013656	0.000024	-0.000000	-0.001626	0.000466	-0.000012	0.000000
30	0.498656	0.043375	0.000751	0.000001	-0.001097	0.000399	0.000007	-0.000001
40	0.558112	0.079819	0.003535	0.000041	-0.000706	0.000212	0.000048	-0.000002
50	0.600493	0.116943	0.009048	0.000253	-0.000474	0.000082	0.000072	0.000002
60	0.632628	0.152254	0.017134	0.000831	-0.000334	0.000009	0.000077	0.000009
70	0.658062	0.184933	0.027265	0.001936	-0.000244	-0.000029	0.000070	0.000017
80	0.678835	0.214854	0.038860	0.003647	-0.000185	-0.000047	0.000059	0.000023
90	0.696214	0.242165	0.051414	0.005962	-0.000143	-0.000055	0.000047	0.000026
100	0.711031	0.267103	0.064525	0.008821	-0.000114	-0.000057	0.000036	0.000027
110	0.723858	0.289921	0.077885	0.012133	-0.000092	-0.000055	0.000027	0.000025
120	0.735103	0.310856	0.091268	0.015799	-0.000076	-0.000053	0.000019	0.000023
130	0.745065	0.330124	0.104507	0.019720	-0.000063	-0.000049	0.000013	0.000019
140	0.753971	0.347909	0.117482	0.023808	-0.000053	-0.000045	0.000007	0.000016
150	0.761993	0.364373	0.130110	0.027989	-0.000045	-0.000042	0.000003	0.000012
160	0.769267	0.379654	0.142330	0.032199	-0.000039	-0.000038	0.000000	0.000009
170	0.775900	0.393872	0.154107	0.036388	-0.000034	-0.000035	-0.000003	0.000006
180	0.781978	0.407127	0.165415	0.040518	-0.000030	-0.000032	-0.000006	0.000004
190	0.787573	0.419509	0.176243	0.044558	-0.000026	-0.000030	-0.000007	0.000002
200	0.792741	0.431094	0.186589	0.048486	-0.000023	-0.000028	-0.000009	0.000000
210	0.797530	0.441948	0.196455	0.052287	-0.000021	-0.000026	-0.000010	-0.000001
220	0.801982	0.452130	0.205849	0.055949	-0.000018	-0.000024	-0.000011	-0.000003
230	0.806128	0.461691	0.214782	0.059466	-0.000017	-0.000022	-0.000011	-0.000003
240	0.809999	0.470678	0.223268	0.062835	-0.000015	-0.000021	-0.000012	-0.000004
250	0.813618	0.479132	0.231321	0.066054	-0.000014	-0.000020	-0.000012	-0.000005
260	0.817008	0.487089	0.238960	0.069125	-0.000013	-0.000019	-0.000012	-0.000005
270	0.820187	0.494583	0.246199	0.072050	-0.000012	-0.000018	-0.000012	-0.000005
280	0.823172	0.501645	0.253057	0.074831	-0.000011	-0.000017	-0.000012	-0.000006
290	0.825977	0.508301	0.259552	0.077474	-0.000010	-0.000016	-0.000012	-0.000006
300	0.828614	0.514577	0.265699	0.079982	-0.000009	-0.000015	-0.000012	-0.000006

Table A.5 - Unit step responses of the lumped model ROD2, for n = 15, in the points $z = \ell/8, 3\ell/8, \ldots, 7\ell/8$. The step responses y_{th_i} of the infinite dimensional system (2.1) are obtained from (3.59) in Chapter 2. The calculations are based on the parameter values $a = 1.159 \cdot 10^{-4}$ m^2/s and $\eta = 3.6 \cdot 10^{-5}$ 1/s.

Time	Step responses				Errors: $e_i = y_i - y_{th_i}$, i = 1, 3, ..., 7			
t	y_1	y_3	y_5	y_7	e_1	e_3	e_5	e_7
s	°C	°C	°C	°C	°C	°C	°C	°C
0	0.000000	0.000000	0.000000	0.000000	0.000000	0.000000	0.000000	0.000000
10	0.242920	0.000576	0.000000	0.000000	0.000297	0.000119	0.000000	0.000000
20	0.406911	0.013679	0.000044	0.000000	-0.001680	0.000489	0.000008	0.000000
30	0.498622	0.043335	0.000783	0.000003	-0.001131	0.000360	0.000039	0.000001
40	0.558093	0.079777	0.003558	0.000046	-0.000725	0.000170	0.000071	0.000003
50	0.600483	0.116910	0.009059	0.000260	-0.000485	0.000049	0.000083	0.000009
60	0.632623	0.152230	0.017135	0.000838	-0.000339	-0.000016	0.000078	0.000016
70	0.658059	0.184915	0.027260	0.001941	-0.000247	-0.000047	0.000066	0.000022
80	0.678834	0.214841	0.038853	0.003650	-0.000186	-0.000060	0.000052	0.000026
90	0.696214	0.242156	0.051405	0.005963	-0.000144	-0.000064	0.000038	0.000027
100	0.711031	0.267096	0.064515	0.008820	-0.000114	-0.000064	0.000027	0.000026
110	0.723858	0.289916	0.077876	0.012131	-0.000092	-0.000061	0.000018	0.000023
120	0.735103	0.310852	0.091259	0.015796	-0.000075	-0.000057	0.000010	0.000020
130	0.745066	0.330120	0.104499	0.019717	-0.000062	-0.000052	0.000005	0.000016
140	0.753971	0.347906	0.117475	0.023805	-0.000053	-0.000048	0.000000	0.000013
150	0.761993	0.364371	0.130103	0.027986	-0.000045	-0.000044	-0.000004	0.000009
160	0.769267	0.379653	0.142324	0.032196	-0.000038	-0.000040	-0.000006	0.000006
170	0.775900	0.393870	0.154101	0.036385	-0.000033	-0.000037	-0.000009	0.000004
180	0.781979	0.407126	0.165410	0.040515	-0.000029	-0.000034	-0.000010	0.000001
190	0.787573	0.419508	0.176239	0.044556	-0.000026	-0.000031	-0.000012	-0.000001
200	0.792741	0.431093	0.186585	0.048484	-0.000023	-0.000029	-0.000012	-0.000002
210	0.797531	0.441947	0.196452	0.052285	-0.000020	-0.000027	-0.000013	-0.000003
220	0.801982	0.452129	0.205846	0.055947	-0.000018	-0.000025	-0.000014	-0.000004
230	0.806128	0.461691	0.214779	0.059465	-0.000016	-0.000023	-0.000014	-0.000005
240	0.809999	0.470678	0.223266	0.062834	-0.000015	-0.000021	-0.000014	-0.000005
250	0.813618	0.479132	0.231320	0.066053	-0.000014	-0.000020	-0.000014	-0.000006
260	0.817008	0.487089	0.238958	0.069124	-0.000012	-0.000019	-0.000014	-0.000006
270	0.820187	0.494583	0.246198	0.072049	-0.000011	-0.000018	-0.000014	-0.000006
280	0.823172	0.501644	0.253056	0.074830	-0.000011	-0.000017	-0.000013	-0.000006
290	0.825977	0.508301	0.259551	0.077473	-0.000010	-0.000016	-0.000013	-0.000006
300	0.828614	0.514577	0.265698	0.079982	-0.000009	-0.000015	-0.000013	-0.000006

Table A.6 - Unit step responses of the lumped model ROD3, for n = 15, in the points $z = \ell/8, 3\ell/8, \ldots, 7\ell/8$. The step responses y_{th_i} of the infinite dimensional system (2.1) are obtained from (3.59) in Chapter 2. The calculations are based on the parameter values $a = 1.159 \cdot 10^{-4}$ m^2/s and $\eta = 3.6 \cdot 10^{-5}$ 1/s.

CHAPTER 4

SYSTEM IDENTIFICATION

1. INTRODUCTION

Theoretical models of the rod were derived in Chapter 2. These models were linear and infinite dimensional. The modal expansion of the transfer function for one of these models, relating the temperature at a point z to one end temperature of the rod, is given by

$$G(z,s) = \sum_{k=1}^{\infty} \frac{K_k(z)}{1+T_k s} \qquad (1.1)$$

Lumped state space models of the rod were given in Section 2 of Chapter 3.

In this chapter the dynamics of the diffusion process will be determined using system identification methods. First a straight forward parametric maximum likelihood method is used. The orders of the employed models are successively increased and order tests are performed. These tests indicate that the appropriate orders of the models are relatively low. Given the appropriate order of the model, the parameters of an extended model are identified. The results obtained from this identification are the final results.

The relatively low model orders are partly explained by the fact that the models are identified from sampled data. It has been found empirically that successive terms in the expansion (1.1), which have gain factors of the same sign, are identified as a single term

$$\frac{K}{1+sT}$$

where K is approximately equal to the sum of the gain factors of the clustered terms and T is an average value of the time constants of these terms. This also explains the relatively low order of the models.

The study shows that the first term in the expansion (1.1) is accurately estimated in all cases. It is also found that the infinite number of terms in this expansion, which have time constants T_k close to or less than the inverse Nyquist frequency, are identified as a first order term or a second order term, depending on the relative differences of the time constants T_k. If this difference is large, then the rest terms in (1.1) are identified as a first order term. Otherwise, these rest terms are identified as a second order term, with well damped complex poles.

Models are estimated from the series S1 and S3, defined in Section 4 of Chapter 2. The sampling period of these series are 10 s and 2 s respectively. The dominant time constant of the rod is 176 s. An order test indicates that the appropriate orders of the models are 4 and 5. The coefficients of the characteristic polynomials of the identified models are estimated very accurately in all cases. The standard deviations of the residuals of the different models are extremely small. These standard deviations are 0.0003 ^{o}C - 0.0008 ^{o}C whereas the corresponding output swings are 0.4 ^{o}C - 1.3 ^{o}C.

2. OUTLINE OF THE MAXIMUM LIKELIHOOD METHOD

The maximum likelihood method [1] may be used effectively to identify linear, single-output, time-invariant and discrete-time stochastic systems of the form

$$A^*(q^{-1})y(t) = B^*(q^{-1})u(t) + \lambda C^*(q^{-1})e(t) \qquad (2.1)$$

where u is the input, y is the output and {e(t)} is a sequence of independent, normal (0,1) random variables. The variable e(t) is also assumed to be independent of the input u(s) for all s and t. The shift operator is denoted q and $A^*(q^{-1})$, $B^*(q^{-1})$ and $C^*(q^{-1})$ are polynomials

$$A^*(q^{-1}) = 1 + a_1 q^{-1} + \ldots + a_n q^{-n}$$

$$B^*(q^{-1}) = b_1 q^{-1} + \ldots + b_n q^{-n}$$

$$C^*(q^{-1}) = 1 + c_1 q^{-1} + \ldots + c_n q^{-n} \qquad (2.2)$$

where n is the order of the system (2.1).

Following [1] and [4], the parameters of (2.1) are determined using the maximum likelihood method. Given a record of input-output data $\{u(t), y(t) \mid t=1,2, \ldots, N\}$ of length N, the negative logarithm of the likelihood function becomes

$$-\ln L(\alpha,\lambda) = \frac{1}{2\lambda^2} \sum_{t=1}^{N} \varepsilon^2(t) + N \ln\lambda + \frac{N}{2} \ln 2\pi \qquad (2.3)$$

where the residuals $\varepsilon(t)$ are obtained recursively from

$$C^*(q^{-1})\varepsilon(t) = A^*(q^{-1})y(t) - B^*(q^{-1})u(t) \qquad (2.4)$$

The likelihood function is considered as a function of α and λ, where α is a vector whose components are the parameters $a_1, a_2, \ldots, a_n, b_1, b_2, \ldots, b_n, c_1, c_2, \ldots, c_n$ and the n initial conditions $d_1, d_2, \ldots d_n$ of (2.4).

The maximization of $L(\alpha,\lambda)$ can be performed separately with respect to α and λ. According to [1] and [4], the maximum of $L(\alpha,\lambda)$ is obtained by finding α which minimizes

$$V(\alpha) = \frac{1}{2} \sum_{t=1}^{N} \varepsilon^2(t) \tag{2.5}$$

The maximization with respect to λ can then be done analytically to yield

$$\hat{\lambda}^2 = \frac{2}{N} \min_{\alpha} V(\alpha) \tag{2.6}$$

The estimation problem is thus equivalent to minimizing a function of several variables.

Under the restrictive assumption that the data were actually generated by a system (2.1), where $\{e(t)\}$ is a sequence of independent, equally distributed gaussian random variables, it is possible to pose and solve several statistical problems. With mild additional assumptions, it can be shown [1] that the likelihood estimates are consistent, asymptotically efficient and asymptotically normal $(\alpha_0, \lambda^2 V_{\alpha_0}^{-1} \alpha_0)$, where α_0 stands for the true parameter value. Some means to detect possible violation of the prerequisities for the maximum likelihood identification are given in [5]. With mild additional assumptions, it follows from [5] that the maximum likelihood method yields a model with correct input- and noise-transfer functions if and only if $r_{\varepsilon}(\tau) = E\{\varepsilon(t+\tau)\varepsilon(t)\} = 0$ for $\tau \geq 1$ and $r_{\varepsilon u}(\tau) = E\{\varepsilon(t+\tau)u(t)\}$ for $\tau \geq 0$.

To test if the reduction of the loss function is significant, when the order of the model (2.1) is increased from n to n+k, the following test quantity is used

$$t_{n+k,n} = \frac{V_n - V_{n+k}}{V_{n+k}} \frac{n-4(n+k)}{4k} \tag{2.7}$$

where V_n and V_{n+k} are the minimum values of the loss function for a model of order n and n+k respectively. It can be shown [2] that the random variable $4k \cdot t$, for large N, is asymptotically $\chi^2(4k)$ distributed under the null hypothesis

$$H_0 : a_{n+1} = a_{n+2} = \ldots = a_{n+k} = b_{n+1} = b_{n+2} = \ldots = b_{n+k} = c_{n+1} = c_{n+2} = \ldots = c_{n+k} = d_{n+1} = d_{n+2} = \ldots = d_{n+k} = 0 \qquad (2.8)$$

If the order of the model (2.1) is increased from n to n+1, then k=1. At a risk level of 1 %, the corresponding loss function is significantly reduced if $t_{n+1,n}$ is greater than 3.3. This means that the null hypothesis H_0 is rejected. The Fortran programs used for the identification procedure are described in [6].

3. IDENTIFICATION RESULTS FROM THE SERIES S1

In this section typical maximum likelihood identification results from the series S1 are presented. The experimental set-up, used to obtain the data of this series, and the experimental conditions are described in Section 4 of Chapter 2. The identification results from the input-output data (u_1,y_2), (u_1,y_4) and (u_1,y_6) will be presented.

In Tables A.1, A.2 and A.3 the results of identification are given for successively increasing order of the model. The small values of the estimated standard deviations of the a-parameters should be observed. As the signal to noise ratio decreases with z, it is natural that the relative errors of the b-parameters increases with z for a model with given order. The large values of the d-parameters are due to the initial nonzero temperature gradient of the rod. It should be observed that the models in Tables A.1, A.2 and A.3 contain redundant parameters at a risk level of 1 %.

Below the values of the test quantities $t_{n+1,n}$ are shown when testing the reduction of the loss function for a model of order n+1 compared to a model of order n.

$z = \ell/4$	$z = \ell/2$	$z = 3\ell/4$	
$t_{3,2} = 875$	$t_{3,2} = 2398$	$t_{3,2} = 355$	
$t_{4,3} = 758$	$t_{4,3} = 430$	$t_{4,3} = 266$	
$t_{5,4} = 4.7$	$t_{5,4} = 6.4$	$t_{5,4} = 1.4$	(3.1)

The test quantities in (3.1) indicate that the models obtained for $z = \ell/4$ and $\ell/2$ are at least of order 5. The prerequisities for the order tests are, however, not fulfilled for these models (compare Fig. 3.1 and 3.2). Therefore, the tests are not quite relevant. The 5th order models obtained for $z = \ell/4$ and $\ell/2$ have poles on the negative real axis and, hence, have no continuous correspondences. Moreover, the test quantities $t_{5,4}$ for these models are relatively low. Therefore, the orders of the models for $z = \ell/4$ and $\ell/2$ are chosen to $n = 4$. The prerequisities for the order tests are fulfilled for the model obtained for $z = 3\ell/4$ (compare Fig. 3.3) and, consequently, by (3.1), the appropriate order of this model is $n = 4$.

In order to account for possible constant levels in the outputs y_2, y_4 and y_6, the parameters of the following model were estimated

$$A^*(q^{-1})y(t) = \delta_0 + B^*(q^{-1})u(t) + \lambda C^*(q^{-1})e(t) \qquad (3.2)$$

for $n = 4$. In (3.2) the zero adjustment error of the transducer recording the temperature y is denoted by δ_0. The calculation of the residuals was also modified according to

$$\varepsilon(t) = \begin{cases} \varepsilon(t) & |\varepsilon(t)| \leq 3\hat{\lambda} \\ 3\hat{\lambda}\,\mathrm{sign}(\varepsilon(t)) & |\varepsilon(t)| > 3\hat{\lambda} \end{cases} \qquad (3.3)$$

where $\hat{\lambda}$ denotes the current estimate of the standard deviation of the residuals and sign denotes the signum function. Moreover, the parameter b_1 in the model (3.2) for $z = \ell/2$ and $z = 3\ell/4$ was put equal to zero. This parameter is redundant (2.6 σ limit) in the model (2.1) for $n = 4$, given in Tables A.2 and A.3.

In Table 3.1 the final identification results are given for the series Sl. The models in this table are denoted by $Sl_{\ell/4}$, $Sl_{\ell/2}$ and $Sl_{3\ell/4}$. Compared to the results in Tables A.1, A.2 and A.3 for n = 4, significant reductions of the loss functions occur when the model (3.2) and the limitation (3.3) are used. Notice that the moduluses of the zero adjustment errors in Table 3.1 are less than 0.02 ^{o}C. The roots of the A-, B- and C-polynomials and the static gains of the models $Sl_{\ell/4}$, $Sl_{\ell/2}$ and $Sl_{3\ell/4}$ are given in Table 3.2. From this table it is seen that the A-, B- and C-polynomials of these models have no common factors and that the static gains are estimated well.

The statistical properties of the residuals of the models $Sl_{\ell/4}$, $Sl_{\ell/2}$ and $Sl_{3\ell/4}$ were examined. The sample auto-correlation function of these residuals

$$\rho_{\varepsilon}(\tau) = \frac{c_{\varepsilon}(\tau)}{c_{\varepsilon}(0)} \tag{3.4}$$

where

$$c_{\varepsilon}(\tau) = \frac{1}{N} \sum_{t=1}^{N-\tau} (\varepsilon(t+\tau)-\bar{\varepsilon})(\varepsilon(t)-\bar{\varepsilon}) \tag{3.5}$$

are shown in Fig. 3.1. Moreover, in this figure the sample cross-correlation function of the input u_1 and the residuals

$$\rho_{\varepsilon u_1}(\tau) = \frac{c_{\varepsilon u_1}(\tau)}{\sqrt{c_{\varepsilon}(0)\, c_{u_1}(0)}} \tag{3.6}$$

where

$$c_{\varepsilon u_1}(\tau) = \frac{1}{N} \sum_{t=1}^{N-\tau} (\varepsilon(t+\tau)-\bar{\varepsilon})(u_1(t)-\bar{u}_1). \tag{3.7}$$

	$z = \ell/4$	$z = \ell/2$	$z = 3\ell/4$
a_1	-1.9634 ± 0.0010	-2.0018 ± 0.0007	-2.9564 ± 0.0017
a_2	1.2222 ± 0.0020	1.3338 ± 0.0015	3.2694 ± 0.0049
a_3	-0.2829 ± 0.0015	-0.3464 ± 0.0014	-1.6134 ± 0.0047
a_4	0.0359 ± 0.0006	0.0284 ± 0.0006	0.3025 ± 0.0015
b_1	0.0107 ± 0.0001	0.0000	0.0000
b_2	0.0524 ± 0.0001	$0.5152 \cdot 10^{-3} \pm 0.0221 \cdot 10^{-3}$	$0.1297 \cdot 10^{-3} \pm 0.0124 \cdot 10^{-3}$
b_3	-0.0473 ± 0.0001	$3.8709 \cdot 10^{-3} \pm 0.0411 \cdot 10^{-3}$	$-0.4166 \cdot 10^{-3} \pm 0.0252 \cdot 10^{-3}$
b_4	-0.0071 ± 0.0001	$2.4768 \cdot 10^{-3} \pm 0.0266 \cdot 10^{-3}$	$0.7942 \cdot 10^{-3} \pm 0.0138 \cdot 10^{-3}$
c_1	-0.5145 ± 0.0347	-1.0345 ± 0.0345	-2.4919 ± 0.0365
c_2	-0.6301 ± 0.0418	0.5208 ± 0.0517	2.3331 ± 0.0940
c_3	0.0921 ± 0.0331	-0.1885 ± 0.0509	-0.9918 ± 0.0915
c_4	0.2053 ± 0.0352	0.1410 ± 0.0317	0.1804 ± 0.0344
d_1	-0.6919	-0.4603	-0.2266
d_2	0.6768	0.4611	0.4428
d_3	-0.1217	-0.1523	-0.2960
d_4	0.0304	0.0105	0.0669
λ	$0.8286 \cdot 10^{-3}$	$0.3170 \cdot 10^{-3}$	$0.4279 \cdot 10^{-3}$
V	$0.29594 \cdot 10^{-3}$	$0.43313 \cdot 10^{-4}$	$0.78926 \cdot 10^{-4}$
δ_0	$-1.32 \cdot 10^{-2}$	$-0.60 \cdot 10^{-2}$	$-0.56 \cdot 10^{-2}$

Table 3.1 - Maximum likelihood parameter estimates from the input-output data (u_1, y_2), (u_1, y_4) and (u_1, y_6) of the series S1. All input-output variables are given in degrees centigrade.

	$z = \ell/4$	$z = \ell/2$	$z = 3\ell/4$
A	0.1408±i0.1778 0.7411 0.9406	0.1523 0.3642 0.5417 0.9435	0.6017±i0.1843 0.8097 0.9433
B	-5.6697 -0.1308 0.8912	-6.8075 -0.7062	-1.6060±i1.8827
C	-0.5116±i0.2814 0.7688±i0.1057	-0.1153±i0.4878 0.6325±i0.4014	0.3720±i0.2904 0.8740±i0.2149
K	0.7408	0.4920	0.2440

Table 3.2 - Roots of the A-, B- and C-polynomials and the static gains of the models $Sl_{\ell/4}$, $Sl_{\ell/2}$ and $Sl_{3\ell/4}$.

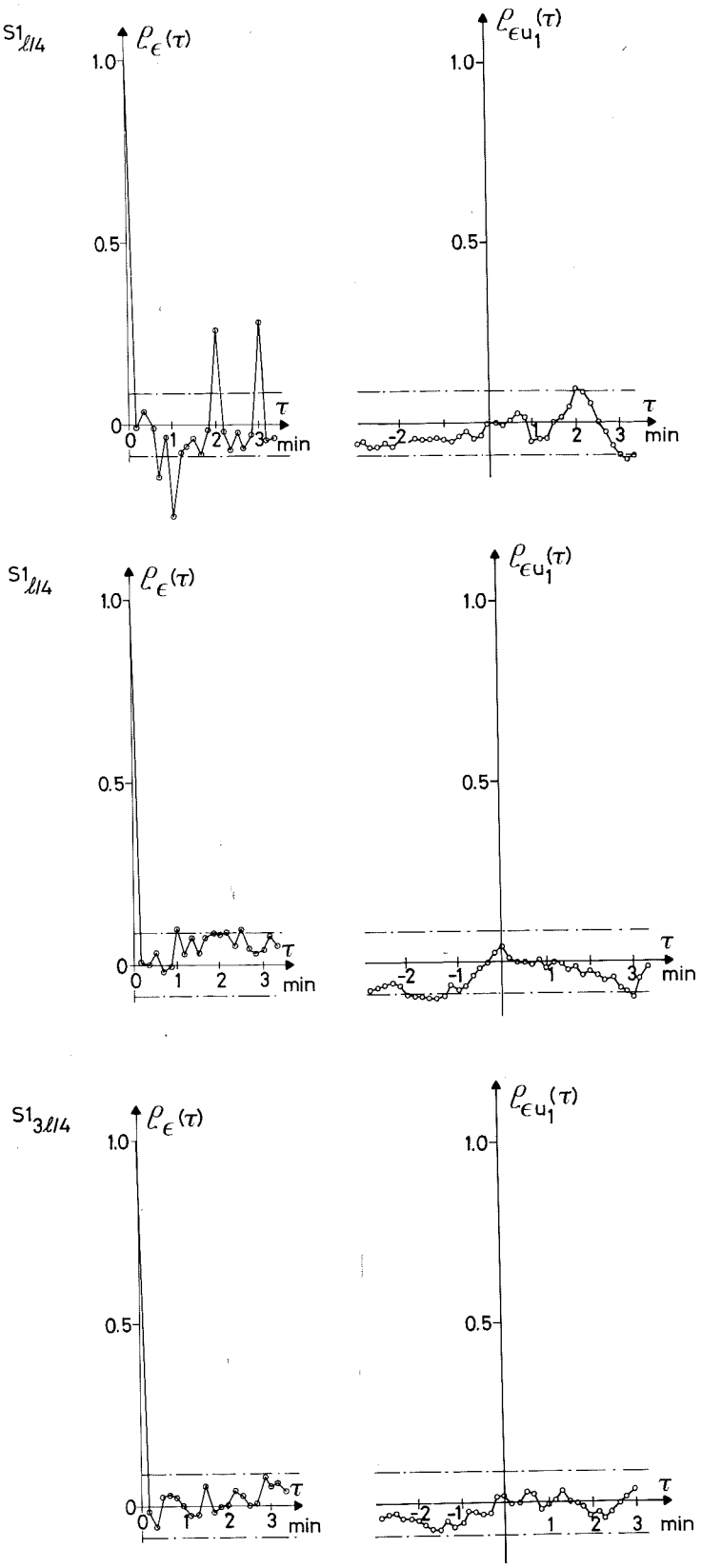

Fig. 3.1. - Sample correlation functions for the models $Sl_{\ell/4}$, $Sl_{\ell/2}$ and $Sl_{3\ell/4}$. The dashed lines give the 99% confidence intervals for $\rho_{\varepsilon}(\tau)$ for $\tau \neq 0$ and for $\rho_{\varepsilon u_1}(\tau)$ $\forall \tau$.

are shown for the considered models. In (3.5) and (3.7) the sample means of the residuals ε and the input u_1 are denoted by $\bar{\varepsilon}$ and $\bar{u}_1$ respectively.

It is seen from Fig. 3.1 that the residuals of the models $Sl_{\ell/4}$ and $Sl_{\ell/2}$ are correlated and that the residuals of the model $Sl_{3\ell/4}$ are uncorrelated at a risk level of 1 %. At the same risk level, this figure also shows that the input u_1 and the residuals of the models $Sl_{\ell/4}$ and $Sl_{\ell/2}$ are correlated and that the input u_1 and the residuals of the model $Sl_{3\ell/4}$ are uncorrelated. In particular, it is found from Fig. 3.1 that the sample auto-correlation function of the model $Sl_{\ell/4}$ contains spikes for τ = 1,2 and 3 min. The minimum pulse length of the PRBS-signal was 1 min. Therefore, it might be expected that the residuals of the model $Sl_{\ell/4}$ assume large values after that a shift has occured in the PRBS-signal. This expectation is confirmed by the plots of the input signal u_1 and the residuals in Fig. 3.2. Owing to the special properties of the identification method [1], the sample cross-correlation function of the model $Sl_{\ell/4}$ does not assume large values for small values of τ.

The residuals of the models $Sl_{\ell/4}$, $Sl_{\ell/2}$ and $Sl_{3\ell/4}$ were tested for normality using a chi-square goodness-of-fit test. The test quantities of these residuals became

$$\chi^2_{\ell/4} = 239$$

$$\chi^2_{\ell/2} = 203$$

$$\chi^2_{3\ell/4} = 55 \qquad (3.8)$$

The number of degrees of freedom was 33. Provided that the test quantity is less than 55, the hypothesis that the residuals are normally distributed is accepted at a risk level of 1 %.

In Fig. 3.2, 3.3 and 3.4 the following signals are plotted

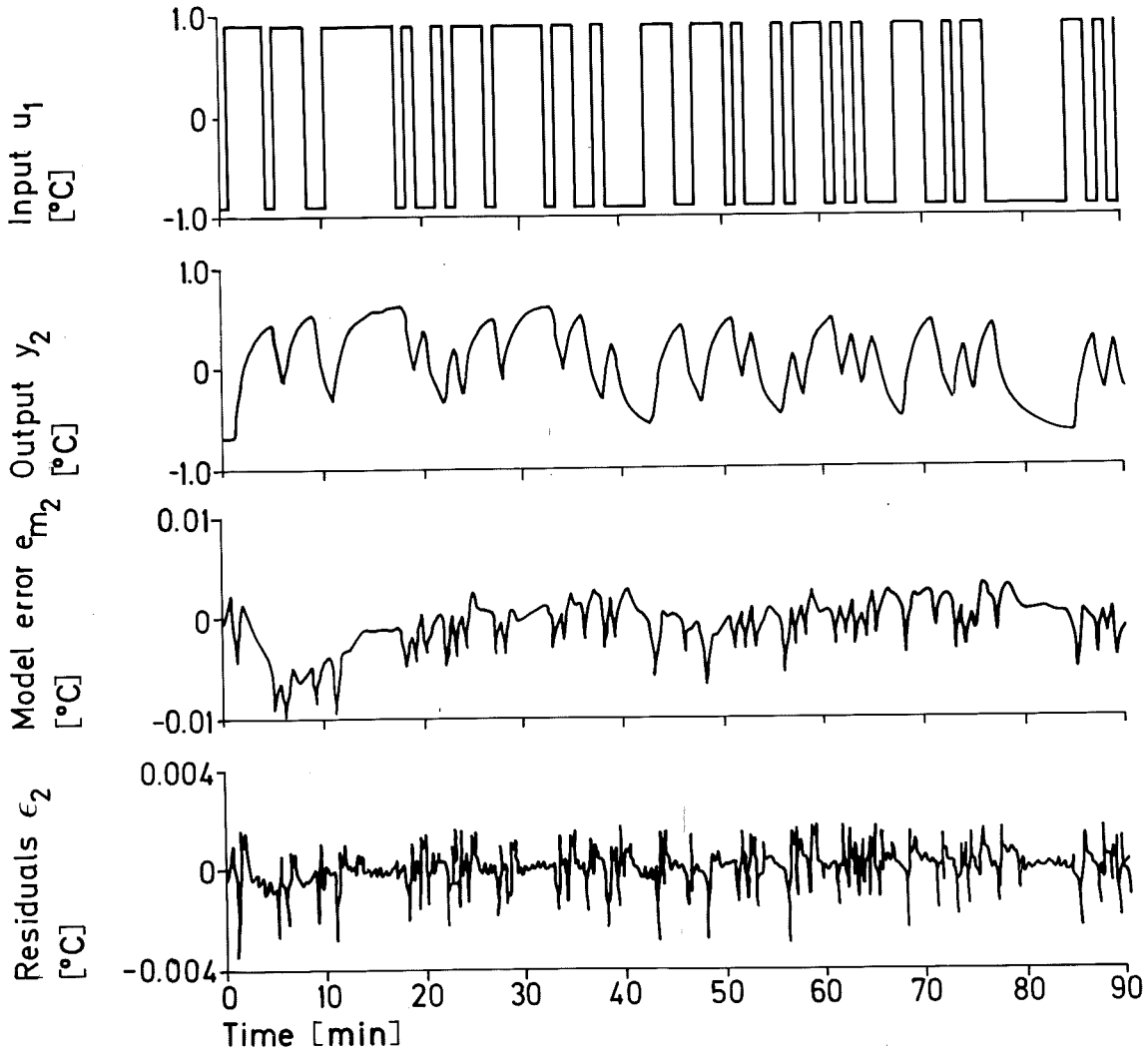

Fig. 3.2 - The model error, the residuals and the input-output variables of the model $Sl_{\ell/4}$.

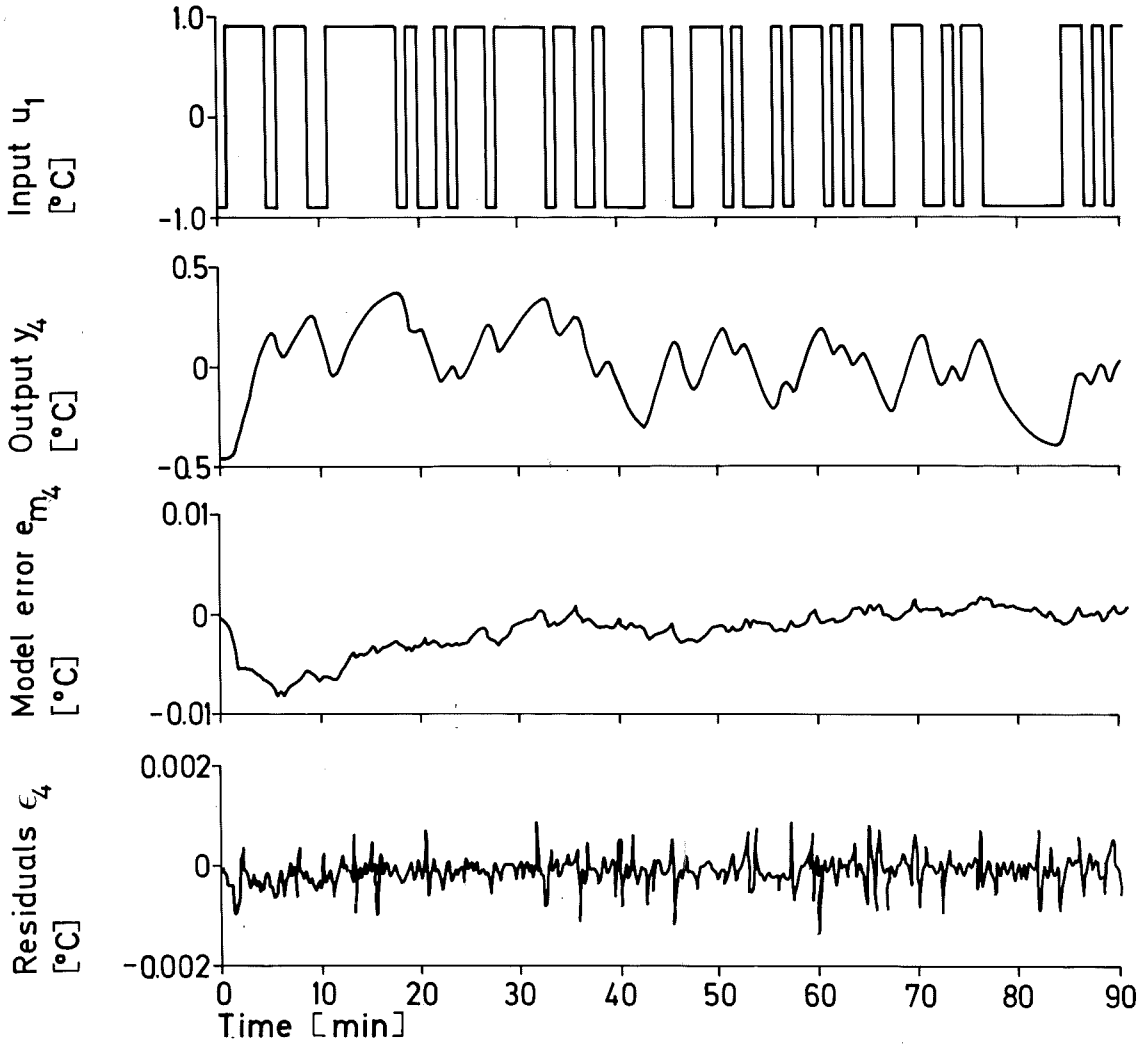

Fig. 3.3 - The model error, the residuals and the input-output variables of the model $S1_{\ell/2}$.

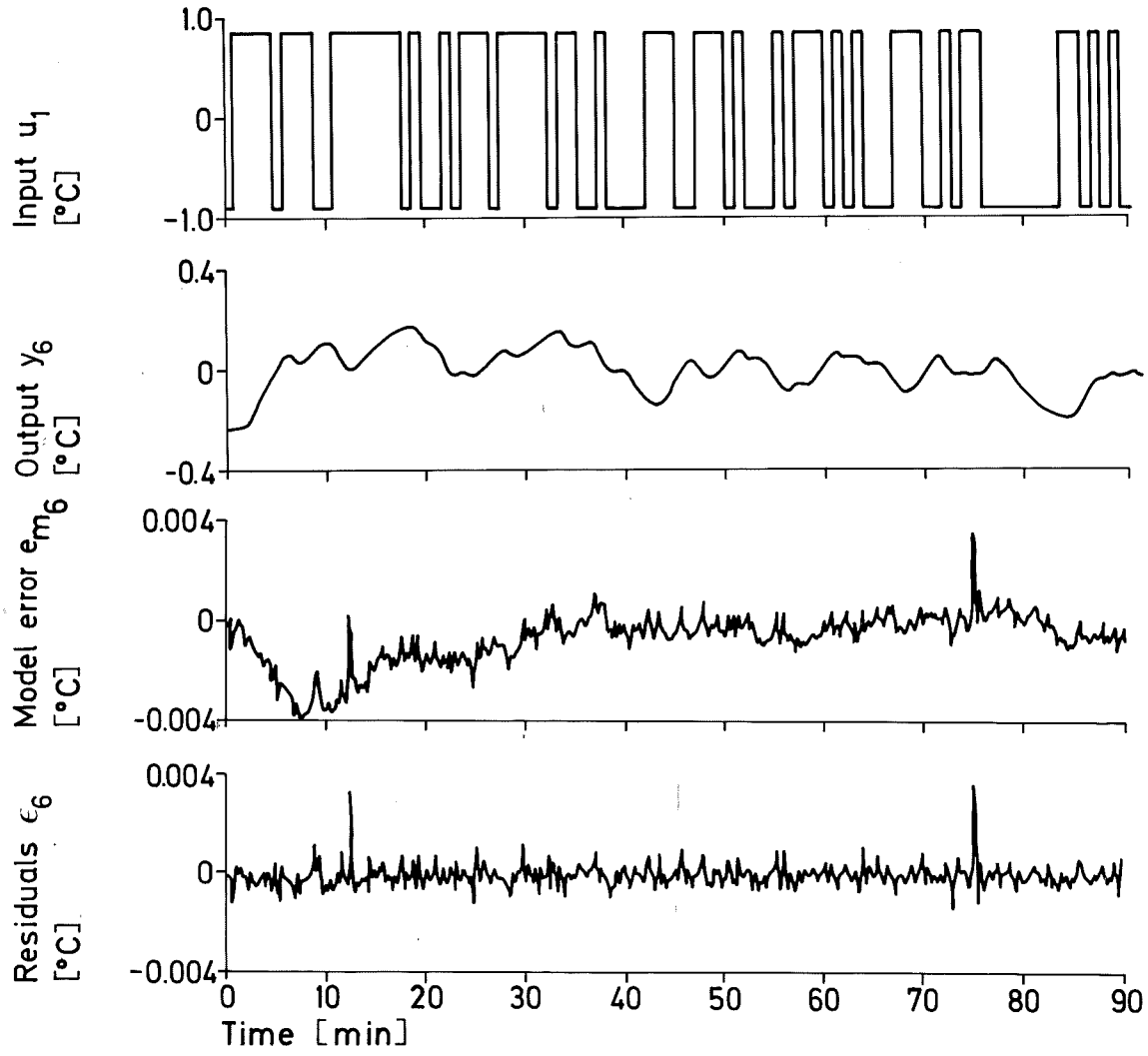

Fig. 3.4 - The model error, the residuals and the input-output variables of the model $Sl_{3\ell/4}$.

- the input signal u_1
- the output signal y
- the model error $e_m = y - \frac{B^*(q^{-1})}{A^*(q^{-1})} u_1$
- the residuals ε

for the models $Sl_{\ell/4}$, $Sl_{\ell/2}$ and $Sl_{3\ell/4}$. The model errors in all these figures contain small negative transient parts in the beginning of the experiment. These parts might be caused by the change of the thermal equilibrium state in the rod that occured since the initial temperature gradient of the rod was nonzero. The model error and the residuals of the model $Sl_{3\ell/4}$ contain two spikes. These spikes were probably due to transient in the AC-mains. Summing up, it is found that the prerequisities for the maximum likelihood identification only were fulfilled for the model $Sl_{3\ell/4}$.

4. IDENTIFICATION RESULTS FROM THE SERIES S3

In this section typical maximum likelihood identification results from the series S3 are given. The experimental set-up, employed in obtaining the data of this series, and the experimental conditions are given in Section 4 of Chapter 2. The sampling period of the series S3 is shorter than the one of the series Sl. Moreover, the number of sampling events of the series S3 is greater than the corresponding number of the series Sl. Finally, the power spectrum of the input signal of the series S3 contains more energy at higher frequencies than the corresponding power spectrum of the series Sl. Therefore, it should be possible to identify the fast dynamics of the process more accurately from the series S3 than from the series Sl. The identification results from the input-output data (u_1, y_2) will be presented.

The results of identification are shown in Table 4.1 for successively increasing order of the model. The shorter sampling period of the series S3 yields a decrease in the b-parameters, compared to the b-parameters of the corresponding models of the series Sl.

At a risk level of 1 %, the models in Table A.4 contain redundant parameters.

Below the values of the test quantities $t_{n+1,n}$ are shown, when testing the reduction of the loss function for a model of order n+1 compared to a model of order n

$$\begin{aligned} t_{4,3} &= 192 \\ t_{5,4} &= 121 \\ t_{6,5} &= 0.2 \end{aligned} \qquad (4.1)$$

The test quantities in (4.1) indicate that the appropriate order of the model is n = 5.

The parameters of the model (3.2) for n = 5 were estimated using the maximum likelihood method. Thereby, the residuals were limited according to (3.3). Moreover, the parameters b_1,b_2 and c_5 in the model (3.2) were put equal to zero. These parameters are redundant (2.6 σ limit) in the model (2.1) for n = 5, given in Table A.4.

The final results of identification are given in Table 4.1 for the series S3. The model in this table is denoted by $S3_{\ell/4}$. According to Tables 4.1 and A.4, a significant reduction of the loss function occurs when the model (3.2) and the limitation (3.3) are used. From Tables 3.1 and 4.1 it follows that the transducer recording the temperature y_4 indicates 0.0096 ^{o}C higher temperature during experiment S3 than during experiment S1. This increase in the zero adjustment error might be due to an increase in the room temperature that occured during the two experiments.

In Table 4.2 the roots of the A-, B- and C-polynomials and the static gain of the model $S3_{\ell/4}$ are given. From this table it can be seen that these polynomials have no common factors and that the static gain is estimated well.

a_1	-3.5157 ± 0.0002		
a_2	4.8648 ± 0.0004		
a_3	-3.3415 ± 0.0005		
a_4	1.1599 ± 0.0005		
a_5	-0.1673 ± 0.0002		
b_1	0.0000	d_1	-0.7192
b_2	0.0000	d_2	1.8093
b_3	$0.5337 \cdot 10^{-3} \pm 0.0144 \cdot 10^{-3}$	d_3	-1.6896
b_4	$1.4695 \cdot 10^{-3} \pm 0.0299 \cdot 10^{-3}$	d_4	0.7147
b_5	$-1.9457 \cdot 10^{-3} \pm 0.0158 \cdot 10^{-3}$	d_5	-0.1186
c_1	-2.4107 ± 0.0229	λ	$0.4532 \cdot 10^{-3}$
c_2	2.2588 ± 0.0555	V	$0.18773 \cdot 10^{-3}$
c_3	-1.0831 ± 0.0549	δ_0	$-0.36 \cdot 10^{-2}$
c_4	0.2362 ± 0.0225		
c_5	0.0000		

Table 4.1 - Maximum likelihood parameter estimates from the input-output data (u_1, y_2) of the series S3. The input-output variables are given in degrees centigrade.

A	0.4339 ± 0.2488	B	-3.7304
	0.7202		0.9772
	0.9397		
	0.9880	C	$0.3686 \pm i0.4624$
			0.6796
			0.9939
		K	0.7448

Table 4.2 - Roots of the A-, B- and C-polynomials and the static gain of the model $S3_{\ell/4}$.

The statistical properties of the residuals of the model $S3_{\ell/4}$ were examined. The sample auto-correlation function (3.4) of the residuals and the sample cross-correlation function (3.6) of the input u_1 and the residuals are shown in Fig. 4.1. From this figure it can be seen that the residuals are correlated at a risk level of

1 %. At the same risk level, this figure also shows that the input u_1 and the residuals are uncorrelated.

The residuals of the model $S3_{\ell/4}$ were tested for normality using a chi-square goodness-of-fit test. The test quantity was

$$\chi^2_{\ell/4} = 195 \qquad (4.2)$$

The number of degrees of freedom was 41. Provided that the test quantity $\chi^2_{\ell/4}$ is greater than 65, the hypothesis that the residuals are normally distributed is rejected at a risk level of 1 %. In Fig. 4.2 the model error, the residuals and the input-output variables of the model $S3_{\ell/4}$ are shown. The four spikes in the residuals were probably due to transients in the AC-mains. Summing up, it is found that the prerequisities for the maximum likelihood identification were not fulfilled for the model $S3_{3\ell/4}$.

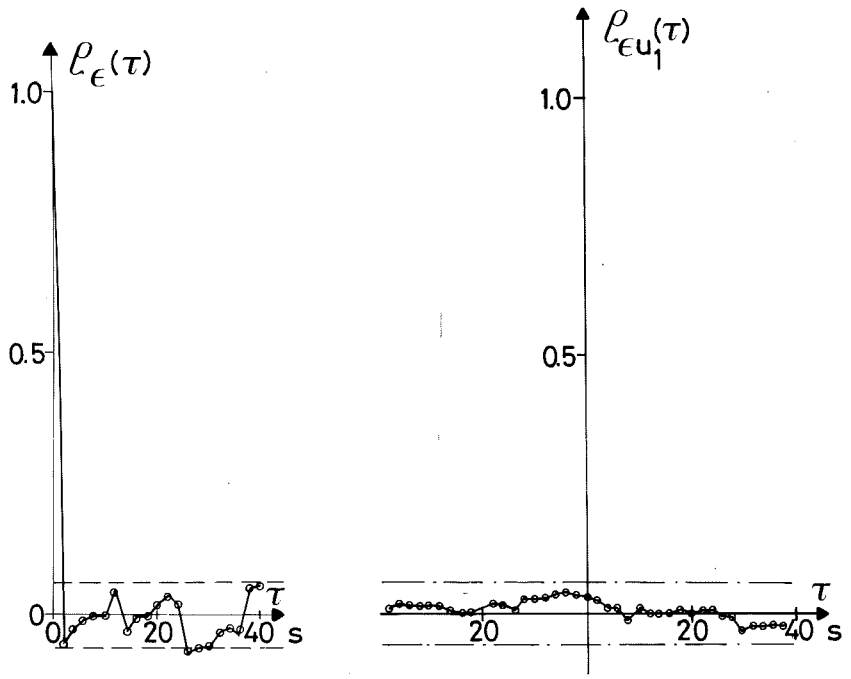

Fig. 4.1 - Sample correlation function for the model $S3_{\ell/4}$. The dashed lines give the 99 % confidence intervals for $\rho_\varepsilon(\tau)$ for $\tau \neq 0$ and for $\rho_{\varepsilon u_1}(\tau)$ $\forall\tau$.

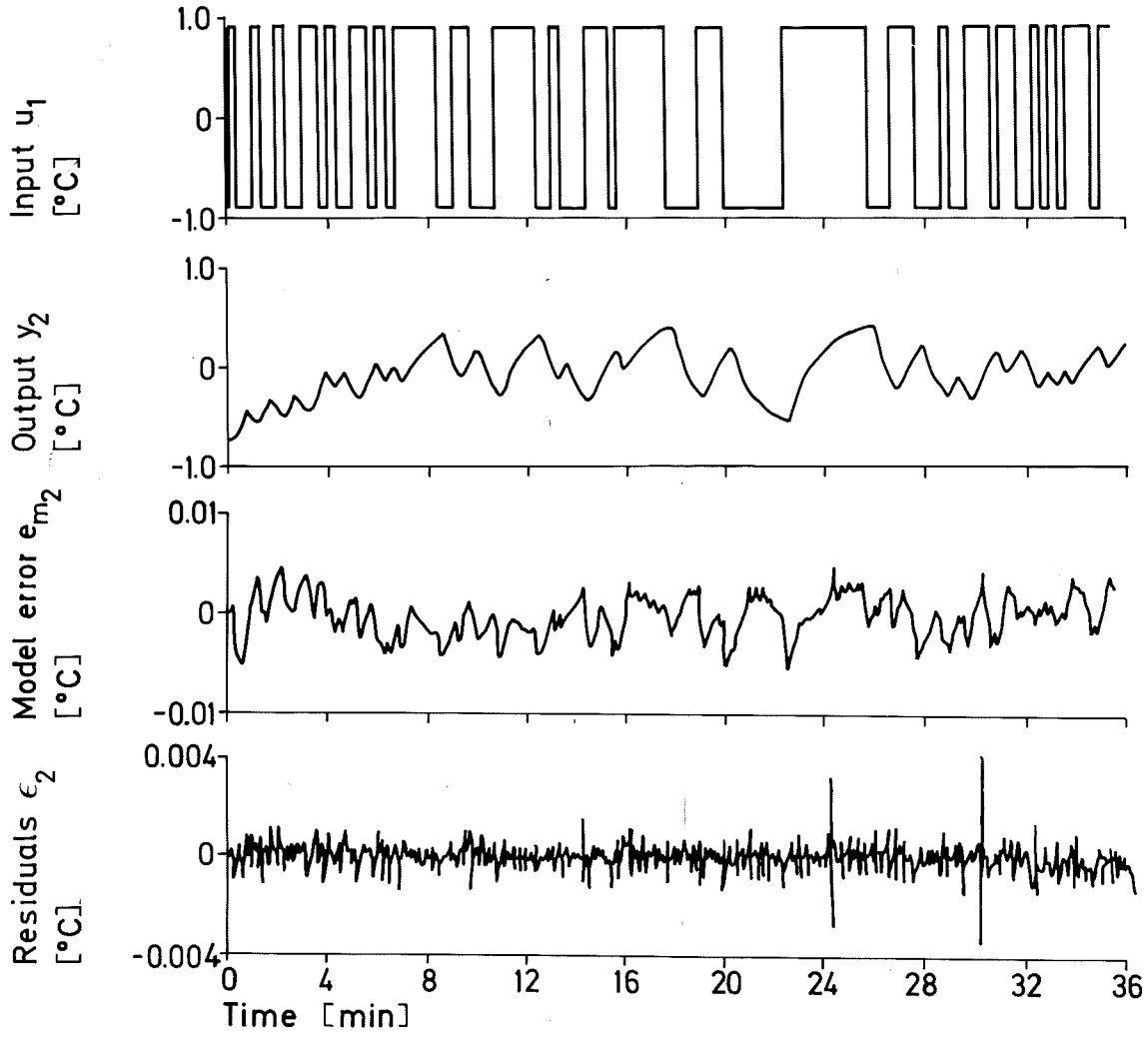

Fig. 4.2 - The model error, the residuals and the input-output variables of the model $S3_{\ell/4}$.

5. DISCUSSION ON THE IDENTIFICATION RESULTS

In this section the continuous modal expansion of the identified discrete time models are calculated. This expansion is compared with the modal expansion of the corresponding infinite dimensional model of the rod. According to (3.57) in Chapter 2, this model has the transfer function

$$G(z,s) = \sum_{k=1}^{\infty} \frac{K_k(z)}{1 + T_k s} \tag{5.1}$$

where

$$K_k(z) = \frac{2\pi(-1)^{k+1} k \sin \frac{\ell - z}{\ell} \pi k}{b + \pi^2 k^2}$$

$$T_k = T/(b + \pi^2 k^2) \tag{5.2}$$

For large values of k, the gain factors $K_k(z)$ are inversely proportional to k and thus decrease very slowly with k. Also, observe that the poles of the transfer function (5.1) are negative and real.

In Table 5.1 the time constants T_k and the gain factors $K_k(\ell/4)$, $K_k(\ell/2)$ and $K_k(3\ell/4)$ of the expansion (5.1) are given for $T_k > 2/\pi$. Notice that the gain factors $K_k(3\ell/4)$ are obtained from the gain factors $K_k(\ell/2)$ by changing sign of the 4th gain factor from the second onwards.

In [3] and [7] the problem of choosing the sampling interval T for parametric identification has been studied. The results in [7] are restricted to the least squares and the white noise discrete-time model structures for white noise inputs. For a system with poles s_k, it is found in [7] that the variances of the estimates of these poles increase rapidly as the product $T|s_k|$ exceed π. Therefore, for a stable system, it should be expected that the poles $\hat{s}_k$, possible to find by identification, should be located inside the following closed region in the complex s-plane

$$|\hat{s}_k| < \pi/T$$
$$\mathrm{Re}(s_k) < 0 \qquad (5.3)$$

where π/T is the Nyquist frequency. The inverse Nyquist frequency is $T_N = T/\pi$. It is interesting to compare (5.3) with the choice of sampling interval recommended for ordinary spectral analysis. This choice of sampling interval must be small enough so that aliasing will not be a problem.

k	Time constants T_k	Gain factors $K_k(z)$ z=ℓ/4	z=ℓ/2	z=3ℓ/4
1	175.906891	0.447307	0.632588	0.447307
2	44.186586	0.317804	-	-0.317804
3	19.655853	0.149947	-0.212056	0.149947
4	11.059841	-	-	-
5	7.079313	-0.090009	0.127292	-0.090009
6	4.916573	-0.106085	-	0.106085
7	3.612345	-0.064300	-0.090934	-0.064300
8	2.765786	-	-	-
9	2.185358	0.050014	0.070730	0.050014
10	1.770167	0.063658	-	-0.063658
11	1.462964	0.040921	-0.057871	0.040921
12	1.229306	-	-	-
13	1.047463	-0.034626	0.048969	-0.034626
14	0.903174	-0.045471	-	0.045471
15	0.786769	-0.030010	-0.042440	-0.030010
16	0.691498	-	-	-

Table 5.1 - Time constants T_k and gain factors $K_k(\ell/4)$, $K_k(\ell/2)$ and $K_k(3\ell/4)$ of the modal expansion (5.1) for $T_k > T/\pi$ T=2. Bars are used to indicate gain factors, which are zero. The employed values of the thermal diffusivity and the coefficient of surface-heat loss are a = $= 1.159 \cdot 10^{-4}$ m^2/s and $\eta = 3.6 \cdot 10^{-5}$ 1/s.

Modal expansion of the models $Sl_{\ell/4}$, $Sl_{\ell/2}$ and $Sl_{3\ell/4}$.

The sampling period of the series Sl is 10 s. Thus the inverse Nyquist frequency become $T_N = 3.18$ s. The continuous modal expansion of the model $Sl_{\ell/4}$ is

$$G_{Sl}(\ell/4,s) = \frac{0.47022}{1 + 163.40s} + \frac{0.44255}{1 + 33.373s} - \\ - \frac{0.57792s + 0.17208}{1 + 9.8491s + 33.195s^2} \qquad (5.4)$$

An inspection of Table 5.1 shows that the first term in the expansion (5.1) is estimated rather well. It is also concluded from this table that the 2nd and 3rd terms in (5.1) are identified as a single term. This single term has the time constant T = 33.373. Moreover, the sum of the gain factors of the two clustered terms is approximately equal to the gain factor of this single term. The model (5.4) also contains a second order term with complex poles. The damping factor of these poles is 0.85. This second order term approximates the infinite number of terms in (5.1) from the 5:th onwards. It should be observed that the gain factors $K_k(\ell/4)$ do not form an alternating series.

The model $Sl_{\ell/2}$ has the following continuous modal expansion

$$G_{Sl}(\ell/2,s) = \frac{0.63337}{1 + 172.00s} - \frac{0.37123}{1 + 16.314s} + \frac{0.28546}{1 + 9.9014s} - \\ - \frac{0.05561}{1 + 5.3138s} \qquad (5.5)$$

The model (5.5) has 4 real poles. From Table 5.1 it can be seen that the first term in the expansion (5.1) is estimated well and that the poles in this expansion are identified more accurately than the corresponding gain factors.

The modal expansion of the model $Sl_{3\ell/4}$ becomes

$$G_{S1}(3\ell/4,s) = \frac{0.45268}{1 + 171.18s} - \frac{0.27613}{1 + 47.380s} +$$

$$+ \frac{1.03112s + 0.06739}{1 + 30.584s + 330.18s^2} \qquad (5.6)$$

From Table 5.1, it is clear that the first two terms in (5.1) are identified rather well. Moreover, this table shows that the infinite number of terms, from the 3rd onwards, are represented by a second order term in (5.6). This term has complex poles with a damping factor of 0.84.

Modal expansion of the model $S3_{\ell/4}$

The sampling period of the series S3 is 2 s. The inverse Nyquist frequency of this series become $T_N = 0.64$ s. The model $S3_{\ell/4}$ has the following partial fraction expansion

$$G_{S3}(\ell/4,s) = \frac{0.44988}{1 + 163.81s} + \frac{0.46523}{1 + 32.251s} - \frac{0.25794}{1 + 6.0921s} +$$

$$+ \frac{0.12884s + 0.06642}{1 + 3.6896s + 5.3260s^2} \qquad (5.7)$$

A comparison with Table 5.1 shows that the first term in the expansion (5.1) is estimated rather well. This table also shows that the 2nd, 3rd and 5th, 6th, 7th term in (5.1) are represented by the 2nd and 3rd terms respectively in (5.7). Thereby, the gain factors of these lumped terms are approximately equal to the sum of the gain factors of the corresponding clustered terms. Moreover, the time constants of the lumped terms equal an average value of the time constants of the corresponding clustered terms. From Table 5.1 it is also clear that the infinite number of terms from the 9th onwards are identified as a second order term in (5.1). The damping factor of the complex poles of this term is 0.80. It should be observed that the gain factors $K_k(\ell/4)$ do not form an alternating series.

Clustering effect

The results above will now be summarized. It is found that the first term in the modal expansion (5.1) is estimated rather well in all models. Moreover, the conclusion is reached that successive terms in (5.1) from the 2nd onwards, which have gain factors of the same sign, are identified as a single term

$$\frac{K}{1+sT}$$

where K is approximately equal to the sum of the gain factors of the clustered terms and T is an average value of the time constants of these terms.

The investigation also shows that the infinite number of terms in (5.1), whose time constants are close to or less than the inverse Nyquist frequency $T_N = T/\pi$, are identified as a first order term or a second order term, depending on the relative differences of the time constants T_k. If this difference is large, then the rest terms in (5.1) are represented by a first order term in the estimated model. Otherwise, the rest terms in (5.1) are represented by a second order term. The complex poles of this second order term are well damped. These two phenomena explain the relatively low orders of the identified models. In [8] it is shown that these conclusions also are valid for maximum likelihood identification results from simulated samples of a rod.

Nonlinearities of the temperature servos

The conclusions stated here are important for the choice of experimental conditions in Chapter 5 and the interpretation of the Kalman filtering results in Chapter 7.

The identification results from the input-output data (u_1, y_2) of the series S1 show that the prerequisities for the maximum likeli-

hood identification are strongly violated. In particular, it is found that this model does not describe the dynamics of the process well, during the first sampling intervals after that a shift has occured in the input signal. The identification results from the data (u_1, y_4) of the series S1 still show that the prerequisities for the maximum likelihood identification are violated. However, it is clear from Fig. 3.1 and 3.2 that the model $S1_{\ell/2}$ describes the fast dynamics of the process essentially better than the model $S1_{\ell/4}$. It is also found that the prerequisities for the maximum likelihood identification are fulfilled for the data (u_1, y_6) of the series S1. Especially, it is seen that the dynamics of the process are well described by the model $S1_{3\ell/4}$.

The results are explained by the fact that the nonlinearities in the response to the input u_1, introduced via the servo, are not effectively filtered out by the process dynamics at $z=\ell/4$ and $\ell/2$. Since the employed model (3.2) can be used to describe a very large class of linear time-invariant stochastic processes and since the choice of n is based on order tests, it follows that there exists no linear time-invariant stochastic model which describes the process perfectly for $z=\ell/4$ and $\ell/2$. However, such a model exists for $z=3\ell/4$ and $S3_{3\ell/4}$ is one such model. This also implies that if an extremely accurate model of the rod and the servos is required, then this model must contain non-linear elements. The conclusions above also apply to the identification results for the input-output data (u_1, y_2) of the series S3.

6. REFERENCES

[1]: Åström, K.J. and Bohlin, T.: "Numerical identification of linear dynamic systems from normal operating records", Paper IFAC Symp. on Theory of Self-Adaptive Control Systems, Teddington, Engl. In Theory of Self-Adaptive Control Systems (Ed. Hammond P.H.), Plenum Press, New York, 1966.

[2]: Åström, K.J.: "Lectures on the identification problem - the least squares method", Report 6806, Lund Inst. of Techn., Div. of Automatic Control, 1968.

[3]: Åström, K.J.: "On the choice of sampling rates in parametric identification of time series". Information Sciences, 1969.

[4]: Åström, K.J. and Eykhoff, P.: "System identification - A survey", Automatica, Vol. 7, 123-162, 1971.

[5]: Bohlin, T.: "On the problem of ambiguities in maximum likelihood identification", Automatica, Vol. 7, 199-210, 1971.

[6]: Gustavsson, I.: "Parametric identification on multiple input, single output linear dynamic systems", Report 6907, Lund Inst. of Techn., Div. of Automatic Control, 1969.

[7]: Gustavsson, I.: "Choice of sampling interval for parametric identification", Report 7103, Lund Inst. of Techn., Div. of Automatic Control, 1971.

[8]: Leden, B.: "Identification of dynamics of a one dimensional heat diffusion process", Report 7121, Lund Inst. of Techn., Div. of Automatic Control, 1971.

APPENDIX 4A

	n=3	n=4	n=5
a_1	-1.9603±0.0024	-1.9437±0.0010	-1.5215±0.0012
a_2	1.2422±0.0037	1.1845±0.0019	0.2957±0.0015
a_3	-0.2620±0.0019	-0.2584±0.0015	0.3784±0.0014
a_4		0.0300±0.0007	-0.1676±0.0014
a_5			0.0315±0.0007
b_1	0.0115±0.0002	0.0107±0.0001	0.0107±0.0001
b_2	0.0507±0.0004	0.0526±0.0001	0.0570±0.0001
b_3	-0.0480±0.0003	-0.0463±0.0001	-0.0247±0.0001
b_4		-0.0079±0.0001	-0.0308±0.0001
b_5			0.0000±0.0001
c_1	-0.5109±0.0467	-0.3934±0.0346	0.0250±0.0337
c_2	-0.3272±0.0638	-0.6072±0.0407	-0.8599±0.0361
c_3	0.4647±0.0666	0.0885±0.0313	-0.1299±0.0378
c_4		0.2457±0.0353	0.3448±0.0337
c_5			0.0627±0.0286
d_1	-0.6918	-0.6918	-0.6920
d_2	0.6767	0.6633	0.3714
d_3	-0.1412	-0.1091	0.2182
d_4		0.0272	-0.0669
d_5			-0.0213
λ	$0.1867 \cdot 10^{-2}$	$0.8720 \cdot 10^{-3}$	$0.8624 \cdot 10^{-3}$
V	$0.15023 \cdot 10^{-2}$	$0.32773 \cdot 10^{-3}$	$0.32054 \cdot 10^{-3}$

Table A.1 - Models of successively increasing order, relating the temperature y_2 [°C] to the end point temperature u_1, [°C] for the series S1.

	n=3	n=4	n=5
a_1	-2.1237 ± 0.0011	-2.0342 ± 0.0007	-1.9329 ± 0.0007
a_2	1.4979 ± 0.0020	1.4028 ± 0.0016	1.1847 ± 0.0015
a_3	-0.3632 ± 0.0010	-0.3958 ± 0.0015	-0.2282 ± 0.0018
a_4		0.0406 ± 0.0006	0.0117 ± 0.0015
a_5			0.0082 ± 0.0006
b_1	$-0.1196\cdot10^{-3}\pm0.0701\ 10^{-3}$	$0.0219\cdot10^{-3}\pm0.0260\cdot10^{-3}$	$0.0237\cdot10^{-3}\pm0.0256\cdot10^{-3}$
b_2	$-0.2136\cdot10^{-3}\pm0.1351\ 10^{-3}$	$0.4645\cdot10^{-3}\pm0.0516\cdot10^{-3}$	$0.4595\cdot10^{-3}\pm0.0490\cdot10^{-3}$
b_3	$5.6447\cdot10^{-3}\pm0.0814\ 10^{-3}$	$3.9032\cdot10^{-3}\pm0.0532\cdot10^{-3}$	$3.9506\cdot10^{-3}\pm0.0561\cdot10^{-3}$
b_4		$2.3003\cdot10^{-3}\pm0.0300\cdot10^{-3}$	$2.7232\cdot10^{-3}\pm0.0499\cdot10^{-3}$
b_5			$0.1290\cdot10^{-3}\pm0.0296\cdot10^{-3}$
c_1	-1.0332 ± 0.0358	-0.8617 ± 0.0358	-0.7653 ± 0.0351
c_2	0.4407 ± 0.0697	0.5379 ± 0.0518	0.4371 ± 0.0412
c_3	0.1057 ± 0.0503	-0.1516 ± 0.0498	-0.0248 ± 0.0403
c_4		0.2445 ± 0.0312	0.0681 ± 0.0413
c_5			0.1846 ± 0.0311
d_1	-0.4605	-0.4604	-0.4603
d_2	0.5172	0.4761	0.4297
d_3	-0.1721	-0.1694	-0.1153
d_4		0.0168	-0.0065
d_5			0.0036
λ	$0.6303\cdot10^{-3}$	$0.3620\cdot10^{-3}$	$0.3565\cdot10^{-3}$
V	$0.17125\cdot10^{-3}$	$0.56465\cdot10^{-4}$	$0.54789\cdot10^{-4}$

Table A.2 - Models of successively increasing order, relating the temperature y_4 [°C] to the end point temperature u_1 [°C] for the series S1.

	n=3	n=4	n=5
a_1	-2.5868±0.0022	-2.9647±0.0018	-2.2107±0.0020
a_2	2.2439±0.0043	3.2909±0.0050	1.0425±0.0053
a_3	-0.6546±0.0021	-1.6323±0.0048	0.8836±0.0065
a_4		0.3081±0.0016	-0.9533±0.0052
a_5			0.2415±0.0018
b_1	$0.5086 \cdot 10^{-3} \pm 0.0511 \cdot 10^{-3}$	$-0.0154 \cdot 10^{-3} \pm 0.0330 \cdot 10^{-3}$	$-0.0120\ 10^{-3} \pm 0.0364 \cdot 10^{-3}$
b_2	$-1.7476 \cdot 10^{-3} \pm 0.1045 \cdot 10^{-3}$	$0.1666 \cdot 10^{-3} \pm 0.0934 \cdot 10^{-3}$	$0.1375\ 10^{-3} \pm 0.0953 \cdot 10^{-3}$
b_3	$1.8677 \cdot 10^{-3} \pm 0.0586 \cdot 10^{-3}$	$-0.4393 \cdot 10^{-3} \pm 0.0962 \cdot 10^{-3}$	$-0.2845\ 10^{-3} \pm 0.1163 \cdot 10^{-3}$
b_4		$0.7897 \cdot 10^{-3} \pm 0.0363 \cdot 10^{-3}$	$0.4457 \cdot 10^{-3} \pm 0.0985 \cdot 10^{-3}$
b_5			$0.5856 \cdot 10^{-3} \pm 0.0402 \cdot 10^{-3}$
c_1	-1.5925±0.0364	-2.3374±0.0372	-1.5773±0.0363
c_2	0.6325±0.0677	2.1375±0.0910	0.3189±0.0621
c_3	0.0668±0.0411	-0.9249±0.0882	0.8192±0.0526
c_4		0.2004±0.0341	-0.6335±0.0653
c_5			0.2056±0.0342
d_1	-0.2267	-0.2267	-0.2266
d_2	0.3602	0.4450	0.2736
d_3	-0.1498	-0.2996	0.0396
d_4		0.0686	-0.1629
d_5			0.0541
λ	$0.7689 \cdot 10^{-3}$	$0.5119 \cdot 10^{-3}$	$0.5101 \cdot 10^{-3}$
V	$0.25483 \cdot 10^{-3}$	$0.11292 \cdot 10^{-3}$	$0.11216 \cdot 10^{-3}$

Table A.3 - Models of successively increasing order, relating the temperature y_6 [°C] to the end point temperature u_1 [°C] for the series S1.

	n=4	n=5 †	n=6
a_1	-2.5101±0.0008	-3.5155±0.0023	-2.5177±0.0009
a_2	2.2999±0.0019	4.8639±0.0083	1.3577±0.0023
a_3	-0.9219±0.0018	-3.3402±0.0119	1.5070±0.0016
a_4	0.1362±0.0008	1.1590±0.0078	-2.1651±0.0017
a_5		-0.1671±0.0020	0.9836±0.0022
a_6			-0.1653±0.0008
b_1	$-0.0404 \cdot 10^{-3} \pm 0.0399 \cdot 10^{-3}$	$0.0420 \cdot 10^{-3} \pm 0.0322 \cdot 10^{-3}$	$0.0529 \cdot 10^{-3} \pm 0.0322 \cdot 10^{-3}$
b_2	$0.0132 \cdot 10^{-3} \pm 0.0835 \cdot 10^{-3}$	$-0.1142 \cdot 10^{-3} \pm 0.1084 \cdot 10^{-3}$	$-0.1109 \cdot 10^{-3} \pm 0.0804 \cdot 10^{-3}$
b_3	$0.5438 \cdot 10^{-3} \pm 0.0843 \cdot 10^{-3}$	$0.6463 \cdot 10^{-3} \pm 0.1543 \cdot 10^{-3}$	$0.5935 \cdot 10^{-3} \pm 0.0784 \cdot 10^{-3}$
b_4	$2.0224 \cdot 10^{-3} \pm 0.0416 \cdot 10^{-3}$	$1.4163 \cdot 10^{-3} \pm 0.1131 \cdot 10^{-3}$	$2.0017 \cdot 10^{-3} \pm 0.0770 \cdot 10^{-3}$
b_5		$-1.9316 \cdot 10^{-3} \pm 0.0360 \cdot 10^{-3}$	$-0.4797 \cdot 10^{-3} \pm 0.0830 \cdot 10^{-3}$
b_6			$-1.9405 \cdot 10^{-3} \pm 0.0363 \cdot 10^{-3}$
c_1	-0.9927±0.0245	-2.3828±0.0235	-1.3843±0.0234
c_2	0.7059±0.0378	2.2453±0.0605	-0.1316±0.0400
c_3	-0.1246±0.0369	-1.0767±0.0780	1.1566±0.0372
c_4	0.1976±0.0221	0.2403±0.0645	-0.8210±0.0360
c_5		-0.0027±0.0252	0.2255±0.0433
c_6			0.0016±0.0257
d_1	-0.7192	-0.7192	-0.7192
d_2	1.0861	1.8092	1.0916
d_3	-0.5680	-1.6893	0.1148
d_4	0.0959	0.7142	-0.9681
d_5		-0.1185	0.5911
d_6			-0.1173
λ	$0.6566 \cdot 10^{-3}$	$0.5236 \cdot 10^{-3}$	$0.5233 \cdot 10^{-3}$
V	$0.39410 \cdot 10^{-3}$	$0.25056 \cdot 10^{-3}$	$0.25029 \cdot 10^{-3}$

Table A.4 - Models for successively increasing order, relating the temperature y_2 [°C] to the end point temperature u_1 [°C] for the series S3.

† This model has an indefinite matrix of second order partial derivatives $V_{\alpha\alpha}$.

CHAPTER 5

ESTIMATION OF THERMAL DIFFUSIVITY

1. INTRODUCTION

Several mathematical and experimental methods for determining the thermal diffusivity of solid materials have been developed during the past hundred years. A review of the mathematical development may be found in e.g. Jakob [8] and Carslaw and Jaeger [5]. Recent accounts for the experimental development have been given by Danielson and Sidles [6] and Touloukain et al. [13].

The methods fall into two main classes, periodic heat-flow methods and transient heat-flow methods. In the periodic heat-flow methods, the thermal energy supplied to the sample varies periodically with a fix period. Consequently, the temperatures at all points in the sample vary with the same period and the thermal diffusivity is determined from measurements of the amplitude and phase relationships. A steady-state condition prevails in the sense that the temperatures are periodic.

In the transient heat-flow methods, the sample is initially in a steady-state condition. Energy is then added or removed from the sample which induces a transient temperature change. The thermal diffusivity is determined from measurements of the temperature as a function of time at one or more points on the sample. In this class of experimental methods, it is often crucial to measure the temperature a short time after that the perturbation is introduced whereas in the other methods temperature measurements may be performed at any time.

Following [13], the two main classes can be further classified,

according to the originator or the nature of the technique used, in the following subclasses:

A. Periodic heat-flow methods:
Ångström's method, Temperature wave velocity method, Temperature wave amplitude-decrement method, Modified Ångström's methods, Phase-lag methods, Thermoelectric methods, Radial-wave method and Cryogenic method.

B. Transient heat-flow methods:
Long bar methods, Moving heat-source method, Small-area-contact method, Thermoelectric effect method, Semi-infinite plate method, Radial heat-flow methods, High-intensity arc method, Flash methods, Electrically-heated rod methods.

In this chapter two different methods are compared for determining the thermal diffusivity of the rod. The first method is a modified Ångström's method which makes use of a long bar. In 1861 the Swedish physicist Ångström [2] published his method for determining the thermal diffusivity of metals. This method and its modifications are highly accurate methods for determining the diffusivity. The modified Ångström's methods, proposed by Sidles and Danielson [12] and Abeles et al. [1], make use of a sinusoidal input signal and Lissajou's figure techniques to determine the thermal diffusivity.

There are several interesting features in Ångström's original method whose importance have not been clearly understood by the rediscoverers of the method. The most prominent feature to be mentioned is the least squares technique used by Ångström to filter out the first harmonics in the periodic temperature variation. In the author's experimental approach, the rod is excited by a sinusoidal signal and a digital filter is used to filter out the fundamental harmonics of the temperatures in two properly chosen points, using the correlation method [4].

The second method is a long bar method. This method resembles in some respect the method proposed by Kennedy et al. [9] in 1962. Kennedy et al. made use of a guarded sample, attached in

one end to an electrical resistance heater. Three thermocouples were mounted at equally spaced intervals along the rod. After the heater was turned on, the temperature changes occuring at each thermocouple were recorded. The temperature at the two outer thermocouples determined the boundary conditions for the heat equation. The thermal diffusivity was determined such that the following model error was minimized

$$V = \frac{1}{N} \sum_{t=1}^{N} \left(y(t) - \hat{y}(t) \right)^2 \qquad (1.1)$$

where y was the measured mid-point temperature, $\hat{y}$ was the calculated mid-point temperature and N was the number of data points.

It is here proposed to use the principle of maximum likelihood to estimate several parameters of the heat process. These parameters are the thermal diffusivity, the coefficient of surface-heat loss, the slope and the zero adjustment errors of the mid-point transducer. By including a heat loss term in the heat equation, it is possible to account for radial heat loss from the rod. Moreover, the influence of the calibration errors of the transducers are eliminated by estimating the slope and zero adjustment errors of the mid-point transducer. The rod is excited by a PRBS-signal which is known to be a more effective input signal for system identification purposes than the step signal used by Kennedy. By employing this method, it is also possible to assign accuracies to the parameter estimates.

The experimental set-up employed differs from that of Kennedy in two respects, the heating is done with Peltier elements and thermistor sensors are used. By this arrangement, it is possible to control the end temperatures of the rod more accurately and to measure the temperature profile of the rod with better precision.

2. MODIFIED ÅNGSTRÖM'S METHOD

Outline of the method

In a modified Ångström's method [1] and [12] one end of the rod is subjected to sinusoidal temperature variations. This causes a heat-wave to progress down the rod. The period of the temperature variations is chosen small enough for the free end temperature of the rod to be unchanged. After the cyclic temperature variations have been continued for a sufficiently long time for the heat-wave to become stationary, the thermal diffusivity is determined by analysing the attenuation and phase shift of the heat-wave. The conduction of heat in the rod is assumed to be described by

$$a \frac{\partial^2 \theta}{\partial z^2} = \frac{\partial \theta}{\partial t} + \eta\theta \tag{2.1}$$

It follows from [4] that the transfer function for a semi-infinite rod (2.1), relating the temperature at a point z_0+d to the temperature at a point z_0 on the rod, is given by

$$G(s) = \exp\left(- d\sqrt{(s+\eta)/a}\right) \tag{2.2}$$

Straightforward calculations show that

$$\begin{aligned} \ln|G(i\omega)| &= - d\sqrt{\left(\sqrt{\omega^2+\eta^2}+\eta\right)/(2a)} \\ \arg G(i\omega) &= - d\sqrt{\left(\sqrt{\omega^2+\eta^2}-\eta\right)/(2a)} \end{aligned} \tag{2.3}$$

Though obtained in a neater fashion, multiplication now gives the result discovered by Ångström [2] more than a century ago

$$\ln|G(i\omega)| \cdot \arg G(i\omega) = \frac{d^2\omega}{2a} \tag{2.4}$$

By measuring the value of the transfer function G(s) at one particular frequency ω, the thermal diffusivity can thus easily be

determined from the Ångström's formula (2.4). Rewriting (2.4), it follows that

$$a = \frac{\pi d^2}{T_p \ln|G(i\omega)| \cdot \arg G(i\omega)} \qquad (2.5)$$

where the period T_p of the sinusoidal input signal has been introduced.

Experimental approach

When measuring the thermal diffusivity, using the modified Ångström's method, the transfer function G was determined for one value of ω by frequency analysis, employing the correlation method [4]. The diffusivity was then obtained from (2.5). The experimental arrangement is shown in Fig. 2.1. The synchronized sine and cosine signals of the signal generator are generated in software by a process computer. The sine signal is converted to analogue form and this signal serves as input signal to the process. The signals y_1 and y_2 are converted to digital form, and the multiplication and the integration are performed in software by the computer.

If the influence of the disturbances is neglected, the signals y_1 and y_2 are given by

$$y_k = y_{0_k} \sin(\omega t+\varphi_k), \qquad k = 1, 2 \qquad (2.6)$$

The outputs of the integrators are functions of the integration time T. These functions are only considered at discrete times, where ωT is an integer multiple of π. Short calculations give that

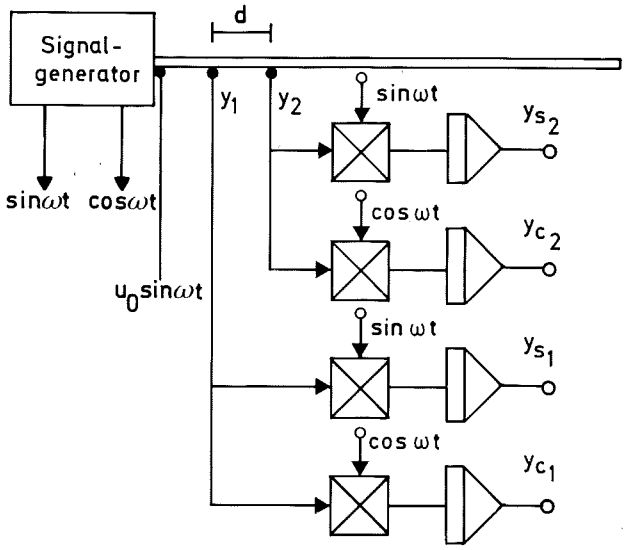

Fig. 2.1 - Block diagram of an experimental arrangement for determining the thermal diffusivity.

$$y_{s_k} = \int_0^T y_k(t) \sin \omega t \, dt = \frac{1}{2} T \, y_{0_k} \cos \varphi_k$$

$$y_{c_k} = \int_0^T y_k(t) \cos \omega t \, dt = \frac{1}{2} T \, y_{0_k} \sin \varphi_k, \qquad k = 1, 2 \tag{2.7}$$

and

$$y_{0_k} = \frac{2}{T} \sqrt{y_{s_k}^2 + y_{c_k}^2}$$

$$\varphi_k = \operatorname{arctg}(y_{c_k}/y_{s_k}), \qquad k = 1, 2 \tag{2.8}$$

It follows from (2.8) that

$$|G(i\omega)| = \sqrt{(y_{s_2}^2 + y_{c_2}^2)/(y_{s_1}^2 + y_{c_1}^2)}$$

$$\arg G(i\omega) = \operatorname{arctg}\left[(y_{c_2}/y_{s_2} - y_{c_1}/y_{s_1})/(1 + y_{c_2}/y_{s_2} \cdot y_{c_1}/y_{s_1}) \right] \tag{2.9}$$

According to [4], the correlation method effectively eliminates disturbances and, if ωT is an integer multiple of 2π, constant measurement errors. It can also be shown that continuous simple nonlinearities [7] in the A/D-converters of the computer interface do not affect the measurement of the phase shift arg $G(i\omega)$, provided that ωT is an integer multiple of 2π. The influence of continuous simple nonlinearities on the amplitude ratio $|G(i\omega)|$ can be eliminated either by repeating the experiment with the A/D-channels interchanged or by correcting the value of $|G(i\omega)|$ with the result obtained for the transfer function $G(s) = 1$.

Results

The rod was excited by a sinusoidal input signal of amplitude $2.3^{\circ}C$ and period 60 s, and the system was allowed to reach equilibrium. The amplitude of the free end temperature variations may be estimated from (2.3), using the specification (3.13) in Chapter 2. Provided that $\eta << \omega$, an estimate of this amplitude becomes $0.0002^{\circ}C$. This implies that the rod was effectively semi-infinite. The integration was carried out during 5-10 periods. The influence of simple nonlinearities in the A/D-converters was eliminated by correcting the value of $|G(i\omega)|$ with the result obtained for the transfer function $G(s) = 1$.

The thermal diffusivity was determined from the signals y_1 and y_2. The amplitude ratio $|G(i\omega)|$ and the phase shift arg $G(i\omega)$ and their standard deviations obtained from 8 different experiments were

$$|G(i\omega)| = 0.3032 \pm 0.0001$$

$$\arg G(i\omega) = -1.1939 \pm 0.0004 \text{ rad} \qquad (2.10)$$

The reproducability was thus very good. However, the measurements were not free from systematic errors.

Since the influence of simple nonlinearities in the A/D-converters was eliminated, it follows from (2.5) and (2.9) that the

systematic errors were due to errors in the sensor position, errors in the period T_p and errors in the calibration of the transducers. According to (2.5) and (2.9) the maximal systematic error in the diffusivity becomes

$$\left|\frac{\Delta a}{a}\right|_{max} = 2\left|\frac{\Delta d}{d}\right|_{max} + \left|\frac{\Delta T_p}{T_p}\right|_{max} + \left|\frac{1}{\ln|G(i\omega)|}\right|\left(|\delta_{s_1}|_{max} + |\delta_{s_2}|_{max}\right) \tag{2.11}$$

where δ_{s_1} and δ_{s_2} are the slope errors of the transducers recording the signals y_1 and y_2 respectively. From (2.1) in Chapter 2, it follows that the sensor separation and its maximal error were $d = 0.05625$ m and 0.3 % respectively. Moreover, by (2.5) in Chapter 2, the maximal errors in δ_{s_1} and δ_{s_2} were both 0.2%. Neglecting the error in the period T_p, it then follows from (2.5), (2.10) and (2.11) that the thermal diffusivity and its maximal error become

$$a = 1.163 \pm 0.009 \tag{2.12}$$

It should be observed the random errors were small compared to the systematic errors. Also observe that the errors in the phase shift arg $G(i\omega)$ were negligible. Finally, notice that the errors in the sensor position (0.6%) dominated over the calibration errors of the transducers (0.3%). These calibration errors could therefore not be eliminated by simply repeating the experiments with the thermistor sensors interchanged.

A process computer PDP-15/35, with floating point arithmetic in hardware, was used in the experiments. The sampling rate was 20 ms and the time delay between the readings of two arbitrary analogue input channels, during the same sampling period, was 20 μs. The resolutions of the A/D- and D/A-converters corresponded to $0.002^{\circ}C$ and $0.02^{\circ}C$ respectively. A storage capacity of 1.8 K words was required for the program, including the system subroutines but excluding the executive and the programs for data acquisition.

3. MAXIMUM LIKELIHOOD METHOD

Method of identification

Consider a linear, single-output, time-invariant and discrete-time system

$$x(t+1) = \Phi x(t) + \Gamma u(t)$$

$$y(t) = Cx(t) + \delta_0 + e(t) \qquad (3.1)$$

where x is an n-vector, the input u is m-vector, the output y is a scalar, $\{e(t)\}$ is a sequence of independent normal $(0,\lambda^2)$ random variables and δ_0 is a constant level in the output. The variable e(t) is also assumed to be independent of the input u(s) for all s and t.

Following Section 2 of Chapter 4, the parameters of (3.1) are determined using the maximum likelihood method. Given a record of input-output data $\{u(t), y(t) \mid t = 1, 2, \ldots, N\}$ of length N, the negative logarithm of the likelihood function for the system (3.1) becomes

$$-\ln L(\alpha,\lambda) = \frac{1}{2\lambda^2} \sum_{t=1}^{N} \varepsilon^2(t) + N \ln \lambda + \frac{N}{2} \ln 2\pi \qquad (3.2)$$

where the residuals $\varepsilon(t)$ are obtained recursively from

$$\varepsilon(t) = y(t) - Cx(t) - \delta_0$$

$$x(t+1) = \Phi x(t) + \Gamma u(t)$$

$$x(0) = x_0 \qquad (3.3)$$

The likelihood function is considered as a function of α and λ where α is a vector whose components are the unknown elements of the matrices Φ, Γ, C, δ_0 and the n initial conditions x_0.

From Section 2 of Chapter 4, it follows that the maximum of the likelihood function is obtained by finding α which minimizes

$$V(\alpha) = \frac{1}{2} \sum_{t=1}^{N} \varepsilon^2(t) \tag{3.4}$$

An estimate of λ is then given by

$$\hat{\lambda}^2 = \frac{2}{N} \min_{\alpha} V(\alpha) \tag{3.5}$$

A number of properties of the maximum likelihood estimates and some means to detect possible violation of the prerequisities for the maximum likelihood identification are given in Section 2 of Chapter 4. The maximum likelihood identification for a general multiple-output system (3.1) are discussed in [3], [10] and [14].

The estimates were computed by minimizing the loss function V numerically. The accuracy of the vector $\hat{\alpha}$ was estimated from the matrix $\hat{\lambda}^2 V^{-1}_{\hat{\alpha}\hat{\alpha}}$ according to Section 2 of Chapter 4. The matrix $V_{\hat{\alpha}\hat{\alpha}}$ was computed by means of difference approximations.

State-space model of the rod

The lumped model ROD2 of the rod is used for maximum likelihood identification. This state-space model is given by

$$\dot{x} = Ax + Bv \tag{3.6}$$

where the matrices A and B are defined by (2.10) in Section 2 of Chapter 3. The state vector x approximates the temperature in n-1 equidistant nodal points along the rod whereas the components the input vector v are the boundary temperatures of the rod.

The discrete model corresponding to (3.6) becomes

$$\tilde{x}(t+1) = \Phi\tilde{x}(t) + \Gamma\tilde{v}(t) \tag{3.7}$$

where

$$\Phi = e^{A}$$

$$\Gamma = \int_0^1 e^{As}ds\ B \tag{3.8}$$

The sampling period T is for convenience chosen as the time unit. At the sampling instants the responses of the models (3.6) and (3.7) are the same to a piecewise constant input vector.

The input vector is not piecewise constant in the particular case. By approximating the input signals with polynomials in t, of order k, and by enlarging the state space vector with 2k components, it is possible to set up an enlarged continuous state-space model of the rod with a piecewise constant input vector. Thereby, the new components of the state vector consist of the approximated input signals and their k-1 first derivatives. Moreover, the new input vector consists of the k:th derivatives of the approximated input signals. In the time interval $j \leq t < j+1$ Lagrange polynomials of order 3 defined by

$$P_i(j-1) = v_i(j-1)$$

$$P_i(j) = v_i(j)$$

$$P_i(j+1) = v_i(j+1)$$

$$P_i(j+2) = v_i(j+2), \qquad i = 1, 2 \tag{3.9}$$

are employed to perform the approximation.

The enlarged state-space model becomes

$$\dot{\hat{x}} = \left[\begin{array}{ccc|c|ccc} 0 & 0 & 0 & & & & \\ 1 & 0 & 0 & 0 & & 0 & \\ 0 & 1 & 0 & & & & \\ \hline 0 & 0 & a_2 & & 0 & 0 & 0 \\ 0 & 0 & -b_3 & & 0 & 0 & 0 \\ 0 & 0 & 0 & & 0 & 0 & 0 \\ \vdots & \vdots & \vdots & A & \vdots & \vdots & \vdots \\ 0 & 0 & 0 & & 0 & 0 & 0 \\ 0 & 0 & 0 & & -b_3 & 0 & 0 \\ 0 & 0 & 0 & & a_2 & 0 & 0 \\ \hline & & & & 0 & 1 & 0 \\ & 0 & & & 0 & 0 & 1 \\ & & & & 0 & 0 & 0 \end{array}\right] \hat{x} + \left[\begin{array}{cc} 1 & 0 \\ 0 & 0 \\ 0 & 0 \\ 0 & 0 \\ 0 & 0 \\ 0 & 0 \\ \vdots & \vdots \\ 0 & 0 \\ 0 & 0 \\ 0 & 0 \\ 0 & 0 \\ 0 & 0 \\ 0 & 1 \end{array}\right] \hat{v} = \hat{A}\hat{x} + \hat{B}\hat{v} \qquad (3.10)$$

where the matrix A and the parameters a_2 and b_3 are defined by (3.6) and (2.11) in Chapter 3 respectively. The null matrix is denoted by 0 .

Given a record of input-output data $\{v(t), y(t) \mid t = 1, 2, \ldots, N\}$, the parameter vector α and the parameter λ are estimated from the model (3.1). Thereby, the matrices Φ and Γ of (3.1) are obtained from (3.8) with $A = \hat{A}$ and $B = \hat{B}$. Moreover, the input vector $u = \hat{v}$ of (3.1) is calculated from the given input vector v in accordance with (3.9). Finally, the components x_1, x_2, x_3, x_{n-2}, x_{n-1} and x_n of the state-vector x of (3.1) are updated conformably with (3.9) at each sampling instant. The order of the model used for identification was n = 21.

Results

The objective of the identification was to determine the diffusivity a and the coefficient of surface-heat loss η of the model (2.1). In order to eliminate the influence of the calibration errors of the transducers, the slope error δ_s and the zero-adjustment error δ_0 of the output transducer was also estimated. The slope errors could not be eliminated in the Ångström's method.

The signals y_2, y_4 and y_6 of the series S2, defined in Section 4 of Chapter 2, were used for identification. The boundary conditions for the heat equation was thus determined by y_2 and y_6, and y_4 was chosen as the output variable. This selection of boundary conditions eliminated the influence of nonlinearities of the servos, discussed in Section 5 of Chapter 4, and is therefore crucial for the choice of experimental conditions. The matrix C in (3.1) became

$$C = (0 \ldots 0 \ 1+\delta_s \ 0 \ldots 0) \tag{3.11}$$

To save computer time the computations were based on a record of length N = 205. The transient caused by the initial nonzero temperature gradient in the rod was eliminated by not using the first part of the series S2. The chosen record contained 18 bad readings. These readings were substituted using Lagrange interpolation.

The results of the identification were

$$a = 1.1589 \cdot 10^{-4} \pm 0.0001 \cdot 10^{-4} \ m^2/s$$

$$\eta = 3.56 \cdot 10^{-5} \pm 0.05 \cdot 10^{-5} \ 1/s$$

$$\delta_0 = 3.92 \cdot 10^{-3} \pm 0.01 \cdot 10^{-3} \ ^oC$$

$$\delta_s = 6 \cdot 10^{-5} \pm 1 \cdot 10^{-5}$$

$$\hat{\lambda} = 1.42 \cdot 10^{-4} \ ^oC \tag{3.12}$$

The random errors were thus very small. However, the measurements were not free from systematic errors. The model used for identification were based on the partial differential equation (2.1). From (2.1) it is immediate that the only quantities involved in the estimation of the thermal diffusivity are the time t, the length z and the temperature θ. Since the slope and zero adjustment errors of the output transducer were estimated, the

errors in the measurement of the temperature θ were eliminated.

To be more specific the identification was based on the lumped model (2.10) with the parameters (2.11) in Chapter 3. From (2.10) and (2.11) it follows that a systematic error in the length scale influenced a quadratically whereas a systematic error in the time scale influenced a and η linearly. In this experiment the sensor separation was D = 2d. Since the parameters were determined using an optimization algorithm, it follows that the maximal systematic error in a and η become

$$\left|\frac{\Delta a}{a}\right|_{max} = 2\left|\frac{\Delta D}{D}\right|_{max} + \left|\frac{\Delta T}{T}\right|_{max}$$

$$\left|\frac{\Delta \eta}{\eta}\right|_{max} = \left|\frac{\Delta T}{T}\right|_{max} \qquad (3.13)$$

From (2.1) in Chapter 2 it follows that the maximal error in D was 0.15%. Moreover, the errors in the sampling period were neglectable. Therefore, by (3.12) and (3.13) the values of a and η and their maximal errors become

$$a = 1.159 \cdot 10^{-4} \pm 0.003 \cdot 10^{-4} \ m^2/s$$

$$\eta = 3.6 \cdot 10^{-5} \pm 0.1 \cdot 10^{-5} \ 1/s \qquad (3.14)$$

It should be observed that the random errors were negligible, compared to the systematic errors in this experiment. It follows from (3.12) that the standard deviation of the residuals is $0.0001^{o}C$. This means that the state-space model ROD2 describes the conduction of heat in the rod extremely well.

The statistical properties of the residuals of the identified model were examined. The sample auto-correlation function (3.4) in Chapter 4 of the residuals and the sample cross-correlation function (3.6) in Chapter 4 of the inputs u_1, u_2 and the residuals are shown in Fig. 3.1. From this figure it is clear that the residuals are uncorrelated. Moreover, by this figure, the

inputs u_1, u_2 and the residuals are uncorrelated.

The residuals were tested for normality using a chi-square goodness-of-fit test. The test quantity was $\chi^2 = 34$. The number of degrees of freedom was 21. Provided that χ^2 is less than 39 the hypothesis that the residuals are normally distributed is accepted at a risk level of 1%.

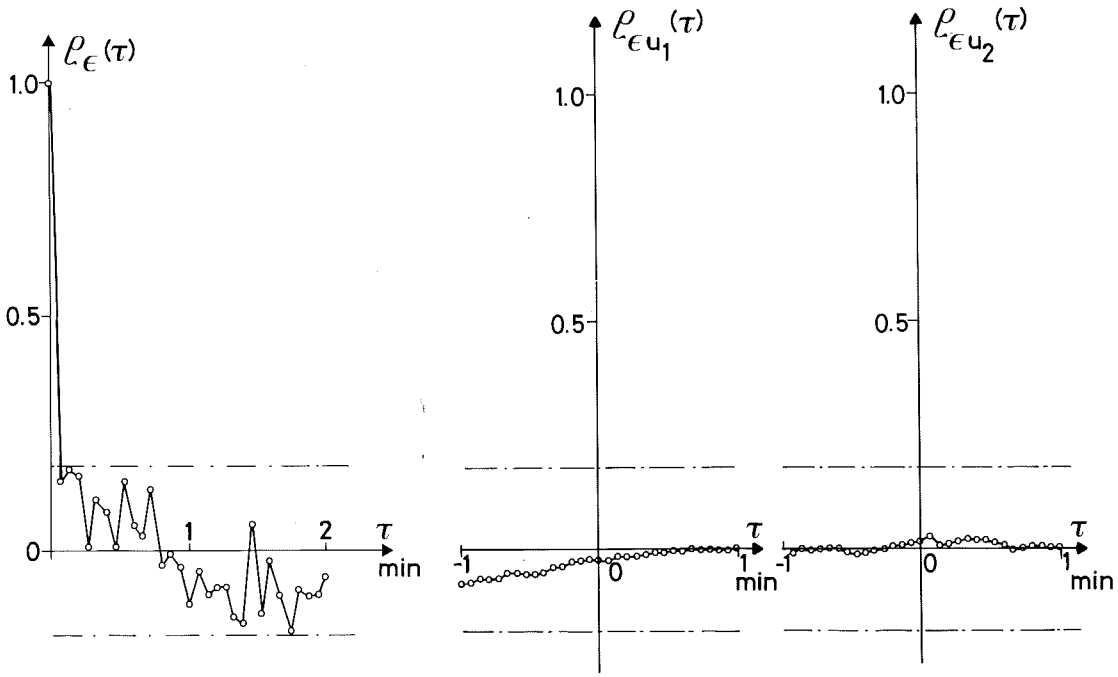

Fig. 3.1 - Sample correlation functions of the identified model. The signals u_1 and u_2 are the boundary temperatures y_2 and y_6 whereas the signal y_4 is the output temperature. The dashed lines give the 99% confidence interval for $\rho_\varepsilon(\tau)$ for $\tau \neq 0$ and for $\rho_{\varepsilon u_1}(\tau)$ and $\rho_{\varepsilon u_2}(\tau)$ $\forall\ \tau$.

The results of identification are illustrated in Fig. 3.2. This figure shows:

- the boundary temperatures y_2 and y_6
- the output temperature y_4
- the model error $e_{m_4} = y_4 - y_{m_4}$, where y_{m_4} is the output of the model

$$\dot{\hat{x}} = \hat{A}\hat{x} + \hat{B}\hat{v}$$

$$y_{m_4} = C\hat{x} + \delta_0$$

with parameters (3.12)

for the identified model. Summing up, it is found that the prerequisities for the maximum likelihood identification were fulfilled at a risk level of 1% (compare the results for the model $Sl_{\ell/4}$ in Section 3 of Chapter 4).

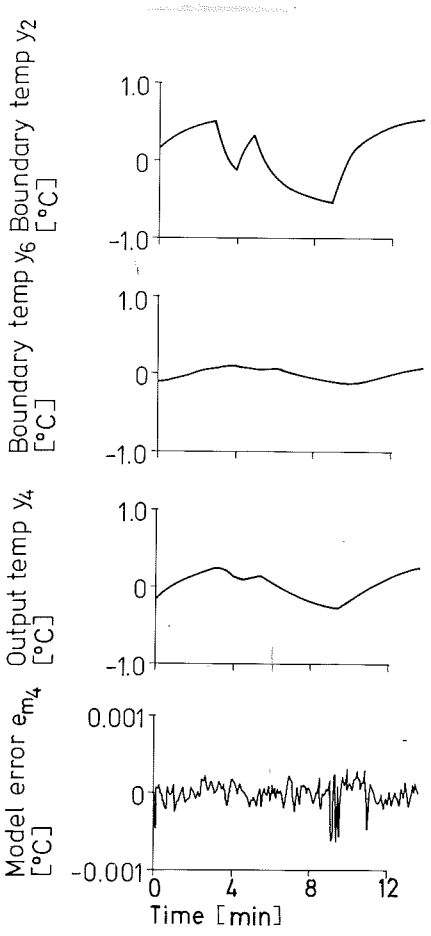

Fig. 3.2 - The boundary temperatures y_2 and y_6, the output temperature y_4, and the model error e_{m_4} of the identified model.

On a Univac 1108 computer the storage capacity required for the programs and the data was 5.6 K words and 9.9 K words respectively. The system subroutines required extra 4.4 K words. The time required to compute the optimum parameter vector α was 6 min for a reasonable initial guess. The algorithm used for the numerical minimization was based on [11].

4. CONSISTENCY AND CONCLUSIONS

Consistency

In [13] the recommended value of the thermal diffusivity for well-annealed high-purity copper is $a = 1.17 \cdot 10^{-4} \pm 0.04 \cdot 10^{-4}$ m^2/s. The values of a estimated by the Ångström's method and the maximum likelihood method are consistent with this result, according to (2.12) and (3.14). Moreover, by (2.12) and (3.14), the value obtained from the Ångström's method and the maximum likelihood method are also mutually consistent. According to (3.46) in Chapter 2, a lower bound of η is given by $\eta = 2.0 \cdot 10^{-5}$ 1/s. The lower bound applies to a case when the end point temperatures of the rod are perturbed very slowly. From (3.14) it can be seen that the heat loss from the rod only is increased by a factor 1.8, compared to this case, in the experiment S2. By (3.12), the estimated values of δ_0 and δ_s are consistent with (2.5) in Chapter 2.

Conclusions

The modified Ångström's method and the maximum likelihood method are very accurate methods for determining the thermal diffusivity. Errors in measuring the diffusivity originate mainly from systematic errors in the sensor position and the calibration of the transducers. Ångström's method applies to a semi-infinite rod and, therefore, requires a smaller sensor separation than the maximum likelihood method. This is a distinct disadvantage of the Ångström's method. The influence of the calibration errors of the transducers can be eliminated by estimating the slope and zero ad-

justment errors of the output transducer using the maximum likelihood method. These errors effect the determination of the thermal diffusivity in Ångström's method.

In both methods the random errors are very small compared to the systematic errors. The measurement times used in both cases are relatively short. Therefore, these methods possess a possible potential for determining the thermal diffusivity even more accurately. The results in this chapter indicate that the thermal diffusivity can be determined more accurately if thermistor sensors of smaller sizes are used. In the present apparatus, errors in determining the thermal diffusivity are of the order of 0.9% and 0.3% for the Ångström's method and the maximum likelihood method respectively.

5. REFERENCES

[1]: Abeles, B., Cody, G.P. and Beers, D.S.: "Apparatus for the measurement of the thermal diffusivity of solids at high temperatures", J. Appl. Phys., Vol. 31, 1585-1592, 1960.

[2]: Ångström, A.J.: "Neue Methode das Wärmeleitungsvermögen den Körper zu bestimmen", Ann. der Phys. u. Chem., Poggendorff's Annal., Vol. 114, 513-530, 1861.

[3]: Åström, K.J. and Eykhoff, P.: "System identification - A survey", Automatica, Vol. 7, 123-152, 1971.

[4]: Åström, K.J.: "Lectures on system identification, Chapter 3, Frequency response analysis", Report 7504, Lund Inst. of Techn., Div. of Automatic Control, 1975.

[5]: Carslaw, H.S. and Jaeger, J.C.: "Conduction of heat in solids", 2nd ed., Clarendon Press, Oxford, 1959.

[6]: Danielson, G.C. and Sidles, P.H.: "Thermal diffusivity and other non-steady-state methods". In "Thermal conductivity" (Ed. Tye, R.P.), Vol. 2, 149-201, Academic Press, London, 1969.

[7]: Graham, D. and McRuer, D.: "Analysis of nonlinear control systems", John Wiley, New York, 1961.

[8]: Jakob, M.: "Heat transfer", 8th ed., John Wiley, New York 1962.

[9]: Kennedy, W.L., Sidles, P.H. and Danielson, G.C.: "Thermal diffusivity measurements on finite samples", Advanced Energy Conversion, Vol. 2, 53-58, 1962.

[10]: Ljung, L.: "On consistency for prediction error identification methods", Report 7405, Lund Inst. of Techn., Div. of Automatic Control, 1974.

[11]: Powell, M.J.D.: "An efficient method of finding the minimum of a function of several variables without calculating derivatives", Computer J., Vol. 7, 155-162, 1964.

[12]: Sidles, P.H. and Danielson, G.C.: "Thermal diffusivity of metals at high temperatures", J. Appl. Phys., Vol. 25, 58-66, 1954.

[13]: Touloukain, Y.S., Powell, R.W., Ho, C.Y. and Nicolaou, M.C.: "Thermal diffusivity", Thermophysical properties of matters Vol. 10, IFI/Plenum Data Corporation, New York, 1973.

[14]: Woo, K.T.: "Maximum likelihood identification of noisy systems", 2nd IFAC Symp. on Identification and Process Parameter Estimation, Prague, paper 3.1, 1970.

CHAPTER 6

MULTIVARIABLE DEAD-BEAT CONTROLLERS

1. INTRODUCTION

During the past two decades the state space approach to dead-beat control theory has been given much attention. Early contributions to the topic were given by Kalman et al. [9] and [10] in 1958 and 1960. Kalman solves the problem of transferring the state of a single-input sampled-data system from any initial state to equilibrium with zero error in a minimum number of time steps. The solution was given as a linear state feedback. In solving this problem Kalman [10] introduces the concepts of reachability and observability. The possibility to design a sampled-data regulator in such a way that the error in the response to a step input is identically zero in the sampling instants after a certain number of time steps was first pointed out by Bergen and Ragazzini [5] in 1954.

Bertram and Sarachik [6] relaxed the minimality condition, introduced by Kalman, and demanded that the output of the system from any initial state should be transferred to the origin, possibly with a small error, in a given a number of time steps. Instead the control strategies were made to satisfy other desiderata, for instance, minimizing the energy consumption required for the transfer. The strategies were control programs applicable to multivariable systems. Dead-beat regulators that force the state of a multivariable system to zero were first derived by Farison et al. [7] and Kučera [12] in 1970 and 1971. The problem of constructing a linear state feedback which forces the output of a single-input, single-output system from its initial state to zero in a minimum number of time steps was considered by Kučera

in [13].

The dead-beat regulators are intimately connected to canonical structures of linear systems. In fact such regulators which force the state of a multivariable system to the origin can be obtained directly from one controllable canonical form [14] of the system. This fact was used by Ackerman [1] to obtain dead-beat response. However, there exist no canonical structures which give the corresponding controllers for the output case. The computation of the canonical structures which yield the dead-beat regulators is numerically ill-conditioned for systems with a large number of state variables.

In this chapter a unified approach to the theory of multivariable dead-beat control is given. The approach covers and extends all results on the topic given in the cited literature. Special attention is given to the connection between dead-beat control strategies and the solution of a singular optimal control problem which gives time-variable dead-beat controllers. Some of the algorithms which yield the dead-beat regulators are numerically ill-conditioned if the sampled-data system has eigenvalues close to the origin. It is shown how the condition can be improved by splitting of these eigenvalues of the system. The algorithms may be viewed as special algorithms for pole assignement. The approach is basically geometric and much inspiration comes from Wonham and Morse [15], [17] and [18].

2. PRELIMINARIES

Notation

Below, capital italic letters A, B, C, ... denote linear maps and script letters $\mathcal{X}$, $\mathcal{Y}$, $\mathcal{Z}$, ... denote linear vector spaces. Elements of a vector space are denoted by lower case italic letters x, y, z,... .The same letter is used to denote both a matrix and its map. All maps, matrices and spaces are defined over the field of real numbers. Transpose it denoted by a prime. The orthogonal com-

plement of a subspace $\mathcal{V}$ is written $\mathcal{V}^{\perp}$. The dimension of a subspace $\mathcal{V}$ is denoted by $\dim(\mathcal{V})$. A matrix V is said to be a basis matrix for $\mathcal{V}$ if the column vectors of V are linearly independent and span $\mathcal{V}$. The symbol 0 stands for a number, a vector or a subspace which is zero.

Assume that k is a positive integer. Then $\underline{k}$ and $\underline{k}_0$ are the set of integers $\{1, 2, \ldots, k\}$ and $\{0, 1, \ldots, k\}$ respectively. A set of elements $\{a_1, a_2, \ldots, a_k\}$ is written $\{a_i\}_{i\in\underline{k}}$ or $\{a_i\}_{i=1}^{k}$. The empty set is written ϕ. The symbol 0_n is used to denote a null matrix with n-columns, whose number of rows is to be understood from the context. To represent a $n\times n$ unit matrix the symbol I_n is used.

Background algebra

Assume that $\mathcal{X}$ and $\mathcal{Y}$ are linear vector spaces and assume that $A:\mathcal{X}\to\mathcal{Y}$ is a linear map. The kernel of A is the subspace $\mathrm{Ker}(A) = \{x \mid x\in\mathcal{X},\ Ax=0\}$ and the image of A is the subspace $\mathrm{Im}(A) = \{y \mid y\in\mathcal{Y},\ \exists x\in\mathcal{X}: y=Ax\}$. Sometimes the image of A is written A. The nullity and the rank of a map A are defined according to $\nu(A) = \dim(\mathrm{Ker}(A))$ and $\mathrm{rk}(A) = \dim(\mathrm{Im}(A))$ respectively. The image of $\mathcal{V}\subset\mathcal{X}$ under A is the subspace $A\mathcal{V} = \{y \mid y\in\mathcal{Y},\ \exists x\in\mathcal{V}: y=Ax\}$. Moreover, the subspace $A^{-1}\mathcal{W} = \{x \mid x\in\mathcal{X},\ Ax\in\mathcal{W}\}$ is the inverse image of $\mathcal{W}\subset\mathcal{Y}$ under A.

Assume that $A:\mathcal{X}\to\mathcal{X}$ is a linear map. Let $\mathcal{V}\subset\mathcal{X}$ and let $A\mathcal{V}\subset\mathcal{V}$. The subspace $\mathcal{V}$ is then said to be an A-invariant subspace. Assume that V is a basis matrix for $\mathcal{V}$. Then the map corresponding to the matrix $\bar{A}$ which satisfies $AV = V\bar{A}$ is called the restriction of A to $\mathcal{V}$. This map is denoted by $A|\mathcal{V}$. If there exists a subspace $\mathcal{W}\subset\mathcal{X}$ such that $A\mathcal{W}\subset\mathcal{W}$ and $\mathcal{V}\oplus\mathcal{W} = \mathcal{X}$, then A is said to be reduced by the pair $(\mathcal{V},\mathcal{W})$ which is written $A = A|\mathcal{V} \oplus A|\mathcal{W}$. The subspace $\{A|\mathcal{B}\}$ is defined by $\{A|\mathcal{B}\} = \mathcal{B} + A\mathcal{B} + \ldots + A^{n-1}\mathcal{B}$ where $\mathcal{B}\subset\mathcal{X}$ and $\dim(\mathcal{X}) = n$.

Let $\mathcal{X}$ and $\mathcal{U}$ be linear vector spaces and let $A:\mathcal{X}\to\mathcal{X}$ and $B:\mathcal{U}\to\mathcal{X}$ be two linear maps. A subspace $\mathcal{V}$ is called an (A,B)-invariant subspace if $A\mathcal{V}\subset\mathcal{V}+\mathcal{B}$. According to [15], there exists a map $L:\mathcal{X}\to\mathcal{U}$

such that $(A+BL)V \subset V$ if and only if $AV \subset V+\mathcal{B}$. Associated with an (A,B)-invariant subspace V, there are many linear maps L such that $(A+BL)V \subset V$. The feedback class $\underline{L}(V)$ is the set of all such linear maps, i.e.

$$\underline{L}(V) = \{L \mid (A+BL)V \subset V\} \tag{2.1}$$

A set of (A,B)-invariant subspaces $\{V_i\}_{i\in\underline{k}}$ is said to be compatible if

$$\bigcap_{i=1}^{k} \underline{L}(V_i) \neq \phi \tag{2.2}$$

Let $A: X \to X$ and $B: \mathcal{U} \to X$ be two linear maps. Assume that $\mathcal{W}$ is a given subspace in X. Then, according to [15], there exists a unique maximal (A,B)-invariant subspace V^* contained in $\mathcal{W}$. Thus if V is any (A,B)-invariant subspace, then $V \subset V^* \subset \mathcal{W}$. From [15] it follows that the maximal subspace V^* is generated by the following sequence

$$V_0 = \mathcal{W}$$

$$V_i = \mathcal{W} \cap A^{-1}(V_{i-1}+\mathcal{B}) = V_{i-1} \cap A^{-1}(V_{i-1}+\mathcal{B}), \qquad i = 1, 2, \ldots \tag{2.3}$$

The sequence converge in at most $\dim(\mathcal{W})$ steps and if k is the least positive integer such that $V_{k+1} = V_k$ then $V^* = V_k$.

Assume that X is a linear space and that $A: X \to X$ is a linear map. Let $\alpha(\lambda) = \alpha_1^{m_1}(\lambda)\alpha_2^{m_2}(\lambda) \ldots \alpha_\ell^{m_\ell}(\lambda)$ be a prime factorization over $\mathbb{R}$ of the minimal polynomial (m.p.) of A and let $N_i = \operatorname{Ker}(\alpha_i^{m_i}(A))$ for $i \in \underline{\ell}$. Then

$$X = N_1 \oplus N_2 \oplus \ldots \oplus N_\ell$$

$$AN_i \subset N_i, \qquad i \in \underline{\ell} \tag{2.4}$$

and the m.p. of $A \mid N_i$ is α_i for $i \in \underline{\ell}$. Moreover, $X = N_1 \oplus N_2 \oplus \ldots \oplus N_\ell$ provides a modal decomposition of X, relative to A, which is unique. The index ν_i of an eigenvalue λ_i of A such that $\alpha_i(\lambda_i) = 0$

is the least positive integer satisfying $N_i^{\nu_i+1} = N_i^{\nu_i}$ where $N_i^{\nu_i} = \mathrm{Ker}\left(\alpha_i(A)^{\nu_i}\right)$ for $i\in\underline{\ell}$. Henceforth, N_i is said to be a generalized eigenvector space of A of index $\nu_i = m_i$ associated with the eigenvalue $\lambda_i\in\mathbb{R}$ or $\lambda_i,\lambda_i^*\in\mathbb{C}$ for $i\in\underline{\ell}$.

Moore-Penrose pseudoinverse

Let X and Y be linear vector spaces and let $A:X\to Y$ be a linear map. The Moore-Penrose pseudoinverse of A is the linear map $A^+:Y\to X$ uniquely defined by the following four axioms [2] and [11].

$$AA^+A = A \tag{2.5a}$$
$$A^+AA^+ = A^+ \tag{2.5b}$$
$$(AA^+)' = AA^+ \tag{2.5c}$$
$$(A^+A)' = A^+A \tag{2.5d}$$

It can be shown [2] that these axioms imply

$$(A')^+ = (A^+)' \tag{2.6a}$$
$$A^+ = (A'A)^+A' = A'(AA')^+ \tag{2.6b}$$

A^+A is the orthogonal projection of X on $\mathrm{Im}(A')$ (2.7a)
$I-A^+A$ is the orthogonal projection of X on $\mathrm{Ker}(A)$ (2.7b)
AA^+ is the orthogonal projection of Y on $\mathrm{Im}(A)$ (2.7c)
$I-AA^+$ is the orthogonal projection of Y on $\mathrm{Ker}(A')$ (2.7d)

$$\mathrm{Ker}(A^+) = \mathrm{Im}(A')^\perp = \mathrm{Ker}(A) \tag{2.8a}$$
$$\mathrm{Im}(A^+) = \mathrm{Ker}(A)^\perp = \mathrm{Im}(A') \tag{2.8b}$$

The Penrose inverse can be used to give an explicit representation for the minimum norm solution to a least squares problem.

Lemma 2.1: Given two linear vector spaces X and Y, a constant vector $z \in Y$ and a linear map $A: X \to Y$. Then $\hat{x} = A^{+}z$ is the vector of minimum norm among those $x \in X$ which minimize

$$\| Ax-z \|^2 \tag{2.9}$$

The minimum value of $\| Ax-z \|$ is given by

$$\| A\hat{x}-z \|^2 = \| z \|^2 - \| A\hat{x} \| = \| (I-AA^{+})z \| \tag{2.10}$$

Moreover, a value of x that minimizes (2.9) is unique if and only if $\mathrm{Ker}(A) = 0$.

System description

Consider a finite dimensional, time-invariant, linear and discrete-time system described by the difference equation

$$x_{t+1} = Ax_t + Bu_t$$

$$y_t = Cx_t \tag{2.11}$$

where $x_t \in X$ is an n-vector, $u_t \in U$ is an m-vector and $y_t \in Y$ is a p-vector. The Euclidean spaces $X = \mathbb{R}^n$, $U = \mathbb{R}^m$ and $Y = \mathbb{R}^p$ are the state, the input and the output spaces respectively. The system (2.11) is denoted by $S(A,B,C)$. When the complete state is considered, the shorter notation $S(A,B)$ is used. The system $S(A,B,C)$ is called completely reachable if $\{A|B\} = X$. The maximal (A,B)-invariant subspace in $\mathrm{Ker}(C)$ for the system $S(A,B,C)$ is denoted by V^M.

System classes

In order to simplify the mathematics all results in this chapter will not be given in its most general form but different restrictions will be made on the considered systems. The consequences of these restrictions will be discussed in detail in Section 7. The following four system classes will in the sequel be devoted much attention.

$$S^1 = \{S(A,B,C)\}$$

$$S^2 = \left\{S(A,B,C) \mid \mathrm{Ker}(B) = \mathrm{Ker}(C') = 0,\ \{A|B\} = X\right\}$$

$$S^3 = \left\{S(A,B,C) \mid S(A,B,C)\in S^2,\ A \text{ invertable}\right\}$$

$$S^4 = \left\{S(A,B,C) \mid S(A,B,C)\in S^3,\ V^M \cap A^{-1}B = 0\right\} \qquad (2.12)$$

3. STATE DEAD-BEAT CONTROLLERS

Consider a system $S(A,B)$ in the class S^3 controlled by linear time-invariant state feedbacks

$$u_t = Lx_t, \quad t = 0, 1, \ldots \qquad (3.1)$$

such that the state of the system from any x_0 at $t = 0$ is forced to the origin in a finite number of time steps. A state dead-beat controller is such a controller which for each x_0 requires the minimum number of time steps. This number depends on x_0. It should be observed that the state feedback L must not depend on x_0.

Preliminaries

Assuming that the state of the system $S(A,B) \in S^3$ is x_0 at $t = 0$, the state at the k:th sampling instant is

$$x_k = A^k x_0 + W_k \beta_k' \tag{3.2}$$

where $\beta_k = [u_{k-1}', u_{k-2}', \ldots, u_0']$ contains the sequence of control vectors and W_k is the reachability matrix, i.e.

$$W_k = [B, AB, \ldots, A^{k-1}B]$$

$$W_0 = 0 \tag{3.3}$$

Since A is invertable, it follows from (3.2) that the set of states (subspace) which can be transferred to the origin in no more than k time steps for some choice of the input sequence β_k is $Z_k = \mathrm{Im}(Z_k)$,

$$Z_k = [A^{-1}B, A^{-2}B, \ldots, A^{-k}B]$$

$$Z_0 = 0 \tag{3.4}$$

This fundamental result was first pointed out by Kalman [10]. The reachability index ν of the system S(A,B) is the least positive integer such that $\mathrm{rk}(W_\nu) = n$. It is clear that $\dim(Z_\nu) = \mathrm{rk}(W_\nu)$, since A is invertable. Therefore, the state of a system $S(A,B \in S^3$ can be driven to zero in no more than ν time steps for any initial state x_0. Moreover, by (3.2), ν is the smallest positive integer for which this is true.

Selection procedure

The first step in the development of a state dead-beat controller is the selection of n linearly independent column vectors from the full rank matrix Z_ν. Procedures which accomplish such a selection are discussed in [14]. In the selection here the column vectors of Z_ν should be examined in the following order

$$A^{-1}b_{i_1}, A^{-1}b_{i_2}, \ldots, A^{-1}b_{i_m}, A^{-2}b_{i_1}, A^{-2}b_{i_2}, \ldots,$$

$$\ldots, \ldots, A^{-m}b_{i_m} \qquad (3.5)$$

where the integers $\{i_j\}_{j\in\underline{m}}$ is a permutation of $\underline{m}$. It tends to produce several chains $A^{-1}b_j, A^{-2}b_j, \ldots, A^{-r_i}b_j$, $j\in\underline{m}$, of nearly equal length. The essential restriction on the selection procedure is that no vector of the form $A^{-i}b_j$ is selected unless all lower powers of A^{-1} times b_j are selected.

The sequential selection of vectors from (3.5) is made according to the following scheme:

(i) select one of the columns of $A^{-1}B$

(ii) select another column vector of $A^{-1}B$ $(m>1)$. If the vector is linearly independent of the previously selected vectors, keep it, otherwise omit it from the selection

(iii) at any stage of the process, select a new vector of the form $A^{-i}b_j$ where all lower powers of A^{-1} times b_j have already been kept. If the new vector is linearly independent of the previously selected vectors, keep it, otherwise omit it from the selection

(iv) the selection procedure terminates when n linearly independent vectors are selected.

(SP1)

It is clear that the outcome of the selection procedure may depend on which permutation of the vectors in B that is used. In [14] it is shown that the process does not terminate until n linearly independent vectors have been selected.

The notation $A^{-1}B(1), A^{-2}B(2), \ldots, A^{-k}B(k)$ is used to denote the linearly independent column vectors selected from the matrices $A^{-1}B, A^{-2}B, \ldots, A^{-k}B$ respectively for $k\in\underline{\nu}$. By construction, the selection is carried out such that

$$\mathrm{Im}\left(B^{(1)}\right) = \mathrm{Im}(B)$$

$$\mathrm{Im}\left(B^{(k)}\right) \subset \mathrm{Im}\left(B^{(k-1)}\right) \subset \ldots \subset \mathrm{Im}\left(B^{(1)}\right), \quad k \in \underline{\nu} \tag{3.6}$$

Introduce the following compact notation

$$R_k = \left[A^{-1}B(1),\ A^{-2}B(2),\ \ldots,\ A^{-k}B(k)\right]$$

$$r_i = \mathrm{rk}\left(B^{(1)}\right), \quad i \in \underline{k} \quad k \in \underline{\nu} \tag{3.7}$$

where $r_1 = m$ and

$$n = \sum_{i=1}^{\nu} r_i$$

The selection procedure is constructed so that

$$Z_k = \mathrm{Im}(R_k), \quad k \in \underline{\nu} \tag{3.8}$$

which means that R_k is a basis matrix for Z_k for all $k \in \underline{\nu}$.

Main result

The theorem stated below gives an algorithm for constructing a state dead-beat controller. For a multivariable system special cases of the theorem is given in [7] and [12]. The results in [7] apply to systems where the columns of the reachability matrix form a basis for X. For such systems no selection procedure is required to obtain the state dead-beat controller. The general case is studied in [12], but here the author only proves that the state of the system can be forced to zero in no more than ν time units for any initial state. Below, it is shown that, in fact, it is possible to construct a controller which brings the state of the system from each initial state x_0 to zero in the minimum number of time steps. An example which illustrates the use of the theorem is also given.

Theorem 3.1: Assume that $S(A,B) \in \mathcal{S}^3$. Then a state dead-beat controller is given by the m×n matrix solution to

$$L\left[A^{-1}B(1),\ A^{-2}B(2),\ \ldots,\ A^{-\nu}B(\nu)\right] = \left[-I_{r_1},\ 0_{r_2},\ \ldots,\ 0_r\right] \qquad (3.9)$$

Moreover, the matrix A+BL is nilpotent of index ν.

Proof: Let $k \in \underline{\nu}$ be a positive integer. Then (3.9) implies that

$$BLA^{-1}B(j) = B(j), \qquad j \in \underline{k}$$

$$LA^{-i}B(j) = 0, \qquad i = 2, 3, \ldots, j \qquad (3.10)$$

since, by (3.6), $\mathrm{Im}(B(j)) \subset \mathrm{Im}(B(j-1)) \subset \ldots \subset \mathrm{Im}(B(1))$ and $\mathrm{Im}(B(1)) = \mathrm{Im}(B)$ for $j \in \underline{k}$. Therefore, it follows from (3.9) and (3.10) that

$$(A+BL)^k A^{-j}B(j) = (A+BL)^{k-1}A^{-(j-1)}B(j) = \ldots =$$

$$= (A+BL)^{k-j+1}A^{-1}B(j) = (A+BL)^{k-j}\left(B(j) - B(j)\right) = 0$$

$$\forall j \in \underline{k} \qquad (3.11)$$

Hence, $R_k = \mathrm{Im}\left([A^{-1}B(1),\ A^{-2}B(2),\ \ldots,\ A^{-k}B(k)]\right)$ belongs to the generalized eigenvector space of A+BL associated with the eigenvalue $\lambda = 0$ and $R_k \subset \mathrm{Ker}\left((A+BL)^k\right)$ for $k \in \underline{\nu}$.

Let x_0 be arbitrary. Since $Z_\nu = X$, there exists an integer $k \geq 1$ such that $x_0 \notin Z_{k-1}$ and $x_0 \in Z_k$. Then, by (3.4), there exists some choice of β_k such that the state is forced to zero in k time steps for the considered x_0 and k is the least positive integer for which such a choice exists. But, according to (3.8), $R_k = Z_k$ for all $k \in \underline{\nu}$. Therefore, by (3.11), the controller L forces the state to zero in k time steps for the given x_0. But x_0 is arbitrary and, consequently, L is a state dead-beat controller. Moreover, since $R_\nu = X$, it follows from (3.11) that A+BL is nilpotent of index ν.

□

Remark 1: The theorem is a straightforward generalization of the scalar case discussed in e.g. [12].

Remark 2: Let $k \in \underline{\nu}$ be an integer. Then (3.11) implies that

$$(A+BL)Z_i \subset Z_{i-1}, \quad i = 1, 2, \ldots, k$$
$$Z_0 = 0 \tag{3.12}$$

Remark 3: Assume that there exists a sequence of inputs β_k which drives the state of a system $S(A,B) \in S^2$ from a given x_0 to zero in the minimum number of time steps k. Then there also exists a linear state feedback (3.1) which forces the state to zero in k time steps for the considered x_0.

Example 3.1: Consider the linear and discrete-time system

$$x_{t+1} = \begin{bmatrix} 1 & 0 & 0 \\ 0 & 0.9 & 0 \\ 0 & 0 & 0.8 \end{bmatrix} x_t + \begin{bmatrix} 1 & 1 \\ 1 & 0 \\ 2 & 1 \end{bmatrix} u_t \tag{3.13}$$

It is straightforward to verify that the system (3.13) belongs to the system class S^3. The reachability index of the system is $\nu = 2$. To construct a state dead-beat controller invoke the selection procedure (SP1). The following two outcomes of the procedure exist

$$\left[A^{-1}B, \; A^{-2}b_1\right] = \begin{bmatrix} 1 & 1 & 1 \\ 1.11111 & 0 & 1.23457 \\ 2.5 & 1.25 & 3.125 \end{bmatrix} \tag{3.14}$$

and

$$\left[A^{-1}B, \; A^{-2}b_2\right] = \begin{bmatrix} 1 & 1 & 1 \\ 1.11111 & 0 & 0 \\ 2.5 & 1.25 & 1.5625 \end{bmatrix} \tag{3.15}$$

According to (3.9), the outcomes (3.14) and (3.15) correspond to the controllers

$$L_1 = \begin{bmatrix} 2.85714 & -3.47143 & 2.28571 \\ -0.71429 & 1.15714 & 0.22857 \end{bmatrix} \tag{3.16}$$

and

$$L_2 = \begin{bmatrix} 0 & -0.9 & 0 \\ -5 & -2.7 & 3.2 \end{bmatrix} \tag{3.17}$$

respectively. The closed loop systems associated with the controllers L_1 and L_2 become

$$x_{t+1} = \begin{bmatrix} -2.57143 & -2.31429 & 2.05714 \\ -2.85714 & -2.57143 & 2.28571 \\ -6.42857 & -5.78571 & 5.14286 \end{bmatrix} x_t \tag{3.18}$$

and

$$x_{t+1} = \begin{bmatrix} -4 & -3.6 & 3.2 \\ 0 & 0 & 0 \\ -5 & -4.5 & 4 \end{bmatrix} \tag{3.19}$$

respectively. The ch.p. of those systems are

$$d(z) = \det\left(zI - (A+BL_1)\right) = \det\left(zI - (A+BL_2)\right) = z^3 \tag{3.20}$$

For $x_0 = (111)'$ the trajectories and the input sequences of the system controlled with the linear feedbacks L_1 and L_2 become

t	0	1	2	t	0	1
x_t	$\begin{bmatrix} 1 \\ 1 \\ 1 \end{bmatrix}$	$\begin{bmatrix} -2.82857 \\ -3.14286 \\ -7.07143 \end{bmatrix}$	$\begin{bmatrix} 0 \\ 0 \\ 0 \end{bmatrix}$	u_t	$\begin{bmatrix} -4.04286 \\ 0.21429 \end{bmatrix}$	$\begin{bmatrix} 2.82857 \\ 0 \end{bmatrix}$
x_t	$\begin{bmatrix} 1 \\ 1 \\ 1 \end{bmatrix}$	$\begin{bmatrix} -4.4 \\ 0 \\ -5.5 \end{bmatrix}$	$\begin{bmatrix} 0 \\ 0 \\ 0 \end{bmatrix}$	u_t	$\begin{bmatrix} -0.9 \\ -4.5 \end{bmatrix}$	$\begin{bmatrix} 0 \\ 4.4 \end{bmatrix}$

(3.21)

respectively. Both the controllers L_1 and L_2 force the state of the system (3.13) to zero in $\nu = 2$ time steps.

4. OUTPUT DEAD-BEAT CONTROLLERS

Consider a system S(A,B,C) in the class $\mathcal{S}^4$ controlled by linear state feedbacks (3.1) such that the output is forced to zero and kept zero for any initial state x_0 in a finite number of time steps. Let k(L) be the number of time steps required at most for a certain feedback L. Define $\mu = \min_L k(L)$. An output dead-beat controller is then a linear state feedback (3.1) which forces the output of the system S(A,B,C) to zero in at most μ time steps and thereafter keeps it zero for any initial state x_0. If in addition the controller for each x_0 actually requires only the minimum number of time steps then the controller is said to be a strict output dead-beat controller.

If the system S(A,B,C) is obtained by sampling a continuous system then the output of this system need not be zero between the sampling points after μ time steps. However, for a state dead-beat controller it was required that the complete state should reach the equilibrium point. As a result the state would remain zero.

Preliminaries

The subspace $\mathcal{V}^M$ plays a fundamental role when constructing dead-beat contollers. For any $L \in \underline{L}(\mathcal{V}^M)$ the subspace $\mathcal{V}^M$ is an unobservable subspace to the pair (C,A+BL). The unobservability is introduced into the system by applying a linear state feedback (3.1). The system class $\mathcal{S}^4$ consists of all systems $S(A,B,C) \in \mathcal{S}^3$ such that $\mathcal{V}^M \cap A^{-1}\mathcal{B} = 0$. A technical consequence of this restriction is given in the following lemma.

Lemma 4.1: Assume that $S(A,B,C) \in \mathcal{S}^4$. Then the restriction of A+BL to $\mathcal{V}^M$ $(A+BL) \mid \mathcal{V}^M$ is invertable for all $L \in \underline{L}(\mathcal{V}^M)$.

The proof of the lemma is given in the Appendix 6A.

The construction of dead-beat controllers is simplified when the system S(A,B,C) is left invertable. A neat geometric condition for

a system to be left invertable is given in [15]:

S(A,B,C) is left invertable if and only if

$$\text{Ker}(B) = 0 \text{ and } V^M \cap \mathcal{B} = 0 \tag{4.1}$$

For a non left invertable system the decomposition $V^M = \hat{V} \oplus V^M \cap \mathcal{B}$ yield a subspace $\hat{V} \subset V^M$ which is compatible with V^M and has the property $\hat{V} \cap \mathcal{B} = 0$.

Lemma 4.2: Let

$$V^M = \hat{V} + V^M \cap \mathcal{B}$$

be a decomposition of V^M. Then

$\hat{V}$ and $\mathcal{B}$ are independent (4.2a)

$\hat{V}$ is an (A,B)-invariant subspace (4.2b)

$\hat{V}$ and V^M are compatible (4.2c)

$d_1(z)$ = ch.p. of $(A+BL)|\hat{V}$ divides $d_2(z)$ = ch.p. of $(A+BL)|V^M$, if $L \in \underline{L}(\hat{V}) \cap L(V^M)$ (4.2d)

The Appendix 6A contains a proof of the lemma.

The following lemma gives a lower bound for the number of time steps required to force the output of a system S(A,B,C) from any initial state x_0 to zero and thereafter keep the output zero using a linear state feedback (3.1).

Lemma 4.3: Assume that $S(A,B,C) \in S^4$. If there exists a linear state feedback (3.1) which brings the output of the system S(A,B,C) from any initial state to zero in at most k time steps and thereafter keeps the output zero, then $X = Z_k + V^M$.

Proof: Assume that $L: X \to U$ is a linear state feedback which forces the output of the system S(A,B,C) from any initial state x_0 to zero

in at most k time steps and thereafter keeps the output zero. Let

$$X = N_1 \oplus N_2 \oplus \ldots \oplus N_\ell$$

$$(A+BL)\,N_i \subset N_i, \quad i \in \underline{\ell} \tag{4.3}$$

be a modal decomposition of X, relative to A+BL. Assume that N_i is a basis matrix for N_i and assume that $(\overline{A+BL})$ is the induced matrix representation for $(A+BL)\,|\,N_i$. Putting

$$M_i = (A+BL)^k N_i, \quad i \in \underline{\ell} \tag{4.4}$$

it then follows that

$$M_i = (A+BL)^{k-1} N_i (\overline{A+BL}) = \ldots = N_i (\overline{A+BL})^k, \quad i \in \underline{\ell} \tag{4.5}$$

Since by hypothesis, $y_k = C(A+BL)^k x_0 = 0$ for all $x_0 \in N_i$, it follows that $M_i \subset \mathrm{Ker}(C)$. Moreover, (4.5) implies that M_i is an (A,B)-invariant subspace. Therefore, the maximal property of V^M yields that

$$M_i \subset V^M, \quad i \in \underline{\ell} \tag{4.6}$$

(i) Assume that N_i is associated with $\lambda_i \neq 0$.

Then $(\overline{A+BL})$ is invertable. Thus, by (4.5) and (4.6), $N_i = M_i \subset V^M$

(ii) Assume that N_i is associated with $\lambda_i = 0$.

First assume that $M_i = 0$. Then by (4.5), $x_k = (A+BL)^k x_0 = 0$ for all $x_0 \in N_i$. Therefore, by (3.4), $N_i \subset Z_k$. Now assume that $M_i \neq 0$. Since M_i is a generalized eigenvector space of A+BL associated with the eigenvalue $\lambda_i = 0$, there exists a $0 \neq v \in M_i$ such that

$$(A+BL)v = 0 \tag{4.7}$$

This implies that $v = -A^{-1}BLv$ and, hence, $v \in A^{-1}\mathcal{B}$. Therefore, by (4.5), $0 \neq V^M \cap A^{-1}\mathcal{B}$, since $v \neq 0$. This contradicts that $S(A,B,C) \in S^4$.

Hence $N_i \subset Z_k$.

Together (i) and (ii) imply that $X = N_1 \oplus N_2 \oplus \ldots \oplus N_\ell \subset Z_k + V^M$. Since $Z_k + V^M \subset X$, it then follows that $X = Z_k + V^M$. □

Remark: If there exists a linear state feedback (3.1) which forces the output of the system S(A,B,C) to zero in at most k time steps and thereafter keeps the output zero, then $x_0 \in Z_k + V^M$.

Let μ be the least positive integer such that

$$X = Z_\mu + V^M \tag{4.8}$$

Then by Lemma 4.3, there does not exist a linear feedback (3.1) which forces the output of the system S(A,B,C) from any initial state to zero in less than μ time steps and thereafter keeps the output zero.

Selection procedure

By Theorem 3.1 there exist linear maps $L: X \to U$ such that Z_μ belongs to the generalized eigenvector space of A+BL associated with the eigenvalue $\lambda = 0$. According to Lemma 4.1, there also exist linear maps $L: X \to U$ such that V^M belongs to the sum of the generalized eigenvector spaces of A+BL associated with the eigenvalues $\lambda \neq 0$. In general, there exists no common map L such that Z_μ and V^M have the two properties. However, by invoking a selection procedure similar to (SP1) it is possible to split $X = Z_\mu + V^M$ into two independent subspaces $X = \hat{R}_\mu \oplus \hat{V}$ which have these properties.

Some results are needed before the selection procedure can be given. Let L_0 be a given element in $\underline{L}(V^M)$. If V^M is a basis matrix for V^M then

$$(A+BL_0)V^M = V^M(\overline{A+BL_0}) \tag{4.9}$$

where $\overline{(A+BL_0)}$ is the induced matrix representation for $(A+BL)\,|\,V^M$. By (4.9), it follows that

$$V^M = A^{-1}V^M(\overline{A+BL_0}) - A^{-1}BL_0V^M \tag{4.10}$$

Decompose V^M according to Lemma 4.2

$$V^M = \hat{V} \oplus V^M \cap B \tag{4.11}$$

and let $\hat{V}$ be a basis matrix for $\hat{V}$. Then

$$\begin{aligned} X &= \mathrm{Im}\left([A^{-1}B,\ A^{-2}B,\ \ldots,\ A^{-\mu}B,\ V^M]\right) \\ &= \mathrm{Im}\left([A^{-1}B,\ A^{-2}B,\ \ldots,\ A^{-\mu}B,\ A^{-1}V^M(\overline{A+BL_0}) - A^{-1}BL_0V^M]\right) \\ &= \mathrm{Im}\left([A^{-1}B,\ A^{-2}B,\ \ldots,\ A^{-\mu}B,\ A^{-1}V^M]\right) \\ &= \mathrm{Im}\left([A^{-1}B,\ A^{-2}B,\ \ldots,\ A^{-\mu}B,\ A^{-1}\hat{V}]\right) \end{aligned} \tag{4.12}$$

where the first equality follows from (4.8), the second equality follows from (4.10), the third equality follows from Lemma 4.1 and $\mathrm{Im}(GH)\subset\mathrm{Im}(G)$ and the fourth equality follows from (4.11).

In the selection procedure it will be required that n linearly independent column vectors are selected from the full rank matrix

$$[A^{-1}B,\ A^{-2}B,\ \ldots,\ A^{-\mu}B,\ A^{-1}\hat{V}] \tag{4.13}$$

Thereby the column vectors of (4.13) should be examined in the following order

$$\begin{aligned} &A^{-1}\hat{v}_1,\ A^{-1}\hat{v}_2,\ \ldots,\ A^{-1}\hat{v}_{\hat{s}},\ A^{-1}b_{i_1},\ A^{-1}b_{i_2},\ \ldots,\ A^{-1}b_{i_m}, \\ &\qquad A^{-2}b_{i_1},\ A^{-2}b_{i_2},\ \ldots,\ \ldots,\ \ldots,\ A^{-\mu}b_{i_m} \end{aligned} \tag{4.14}$$

where $\hat{s} = \mathrm{rk}(\hat{V})$ and $\{i_j\}_{j\in\underline{m}}$ is a permutation of $\underline{m}$. The essential restriction on the selection procedure is that no vector of the form $A^{-i}b_j$ is selected unless all lower powers of A^{-1} times b_j are selected.

The sequential selection of vectors from (4.14) is made according to the following scheme:

(i) select all the column vectors $A^{-1}\hat{V}$

(ii) select one of the column vectors of $A^{-1}B$

(iii) select another column vector of $A^{-1}B$ (m>1). If the vector is linearly independent of the previously selected vectors, keep it, otherwise omit it from the selection

(iv) at any stage of the process, select a new vector of the form $A^{-i}b_j$ where all lower power of A^{-1} times b_j already have been kept. If the new vector is linearly independent of the previously selected vectors, keep it, otherwise omit it from the selection

(v) the selection terminates when n linearly independent vectors are found (SP2).

It is shown in Lemma 4.4 in the Appendix 6A that this selection procedure does not terminate until n linearly independent vectors have been selected.

The notation $A^{-1}\hat{B}(1)$, $A^{-2}\hat{B}(2)$, ..., $A^{-k}\hat{B}(k)$ is used to denote the linearly independent column vectors selected from the matrices $A^{-1}B$, $A^{-2}B$, ..., $A^{-k}B$ respectively for $k\in\underline{\mu}$. By construction and by (4.2a) the selection procedure has the properties

$$\mathrm{Im}\left(\hat{B}(1)\right) = \mathrm{Im}(B)$$

$$\mathrm{Im}\left(\hat{B}(k)\right)\subset\mathrm{Im}\left(\hat{B}(k-1)\right)\subset\ldots\subset\mathrm{Im}\left(\hat{B}(1)\right), \quad k\in\underline{\mu} \tag{4.15}$$

Introduce the following compact notation

$$\hat{R}_k = [A^{-1}\hat{B}(1),\ A^{-2}\hat{B}(2),\ \ldots,\ A^{-k}\hat{B}(k)]$$

$$\hat{r}_i = \mathrm{rk}\left(\hat{B}(i)\right), \quad i\in\underline{k}, \quad k\in\underline{\mu}$$

$$\hat{s} = \mathrm{rk}(\hat{V})$$

$$\hat{q} = \sum_{i=1}^{\mu}\hat{r}_i \tag{4.16}$$

where $\hat{r}_1 = m$ and $n = \hat{s} + \hat{q}$.

The subspaces $\hat{R}_\mu$ and $\hat{V}$ are independent and span X, since

$$X = \mathrm{Im}[A^{-1}\hat{B}(1),\ A^{-2}\hat{B}(2),\ \ldots,\ A^{-\mu}\hat{B}(\mu),\ A^{-1}\hat{V}]$$

$$= \mathrm{Im}[A^{-1}\hat{B}(1),\ A^{-2}\hat{B}(2),\ \ldots,\ A^{-\mu}\hat{B}(\mu),\ A^{-1}\hat{V}(\overline{A+BL_0}) - A^{-1}BL_0\hat{V}]$$

$$= \mathrm{Im}[A^{-1}\hat{B}(1),\ A^{-2}\hat{B}(2),\ \ldots,\ A^{-\mu}\hat{B}(\mu),\ \hat{V}] = \hat{R}_\mu \oplus \hat{V} \qquad (4.17)$$

where the second equality follows from Lemma 4.1 and $\mathrm{Im}(GH) \subset \mathrm{Im}(G)$ and the third equality follows from (4.10).

Main results

The theorem stated here gives a nice way to construct an output dead-beat controller. A sufficient condition for this controller to be a strict dead-beat controller is given in the corollary. In [13] an output dead-beat controller is proposed for a system with one input and one output. An example which illustrates the use of the theorem is also given.

Theorem 4.1: Assume that $S(A,B,C) \in \mathcal{S}^4$. Then an output dead-beat controller is given by the $m \times n$ matrix solution to

$$L[A^{-1}\hat{B}(1),\ A^{-2}\hat{B}(2),\ \ldots,\ A^{-\mu}\hat{B}(\mu),\ A^{-1}\hat{V}] =$$

$$= [-I_{\hat{r}_1},\ 0_{\hat{r}_2},\ \ldots,\ 0_{\hat{r}_\mu},\ 0_{\hat{s}}] \qquad (4.18)$$

Moreover, $L \in \underline{L}(\hat{V})$ and

$$d(z) = \text{ch.p. of } A+BL = z^{\hat{q}} d_1(z) \qquad (4.19)$$

where $d_1(z) = \text{ch.p. of } (A+BL)|\hat{V}$ divides $d_0(z) = \text{ch.p. of } (A+BL_0)|V^M$ for any $L_0 \in \underline{L}(\hat{V}) \cap \underline{L}(V^M)$.

Proof: Analogous to (3.12), it is possible to show that

$$(A+BL)\hat{R}_k \subset \hat{R}_{k-1}, \qquad k = 1, 2, \ldots, \mu$$

$$\hat{R}_0 = 0 \tag{4.20}$$

Therefore, $\hat{R}_\mu$ belongs to the generalized eigenvector space of A+BL associated with the eigenvalue $\lambda = 0$ and $\hat{R}_\mu \subset \mathrm{Ker}\left((A+BL)^\mu\right)$.

Assume that $L_0 \in \underline{L}(\hat{V}) \cap \underline{L}(V^M) \neq 0$. Let $\hat{V}$ be a basis matrix for $\hat{V}$ and let $(\overline{A+BL_0})$ be the induced matrix representation for $(A+BL_0)|\hat{V}$. Then

$$(A+BL_0)\hat{V} = \hat{V}(\overline{A+BL_0}) \tag{4.21}$$

which implies

$$\hat{V} = A^{-1}\hat{V}(\overline{A+BL_0}) - A^{-1}BL_0\hat{V} \tag{4.22}$$

Therefore, by (4.18), it follows that

$$\begin{aligned}(A+BL)\hat{V} &= A\hat{V} + BL\hat{V} \\ &= A\hat{V} + BL\left(A^{-1}\hat{V}(\overline{A+BL_0}) - A^{-1}BL_0\hat{V}\right) \\ &= A\hat{V} + BL_0\hat{V} = (A+BL_0)\hat{V} = \hat{V}(\overline{A+BL_0})\end{aligned} \tag{4.23}$$

Hence $L \in \underline{L}(\hat{V})$.

Let $x_0 \in X$ be arbitrary. Since by (4.17), $X = \hat{R}_\mu \oplus \hat{V}$ there exists a unique decomposition of x_0 such that

$$x_0 = x_0^{(1)} + x_0^{(2)} \tag{4.24}$$

where $x_0^{(1)} \in \hat{R}_\mu$ and $x_0^{(2)} \in \hat{V}$. Then (4.20) and (4.23) imply that

$$\begin{aligned}x_{\mu+k} &= (A+BL)^{\mu+k}x_0 = (A+BL)^{\mu+k}x_0^{(1)} + (A+BL)^{\mu+k}x_0^{(2)} \\ &= (A+BL)^{\mu+k}x_0^{(2)} \subset \hat{V} \subset \mathrm{Ker}(C), \quad \forall k \geq 0\end{aligned} \tag{4.25}$$

By (4.25), $y_{\mu+k} = Cx_{\mu+k} = 0$ for all $k \geq 0$. Since x_0 is arbitrary,

it is clear that L is an output dead-beat controller.

From (4.23) it follows that $d_1(z)$ = ch.p. of $(A+BL)|\hat{V}$ = ch.p. of $(A+BL_0)|\hat{V}$. Therefore, since $\hat{V}\subset V^M$, (4.2d) implies that $d_1(z)$ divides $d_0(z)$. By (4.17), (4.20) and (4.23), the pair $(\hat{R}_\mu,\hat{V})$ reduces A+BL. Hence

$$d(z) = \text{ch.p. of } (A+BL) = \text{ch.p. of } (A+BL)|\hat{R}_\mu \cdot$$

$$\cdot \text{ ch.p. of } (A+BL)|\hat{V} = z^q d_1(z) \qquad (4.26)$$

where $d_1(z)$ divides $d_0(z)$. This establishes (4.19). □

Remark 1: For a left invertable system the zeroes of $d_1(z)$ coincide with the zeroes [3] of the system S(A,B,C).

Remark 2: If $d_1(z)$ has zeroes outside the unit circle, then the closed loop system S(A+BL,B,C) will be unstable.

In general the dead-beat controller (4.18) is not a strict output dead-beat controller. A sufficient condition for this to be the case is given in the corollary.

Corollary 4.1: If the system $S(A,B,C)\in S^4$ is left invertable, then the controller (4.18) is a strict output dead-beat controller.

Proof: Assume that S(A,B,C) is left invertable. Then by (4.1), $V^M\cap B = 0$. Therefore, Theorem 4.1 implies that

$$\hat{V} = V^M$$

$$L\in \underline{L}(V^M) \qquad (4.27)$$

By construction of (SP2), it follows that

$$\hat{R}_i + V^M = Z_i + V^M, \quad i \geq 0 \tag{4.28}$$

Since $V = V^M$, it follows from (4.25) and (4.29) that the controller L forces the output of the system S(A,B,C) to zero in $k \geq 0$ time steps and thereafter keeps the output zero, if $x_0 \in Z_k + V^M$. Hence, it is clear from the remark of Lemma 4.3 that L is a strict output dead-beat controller.

□

Example 4.1: Consider a linear system with the transfer function

$$G(z) = \begin{bmatrix} \dfrac{z^2 - 1.8z + 0.8}{z^3 - 1.9z^2 + 1.5z - 0.4} \\ \\ \dfrac{z^3 - 1.3z + 0.4}{z^3 - 1.9z^2 + 1.5z - 0.4} \end{bmatrix} \tag{4.29}$$

A minimal realization of G(z) is given by

$$x_{t+1} = \begin{bmatrix} 1.9 & -1.5 & 0.4 \\ 1 & 0 & 0 \\ 0 & 1 & 0 \end{bmatrix} x_t + \begin{bmatrix} 1 \\ 0 \\ 0 \end{bmatrix} u_t \triangleq Ax_t + Bu_t$$

$$y_t = \begin{bmatrix} 1 & -1.8 & 0.8 \\ 1 & -1.3 & 0.4 \end{bmatrix} x_t \triangleq Cx_t \tag{4.30}$$

It is straightforward to verify that the system (4.30) belongs to the class S^3. According to (2.3), the maximal (A,B)-invariant subspace in Ker(C) becomes

$$V^M = \mathrm{Im} \begin{bmatrix} 0.64 \\ 0.8 \\ 1 \end{bmatrix} \tag{4.31}$$

The system (4.30) belongs to the class S^4, since $S(A,B,C) \in S^3$ and since $V^M \cap A^{-1}B = 0$. Moreover, the system is left invertable, since $\mathrm{Ker}(B) = 0$ and $V^M \cap B = 0$.

The least positive integer such that $X = Z_\mu + V^M$ is $\mu = 2$. To construct an output dead-beat controller invoke the selection procedure (SP2). The outcome of this selection procedure becomes

$$\left[A^{-1}B,\ A^{-2}B,\ A^{-1}V^M\right] = \begin{bmatrix} 0 & 0 & 0.8 \\ 0 & 2.5 & 1 \\ 2.5 & 9.375 & 1.55 \end{bmatrix} \tag{4.32}$$

where V^M is a basis matrix for V^M. Then, by (4.18), the corresponding output dead-beat controller is

$$L = [-1.1 \quad 1.5 \quad -0.4] \tag{4.33}$$

The closed loop system associated with the controller L is

$$x_{t+1} = \begin{bmatrix} 0.8 & 0 & 0 \\ 1 & 0 & 0 \\ 0 & 1 & 0 \end{bmatrix} x_t \triangleq (A+BL)x_t$$

$$y_t = \begin{bmatrix} 1 & -1.8 & 0.8 \\ 1 & -1.3 & 0.4 \end{bmatrix} x_t \tag{4.34}$$

Since

$$(A+BL)V^M = V^M \cdot 0.8 \triangleq V^M(\overline{A+BL}) \tag{4.35}$$

it follows that $L \in \underline{L}(V^M)$. Moreover, since the system (4.30) is left invertable, [3] gives that the system has a zero $z = 0.8$. The ch.p. of the closed loop system (4.34) is

$$d(z) = z^2(z-0.8) \tag{4.36}$$

Thus the zero $z = 0.8$ appears as a pole of the closed loop system (4.34). This is a simple consequence of (4.19).

For $x_0 = (111)'$ the trajectory, the input and output sequences of the system (4.30) controlled with the linear state feedback (4.33) become

$$
\begin{array}{lccccccc}
t & 0 & 1 & 2 & 3 & 4 & 5 & 6 \\
x_t & \begin{bmatrix}1\\1\\1\end{bmatrix} & \begin{bmatrix}0.8\\1\\1\end{bmatrix} & \begin{bmatrix}0.64\\0.8\\1\end{bmatrix} & \begin{bmatrix}0.562\\0.64\\0.8\end{bmatrix} & \begin{bmatrix}0.4096\\0.512\\0.64\end{bmatrix} & \begin{bmatrix}0.32768\\0.4096\\0.512\end{bmatrix} & \begin{bmatrix}0.26214\\0.32768\\0.4096\end{bmatrix} \\
y_t & \begin{bmatrix}0\\0.1\end{bmatrix} & \begin{bmatrix}-0.2\\-0.1\end{bmatrix} & \begin{bmatrix}0\\0\end{bmatrix} & \begin{bmatrix}0\\0\end{bmatrix} & \begin{bmatrix}0\\0\end{bmatrix} & \begin{bmatrix}0\\0\end{bmatrix} & \begin{bmatrix}0\\0\end{bmatrix} \\
u_t & 0 & 0.22 & 0.096 & 0.0768 & 0.6144 & 0.04915 & 0.03932
\end{array}
\qquad (4.37)
$$

It should be observed that the output y_t becomes zero after $\mu = 2$ time steps whereas the trajectory x_t slowly tends to the origin. Since the system (4.30) is left invertable, it follows from Corollary 4.1 that the controller L is a strict output dead-beat controller.

5. CONSTRAINED OUTPUT DEAD-BEAT CONTROLLERS

In the previous section it was found that the output dead-beat control strategy gives an unstable closed loop system if any of the zeroes [3] of the system S(A,B,C) is located outside the unit circle. If the system is obtained by sampling a continuous system, the output of this system will oscillate between the sampling instants with an exponentially growing amplitude. Moreover, if the dead-beat controller is computed from a model which does not describe the continuous system exactly the output will also deviate considerably from zero in the sampling instants after some time. This means that the closed loop sampled-data system is extremely sensitive to parameter variations. Clearly, in this case, the output dead-beat controller cannot be used successfully to control the system.

When the system S(A,B,C) has any zero outside the unit circle, it is of interest to search for linear state feedbacks (3.1) which forces the output of the system from any initial state x_0 to zero in at most $n \in (\mu, \nu]$ time steps and thereafter keeps the output zero

and which give a stable closed loop system. Clearly, the state dead-beat controller is an example of such a state feedback. It will be shown below that there also exist other linear state feedbacks (3.1) with the mentioned properties. Henceforth, all such feedbacks will be called constrained output dead-beat controllers.

Preliminaries

Consider a system $S(A,B,C)$ in the class S^4. Assume that L_0 is a given element in the feedback class $\underline{L}(\mathcal{V}^M)$. Let

$$\mathcal{V}^M = \mathcal{V}_1 \oplus \mathcal{V}_2 \oplus \ldots \oplus \mathcal{V}_\ell$$

$$(A+BL_0)\mathcal{V}_i \subset \mathcal{V}_i, \qquad i \in \underline{\ell} \tag{5.1}$$

be a modal decomposition of $\mathcal{V}^M$, relative to $A+BL_0$. According to [3], this decomposition is independent of the choice of $L_0 \in \underline{L}(\mathcal{V}^M)$ if and only if the system $S(A,B,C)$ is left invertable. Introduce the subspace

$$\mathcal{V}^{M^-} = \left\{ \mathcal{V}_i \mid \mathcal{V}_i \text{ is associated with } |\lambda_i| < 1,\ \mathcal{V}_i \cap \mathcal{B} = 0 \right\} \tag{5.2}$$

which is contained in the subspace of stable modes of $\mathcal{V}^M$, relative to $A+BL_0$. Let V^{M^-} be a basis matrix for $\mathcal{V}^{M^-}$ and let $(\overline{A+BL_0})$ be the induced matrix representation for $(A+BL_0)|\mathcal{V}^{M^-}$. Then (5.1) implies that

$$(A+BL_0)V^{M^-} = V^{M^-}(\overline{A+BL_0}) \tag{5.3}$$

By (5.3), it follows that

$$V^{M^-} = A^{-1}V^{M^-}(\overline{A+BL_0}) - A^{-1}BL_0V^{M^-} \tag{5.4}$$

Define η as the least positive integer such that

$$X = Z_\eta + \mathcal{V}^{M^-} \tag{5.5}$$

It is clear from (5.4) and (5.5) that

$$X = \mathrm{Im}\left([A^{-1}B,\ A^{-2}B,\ \ldots,\ A^{-\eta}B,\ V^{M^-}]\right)$$

$$= \mathrm{Im}\left([A^{-1}B,\ A^{-2}B,\ \ldots,\ A^{-\eta}B,\ A^{-1}V^{M^-}]\right) \tag{5.6}$$

Selection procedure

In order to select n linearly independent column vectors from the full rank matrix

$$[A^{-1}B,\ A^{-2}B,\ \ldots,\ A^{-\eta}B,\ A^{-1}V^{M^-}] \tag{5.7}$$

the selection procedure (SP2) is invoked where the matrix $\hat{V}$ is replaced by the matrix V^{M^-}. The notation $A^{-1}\tilde{B}(1)$, $A^{-2}\tilde{B}(2)$, ..., $A^{-\eta}\tilde{B}(\eta)$ is used to denote the column vectors selected from the matrices $A^{-1}B$, $A^{-2}B$, ..., $A^{-\eta}B$ respectively. By construction and by (5.2) the selection of vectors in (SP2) is performed such that

$$\mathrm{Im}\left(B^{(1)}\right) = \mathrm{Im}(B)$$

$$\mathrm{Im}\left(B^{(\eta)}\right) \subset \mathrm{Im}\left(B^{(\eta-1)}\right) \subset \ \ldots\ \subset \mathrm{Im}\left(B^{(1)}\right) \tag{5.8}$$

The following compact notation is introduced

$$\tilde{R}_\eta = [A^{-1}\tilde{B}(1),\ A^{-2}\tilde{B}(2),\ \ldots,\ A^{-\eta}\tilde{B}(\eta)]$$

$$\tilde{r}_i = \mathrm{rk}\left(\tilde{B}^{(i)}\right),\ i \in \underline{\eta}$$

$$\tilde{s} = \mathrm{rk}(V^{M^-})$$

$$\tilde{q} = \sum_{i=1}^{\eta} \tilde{r}_i \tag{5.9}$$

where $\tilde{r}_1 = m$ and $n = \tilde{q} + \tilde{s}$. Employing (5.4), it can be shown similar to (4.17) that

$$X = \tilde{R}_\mu \oplus V^{M^-} \tag{5.10}$$

Main result

A constrained output dead-beat controller is given by the theorem below. It is also given an example which illustrates the use of the theorem.

Theorem 5.1: Assume that $S(A,B,C) \in S^4$. Then a constrained output dead-beat controller is given by the m×n matrix solution to

$$L[A^{-1}\tilde{B}(1),\ A^{-2}\tilde{B}(2),\ \ldots,\ A^{-\eta}\tilde{B}(\eta),\ A^{-1}V^{M^-}] =$$

$$= [-\ I_{\tilde{r}_1},\ 0_{\tilde{r}_2},\ \ldots,\ 0_{\tilde{r}_\eta},\ 0_{\tilde{s}}] \qquad (5.11)$$

Moreover, $L \in \underline{L}(V^{M^-})$ and

$$d(z) = \text{ch.p. of } A+BL = z^{\tilde{q}} d_1(z) \qquad (5.12)$$

where $d_1(z)$ = ch.p. of $(A+BL)\,|\,V^{M^-}$.

Proof: The theorem may be proved analogous to Theorem 4.1. □

Remark 1: Notice that V^{M^-} depends on the choice of $L_0 \in \underline{L}(V^M)$.

Remark 2: If the system S(A,B,C) is left invertable then η and the zeroes of $d_1(z)$ are independent of the choice of $L_0 \in \underline{L}(V^M)$.

Remark 3: For a left invertable system there exists no linear state feedback (3.1) which forces the output of the system $S(A,B,C) \in S^4$ from any initial state to zero in less than η time steps and thereafter keeps the output zero and which gives a stable closed loop system.

Example 5.1: The continuous linear system with the transfer function

$$G(s) = \begin{bmatrix} \frac{1}{s+1} & \frac{2}{s+3} \\ \frac{1}{s+1} & \frac{1}{s+1} \end{bmatrix} \qquad (5.13)$$

has been used by Rosenbrock [16] to illustrate non-minimum phase behaviour of multivariable systems. A minimal realization of G(s) is given by

$$\dot{x} = \begin{bmatrix} -1 & 0 & 0 \\ 0 & -1 & 0 \\ 0 & 0 & -3 \end{bmatrix} x + \begin{bmatrix} 1 & 0 \\ 0 & 1 \\ 0 & 2 \end{bmatrix} u$$

$$y = \begin{bmatrix} 1 & 0 & 1 \\ 1 & 1 & 0 \end{bmatrix} x \qquad (5.14)$$

For the sampling period T = 0.8 s the discrete-time system corresponding to (5.14) becomes

$$x_{t+1} = \begin{bmatrix} 0.44933 & 0 & 0 \\ 0 & 0.44933 & 0 \\ 0 & 0 & 0.09072 \end{bmatrix} x_t +$$

$$+ \begin{bmatrix} 0.55067 & 0 \\ 0 & 0.55067 \\ 0 & 0.60619 \end{bmatrix} u_t \triangleq Ax_t + Bu_t$$

$$y_t = \begin{bmatrix} 1 & 0 & 1 \\ 1 & 1 & 0 \end{bmatrix} x_t \triangleq Cx_t \qquad (5.15)$$

It is straightforward to verify that the system (5.15) belongs to the system class S^3. The maximal (A,B)-invariant subspace in Ker(C) is

$$V^M = \mathrm{Im} \begin{bmatrix} 1 \\ -1 \\ -1 \end{bmatrix} \qquad (5.16)$$

The system (5.15) belongs to the class S^4, since $S(A,B,C) \in S^3$ and since $V^M \cap A^{-1}\mathcal{B} = 0$. Moreover, the system is left invertable, since Ker(B) = 0 and $V^M \cap \mathcal{B} = 0$.

The least positive integer μ such that $X = Z_\mu + V^M$ is $\mu = 1$. In-

voke the selection procedure (SP2) to construct an output time-optimal controller. The outcome of the process (SP2) becomes

$$\left[A^{-1}B,\ A^{-1}V^M\right] = \begin{bmatrix} 1.22554 & 0 & 2.22554 \\ 0 & 1.22554 & -2.22554 \\ 0 & 6.68212 & -11.0232 \end{bmatrix} \tag{5.17}$$

where V^M is a basis matrix for $\mathcal{V}^M$. According to (4.18), the corresponding output dead-beat controller is

$$L = \begin{bmatrix} -0.81597 & -8.90951 & 1.63406 \\ 0 & 8.09354 & -1.63406 \end{bmatrix} \tag{5.18}$$

The closed loop system associated with the controller L is

$$x_{t+1} = \begin{bmatrix} 0 & -4.90621 & 0.89983 \\ 0 & 4.90621 & -0.89983 \\ 0 & 4.90621 & -0.89983 \end{bmatrix} x_t$$

$$y_t = \begin{bmatrix} 1 & 0 & 1 \\ 1 & 1 & 0 \end{bmatrix} x_t \tag{5.19}$$

Since

$$(A+BL)V^M = V^M \cdot 4.00638 \tag{5.20}$$

it follows that $L \in \underline{L}(\mathcal{V}^M)$. The ch.p. of A+BL becomes

$$d(z) = z^2(z-4.00638) \tag{5.21}$$

Hence, the closed loop system (5.19) is unstable.

For $x_0 = (111)'$ the trajectory, the output and the input sequence of the system (5.15), controlled with the linear state feedback (5.18) become

$$
\begin{array}{lcccccc}
t & 0 & 1 & 2 & 3 & 4 & 5 \\
x_t & \begin{bmatrix}1\\1\\1\end{bmatrix} & \begin{bmatrix}-4.00638\\4.00638\\4.00638\end{bmatrix} & \begin{bmatrix}-16.0511\\16.0511\\16.0511\end{bmatrix} & \begin{bmatrix}-64.3067\\64.3067\\64.3067\end{bmatrix} & \begin{bmatrix}-257.637\\257.637\\257.637\end{bmatrix} & \begin{bmatrix}-1032.19\\1032.19\\1032.19\end{bmatrix} \\
y_t & \begin{bmatrix}2\\2\end{bmatrix} & \begin{bmatrix}0\\0\end{bmatrix} & \begin{bmatrix}0\\0\end{bmatrix} & \begin{bmatrix}0\\0\end{bmatrix} & \begin{bmatrix}0\\0\end{bmatrix} & \begin{bmatrix}0\\0\end{bmatrix} \\
u_t & \begin{bmatrix}-8.09141\\6.45948\end{bmatrix} & \begin{bmatrix}-25.8791\\25.8791\end{bmatrix} & \begin{bmatrix}-103.682\\103.682\end{bmatrix} & \begin{bmatrix}-415.388\\415.388\end{bmatrix} & \begin{bmatrix}-1664.20\\1664.20\end{bmatrix} &
\end{array}
\qquad (5.22)
$$

The output of this system becomes zero in $\mu = 1$ step. However, since the unobservable mode of the pair (C,A+BL) is located outside the unit circle the trajectory and the input sequence are growing unboundedly.

In this particular case $V^{M^-} = 0$ for all $L_0 \in \underline{L}(V^M)$. This follows since the decomposition (5.1) is unique for a left invertable system. Therefore, all constrained output dead-beat controllers of the system (5.15) are state dead-beat controllers. These controllers may be calculated by means of the selection procedure (SP1) and Theorem 3.1. One state dead-beat controller is given by

$$
L = \begin{vmatrix} -0.81597 & 0 & 0 \\ 0 & -1.02238 & 0.03786 \end{vmatrix} \qquad (5.23)
$$

For $x_0 = (111)'$ the trajectory, the output and the input sequence of the system (5.15) controlled with linear state feedback (5.23) is

$$
\begin{array}{lccc}
t & 0 & 1 & 2 \\
x_t & \begin{vmatrix}1\\1\\1\end{vmatrix} & \begin{vmatrix}0\\-0.09282\\-0.50609\end{vmatrix} & \begin{vmatrix}0\\0\\0\end{vmatrix} \\
y_t & \begin{vmatrix}2\\2\end{vmatrix} & \begin{vmatrix}-0.50609\\-0.09282\end{vmatrix} & \begin{vmatrix}0\\0\end{vmatrix} \\
u_t & \begin{vmatrix}-0.81597\\-0.98452\end{vmatrix} & \begin{vmatrix}0\\0.07574\end{vmatrix} &
\end{array}
\qquad (5.24)
$$

The constrained output dead-beat controller drives all state variables of the system (5.15) to zero in $\nu = \eta = 2$ time steps.

6. MINIMUM GAIN DEAD-BEAT CONTROLLERS

Time-invariant dead-beat regulators were derived in the previous sections. In this section time-variable dead-beat controllers are considered. The regulators are obtained by constructing control laws for systems S(A,B,C) which give input signals minimizing the criterion

$$\min_{u_t, u_{t+1}, \ldots, u_{t_1-1}} x'_{t_1} Q_0 x_{t_1}, \quad Q_0 \geq 0 \tag{6.1}$$

It turns out that these control laws are not unique. To obtain a unique sequence of control laws the minimum gain dead-beat controller is chosen.

Preliminaries

The solution to the problem (6.1) is given by the following lemma. A similar result has been proved in [11].

Lemma 6.1: Assume that $S(A,B,C) \in S^1$. The solution to the optimization problem

$$\min_{u_t, u_{t+1}, \ldots, u_{t_1-1}} x'_{t_1} Q_0 x_{t_1}, \quad Q_0 \geq 0 \tag{6.1}$$

is given by

$$u_s = L_s x_s, \quad s = t, t+1, \ldots, t_1-1 \tag{6.2}$$

where

$$L_t = - (B'S_{t+1}B)^{+}B'S_{t+1}A \tag{6.3}$$

and S_t is given by the recursive equation

$$S_t = A'S_{t+1}A - A'S_{t+1}B(B'S_{t+1}B)^{+}B'S_{t+1}A$$

$$= (A+BL_t)'S_{t+1}A = (A+BL_t)'S_{t+1}(A+BL_t)$$

$$S_{t_1} = Q_0 \tag{6.4}$$

If $u_s = F_s x_s$ for $s = t, t+1, \ldots, t_1-1$ is any other solution to the optimization problem,

$$\min_{u_t}(\min_{u_{t+1}} (\ldots(\min_{u_{t_1-1}} x'_{t_1} Q_0 x_{t_1}) \ldots)) \tag{6.1a}$$

then

$$F_s'F_s \geq L_s'L_s, \quad s = t, t+1, \ldots, t_1-1 \tag{6.5}$$

Moreover, the minimum value of the performance index (6.1) is given by

$$V(x_t,t) = x_t'S_t x_t \tag{6.6}$$

The lemma is proved in the Appendix 6A.

In order to rewrite the Riccati equation (6.4) the following lemma is useful.

Lemma 6.2: Assume that $U_0, U_1, \ldots, U_{\ell-1}$ is a sequence of $n \times p$ matrices. Let

$$P_{k+1} = P_k - P_k U_k (U_k'P_k U_k)^{+} U_k'P_k, \quad k = 0, 1, \ldots, \ell-1$$

$$P_0 = I \tag{6.7}$$

and let

$$Q_k = I - T_k T_k^+, \qquad k = 0, 1, 2, \ldots, \ell \tag{6.8}$$

where

$$T_k = \sum_{i=0}^{k-1} U_i U_i' = [U_0, U_1, \ldots, U_{k-1}][U_0, U_1, \ldots, U_{k-1}]'$$

$$T_0 = 0 \tag{6.9}$$

Then $P_k = Q_k$ and Q_k is the orthogonal projection of $X = \mathbb{R}^n$ on $\mathrm{Im}([U_0, U_1, \ldots, U_{k-1}])^\perp$ for all $k \in \underline{\ell}_0$.

The Appendix A contains a proof of the lemma.

By means of Lemma 6.2 it is now straightforward to obtain an explicit solution to the Riccati equation (6.4).

Lemma 6.3: Assume that $S(A,B,C) \in S^1$. Let

$$S_{t_1-k} = A'S_{t_1-(k-1)}A - A'S_{t_1-(k-1)}B(B'S_{t_1-(k-1)}B)^+B'S_{t_1-(k-1)}A$$

$$k = 1, 2, \ldots, \ell$$

$$S_{t_1} = C'C \tag{6.10}$$

and let

$$Q_k = I - T_k T_k^+$$

$$T_k = \sum_{i=0}^{k-1} CA^iB(CA^iB)' = [CB, CAB, \ldots, CA^{k-1}B][CB, CAB, \ldots, CA^{k-1}B]' \triangleq$$

$$\triangleq M_k M_k'$$

$$T_0 = M_0 = 0 \tag{6.11}$$

Then

$$S_{t_1-k} = A'^{k} C' Q_k C A^k, \quad k = 0, 1, \ldots, \ell \tag{6.12}$$

where Q_k is the orthogonal projection of $X = \mathbb{R}^n$ on $\mathrm{Im}(M_k)^{\perp}$ for all $k \in \underline{\ell}_0$.

The lemma is proved in the Appendix A.

Consider a system $S(A,B,C) \in S^3$. By (3.2), the output of this system at the k:th sampling instant is

$$y_k = CA^k x_0 + M_k \beta_k' \tag{6.13}$$

where $\beta_k = [u_{k-1}', u_{k-2}', \ldots, u_0']$ contains the sequence of control vectors and x_0 is the state at $t = 0$. Necessary and sufficient conditions for the existence of a sequence of control vectors β_k which forces the output of the system $S(A,B,C)$ from any initial state to the origin in at most k time steps is given by the following lemma.

Lemma 6.4: Assume that $S(A,B,C) \in S^3$. Then k is a positive integer such that $S_{t_1-k} = 0$ if and only if $\mathrm{rk}(M_k) = p$.

The lemma is proved in the Appendix A.

Define ξ as the least positive integer such that

$$S_{t_1-\xi} = 0 \tag{6.14}$$

It follows from Lemma 6.1 that a minimum gain dead-beat controller drives the state (output) of the system $S(A,B,C)$ from any initial state x_0 to zero in at most ξ time steps and that ξ is the least positive integer for which this is true.

Properties of the sequence $\{L_{t_1-k}\}_{k=1}^{\xi}$

Some properties of the sequence $\{L_{t_1-k}\}_{k=1}^{\xi}$ will be exploited here. It will be assumed from now on that the system $S(A,B,C)$ belongs to the class S^3.

Lemma 6.5: Assume that $S(A,B,C)\in S^3$. Then

$$\mathrm{Ker}(A+BL_{t_1-k}) = \mathrm{Im}\left(A^{-1}\bar{B}^{(k)}\right),\quad \bar{B}^{(k)}=B(B'S_{t_1-(k-1)}B)^{+},\quad k\in\underline{\xi} \tag{6.15a}$$

$$\mathrm{Ker}(L_{t_1-k})\supset\mathrm{Im}\left([A^{-2}B,\ A^{-3}B,\ldots,A^{-k}B]\right),\qquad k=2,3,\ldots,\xi \tag{6.15b}$$

$$\mathrm{Ker}(A+BL_{t_1-k})\cap\mathrm{Ker}(L_{t_1-k}) = 0,\qquad k=2,3,\ldots,\xi \tag{6.15c}$$

The lemma is proved in the Appendix 6A.

Introduce the following notation

$$\bar{B}^{(k)} = B(B'S_{t_1-(k-1)}B)^{+}$$

$$\bar{r}_k = \mathrm{rk}(\bar{B}^{(k)}),\qquad k\in\underline{\xi} \tag{6.16}$$

Since $\mathrm{Ker}(B) = 0$, it follows from (2.8b) that

$$\bar{r}_k = \mathrm{rk}\left((B'S_{t_1-(k-1)}B)^{+}\right) = \mathrm{rk}(B'S_{t_1-(k-1)}B),\quad k\in\underline{\xi} \tag{6.17}$$

Lemma 6.6: Assume that $S(A,B,C)\in S^3$. Then

$$\mathrm{Ker}\left((A+BL_{t_1-k})^{k}\right) = \mathrm{Im}\left([A^{-1}\bar{B}^{(k)},\ A^{-2}\bar{B}^{(k)},\ \ldots,\ A^{-k}\bar{B}^{(k)}]\right) \tag{6.18a}$$

$$\nu\left((A+BL_{t_1-k})^{k}\right) = k\cdot\bar{r}_k,\qquad k\in\underline{\xi} \tag{6.18b}$$

A proof of the lemma is given in the Appendix 6A.

The sequence $\{\bar{r}_k\}_{k=1}^{\xi}$ reflects some fundamental properties of the reachability matrix W_ξ when $Q_0 = I$. This is established by the following lemma.

Lemma 6.7: Let $S(A,B,C)\in S^3$ and let $Q_0 = I$. Then

$\{\bar{r}_i\}_{i=1}^{\xi}$ is a non-increasing sequence of integers (6.19a)

$\bar{r}_k = m \Leftrightarrow \mathrm{Im}(A^{k-1}B)\cap\mathrm{Im}\left([B,AB,\ldots,A^{k-2}B]\right) = 0, k\in\{2,3,\ldots,\xi\}$ (6.19b)

$\bar{r}_\xi = m \Leftrightarrow \mathcal{X} = \mathcal{B}\oplus A\mathcal{B}\oplus \ldots \oplus A^{\xi-1}\mathcal{B}$ (6.19c)

The lemma is proved in the Appendix 6A.

Main result

When $Q_0 = I$ the theorem stated here gives necessary and sufficient conditions for the gain $L_{t_1-\xi}$ of the time-variable dead-beat controller to be a time-invariant dead-beat controller. Apart from being a curiosity, the result is practically useful because it gives an alternative method for computing a state dead-beat controller. When using Theorem 3.1 to construct such a controller, it is necessary to select a number of linearly independent column vectors from the reachability matrix W_ξ which requires tests. If Theorem 6.1 may be used, the state dead-beat controller is obtained simply by iterating the Riccati equation (6.4). This is a numerically well conditioned procedure. It is still an open problem if the output dead-beat controller may be obtained in a similar way.

Theorem 6.1: Let $S(A,B,C)\in S^3$ and let $Q_0 = I$. Then $L_{t_1-\xi}$ is a state dead-beat controller if and only if $\bar{r}_\xi = m$.

Proof: (only if) Assume that $L_{t_1-\xi}$ is a state dead-beat controller. Then, by (3.4), ξ is the smallest positive integer such that

$$n = \mathrm{rk}\left([B,\ AB,\ \ldots,\ A^{\xi-1}B]\right) \tag{6.20}$$

Moreover, (6.18a) implies that

$$\begin{aligned} n &= \mathrm{rk}\left([A^{-1}\bar{B}(\xi),\ A^{-2}\bar{B}(\xi),\ \ldots,\ A^{-\xi}\bar{B}(\xi)]\right) \\ &= \mathrm{rk}\left([\bar{B}(\xi),\ A\bar{B}(\xi),\ \ldots,\ A^{\xi-1}\bar{B}(\xi)]\right) \end{aligned} \tag{6.21}$$

since A is invertable. Together (6.20) and (6.21) give $\bar{r}_\xi = m$.

(if) Assume that $\bar{r}_\xi = m$. Then (6.19c) yields that

$$X = B \oplus AB \oplus \ldots \oplus A^{\xi-1}B \tag{6.22}$$

Therefore, by (6.18a), it follows that

$$\nu\left((A+BL_{t_1-\xi})^{\xi}\right) = \xi \cdot \bar{r}_\xi = \xi \cdot m = n \tag{6.23}$$

Hence $L_{t_1-\xi}$ is a state dead-beat controller. □

Remark: For a single-input system S(A,B,C) the gain $L_{t_1-\xi}$ is always a state dead-beat controller.

Example 6.1: A state dead-beat controller for the following system was constructed in Example 3.1.

$$x_{t+1} = \begin{bmatrix} 1 & 0 & 0 \\ 0 & 0.9 & 0 \\ 0 & 0 & 0.8 \end{bmatrix} x_t + \begin{bmatrix} 1 & 1 \\ 1 & 0 \\ 2 & 1 \end{bmatrix} u_t \qquad (3.13) = (6.24)$$

In that example it was found that the system belonged to the class S^3, and that $\nu = 2$. Here a minimal gain dead-beat controller which drives the state of the system (6.24) from any initial state to zero in at most $\nu = 2$ time steps will be constructed. Provided that $Q_0 = I$, Lemma 6.1 yields that

$$S_{t_1} = \begin{bmatrix} 1 & 0 & 0 \\ 0 & 1 & 0 \\ 0 & 0 & 1 \end{bmatrix}$$

$$S_{t_1-1} = \begin{bmatrix} 0.33333 & 0.3 & -0.26667 \\ -0.3 & 0.27 & -0.24 \\ -0.26667 & -0.24 & 0.21333 \end{bmatrix}$$

$$S_{t_1-2} = 0 \tag{6.25}$$

and

$$L_{t_1-1} = \begin{bmatrix} 0.33333 & -0.6 & -0.26667 \\ -1 & 0.9 & 0 \end{bmatrix}$$

$$L_{t_1-2} = \begin{bmatrix} -2.30769 & -1.86923 & 1.47692 \\ -1.53846 & -1.24615 & 0.98462 \end{bmatrix} \qquad (6.26)$$

The matrix S_{t_1-k} becomes zero in $k = 2$ time steps. The matrices $A+BL_{t_1-1}$ and $A+BL_{t_1-2}$ become

$$A+BL_{t_1-1} = \begin{bmatrix} -2.84615 & -3.11538 & 2.46154 \\ -2.30769 & -0.96932 & 1.47692 \\ -6.15384 & -4.98461 & 4.73846 \end{bmatrix} \qquad (6.27)$$

and

$$A+BL_{t_1-2} = \begin{bmatrix} 0.33333 & 0.3 & -0.26667 \\ 0.33333 & 0.3 & -0.26667 \\ -0.33333 & -0.3 & 0.26667 \end{bmatrix} x_t \qquad (6.28)$$

respectively. The ch.p. of (6.27) and (6.28) are

$$d(z) = z^2(z-0.92308) \qquad (6.29)$$

and

$$d(z) = z^2(z-0.9) \qquad (6.30)$$

respectively. By (6.30), L_{t_1-2} is not a state dead-beat controller.

For $x_0 = (111)'$ the trajectory and input sequence of the closed loop system

$$x_{t+1} = \begin{bmatrix} 1 & 0 & 0 \\ 0 & 0.9 & 0 \\ 0 & 0 & 0.8 \end{bmatrix} x_t + \begin{bmatrix} 1 & 1 \\ 1 & 0 \\ 2 & 1 \end{bmatrix} u_t$$

$$u_t = L_t x_t \tag{6.31}$$

becomes

t	0	1	2	t	0	1
x_t	$\begin{bmatrix} 1 \\ 1 \\ 1 \end{bmatrix}$	$\begin{bmatrix} -3.5 \\ -1.8 \\ -6.4 \end{bmatrix}$	$\begin{bmatrix} 0 \\ 0 \\ 0 \end{bmatrix}$	u_t	$\begin{bmatrix} -2.7 \\ \\ -1.8 \end{bmatrix}$	$\begin{bmatrix} 1.62 \\ \\ 1.88 \end{bmatrix}$

(6.32)

where $t_1 = \nu$ have been used.

In the table below the norms of the input signals $\{u_i\}'_{t=0}$ of the system (6.24) are shown for $x_0 = (111)'$ when the system is controlled with the state dead-beat controllers L_1 and L_2 in Example 3.1 and the minimum gain dead-beat controller $\{L_{t_1-k}\}_{k=1}^{2}$.

$\|u(t)\| = \sqrt{u_1(t)^2 + u_2(t)^2}$ Controller		t=0	t=1
State dead-beat controller (Example 3.1)	L_1	4.04853	2.82857
	L_2	4.58912	4.4
Minimum gain dead beat controller $\{L_{t_1-i}\}_{i=1}^{2}$		3.245	2.48169

Notice that the norms of the input vectors $\{u_t\}_{t=0}^{1}$ are smaller when the system (6.24) is controlled by the minimum gain controller compared to the time-invariant controllers.

Example 6.2: An output dead-beat controller was derived for the following system in Example 4.1

$$x_{t+1} = \begin{bmatrix} 1.9 & -1.5 & 0.4 \\ 1 & 0 & 0 \\ 0 & 1 & 0 \end{bmatrix} x_t + \begin{bmatrix} 1 \\ 0 \\ 0 \end{bmatrix} u_t$$

$$y_t = \begin{bmatrix} 1 & -1.8 & 0.8 \\ 1 & -1.3 & 0.4 \end{bmatrix} x_t \qquad (4.30) = (6.33)$$

In that example it was found that the system belonged to the class S^3 and that $\mu = 2$. Here a minimal gain dead-beat controller which forces the output of the system (6.33) from any initial state to zero in at most $\mu = 2$ time steps will be constructed. When $Q_0 = C'C$ Lemma 6.1 yields that

$$S_{t_1} = \begin{bmatrix} 2 & -3.1 & 1.2 \\ -3.1 & 4.93 & -1.96 \\ 1.2 & -1.96 & 0.8 \end{bmatrix}$$

$$S_{t_1-1} = \begin{bmatrix} 0.125 & -0.1 & 0 \\ -0.1 & 0.08 & 0 \\ 0 & 0 & 0 \end{bmatrix}$$

$$S_{t_1-2} = 0 \qquad (6.34)$$

and

$$L_{t_1-1} = [-0.35 \quad 0.9 \quad -0.4]$$

$$L_{t_1-2} = [-1.1 \quad 1.5 \quad -0.4] \qquad (6.35)$$

The matrix S_{t_1-k} become zero in $k = 2$ time steps. The matrices $A+BL_{t_1-1}$ and $A+BL_{t_1-2}$ become

$$A+BL_{t_1-1} = \begin{bmatrix} 1.55 & -0.6 & 0 \\ 1 & 0 & 0 \\ 0 & 1 & 0 \end{bmatrix} \qquad (6.36)$$

and

$$A+BL_{t_1-2} = \begin{bmatrix} 0.8 & 0 & 0 \\ 1 & 0 & 0 \\ 0 & 1 & 0 \end{bmatrix} \tag{6.37}$$

respectively. The ch.p. of (6.36) and (6.37) are

$$d(z) = z(z-1.55)(z+0.6) \tag{6.38}$$

and

$$d(z) = z^2(z-0.8) \tag{6.39}$$

respectively. Notice that the controller L_{t_1-2} is equal to the controller L in Example 4.1. Hence $L_{t_1-2} \in \underline{L}(V^M)$.

7. DISCUSSION ON SYSTEM CLASSES

The theory in the previous sections has arisen from efforts to find synthesis methods for designing multivariable sampled-data control systems. The plant is assumed to be governed by linear differential equations with constant coefficients of the form

$$\dot{x} = A_c x + B_c u$$

$$y = C_c x \tag{7.1}$$

It is also assumed that the sampling period is constant. At the sampling instants the behaviour of the system (7.1) is described by the equation (2.11). This means that any sampled-data system (7.1) will at least belong to the system class $\mathcal{S}^1$.

System class $\mathcal{S}^2$

In this class it is assumed that the system S(A,B,C) has no redundant inputs or measurements and that an arbitrary state $x_1 \in X$ can be reached from the origin. Geometrically these conditions correspond to Ker(B) = Ker(C') = 0 and $\{A|\mathcal{B}\} = X$ respectively.

The two first assumptions are introduced merely for notational convenience. If the third assumption is not satisfied, then the results, given in the previous sections should be applied to the reachable subspace $\{A|B\}$ instead of the space X.

System class S^3

It is well known that the matrix A of any system S(A,B,C) obtained by sampling the continuous system (7.1) is invertable. Therefore, it seems very natural to consider only systems S(A,B,C) which belong to the class S^3. However, it might also be of interest to control linear time-invariant systems with time delays. These systems will in general not belong to the class S^3. The different chains of time delays associated with such a system will give nilpotent submatrices in the Jordan canonical form of the A-matrix of the system.

It is, however, possible to construct suboptimal controllers for a discrete-time system with a singular A-matrix. According to [8] any map $A: X \to X$ can be reduced in the following way

$$A = A|T_q \oplus A|N_q \tag{7.2}$$

where q is the least positive integer such that $\mathrm{Ker}(A^q) = \mathrm{Ker}(A^{q+1})$ $T_q = \mathrm{Im}(A^q)$, $N_q = \mathrm{Ker}(A^q)$, $A|T_q$ is invertable and $A|N_q$ is nilpotent of index q. Let $\{e_i\}_{i=1}^{\ell}$ and $\{e_i\}_{i=\ell+1}^{n}$ be bases for T_q and N_q respectively and choose $\{e_i\}_{i=1}^{n}$ as a basis for X. Then, in this basis, the system (2.11) takes the form

$$z_{t+1} = \begin{bmatrix} A_1 & 0 \\ 0 & A_2 \end{bmatrix} z_t + \begin{bmatrix} B_1 \\ B_2 \end{bmatrix} u_t$$

$$y_t = [C_1 \quad C_2] z_t \tag{7.3}$$

where A_1 is invertable and A_2 is nilpotent of index q.

By construction the system $S(A_1,B_1,C_1)$ belongs to the class S^3. Let L_1 be a linear feedback from the state variables of the sub-

system $S(A_1,B_1,C_1)$. The system (7.3) controlled with this feedback becomes

$$z_{t+1} = \begin{bmatrix} A_1+B_1L_1 & 0 \\ B_2L_1 & A_2 \end{bmatrix} z_t$$

$$y_t = (C_1 \quad C_2) z_t \tag{7.4}$$

A suboptimal state dead-beat controller of the system (7.3) can now simply be obtained by letting L_1 be a state dead-beat controller of the subsystem $S(A_1,B_1,C_1)$. Provided that $A_1+B_1L_1$ is nilpotent of index s any initial state of (7.4) will become zero in at most s+q time steps. Specially, it is possible to show that for a system (7.3) with only one input then n = s + q and there exists no linear feedback (3.1) which forces any initial state of the system (7.3) to zero in less than n time steps.

Consider the problem of constructing a suboptimal output dead-beat controller for the system (7.3). In the special cases when $B_2 = 0$ or $C_2 = 0$ such a controller is obtained by choosing L_1 as an output dead-beat controller of the subsystem $S(A_1,B_1,C_1)$. However, in the general case this procedure will not work, since A_1+BL_1 is not nilpotent. This means that the state variable of the subsystem $S(A_1,B_1,C_1)$ will not decay to zero and, consequently, the output may remains different from zero for all future times. It should be pointed out that by letting L_1 be a state dead-beat controller of the subsystem $S(A_1,B_1,C_1)$, then the output of the system (7.4) will always become zero in no more than s+q time steps for any initial state. Therefore, this controller is a suboptimal output dead-beat controller.

System class S^4

The class S^4 consists of all systems $S(A,B,C) \in S^3$ which satisfy the condition $V^M \cap A^{-1}B = 0$. This condition is a technical condition which guarantees that no generalized eigenvector space of A+BL, contained in V^M, is associated with the eigenvalue $\lambda = 0$ for any

$L \in \underline{L}(\mathcal{V}^M)$. For a left invertable system the condition is equivalent to that the system has no zeroes [3] at the origin. If the discrete-time system is obtained by sampling a continuous system, then in general only very special choices of the sampling period will give systems S(A,B,C) with zeroes at the origin. However, for other discrete-time systems zeroes at the origin arise quite naturally. It is natural to introduce the restriction $\mathcal{V}^M \cap A^{-1}\mathcal{B} = 0$, since the algorithms for computing output dead-beat controllers are essentially clarified and simplified when a system fulfils the restriction.

Consider the problem of constructing suboptimal output dead-beat controllers for left invertable systems which belong to the class S^3 but not to the class S^4. Let L_0 be a given element in the feedback $\underline{L}(\mathcal{V}^M)$. Assume that $d_0(z)$ = ch.p. of $(A+BL_0)|\mathcal{V}^M$. Factor $d_0(z) = d^0(z)d^+(z)$ so that the complex zeroes of $d^0(z)$ and $d^+(z)$ belong to $\mathbb{C}^0 = \{z|z=0\}$ and $\mathbb{C}^+ = \{z||z|>0\}$ respectively. Then there exists a unique decomposition of $\mathcal{V}^M$ such that

$$\mathcal{V}^M = \mathcal{V}^{M0} \oplus \mathcal{V}^{M+}$$

$$(A+BL_0)\mathcal{V}^{M0} \subset \mathcal{V}^{M0}$$

$$(A+BL_0)\mathcal{V}^{M+} \subset \mathcal{V}^{M+} \qquad (7.5)$$

and

$$d^0(z) = \text{ch.p. of } (A+BL_0)|\mathcal{V}^{M0}$$

$$d^+(z) = \text{ch.p. of } (A+BL_0)|\mathcal{V}^{M+} \qquad (7.6)$$

By construction no generalized eigenvector space of $A+BL_0$, contained in $\mathcal{V}^{M+}$, is associated with the eigenvalue $\lambda = 0$. Since $\mathcal{V}^{M0}$ belongs to the generalized eigenvector space of $A+BL_0$ associated with the eigenvalue $\lambda = 0$, there exists a smallest positive integer ℓ such that

$$\mathcal{V}^{M0} \subset A^{-1}\mathcal{B} + A^{-2}\mathcal{B} + \ldots + A^{-\ell}\mathcal{B} \qquad (7.7)$$

Define μ is the least positive integer such that

$$X = Z_{\mu} + V^{M} \tag{7.8}$$

Now assume that $\ell \leq \mu$. Then (7.7) and (7.8) imply that

$$\begin{aligned} X &= \mathrm{Im}\left([A^{-1}B,\ A^{-2}B,\ \ldots,\ A^{-\mu}B,\ V^{M}] \right) \\ &= \mathrm{Im}\left([A^{-1}B,\ A^{-2}B,\ \ldots,\ A^{-\mu}B,\ V^{M^+}] \right) \end{aligned} \tag{7.9}$$

where V^{M} and V^{M^+} are basis matrices for V^{M} and V^{M^+} respectively. If $(\overline{A+BL_0})$ is the induced matrix representation for $(A+BL_0)|V^{M^+}$, then (7.5) gives that

$$(A+BL_0)V^{M^+} = V^{M^+}(\overline{A+BL_0}) \tag{7.10}$$

Therefore

$$V^{M^+} = A^{-1}V^{M^+}(\overline{A+BL_0}) - A^{-1}BL_0V^{M^+} \tag{7.11}$$

By (7.9) and (7.11)

$$X = \mathrm{Im}\left([A^{-1}B,\ A^{-2}B,\ \ldots,\ A^{-\mu}B,\ A^{-1}V^{M^+}] \right) \tag{7.12}$$

since $(\overline{A+BL_0})$ is invertable. Moreover, since $(\overline{A+BL_0})$ is invertable, the selection procedure (SP2) may be used to select n linearly independent column vectors from the full rank matrix

$$\left[A^{-1}B,\ A^{-2}B,\ \ldots,\ A^{-\mu}B,\ A^{-1}V^{M^+} \right] \tag{7.13}$$

Then a suboptimal output dead-beat controller can be calculated by means of Theorem 4.1. This controller will force the output of the system $S(A,B,C)$ to zero in at most μ time steps and thereafter keep the output zero for any initial state $x_0 \in X$.

It can be shown that for any single-input system $S(A,B,C) \in S^3$ this procedure gives a dead-beat controller which forces the output of

the system S(A,B,C) from any initial state to zero in a minimal number of time steps and thereafter keeps the output zero. The minimum number of time steps required is always less than $\mu - \dim(V^{M^0})$. This means that the suboptimal dead-beat controller is in fact a strict output dead-beat controller.

Example 7.1: Consider a system with one input and one output

$$G(z) = \frac{z^2}{z^3 - 1.9z^2 + 1.5z - 0.4} \tag{7.14}$$

A minimal realization of the system is given by

$$x_{t+1} = \begin{bmatrix} 1.9 & -1.5 & 0.4 \\ 1 & 0 & 0 \\ 0 & 1 & 0 \end{bmatrix} x_t + \begin{bmatrix} 1 \\ 0 \\ 0 \end{bmatrix} u_t$$

$$y_t = [1 \quad 0 \quad 0] x_t \tag{7.15}$$

It is straightforward to show that the system belongs to the class S^3. According to (2.3), the maximal (A,B)-invariant subspace in Ker(C) becomes

$$V^M = \mathrm{Im} \begin{bmatrix} 0 & 0 \\ 0 & 1 \\ 1 & 0 \end{bmatrix} \tag{7.16}$$

The system (7.15) is left invertable, since Ker(B) = 0 and $V^M \cap \mathcal{B} = 0$. Straightforward calculations give that

$$A^{-1}\mathcal{B} = \mathrm{Im} \begin{bmatrix} 0 \\ 0 \\ 2.5 \end{bmatrix}, \quad A^{-2}\mathcal{B} = \mathrm{Im} \begin{bmatrix} 0 \\ 2.5 \\ 9.375 \end{bmatrix}, \quad A^{-3}\mathcal{B} = \mathrm{Im} \begin{bmatrix} 2.5 \\ 9.375 \\ 23.2813 \end{bmatrix} \tag{7.17}$$

By (7.17) and (7.18)

$$V^M \subset A^{-1}\mathcal{B} + A^{-2}\mathcal{B} \tag{7.18}$$

An element in the feedback class $\underline{L}(\mathcal{V}^M)$ is

$$L_0 = [0 \quad 1.5 \quad -0.4] \tag{7.19}$$

since $(A+BL_0)\,\mathcal{V}^M \subset \mathcal{V}^M$. Moreover, $(A+BL_0)^2\,\mathcal{V}^M = 0$ and, consequently

$$\mathcal{V}^{M0} = \mathcal{V}^M$$

$$\mathcal{V}^{M+} = 0 \tag{7.20}$$

Thus the suboptimal output dead-beat controller of the system (7.15) is a state dead-beat controller. The state dead-beat controller of this system is

$$L = [-1.9 \quad 1.5 \quad -0.4] \tag{7.21}$$

The closed loop system associated with the controller L is

$$x_{t+1} = \begin{bmatrix} 0 & 0 & 0 \\ 1 & 0 & 0 \\ 0 & 1 & 0 \end{bmatrix} x_t$$

$$y_t = [1 \quad 0 \quad 0]x_t \tag{7.22}$$

Assume that V^M is a basis matrix for $\mathcal{V}^M$. Then since

$$(A+BL)V^M = \begin{bmatrix} 0 & 0 \\ 0 & 1 \\ 1 & 0 \end{bmatrix} \begin{bmatrix} 0 & 1 \\ 0 & 0 \end{bmatrix} \tag{7.23}$$

it follows that $L \in \underline{L}(\mathcal{V}^M)$. The ch.p. of A+BL becomes

$$d(z) = z^3 \tag{7.24}$$

According to (7.17) and (7.18), $\mu = 3$ is the least positive integer such that $X = Z_\mu + \mathcal{V}^M$. However, $C(A+BL) = 0$ and, thus, the output of the system (7.15) is forced to zero in at most 1 time step for any initial state x_0. This clearly demonstrates that the condition $S(A,B,C) \in S^3$ is crucial for Lemma 4.3 to hold. It should

be observed that in this particular example the suboptimal dead-beat controller is a strict output dead-beat controller.

8. ENGINEERING ASPECTS

In this section some engineering aspects on the dead-beat controllers are gathered.

Zeroes

When using output dead-beat controllers the behaviour of the closed loop system is drastically influenced by the zeroes [3] of the system. As shown by Theorem 4.1 those zeroes always appear as poles of the closed loop system. This means that the closed loop system is unstable if any of the zeroes are located outside the unit circle. According to Theorem 5.1, it is always possible to construct constrained output dead-beat controllers which yield a stable closed loop system. Example 5.1 demonstrates the fundamental role played by the zeroes when using output dead-beat control strategies.

Choice of sampling period

In some cases the dead-beat controllers may give unacceptably large control signals. If the plant has real poles or well damped dominant complex poles, the magnitude of the control signals can be decreased by choosing a larger sampling period. Thereby satisfactory control may be achieved. However, if the dominant complex poles of the process are poorly damped or if the process is unstable, then the aliasing effect or the instability give upper bounds for the length of sampling period possible to use. Such systems might only be well controlled by using other types of control strategies than the dead-beat control strategy. A nice example showing the influence of the length of the sampling period on the dead-beat control strategy is given in Section 4 of Chapter 7.

Reference values and state dead-beat controllers

A state $x_{ref} \in X$ is said to be an equilibrium point of the system (7.1) if there exists an input $u_{ref} \in U$ such that

$$A_c x_{ref} + B_c u_{ref} = 0 \tag{8.1}$$

Then putting

$$z = x - x_{ref}$$

$$v = u - u_{ref} \tag{8.2}$$

(7.1) may alternatively be written

$$\dot{z} = A_c z + B_c v \tag{8.3}$$

Therefore, if $v_t = L_t x_t$, $t = 0, 1, \ldots, t_1$, is a sampled-data controller which transfers the system (8.3) from its initial state z_0 to the origin, then the controller

$$u_t = L_t(x - x_{ref}) + u_{ref}, \quad t = 0, 1, \ldots, t_1 \tag{8.4}$$

transfers the system (7.1) from its initial state $z_0 + x_{ref}$ to the equilibrium point x_{ref}. The strategy (8.4) is used in Section 4 of Chapter 7 to control the profile of the diffusion process.

Numerical aspects

The algorithms for computing the time-invariant dead-beat controllers may be numerically ill-conditioned when the system $S(A,B,C) \in S^3$ has eigenvalues close to the origin. In such a case the decomposition (7.3) offers a neat way to overcome the numerical difficulties. Let the m.p. of the matrix A of the system $S(A,B,C)$ be $\alpha(z)$ and factor $\alpha(z) = \alpha^0(z)\alpha^+(z)$ where the complex zeroes of $\alpha^0(z)$ and $\alpha^+(z)$ belong to $\mathbb{C}^0 = \{z \mid |z| \leq \varepsilon\}$ and $\mathbb{C}^+ = \{z \mid |z| > \varepsilon\}$ respectively. Then choose the matrix A_1 and A_2 in (7.3) according to

$$A_1 = A|\mathrm{Ker}\left(\alpha^+(A)\right)$$

$$A_2 = A|\mathrm{Ker}\left(\alpha^0(A)\right)$$

which are the restrictions of A to $\mathrm{Ker}\left(\alpha^+(A)\right)$ and $\mathrm{Ker}\left(\alpha^0(A)\right)$.

By a proper choice of ε the matrix A_1 will always be numerically well-conditioned. The eigenvalues of the matrix A located in $\mathbb{C}^o$ correspond to the fast modes of the underlying continuous system. In general, the gain factors of these poles will be very small and, therefore, the matrix B_2 in (7.3) will be almost zero. This means that the modes of the matrix A_2 will only be slightly excited by the input u_t. Thus a controller constructed for the subsystem $S(A_1,B_1,C_1)$ can be satisfactorily used to control the complete system $S(A,B,C)$. The proposed method may be regarded as a method for model simplification. An example which illustrates the use of the method is given in Section 4 of Chapter 7.

9. REFERENCES

[1]: Ackerman, J.: "Zeitoptimale Mehrfach-Abtastregelsysteme", Preprint IFAC Symp. on Multivariable Control Systems, Band 1, Düsseldorf, 1968.

[2]: Albert, A.: "Regression and the Moore-Penrose pseudoinvers", Academic Press, New York, 1972.

[3]: Bengtsson, G.: "A theory for control of linear multivariable systems", Report 7341, Lund Inst. of Techn., Div. of Automatic Control, 1973.

[4]: Bengtsson, G.: "Lecture notes on a geometric theory for linear dynamical systems", Report 7410, Lund Inst. of Technology, Div. of Automatic Control, 1974.

[5]: Bergen, A.R. and Ragazzini, J.R.: "Sampled-data processing techniques for feedback control systems", Trans. AIEE, Vol.

73, II, 236-244, 1954.

[6]: Bertram, J.E. and Sarachik, P.E.: "On optimal computer control", Preprint 1st Int. IFAC Congr. on Automat. Contr., Vol. 2, 979-982, Moscow, 1960.

[7]: Farison, J.B. and Fu, F.C.: "The matrix properties of minimum-time discrete linear regulator control", IEEE Trans. Automat. Contr., AC-15, 390-391, 1970.

[8]: Halmos, P.R.: "Finite-dimensional vector spaces", 2nd ed., Van Nostrand, New York, 1958.

[9]: Kalman, R.E. and Bertram, J.E.: "General synthesis procedure for computer control of single and multiloop linear systems", Trans. AIEE, Vol. 77, II, 602-609, 1958.

[10]: Kalman, R.E.: "On the general theory of control systems", Preprint 1st IFAC Int. Congr. on Automat. Contr., Vol. 4, 2020-2030, Moscow, 1960.

[11]: Kalman, R.E. and Englar, T.S.: "A user's manual for ASP", NASA Report CR-745, 1966.

[12]: Kučera, V.: "The structure properties of time-optimal discrete linear control", IEEE Trans. Automat. Contr., AC-16, 375-377, 1971.

[13]: Kučera, V.: "State space approach to discrete linear control", Kybernetika, Vol. 8, 233-251, 1972.

[14]: Luenberger, D.G.: "Canonical forms for linear multivariable systems", IEEE Trans. Automat. Contr., AC-12, 290-293, 1967.

[15]: Morse, A.S. and Wonham, W.M.: "Status of noninteracting control", IEEE Trans. Automat. Contr., AC-16, 568-581, 1971.

[16]: Rosenbrock, H.H.: "On the design of linear multivariable systems", Proc. 3rd IFAC Congr., Vol. 1, 1A-9A, 1966.

[17]: Wonham, W.M. and Morse, A.S.: "Decoupling and pole assignement in linear multivariable systems - A geometric approach", SIAM J. Contr., Vol. 8, 1-18, 1970.

[18]: Wonham, W.M.: "Linear multivariable control - A geometric approach", Springer-Verlag, New York, 1974.

APPENDIX 6A

PROOFS OF THE LEMMAS

Proof of Lemma 4.1

Assume that $(A+BL)\,|\,\mathcal{V}^M$ is singular for some $L\in\underline{L}(\mathcal{V}^M)$. Then there exists a vector $0 \neq v\in\mathcal{V}^M$ such that

$$(A+BL)v = 0 \tag{A.1}$$

which implies that $0 \neq v\in A^{-1}\mathcal{B}$. Thus $0 \neq v\in\mathcal{V}^M\cap A^{-1}\mathcal{B}$. This contradiction completes the proof.

□

Proof of Lemma 4.2

(4.2a): Clearly

$$0 = \hat{\mathcal{V}}\cap(\mathcal{V}^M\cap\mathcal{B}) = (\hat{\mathcal{V}}\cap\mathcal{V}^M)\cap\mathcal{B} = \hat{\mathcal{V}}\cap\mathcal{B} \tag{A.2}$$

(4.2b): Since $\mathcal{V}^M\supset\hat{\mathcal{V}}$ is an (A,B)-invariant subspace

$$A\hat{\mathcal{V}}\subset\mathcal{V}^M + \mathcal{B} = \hat{\mathcal{V}}\oplus\mathcal{V}^M\cap\mathcal{B} + \mathcal{B} = \hat{\mathcal{V}} + \mathcal{B} \tag{A.3}$$

(4.2c): By (4.2b), $\mathcal{V}^M\cap\hat{\mathcal{V}} = \hat{\mathcal{V}}$ is an (A,B)-invariant subspace and, therefore, it follows from [4] that $\hat{\mathcal{V}}$ and $\hat{\mathcal{V}}^M$ are compatible.

(4.2d): According to (4.2c) there exists a $0 \neq L\in\underline{L}(\hat{\mathcal{V}})\cap\underline{L}(\mathcal{V}^M)$. Then $\hat{\mathcal{V}}$ and $\mathcal{V}^M$ are two $(A+BL)$-invariant subspaces. Since $\hat{\mathcal{V}}\subset\mathcal{V}^M$, [4] implies that $d_1(z)$ = ch.p. of $(A+BL)\,|\,\hat{\mathcal{V}}$ divides $d_2(z)$ = ch.p. of $(A+BL)\,|\,\mathcal{V}^M$.

□

Lemma 4.4: Let $S(A,B,C) \in S^3$. If $rk[A^{-1}B, A^{-2}B, \ldots, A^{-\mu}B, A^{-1}\hat{v}] = n$, then the selection procedure (SP2) does not terminate until n linearly independent vectors have been selected.

Proof: Assume that the selected vectors are

$$A^{-1}\hat{v}_1, A^{-1}\hat{v}_2, \ldots, A^{-1}\hat{v}_{\hat{s}}, A^{-1}b_1, A^{-2}b_1, \ldots, A^{-\hat{r}_1}b_1, A^{-1}b_2, A^{-2}b_2, \ldots, \ldots, \ldots, A^{-\hat{r}_m}b_m \quad (A.4)$$

and that each of the vectors

$$A^{-\hat{r}_1-1}b_1, A^{-\hat{r}_2-1}b_2, \ldots, A^{-\hat{r}_m-1}b_m \quad (A.5)$$

are linearly dependent on the selected vectors in (A.4), so that the process (SP2) terminates. Then

$$A^{-\hat{r}_k-2}b_k = A^{-1}A^{-\hat{r}_k-1}b_k =$$

$$= A^{-1}\left(\sum_{i=1}^{\hat{s}} \alpha_{0i}A^{-1}\hat{v}_1 + \sum_{i=1}^{m}\sum_{j=1}^{\hat{r}_i} \alpha_{ij}A^{-j}b_i\right), \quad k \in \underline{m} \quad (A.6)$$

where $\alpha_{01}, \alpha_{02}, \ldots, \alpha_{0\hat{s}}, \alpha_{11}, \alpha_{12}, \ldots, \ldots, \ldots, \alpha_{m\hat{r}_m}$ are scalars.

By hypothesis, A^{-1} times any selected vector

$$A^{-1}b_1, A^{-2}b_1, \ldots, A^{-\hat{r}_1}b_1, A^{-1}b_2, A^{-2}b_2, \ldots, \ldots, \ldots, A^{-\hat{r}_m}b_m \quad (A.7)$$

is a linear combination of the vectors in (A.4). By multiplying (4.10) with A^{-1} and rearranging terms it follows that

$$A^{-2}\hat{V}(\overline{A+BL_0}) = A^{-1}\hat{V} + A^{-2}BL_0\hat{V} \quad (A.8)$$

Then

$$\begin{aligned}\mathrm{Im}(A^{-2}\hat{V}) &= \mathrm{Im}\Big(A^{-2}\hat{V}(\overline{A+BL_0})\Big)\\ &\subset \mathrm{Im}\Big([A^{-1}\hat{V},\ A^{-2}BL_0\hat{V}]\Big)\\ &\subset \mathrm{Im}\Big([A^{-1}\hat{V},\ A^{-1}B(1),\ A^{-2}B(2)]\Big)\end{aligned} \qquad (A.9)$$

Where the first equality follows since $(\overline{A+BL_0})$ is invertable, the second equality follows from (A.8) and the third equality follows from $\mathrm{Im}(GH)\subset\mathrm{Im}(G)$ and (SP2). Therefore, A^{-1} times any vector

$$A^{-1}\hat{v}_1,\ A^{-1}\hat{v}_2,\ \ldots,\ A^{-1}\hat{v}_s \qquad (A.10)$$

is also a linear combination of the vectors in (A.4).

Since A^{-1} times any vector in (A.7) and (A.10) is a linear combination of the vectors in (A.4), then (A.6) implies that $A^{-\hat{r}_k-2}b_k$ is contained in the subspace spanned by the vectors in (A.4) for all $k\in\underline{m}$. Therefore, by rewriting

$$A^{-\hat{r}_k-j}b_k = A^{-1}\cdot A^{-1}\ \ldots\ A^{-1}A^{-\hat{r}_k-1}, \quad j\geq 2 \qquad (A.11)$$

it follows that any power of A^{-1} times $A^{-\hat{r}_k}b_k$ is also a linear combination of the vectors in (A.4) for all $k\in\underline{m}$. Then the remaining vectors in (4.14) are linearly dependent on the selected vectors in (A.4). But since the vectors in (4.14) span X, the selection procedure cannot terminate until n linearly independent vectors have been selected. This completes the proof. □

Proof of Lemma 6.1

Introduce the optimal return function

$$V(x_t,t) = \min_{u_t,u_{t+1},\ \ldots,\ u_{t_1-1}} x'_{t_1}Q_0x_{t_1}, \quad Q_0\geq 0 \qquad (6.1) = (A.12)$$

associated with the starting point (x_t,t). By the principle of optimality it follows that

$$V(x_t,t) = \min_{u_t,u_{t+1},\ldots,u_{t_1-1}} x'_{t_1}Q_0x_{t_1}$$

$$= \min_{u_t}\left[\min_{u_{t+1},u_{t+2},\ldots,u_{t_1-1}} x'_{t_1}Q_0x_{t_1}\right] = \min_{u_t} V(x_{t+1},t+1) \qquad (A.13)$$

It is claimed that the functional equation (A.13) has a solution

$$V(x_t,t) = x'_tS_tx_t \qquad (A.14)$$

where S_t is a non-negative definite matrix. This assertion will be proved by induction. The statement is true for $s = t_1$, since $V(x_{t_1},t_1) = x'_tQ_0x_{t_1}$. Assume that the assertion is true for $s = t + 1$. Then there exists a unique non-negative symmetric matrix P_{t+1} such that

$$S_{t+1} = P_{t+1}P_{t+1} \qquad (A.15)$$

From (A.13) and (A.14) it then follows that

$$V(x_t,t) = \min_{u_t} V(x_{t+1},t+1) = \min_{u_t}[(Ax_t+Bu_t)'S_{t+1}(Ax_t+Bu_t)]$$

$$= \min_{u_t}\| P_{t+1}(Ax_t+Bu_t) \| = \min_{u_t}\| P_{t+1}Bu_t + P_{t+1}Ax_t \| \qquad (A.16)$$

By Lemma 2.1, the least squares minimum norm solution of (A.16) is given by

$$u_t^0 = -(P_{t+1}B)^+P_{t+1}Ax_t$$

$$= -(B'S_{t+1}B)^+B'S_{t+1}Ax_t \triangleq L_tx_t \qquad (A.17)$$

and the minimum value of the performance index is given by

$$V(x_t,t) = \left\| \left(I - P_{t+1}B(P_{t+1}B)^{+}\right)P_{t+1}Ax_t \right\|$$

$$= x_t' \left(A' P_{t+1} \left(I - P_{t+1}B(P_{t+1}B)^{+}\right) P_{t+1}A \right) x_t$$

$$= x_t' \left(A'S_{t+1}A - A'S_{t+1}B(B'S_{t+1}B)^{+}B'S_{t+1}A \right) x_t \qquad (A.18)$$

where (A.15) and (2.6b) have been used. Therefore, (A.14) is fulfilled with

$$S_t = A'S_{t+1}A - A'S_{t+1}B(B'S_{t+1}B)^{+}B'S_{t+1}A \qquad (A.19)$$

By (A.18), S_t is a non-negative definite matrix. This completes the induction.

Employing (A.15), (2.5b), (2.6a) and (2.6b), it follows that

$$(A+BL_t)'S_{t+1}B = \left(A' - A'S_{t+1}B(B'S_{t+1}B)^{+}B'\right)S_{t+1}B$$

$$= A'P_{t+1}P_{t+1}B - A'P_{t+1}P_{t+1}B(B'P_{t+1}P_{t+1}B)^{+}B'P_{t+1}P_{t+1}B$$

$$= A'P_{t+1}P_{t+1}B - A'P_{t+1}(P_{t+1}B)(P_{t+1}B)^{+}(P_{t+1}B)$$

$$= A'P_{t+1}P_{t+1}B - A'P_{t+1}P_{t+1}B = 0 \qquad (A.20)$$

Therefore, S_t may alternatively be written

$$S_t = (A+BL_t)'S_{t+1}A$$

$$= (A+BL_t)'S_{t+1}(A+BL_t) \qquad (A.21)$$

Let $u_s = F_s x_s$, $s = t, t+1, \ldots, t_1-1$, be any other solution of the optimization problem (6.1a). Then since $u_s^0 = L_s x_s$, $s = t, t = 1, \ldots, t_1-1$, is the minimum norm solution of (6.1a), it follows that

$$\| F_s x_s \| = \| u_s \| \geq \| u_s^0 \| = \| L_s x_s \|, \quad s = t, t+1, \ldots, t_1-1 \qquad (A.22)$$

which implies that

$$F_s'F_s \geq L_s'L_s, \quad s = t, t+1, \ldots, t_1-1 \tag{A.23}$$

The minimum value of the loss function is given by $V(x_t,t) = x_t S_t x_t$. This completes the proof. □

Proof of Lemma 6.2

It suffices to show that Q_k and P_k are both the unique orthogonal projection of X on $\mathrm{Im}([U_0, U_1, \ldots, U_{k-1}])^{\perp}$ for all $k \in \underline{\ell}_0$. By (2.7d) Q_k is the orthogonal projection of X on $\mathrm{Ker}(T_k')$ for all $k \in \underline{\ell}_0$. But

$$\mathrm{Ker}(T_k') = \mathrm{Im}(T_k)^{\perp} = \mathrm{Im}\left([U_0, U_1, \ldots, U_{k-1}]\right)^{\perp}, \quad k \in \underline{\ell}_0 \tag{A.24}$$

This proves the first part.

It remains to show that P_k is the orthogonal projection of X on $\mathrm{Im}([U_0, U_1, \ldots, U_{k-1}])^{\perp}$ for all $k \in \underline{\ell}_0$. This assertion is proved by induction. The statement is true for $k = 0$, since $P_0 = Q_0 = I$. Assume that the statement is true for index k, i.e.

$$P_k^2 = P_k$$

$$P_k' = P_k$$

$$\mathrm{Ker}(P_k) = \mathrm{Im}\left([U_0, U_1, \ldots, U_{k-1}]\right) \tag{A.25}$$

By hypothesis, (2.5b) and (2.6a), it follows that

$$\begin{aligned} P_{k+1}^2 &= \left(P_k - P_k U_k (U_k' P_k U_k)^{+} U_k' P_k\right)\left(P_k - P_k U_k (U_k' P_k U_k)^{+} U_k' P_k\right) \\ &= P_k - P_k U_k (U_k' P_k U_k)^{+} U_k' P_k - P_k U_k (U_k' P_k U_k)^{+} U_k' P_k \\ &\quad + P_k U_k (U_k' P_k U_k)^{+} U_k' P_k U_k (U_k' P_k U_k)^{+} U_k' P_K \\ &= P_k - P_k U_k (U_k' P_k U_k)^{+} U_k' P_k = P_{k+1} \end{aligned} \tag{A.26}$$

and

$$P'_{k+1} = \left(P_k - P_k U_k (U_k' P_k U_k)^{+} U_k' P_k\right)' = P_{k+1} \tag{A.27}$$

Moreover, the hypothesis and (2.6e) imply that

$$\begin{aligned} \mathrm{Ker}(P_{k+1}) &= \mathrm{Ker}\left(P_k - P_k U_k (U_k' P_k U_k)^{+} U_k' P_k\right) \\ &= \mathrm{Ker}\left(\left(I - P_k U_k (P_k U_k)^{+}\right) P_k\right) \\ &\supset \mathrm{Ker}(P_k) + \mathrm{Im}(U_k) = \mathrm{Im}\left([U_0, U_1, \ldots, U_k]\right) \end{aligned} \tag{A.28}$$

since $\mathrm{Ker}(GH) \supset \mathrm{Ker}(H)$ and since, by (2.5a) $\left(I - P_k U_k (P_k U_k)^{+}\right) P_k U_k = 0$.

But by hypothesis

$$\begin{aligned} \nu(P_{k+1}) &= \nu\left(\left(I - P_k U_k (P_k U_k)^{+}\right) P_k\right) \\ &= \nu(P_k) + \dim\left(\mathrm{Im}\left(P_k U_k (P_k U_k)^{+}\right) \cap \mathrm{Im}(P_k)\right) \\ &= \nu(P_k) + \dim\left(\mathrm{Im}(P_k U_k) \cap \mathrm{Im}(P_k)\right) \\ &= \nu(P_k) + \mathrm{rk}(P_k U_k) \leq \mathrm{rk}[U_0, U_1, \ldots, U_k] \end{aligned} \tag{A.29}$$

where the second equality follows from $\nu(GH) = \nu(H) + \dim\left(\mathrm{Ker}(G) \cap \mathrm{Im}(H)\right)$ and the third follows from (2.7c). It follows from (A.28) and (A.29) that

$$\mathrm{Ker}(P_{k+1}) = \mathrm{Im}\left([U_0, U_1, \ldots, U_k]\right) \tag{A.30}$$

This completes the induction and the proof.

□

Proof of Lemma 6.3

The assertion is proved by induction. The assertion is true for $k = 0$, since $C'Q_0C = S_{t_1}$. Assume that the assertion is true for index k. Then

$$A'^{k+1}C'Q_{k+1}CA^{k+1} = A'A'^{k}C'\Big(Q_k - Q_kCA^kB(B'A'^{k}CQ_kC'A^kB)^{+}\cdot B'A'^{k}C'Q_k\Big)CA^kA$$

$$= A'\Big(S_{t_1-k} - S_{t_1-k}B(B'S_{t_1-k}B)^{+}B'S_{t_1-k}\Big)A =$$

$$= S_{t_1-(k+1)} \qquad (A.31)$$

since, by Lemma 4.2, Q_k satisfies the recursion (6.7) with $U_k = CA^kB$ for $k \geq 0$.

□

Proof of Lemma 6.4

According to Lemma 6.3

$$S_{t_1-k} = A'^{k}C'Q_kCA^k, \qquad k \geq 0 \qquad (A.32)$$

where Q_k is the orthogonal projection of X on $\mathrm{Im}(M_k)^{\perp}$. Since A is invertable and since $\mathrm{Ker}(C') = 0$, it then follows that

$$\mathrm{rk}(S_{t_1-k}) = \mathrm{rk}(Q_k) = p - \mathrm{rk}(M_k), \qquad k \geq 0 \qquad (A.33)$$

Hence, k is an integer such that $S_{t_1-k} = 0$ if and only if $\mathrm{rk}(M_k) = p$.

□

Proof of Lemma 6.5

(6.15a): Assume that $0 \neq x \in \mathrm{Ker}(A+BL_{t_1-k})$ for $k \in \underline{\xi}$. Then

$$(A+BL_{t_1-k})x = 0 \tag{A.34}$$

which implies that

$$x = -A^{-1}BL_{t_1-k}x = -A^{-1}B(B'S_{t_1-(k-1)}B)^{+}B'S_{t_1-(k-1)}Ax \in$$

$$\in \mathrm{Im}(A^{-1}\bar{B}^{(k)}) \tag{A.35}$$

But by (2.5b)

$$(A+BL_{t_1-k})A^{-1}\bar{B}^{(k)} = \bar{B}^{(k)} - B(B'S_{t_1-(k-1)}B)^{+}B'S_{t_1-(k-1)}B(B'S_{t_1-(k-1)}B)^{+}$$

$$= \bar{B}^{(k)} - \bar{B}^{(k)} = 0 \tag{A.36}$$

Together (A.35) and (A.36) establish (6.15a).

(6.15b): By Lemma 6.3

$$L_{t_1-k} = -(B'S_{t_1-(k-1)}B)^{+}B'S_{t_1-(k-1)}A$$

$$= -(B'S_{t_1-(k-1)}B)^{+}B'C'A'^{k-1}Q_{k-1}CA^{k} \tag{A.37}$$

where Q_{k-1} is the orthogonal projection of X on $\mathrm{Im}(M_{k-1})^{\perp}$ for all $k \in \underline{\xi}$. Assume that $x \in \mathrm{Im}([A^{-2}B, A^{-3}B, \ldots, A^{-k}B])$ for $k \in \{2, 3, \ldots, \xi\}$. Then by (A.37), $x \in \mathrm{Ker}(L_{t_1-k})$. This proves (6.15b).

(6.15c): Assume that $x \in \mathrm{Ker}(A+BL_{t_1-k}) \cap \mathrm{Ker}(L_{t_1-k})$ for any $k \in \{2, 3, \ldots, \xi\}$. Then

$$0 = (A+BL_{t_1-k})x = Ax \tag{A.38}$$

Since A is invertable, it follows that $x = 0$. This establishes (6.15c). □

Proof of Lemma 6.6

Assume that $k \in \underline{\xi}$. Then by (6.15a) and (6.15b)

$$(A+BL_{t_1-k})A^{-1}\bar{B}(k) = 0$$

$$(A+BL_{t_1-k})A^{-2}\bar{B}(k) = A^{-1}\bar{B}(k)$$

$$\vdots$$

$$(A+BL_{t_1-k})A^{-k}\bar{B}(k) = \bar{A}(k-1)\bar{B}(k) \qquad (A.39)$$

since $\mathrm{Im}(A^{-i}\bar{B}(k)) \subset \mathrm{Im}(A^{-i}B)$ for $i = 2, 3, \ldots, \xi$. Therefore, $\mathrm{Im}([A^{-1}\bar{B}(k), A^{-2}\bar{B}(k), \ldots, A^{-k}\bar{B}(k)])$ belongs to the generalized eigenvector space of $A+BL_{t_1-k}$ associated with the eigenvalue $\lambda = 0$ and

$$\mathrm{Im}\Big([A^{-1}\bar{B}(k), A^{-2}\bar{B}(k), \ldots, A^{-k}\bar{B}(k)]\Big) \subset \mathrm{Ker}\Big((A+BL_{t_1-k})^k\Big) \qquad (A.40)$$

Since the column vectors of $A^{-1}\bar{B}(k)$ are linearly independent, it can be shown from (A.39) that the subspaces $\left\{\mathrm{Im}(A^{-i}\bar{B}(k))\right\}_{i=1}^{k}$ are linearly independent. Consequently

$$\mathrm{rk}\Big([A^{-1}\bar{B}(k), A^{-2}\bar{B}(k), \ldots, A^{-k}\bar{B}(k)]\Big) = k \cdot \bar{r}_k \qquad (A.41)$$

But

$$\nu\Big((A+BL_{t_1-k})^k\Big) \leq \sum_{i=1}^{k} \nu(A+BL_{t_1-k}) = k \cdot \bar{r}_k \qquad (A.42)$$

since $\nu(GH) \leq \nu(G) + \nu(H)$. Together (A.40), (A.41) and (A.42) establish (6.18a) and (6.18b).

□

Proof of Lemma 6.7

(6.19a): Since C = I, Lemma 6.3 implies that

$$S_{t_1-(k-1)} = A'^{k-1} Q_{k-1} A^{k-1} \tag{A.43}$$

where Q_{k-1} is the orthogonal projection of X on $\mathrm{Im}(W_{k-1})^{\perp}$ for all $k \in \underline{\xi}$. Therefore

$$\begin{aligned}
\bar{r}_k &= \mathrm{rk}\left((B' S_{t_1-(k-1)} B)^{+} \right) \\
&= \mathrm{rk}(B' A'^{k-1} Q_{k-1} A^{k-1} B) \\
&= \mathrm{rk}(Q_{k-1} A^{k-1} B) \\
&= m - \dim \left(\mathrm{Im}(A^{k-1}B) \cap \mathrm{Im}\left([B, AB, \ldots, A^{k-2}B] \right) \right) \triangleq \\
&\triangleq m - \ell_k, \qquad k \in \{2, 3, \ldots, \xi\}
\end{aligned} \tag{A.44}$$

since $\mathrm{Ker}(A) = \mathrm{Ker}(B) = 0$ and since $\mathrm{rk}(GH) = \mathrm{rk}(G) - \dim(\mathrm{Ker}(G) \cap \mathrm{Im}(H))$. Assume that $A^k b_j \in \mathrm{Im}([B, AB, \ldots, A^{k-1}B])$ for any $j \in \underline{m}$. Then $A^{k+1} b_j \in \mathrm{Im}([B, AB, \ldots, A^k B])$. Therefore, $\{\ell_i\}_{i=2}^{\xi}$ is a non-decreasing sequence. Hence, by (A.44), $\{\bar{r}_i\}_{i=1}^{\xi}$ is a non-increasing sequence.

(6.19b): Let $k \in \{2, 3, \ldots, \xi\}$. Then by (A.44)

$$\bar{r}_k = m \Leftrightarrow \mathrm{Im}(A^{k-1}B) \cap \mathrm{Im}\left([B, AB, \ldots, A^{k-2}B] \right) = 0 \tag{A.45}$$

(6.19c): According to (6.19a) and (6.19b)

$$\bar{r}_{\xi} = m \Leftrightarrow$$

$$\mathrm{Im}(A^k B) \cap \mathrm{Im}\left([B, AB, \ldots, A^{k-1}B] \right) = 0, \quad k = 1, 2, \ldots, \xi-1 \Leftrightarrow$$

$$\sum_{k=1}^{\xi-1} \left(\mathrm{Im}(A^k B) \cap \sum_{i=0}^{k-1} \mathrm{Im}(A^i B) \right) = 0 \tag{A.46}$$

Since C = I, Lemma 6.4 gives that

$$X = \mathcal{B} + A\mathcal{B} + \ldots + A^{\xi-1}\mathcal{B} \qquad (A.47)$$

It follows from (A.46) and (A.47) that

$$X = \mathcal{B} \oplus A\mathcal{B} \oplus \ldots \oplus A^{\xi-1}\mathcal{B}$$

□

CHAPTER 7

OPTIMAL FILTERING AND PROFILE CONTROL

1. INTRODUCTION

In this chapter the multivariable dead-beat controllers, developed in Chapter 6, are used to drive the profile of the rod from an arbitrary initial value to a given equilibrium point in a minimum number of time steps. The controllers are computed from the lumped models of the rod given in Chapter 3. In some experiments the state of these models is measured directly whereas in other experiments only the end temperatures of the rod are measured. In the latter case the state of the lumped model is reconstructed from the end temperatures, using Kalman filtering techniques. It turns out that it is enough to measure the end temperatures of the rod to obtain a satisfactory profile control.

The investigation also shows that the profile of the rod may be estimated very accurately from the end temperatures of the rod. It is also found that if the end temperatures of the rod are measured and additional measurements of the temperatures in the mid-section of the rod are made, then the estimation of the profile is only improved marginally. This is of great interest since in a practical application it may only be possible to measure the boundary temperatures of the thermal process.

The study also shows that there is no need to use very elaborate models of the rod for control purposes. This is explained by the fact that the use of dead-beat controllers make it possible to employ a relatively long sampling period, compared to the sampling period required by conventional DDC-controllers. Therefore, it is

not necessary to describe the fast dynamics of the rod very accurately. In fact this points at one of the most interesting features of the dead-beat controllers. Moreover, it is found that it is possible to construct dead-beat controllers for the diffusion process which meet very restrictive requirements on the maximal permissible magnitude of the control signals. These controllers are obtained by choosing a sufficiently long sampling period.

2. A STOCHASTIC MODEL

In this section a stochastic model is set up for the diffusion process tied to a process computer. The result (3.12) of the maximum likelihood identification experiment in Chapter 5 shows that the disturbances acting on the rod are extremely small. Moreover, this result shows that the relative errors of the temperature transducers are very small. In fact, the process disturbances and the transducer errors are negligible compared to the errors of the A/D- and D/A-converters of the computer interface and the errors of the temperature servos. Therefore, to obtain a stochastic model of the diffusion process, tied to the process computer, it is only necessary to model the conversion errors and the errors of the servos.

The conversion errors of the A/D- and D/A-converters are modelled as sequences of uncorrelated and equally-distributed random vectors $\{\xi_{A/D}(t)\}$ and $\{\xi_{D/A}(t)\}$ respectively. The components of these vectors are assumed to be uncorrelated. Moreover, the vectors $\xi_{A/D}(t)$ and $\xi_{D/A}(s)$ are assumed to be uncorrelated for all s and t. Measurements show that the components of $\xi_{A/D}$ and $\xi_{D/A}$ have the probability function shown in Fig. 2.1. According to this figure the mean values and the variances of the components of $\xi_{A/D}$ and $\xi_{D/A}$ are given by

$$E[\xi_{A/D_i}(t)] = E[\xi_{D/A_j}(t)] = 0$$

$$V[\xi_{A/D_i}(t) = V[\xi_{D/A_j}(t)] = 0.6\ a^2,\ i = 1,2;\ j = 1,2,\ldots,\ p \qquad (2.1)$$

$$a = 0.005\ ^{o}C$$

where p denotes the number of measured signals and a denotes the resolution of the converters. The quantization errors of the converters are quite small. On the assumption that these errors are equally-distributed in the interval [-a/2, a/2] their variance become $a^2/12$. This variance is neglected compared to the variance of the conversion errors $0.6\ a^2$.

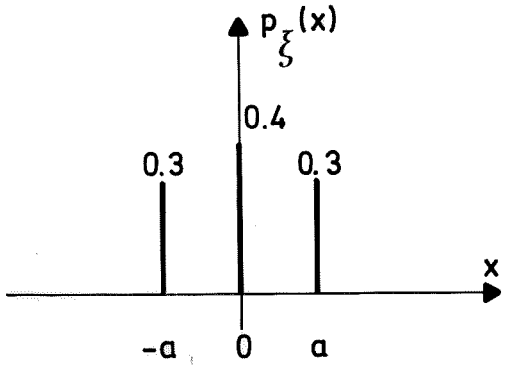

Fig. 2.1 - Probability function $p_\xi(x)$ of the conversion errors of the A/D- and D/A-converters. One bit error in the converters corresponds to $\xi = \pm a$.

In the performed experiments the two control signals will be sequences of uncorrelated random variables. The two sequences will also be uncorrelated. In such a case the errors of the servos ζ may be modelled as a sequence of uncorrelated and equally-distributed random vectors. The components of these vectors are assumed to be uniformly distributed in the interval [-b,b] and to be constant over the sampling period. On this assumption the mean values and variances of the components of ζ become

$$E[\zeta_i(t)] = 0$$
$$V[\zeta_i(t)] = b^2/3, \quad i = 1,2 \qquad (2.2)$$
$$b = 0.006\ ^{o}C$$

Moreover, the conversion errors of the D/A-converters $\xi(t)$ are assumed to be uncorrelated with the errors of the servos $\zeta(s)$ for all s and t.

Consider the deterministic model of the diffusion process

$$\begin{aligned} \dot{x} &= Ax + By \\ y &= Cx \end{aligned} \tag{2.3}$$

where x is the state-vector, u is the control vector and y is the measured vector. Since the stochastic process $\{\xi_{D/A}(t) + \zeta(t)\}$ is constant over the sampling period T, it is simple to set up a stochastic difference equation for the diffusion process tied to the process computer. Putting

$$\begin{aligned} \Phi &= e^{AT} \\ \Gamma &= \int_0^T e^{As} ds \cdot B \end{aligned} \tag{2.4}$$

the difference equation become

$$\begin{aligned} x(t+T) &= \Phi x(t) + \Gamma u(t) + v(t) \\ y(t) &= Cx(t) + e(t) \end{aligned} \tag{2.5}$$

where $v(t) = \Gamma(\xi_{D/A}(t) + \zeta(t))$ and $e(t) = \xi_{A/D}(t)$ have been introduced. The means and the covariances of the second order stochastic processes $\{v(t)\}$ and $\{e(t)\}$ are

$$E[v(t)] = E[e(t)] = 0$$

$$\operatorname{cov}[v(t),v(t)] = R_1 = \Gamma \begin{bmatrix} 0.6\ a^2 + b^2/3 & 0 \\ 0 & 0.6\ a^2 + b^2/3 \end{bmatrix} \Gamma'$$

$$\operatorname{cov}[e(t),e(t)] = \begin{bmatrix} 0.6\ a^2 & & \\ & 0.6\ a^2 & 0 \\ & \ddots & \\ 0 & & 0.6\ a^2 \end{bmatrix} \tag{2.6}$$

3. OPTIMAL FILTERING

Basic theory

Consider the discrete time stochastic system which is described by the state equation

$$x(t+1) = \Phi x(t) + \Gamma u(t) + v(t)$$
$$y(t) = Cx(t) + e(t) \qquad (3.1)$$

where x is an n-dimensional state vector, u is an m-dimensional vector of control signals, y is a p-dimensional vector of observed signals, $\{v(t)\}$ and $\{e(t)\}$ are sequences of uncorrelated and equally-distributed stochastic vectors with zero mean values and covariances R_1 and R_2 respectively. The vectors v(t) and e(s) are also assumed to be independant for all s and t. It is required that the predictor $\hat{x}(t+1)$ of x(t+1) at time t is a linear function of the set of observation $y_t = \{y(t), y(t-1), \ldots, y(t_0)\}$ on the interval $[t_0, t]$. Then it follows from [1] that the optimal predictor in the sense of mean square is given by the Kalman filter.

$$\hat{x}(t+1) = \Phi\hat{x}(t) + \Gamma u(t) + K(t)(y(t) - C\hat{x}(t))$$
$$\hat{x}(t_0) = m = E[x(t_0)] \qquad (3.2)$$

The matrix K(t) is given by

$$K(t) = \Phi P(t)\, C'(CP(t)C' + R_2)^{-1} \qquad (3.3)$$

where P(t) is the covariance of the estimation error obtained from

$$P(t+1) = \Phi P(t)\Phi' + R_1 - \Phi P(t)C'(CP(t)C' + R_2)^{-1}CP(t)\Phi'$$
$$P(t_0) = R_0 = \mathrm{cov}[x(t_0), x(t_0)] \qquad (3.4)$$

The estimation error $\tilde{x}(t) = x(t) - \hat{x}(t)$ is governed by the stochastic difference equation

$$\hat{x}(t+1) = (\Phi - K(t)C)\hat{x}(t) + v(t) - K(t)e(t) \qquad (3.5)$$

The innovations $\varepsilon(t) = y(t) - C\hat{x}(t)$ form a sequence of uncorrelated and equally-distributed random vectors with mean value and covariance given by

$$E[\varepsilon(t)] = 0$$
$$\text{cov}[\varepsilon(t), \varepsilon(t)] = CP(t)C' + R_2 \qquad (3.6)$$

Since the estimation is done for a long time before the control is applied, the assymptotic Kalman gain K_∞, corresponding to the stationary solution P_∞ of the Riccati equation (3.4), is used .

Description of filters

All Kalman filters are based on the lumped 7th order model ROD2 or the 11th order model ROD4. The two servos are modelled by second order systems with the transfer functions

$$G_i(s) = \frac{c_i s + \omega_{0_i}^2}{s^2 + 2\zeta_i \omega_{0_i} + \omega_{0_i}^2}, \quad i = 1,2 \qquad (3.7)$$

The coefficients c_i, ζ_i and ω_{0_i} are determined by parameter adjustment techniques so that the peak time, the overshoot and the settling time of the transfer functions G_1 and G_2 and the corresponding servos agree well. The following values of the parameters are thereby obtained

$$c_1 = 0.753$$
$$\zeta_1 = 2.1$$
$$\omega_{0_1} = 0.18 \qquad (3.8)$$

and

$$
\begin{aligned}
c_2 &= 0.586 \\
\zeta_2 &= 2.1 \\
\omega_{0_2} &= 0.14
\end{aligned}
\tag{3.9}
$$

for the servo 1 and the servo 2 respectively. From simulations it is seen that the rise times of the servos are considerably smaller than the rise times of the transfer functions G_1 and G_2.

The continuous lumped state-space model based on ROD2 becomes

$$
\dot{x} = \left[\begin{array}{cc|c|cc}
0 & -\omega_{0_1}^2 & 0 & 0 & \\
1 & -2\zeta_1\omega_{0_1} & & & \\
\hline
0 & a_2 & & 0 & 0 \\
0 & b_3 & & & \\
0 & 0 & A_2 & 0 & 0 \\
\vdots & \vdots & & \vdots & \vdots \\
0 & 0 & & 0 & 0 \\
\hline
 & 0 & & -b_3 & 0 \\
 & & & a_2 & 0 \\
 & & & -2\zeta_2\omega_{0_2}^2 & 1 \\
0 & & 0 & \omega_{0_2}^2 & 0
\end{array}\right] x + \left[\begin{array}{cc}
\omega_{0_1}^2 & 0 \\
c_1 & 0 \\
0 & 0 \\
\vdots & \vdots \\
0 & 0 \\
0 & c_2 \\
0 & \omega_{0_2}^2
\end{array}\right] u
\tag{3.10}
$$

where the matrix A_2 and the coefficients a_2 and b_3 are defined by (2.10) and (2.11) respectively in Chapter 3. The null matrix is denoted by **0**.

Moreover, the continuous lumped state-space model based on ROD4 becomes

$$\dot{x} = \left[\begin{array}{cc|c|cc} 0 & \omega_{0_1}^2 & & 0 & 0 \\ 1 & -2\zeta_1\omega_{0_1} & 0 & & \\ \hline 0 & a_2 & & 0 & 0 \\ 0 & -b_3 & & & \\ 0 & 0 & & & \\ 0 & -c_3 & & 0 & 0 \\ 0 & d_4 & A_4 & d_4 & 0 \\ 0 & 0 & & -c_3 & 0 \\ & & & 0 & 0 \\ & & & -b_3 & 0 \\ 0 & 0 & & a_2 & 0 \\ \hline & & & -2\zeta_2\omega_{0_2} & 1 \\ & 0 & 0 & \omega_{0_2}^2 & 0 \end{array}\right] x + \left[\begin{array}{cc} \omega_{0_1}^2 & 0 \\ c_1 & 0 \\ 0 & 0 \\ & \\ & \\ & \\ & \\ & \\ & \\ 0 & 0 \\ 0 & c_2 \\ 0 & \omega_{0_2}^2 \end{array}\right] u \qquad (3.11)$$

where the matrix A_4 and the coefficients a_2, b_3, c_3 and d_4 are defined by (2.14) and (2.15) in Chapter 3. The null matrix is denoted by **0**.

In order to denote an asymptotic Kalman filter based on the model RODI the four-tuple (FII, GAI, THIJ, AKIJ) is used. The literal J denotes the number of measured signals. The investigated filters are listed in Table 3.1

Filter	n	T_s	Measured signals
(FI2, GA2, TH22, AK22)	7	20	y_{e_1}, y_{e_2}
(FI2, GA2, TH24, AK24)	7	20	$y_{e_1}, y_3, y_4, y_{e_2}$
(FI4, GA4, TH42, AK42)	11	20	y_{e_1}, y_{e_2}

Table 3.1 - Kalman filters used for estimation of the profile of the rod.

The diagonal elements of P_∞, the gain K_∞, the eigenvalues of $\Phi - K_\infty C$ and the covariance matrix of the innovations R_{ε_∞} for the filters in Table 3.1 are given in Tables A.1, A.2 and A.3. The forms of the gain matrices K_∞ show that the measurements y correct the estimates $\hat{x}$ mainly where they are measured and that the corrections are largest at the ends of the rod. This is natural since the process disturbances are introduced at the ends of the rod and take on small values when they reach the mid-section of the rod, compared to the measurement errors $\sigma = 0.004\ ^oC$. In particular it is found that the variance of the measurement errors $\sigma^2 = 0.15\ 10^{-4}\ ^oC^2$ are considerably larger than the variances of the estimation errors in all internal measurement points on the rod. The theoretical standard deviations of the estimation errors are approximately $0.005\ ^oC$ in the end points of the rod and $0.0005\ ^oC$ in the mid-section of the rod for all filters in Table 3.1.

When the end temperatures of the rod are measured and additional measurements of the temperature in the mid-section of the rod are made Tables A.1 and A.2 show that the estimation errors are only decreased slightly. Tables A.1 and A.3 show that the theoretical estimation errors in any given point on the rod are approximately the same if these errors are computed from the 7th order model ROD2 or the 11th order model ROD4. This means that no elaborate model of the rod is needed to give estimates of the estimation errors.

The lumped models (FI2, GA2) and (FI4, GA4) are controllable. However, these models are not observable from the signals y_{e1} and y_{e2}. The unobservable modes of the pairs (TH22, FI2) and (TH42, FI4) belong to the set of eigenvalues of FI2 - AK22·TH22 and FI4 - AK42·TH42 respectively. The lumped model (FI2, GA2) is observable from the signals y_{e1}, y_3, y_4 and y_{e2}. This implies that the eigenvalues of FI2 and FI2 - AK24·TH24 should be disjoint. The eigenvalues of FI2 and FI4 are given in Table A.4.

Experimental results

The asymptotic Kalman filter (3.2) was implemented on a process computer PDP-15/35. The computer generated two sequences of independent normal (0, 0.5) random variables. The two sequences were also uncorrelated. These sequences were used as control signals. In the experimental set-up used the resolution of the A/D- and D/A-converters were a = 0.005 ^{o}C. Moreover, the errors of the servos were estimated to b = 0.006 ^{o}C.

A typical plot of the control signals, the measured signals and the innovations are shown in Fig. 3.1 for the filter (FI2, GA2, TH24, AK24). The number of sampling events is N = 50. From Fig. 3.1 it is seen that the probability function of the innovations ε_3 and ε_4 is rather well described by the function in Fig. 2.1. Moreover, it is seen that the innovations ε_{e_1} and ε_{e_2} contain several spikes. The spikes in ε_{e_1} and ε_{e_2} occur after a large change in the control signals u_1 and u_2 respectively. This means that the models G_1 and G_2 in (3.7) only describe the servos well for small changes in the control signals. It should be observed that the innovations are only defined at the sampling instants.

The null hypothesis that the process is described by the system (2.5) is tested statistically. The test quantity

$$\chi^2_{ac} = \sqrt{N} \sum_{\tau=1}^{5} \rho_{\varepsilon}(\tau) \qquad (3.12)$$

is used to test if the innovations are uncorrelated. Under the null hypothesis this test quantity is asymptotically $\chi^2(5)$. To test if the control signals are uncorrelated with the residuals the following test quantity is employed

$$\chi^2_{cc} = x' P_x^{-1} x \qquad (3.13)$$

where

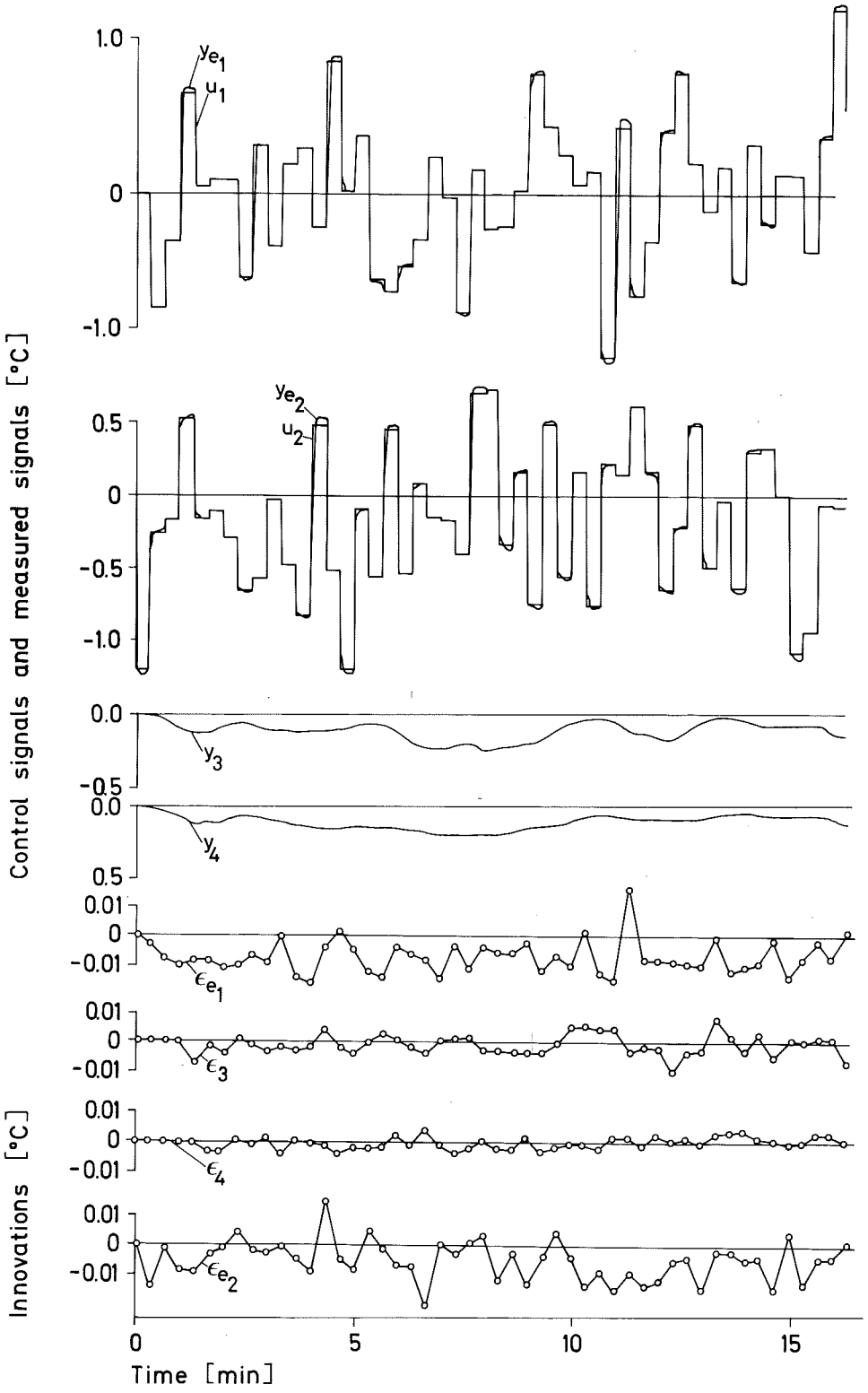

Fig. 3.1 - Kalman filtering experiment with the filter (FI2, GA2, TH24, AK24)

$$x = \begin{bmatrix} \rho_{\varepsilon u}(1) \\ \rho_{\varepsilon u}(2) \\ \vdots \\ \rho_{\varepsilon u}(5) \end{bmatrix} \tag{3.14}$$

and

$$P_x = \begin{bmatrix} \rho_u(0) & \rho_u(1) & \dots & \rho_u(4) \\ \rho_u(1) & \rho_u(0) & \dots & \rho_u(3) \\ \vdots & \vdots & & \vdots \\ \rho_u(4) & \rho_u(3) & \dots & \rho_u(0) \end{bmatrix} \frac{1}{N} \tag{3.15}$$

This test quantity is asymptotically $\chi^2(5)$ under the null hypothesis.

In Table 3.2 the chi-square test quantities for the filter (FI2, GA2, TH24, AK24) are shown

Test quantity \ Innovation	ε_{e_1}	ε_3	ε_4	ε_{e_2}
χ^2_{ac}	5.4	8.8	7.0	2.0
χ^2_{cc} input u_1	2.6	20.5	8.7	5.8
χ^2_{cc} input u_2	2.3	3.5	4.3	4.2

Table 3.2 - Chi-square test quantities for the residuals of the filter (FI2, GA2, TH24, AK24).

At a risk level of 1 % the regions of acceptance for the chi-square test quantities are $\chi^2_{ac} \leq 15.0$ and $\chi^2_{cc} \leq 15.0$. From Table 3.2 it is seen that the control signal u_1 and the innovations ε_3 are not uncorrelated. In Section 5 of Chapter 3 it was found that this correlation was due to the nonlinearities of the servos.

The estimated covariance matrix R_{ε_∞} of the filter (FI2, GA2, TH24, AK24) becomes

$$R_{\varepsilon_\infty} = \begin{bmatrix} 0.35\cdot10^{-4} & -0.16\cdot10^{-5} & 0.34\cdot10^{-6} & -0.25\cdot10^{-5} \\ -0.16\cdot10^{-5} & 0.12\cdot10^{-4} & -0.21\cdot10^{-6} & 0.50\cdot10^{-5} \\ 0.34\cdot10^{-6} & -0.21\cdot10^{-6} & 0.45\cdot10^{-5} & -0.38\cdot10^{-5} \\ -0.25\cdot10^{-5} & 0.50\cdot10^{-5} & 0.38\cdot10^{-5} & 0.46\cdot10^{-4} \end{bmatrix} \qquad (3.16)$$

The theoretical covariance matrix of this filter is given in Table A.2. From this table it is seen that the standard deviations of the innovations ε_{e_1}, ε_3 and ε_{e_2} agree quite well with the theoretical values. However, the standard deviation of the innovation ε_4 is about half of the theoretical value. This may be explained by the fact that the signal y_4 only range over a small interval of the characteristic of the A/D-converter. Summing up, it is found that the diffusion process is rather well described by the model (2.5).

4. PROFILE CONTROL

The dead-beat regulators in Chapter 6 will be used to control the profile of the rod. The controllers are computed from lumped models of the rod. It is required that all state variables of these models reach the given equilibrium point. Therefore, the state dead-beat controller and the minimum gain dead-beat controller are the only regulators of interest.

Description of controllers

All computations of the dead-beat controllers are based on the 7th order model ROD2 or the 11th order model ROD4. The state of the former model may be measured. However, there are not measurement points for all state variables of the model ROD4. The dynamics of the servos will be neglected here. This simplification is realistic since the dynamics of the servos are approximately 100 times faster than the dynamics of the rod. In the Kalman filters it was not straightforward to neglect the dynamics of the servos, since the state of the lumped model of the diffusion process was reconstructed from the end temperatures of the rod. This means that these temperatures should be linear combinations of the state variables of the lumped model. Both time-invariant and time-variable controllers will be studied. The former are calculated by means of Theorem 3.1 in Chapter 6 whereas the latter are calculated from Lemma 6.1 in Chapter 6 with $Q_0 = I$.

A discrete-time system obtained by sampling the model RODI with the sampling time T = J min is denoted by S(FIIJ, GAIJ). To denote a time-invariant (time-variable) controller computed from the system S(FIIJ, GAIJ) the notation FTIIJ (FTVIJ) is used. The investigated controllers are listed in Table 4.1.

Controller	n	T min	Type of controller
FTI21	7	1	time-invariant
FTV21	7	1	time-variable
FTV23	7	3	time-variable
FTV41	11	1	time-variable

Table 4.1 - Dead-beat controllers used for profile control experiments.

The model simplification (8.5) in Chapter 6 is used when computing the controller FTI21. The eigenvalues of the matrix FI21 are

$$\lambda_1 = 0.711317$$
$$\lambda_2 = 0.263492$$
$$\lambda_3 = 0.576040 \cdot 10^{-1}$$
$$\lambda_4 = 0.890062 \cdot 10^{-2}$$
$$\lambda_5 = 0.103496 \cdot 10^{-2}$$
$$\lambda_6 = 0.105942 \cdot 10^{-3}$$
$$\lambda_7 = 0.166351 \cdot 10^{-4} \qquad (4.1)$$

Choosing $\varepsilon = 5 \cdot 10^{-3}$ it follows from (4.1) that the orders of the matrices A_1 and A_2 in (8.5) in Chapter 6 are 4 and 3 respectively. Then it is possible to force any initial state of the subsystem $S(A_1, B_1)$ in (7.3) in Chapter 6 to zero in at most 2 time steps. Since the gain factors of the fast modes of the model ROD2 are small the modes of the subsystem $S(A_2, B_2)$ in (7.3) in Chapter 6 will only be excited slightly. Therefore, it should be expected that the model simplification (8.5) in Chapter 6 work well here. The controller FTI21 becomes

$$L = \begin{bmatrix} -0.357398 & -0.493344 & -0.588792 & -0.531629 \\ -0.110783 & -0.222208 & -0.388699 & -0.531629 \end{bmatrix}$$

$$\begin{bmatrix} -0.388699 & -0.222208 & -0.110783 \\ -0.588792 & -0.493344 & -0.357398 \end{bmatrix} \qquad (4.2)$$

For $x_0 = (1\ 1\ \ldots\ 1)'$ the trajectory and the input sequence of the system S(FI21, GA21) controlled with the state feedback DTI21 become

t	0	1	2	3
x_t	$\begin{bmatrix} 1 \\ 1 \\ 1 \\ 1 \\ 1 \\ 1 \\ 1 \end{bmatrix}$	$\begin{bmatrix} -1.32762 \\ -0.267383 \\ 0.366035 \\ 0.570888 \\ 0.366036 \\ -0.267383 \\ -1.32762 \end{bmatrix}$	$\begin{bmatrix} 0.198716 \cdot 10^{-1} \\ -0.247777 \cdot 10^{-1} \\ -0.165373 \cdot 10^{-2} \\ 0.188904 \cdot 10^{-1} \\ -0.165373 \cdot 10^{-2} \\ -0.247777 \cdot 10^{-1} \\ 0.198716 \cdot 10^{-1} \end{bmatrix}$	$\begin{bmatrix} 0.192789 \cdot 10^{-4} \\ -0.217418 \cdot 10^{-4} \\ -0.735297 \cdot 10^{-5} \\ 0.258069 \cdot 10^{-4} \\ -0.735267 \cdot 10^{-5} \\ -0.217422 \cdot 10^{-4} \\ 0.192788 \cdot 10^{-4} \end{bmatrix}$

$$
\begin{array}{lccc}
t & 0 & 1 & 2 \\
u_t & \begin{bmatrix} -2.69285 \\ -2.69285 \end{bmatrix} & \begin{bmatrix} 0.151595 \\ 0.151595 \end{bmatrix} & \begin{bmatrix} 0.186853 \cdot 10^{-7} \\ 0.180057 \cdot 10^{-7} \end{bmatrix}
\end{array} \qquad (4.3)
$$

Notice the large steps in the absolute values of the control signals after 2 time steps. These steps occur since the state of the subsystem $S(A_1, B_1)$ is forced to zero in 2 time steps for the considered initial state.

In Table A.5 the matrices S_{t_1-1}, S_{t_1-2} and S_{t_1-3}, defined by (6.4) in Chapter 6, are given for the controller FTV21. Since the largest diagonal element of the matrix S_{t_1-3} is $0.61 \cdot 10^{-11}$, it suffices to use 3 sampling intervals to drive the profile of the rod close to the origin. The matrices L_{t_1-1}, L_{t_1-2} and L_{t_1-3}, defined by (6.2) in Chapter 6, specifying the controller FTV21 become

$$
L_{t_1-1} = \begin{bmatrix} -0.216124 & -0.264749 & -0.274409 \\ -0.263994 \cdot 10^{-1} & -0.618784 \cdot 10^{-1} & -0.127741 \end{bmatrix}
$$

$$
\begin{bmatrix} -0.208980 & -0.127741 & -0.618784 \cdot 10^{-1} \\ -0.208980 & -0.274409 & -0.264749 \end{bmatrix}
$$

$$
\begin{bmatrix} -0.263994 \cdot 10^{-1} \\ -0.216124 \end{bmatrix}
$$

$$
L_{t_1-2} = \begin{bmatrix} -0.354382 & -0.488244 & -0.581453 & -0.523726 \\ -0.108449 & -0.217929 & -0.382006 & -0.523725 \end{bmatrix}
$$

$$
\begin{bmatrix} -0.382006 & -0.217929 & -0.108449 \\ -0.581453 & -0.488244 & -0.354382 \end{bmatrix}
$$

$$
L_{t_1-3} = \begin{bmatrix} -0.357715 & -0.493873 & -0.589542 & -0.532425 \\ -0.111003 & -0.222618 & -0.389353 & -0.532415 \end{bmatrix}
$$

$$
\begin{bmatrix} -0.389363 & -0.222625 & -0.111008 \\ -0.589533 & -0.493866 & -0.357710 \end{bmatrix} \qquad (4.4)
$$

Choosing $x_0 = (1\ 1\ \ldots\ 1)'$ the trajectory and the input sequence of the system S(FI21, GA21) controlled with the regulator FTV21

become

$$
\begin{array}{lcccc}
t & 0 & 1 & 2 & 3 \\
x_t & \begin{bmatrix}1\\1\\1\\1\\1\\1\\1\end{bmatrix} & \begin{bmatrix}-1.32999\\-0.268675\\0.365394\\0.570465\\0.365424\\-0.268600\\-1.32985\end{bmatrix} & \begin{bmatrix}0.212137\cdot10^{-1}\\-0.245411\cdot10^{-1}\\-0.202261\cdot10^{-2}\\0.183445\cdot10^{-1}\\-0.201210\cdot10^{-2}\\-0.245341\cdot10^{-1}\\0.211956\cdot10^{-1}\end{bmatrix} & \begin{bmatrix}-0.572191\cdot10^{-6}\\0.269890\cdot10^{-5}\\-0.573247\cdot10^{-5}\\0.718930\cdot10^{-5}\\-0.568340\cdot10^{-5}\\0.265990\cdot10^{-5}\\-0.561853\cdot10^{-6}\end{bmatrix}
\end{array}
$$

$$
\begin{array}{lccc}
t & 0 & 1 & 2 \\
u_t & \begin{bmatrix}-2.69662\\-2.69640\end{bmatrix} & \begin{bmatrix}0.154440\\0.154379\end{bmatrix} & \begin{bmatrix}-0.150569\cdot10^{-3}\\-0.150092\cdot10^{-3}\end{bmatrix}
\end{array}
\qquad (4.5)
$$

It should be observed that the simulation results (4.3) and (4.5) are almost identically. This is explained by the fact that the first seven column vectors in the reachability matrix of the system S(FI21, GA21) are linearly independent. Also notice that the origin is reached with higher precision when the controller FTV21 is used compared to the controller FTI21.

The sampling period of the controller FTV23 is T = 3 min. When this relative long sampling period is used, it can be seen from Table A.6 that it is possible to drive the profile of the rod close to the origin in 2 time steps. The matrices L_{t_1-1} and L_{t_1-2}, defined by (6.2) in Chapter 6, specifying the controller FTV23 become

$$
L_{t_1-1} = \begin{bmatrix}
-0.454905\cdot10^{-1} & -0.665356\cdot10^{-1} & -0.864988\cdot10^{-1} \\
-0.346797\cdot10^{-1} & -0.546867\cdot10^{-1} & -0.777743\cdot10^{-1}
\end{bmatrix}
$$

$$
\begin{bmatrix}
-0.890482\cdot10^{-1} & -0.777743\cdot10^{-1} & -0.546867\cdot10^{-1} \\
-0.890482\cdot10^{-1} & -0.864988\cdot10^{-1} & -0.665356\cdot10^{-1}
\end{bmatrix}
$$

$$
\begin{bmatrix}
-0.346797\cdot10^{-1} \\
-0.454905\cdot10^{-1}
\end{bmatrix}
$$

$$L_{t_1-2} = \begin{bmatrix} -0.561038\cdot10^{-1} & -0.822729\cdot10^{-1} & -0.107301 \\ -0.436581\cdot10^{-1} & -0.686319\cdot10^{-1} & -0.972565\cdot10^{-1} \end{bmatrix}$$

$$\begin{bmatrix} -0.110899 & -0.972565\cdot10^{-1} & -0.686319\cdot10^{-1} \\ -0.110899 & -0.107301 & -0.822729\cdot10^{-1} \end{bmatrix}$$

$$\begin{bmatrix} -0.436581\cdot10^{-1} \\ -0.561038\cdot10^{-1} \end{bmatrix} \qquad (4.6)$$

Putting $x_0 = (1\ 1\ \ldots\ 1)'$ the trajectory and the input sequence of the system S(FI23, GA23) controlled with the regulator FTV23 become

$$\begin{array}{lccc} t & 0 & 1 & 2 \\ x_t & \begin{bmatrix} 1 \\ 1 \\ 1 \\ 1 \\ 1 \\ 1 \\ 1 \end{bmatrix} & \begin{bmatrix} -0.289839 \\ -0.564912\cdot10^{-1} \\ 0.991834\cdot10^{-1} \\ 0.153805 \\ 0.991834\cdot10^{-1} \\ -0.564911\cdot10^{-1} \\ -0.289839 \end{bmatrix} & \begin{bmatrix} 0.814465\cdot10^{-5} \\ -0.186946\cdot10^{-4} \\ 0.173622\cdot10^{-5} \\ 0.181553\cdot10^{-4} \\ 0.173611\cdot10^{-5} \\ -0.186947\cdot10^{-4} \\ 0.814474\cdot10^{-5} \end{bmatrix} \end{array}$$

$$\begin{array}{lcc} t & 0 & 1 \\ u_t & \begin{bmatrix} -0.566122 \\ -0.566122 \end{bmatrix} & \begin{bmatrix} 0.952664\cdot10^{-4} \\ 0.952661\cdot10^{-4} \end{bmatrix} \end{array} \qquad (4.7)$$

Notice that the inputs are considerably decreased as the sampling interval is increased from T = 1 min to T = 3 min.

Finally the controller FTV41 is discussed. This controller is based on the model ROD4 which is a more accurate model than the model ROD2. From Table A.7 it follows that it is possible to drive the profile of the rod close to the origin in 3 sampling intervals even when the temperature at more points are required to be close to zero. The matrices L_{t_1-1}, L_{t_1-2} and L_{t_1-3}, defined by (6.2) in Chapter 6, specifying the controller FTV41 become

$$L_{t_1-1} = \begin{bmatrix} -0.405497\cdot10^{-1} & -0.568116\cdot10^{-1} & -0.405497\cdot10^{-1} \\ -0.359537\cdot10^{-2} & -0.598089\cdot10^{-2} & -0.359537\cdot10^{-2} \end{bmatrix}$$

$$\begin{matrix} -0.179236 & -0.167688 & -0.126097 \\ -0.336965\cdot10^{-1} & -0.708518\cdot10^{-1} & -0.126097 \end{matrix}$$

$$\begin{matrix} -0.708518\cdot10^{-1} & -0.336965\cdot10^{-1} & -0.359537\cdot10^{-2} \\ -0.167688 & -0.179236 & -0.405497\cdot10^{-1} \end{matrix}$$

$$\begin{bmatrix} -0.598089\cdot10^{-2} & -0.359537\cdot10^{-2} \\ -0.568116\cdot10^{-1} & -0.405497\cdot10^{-1} \end{bmatrix}$$

$$L_{t_1-2} = \begin{bmatrix} -0.960250\cdot10^{-1} & -0.138444 & -0.960250\cdot10^{-1} \\ -0.290930\cdot10^{-1} & -0.457472\cdot10^{-1} & -0.290930\cdot10^{-1} \end{bmatrix}$$

$$\begin{matrix} -0.487473 & -0.543600 & -0.504473 \\ -0.215681 & -0.358450 & -0.504472 \end{matrix}$$

$$\begin{matrix} -0.358450 & -0.215682 & -0.290930\cdot10^{-1} \\ -0.543600 & -0.487473 & -0.960250\cdot10^{-1} \end{matrix}$$

$$\begin{bmatrix} -0.457472\cdot10^{-1} & -0.290930\cdot10^{-1} \\ -0.138444 & -0.960250\cdot10^{-1} \end{bmatrix}$$

$$L_{t_1-3} = \begin{bmatrix} -0.987715\cdot10^{-1} & -0.142569 & -0.987715\cdot10^{-1} \\ -0.310763\cdot10^{-1} & -0.488018\cdot10^{-1} & -0.310763\cdot10^{-1} \end{bmatrix}$$

$$\begin{matrix} -0.504145 & -0.565797 & -0.528748 \\ -0.229079 & -0.378327 & -0.528749 \end{matrix}$$

$$\begin{matrix} -0.378325 & -0.229078 & -0.310762\cdot10^{-1} \\ -0.565798 & -0.504146 & -0.987716\cdot10^{-1} \end{matrix}$$

$$\begin{bmatrix} -0.488016\cdot10^{-1} & -0.310762\cdot10^{-1} \\ -0.142569 & -0.987716\cdot10^{-1} \end{bmatrix} \qquad (4.8)$$

For $x_0 = (1\ 1\ \ldots\ 1)'$ the trajectory and the input sequence of the model S(FI41, GA41) controlled with the time-variable feedback FTV41 become

$$
\begin{array}{lccccc}
t & 0 & 1 & 2 & 3 \\
x_t & \begin{bmatrix}1\\1\\1\\1\\1\\1\\1\\1\\1\\1\\1\end{bmatrix} & \begin{bmatrix}-1.96741\\-1.31758\\-0.740175\\-0.259125\\0.377504\\0.584030\\0.377503\\-0.259128\\-0.740178\\-1.31759\\-1.96741\end{bmatrix} & \begin{bmatrix}0.667318\cdot10^{-1}\\0.165423\cdot10^{-1}\\-0.146216\cdot10^{-1}\\-0.243674\cdot10^{-1}\\-0.177607\cdot10^{-2}\\0.182185\cdot10^{-1}\\-0.177641\cdot10^{-2}\\-0.243676\cdot10^{-1}\\-0.146215\cdot10^{-1}\\0.165428\cdot10^{-1}\\0.667329\cdot10^{-1}\end{bmatrix} & \begin{bmatrix}-0.383822\cdot10^{-5}\\0.575654\cdot10^{-5}\\0.313165\cdot10^{-5}\\-0.535614\cdot10^{-5}\\-0.380748\cdot10^{-5}\\0.824057\cdot10^{-5}\\-0.381034\cdot10^{-5}\\-0.535689\cdot10^{-5}\\0.313242\cdot10^{-5}\\0.575749\cdot10^{-5}\\-0.383871\cdot10^{-5}\end{bmatrix}
\end{array}
$$

$$
\begin{array}{lccc}
 & t=0 & 1 & 2 \\
u_t & \begin{bmatrix}-2.65716\\-2.65717\end{bmatrix} & \begin{bmatrix}0.128506\\0.128508\end{bmatrix} & \begin{bmatrix}-0.241430\cdot10^{-4}\\-0.241461\cdot10^{-4}\end{bmatrix}
\end{array}
\qquad (4.9)
$$

The simulation results (4.5) and (4.9) are quite similar. This shows that even for control purposes there is no need to use very elaborate models of the rod.

The reachability index of the model ROD4 is $\nu=6$. Therefore, 6 time steps are required to drive the state of the model ROD4 to zero for any initial state. When the Riccati equation is iterated backwards a good feeling is obtained of how close to the origin it is possible to come in each time step. This is of course specially important when dealing with distributed parameter systems. It should be observed that the model simplification (8.5) in Chapter 6 is automatically done in the Riccati equation.

Experimental results

The time-invariant and the time-variable dead-beat control strategies were implemented on a process computer PDP-15/35. An asymptotic Kalman filter was also implemented. By a simple command it was possible to base the computation of the control signals either on the measured signals or the signals reconstructed from the Kalman filter. In the experimental set-up used the resolution of the A/D-and D/A-converters were a = 0.005°C. Moreover, the errors of the servos were estimated to b = 0.006°C.

First the experimental results for the controllers FTI21, FTV21 and FTV23 are given when the signals required to run the controllers are measured. In Fig. 4.1 and Fig. 4.2 the control signals and the measured signals are shown for the controllers FTI21 and FTV23 respectively. The figure showing the corresponding signals for the controller FTV21 is omitted, since it is almost identically to Fig. 4.1. The initial profiles of the rod were constant and equal to 0.5 (25.5°C) and 1 (26.0°C) at each end. The desired terminal profile was in all cases 0 (25.5°C). From Tables 4.1, 4.2 and 4.3 it is seen that the experimental results and the simulated results (4.3), (4.5) and (4.7) agree quite well. Moreover, these tables show that the desired terminal profile is reached to within the resolution of the A/D-and D/A-converters a = 0.005°C.

Thereafter the results for the controller FTV21 are given when the signals required to run the controller are reconstructed with the Kalman filter (FI2, GA2, TH22, AK22) from the end temperatures of the rod y_{e_1} and y_{e_2}. Before the control experiment started there had elapsed sufficient long time for the Kalman filter to become stationary. The experimental results are given in Table 4.4. A comparison with the results in Table 4.2 shows that almost the same performance of the system is obtained when the state of the model S(FI21, GA21) is measured or reconstructed from the end temperatures of the rod. Since in many practical applications, it is only possible to measure the boundary temperature of a thermal process this result is of great interest.

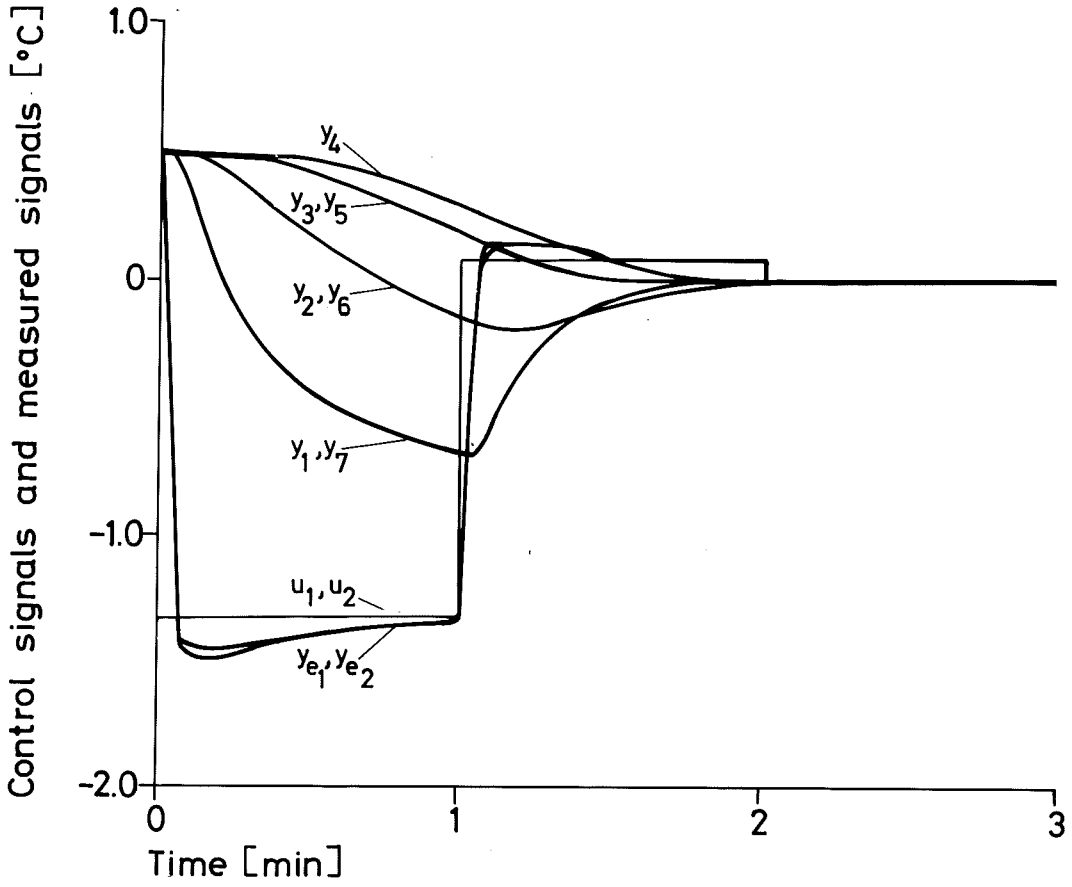

Fig. 4.1 - Dead-beat control experiment with the controller FTI21. The signals required to run the controller are measured directly. All temperatures are referred to T_0 = 25.0°C.

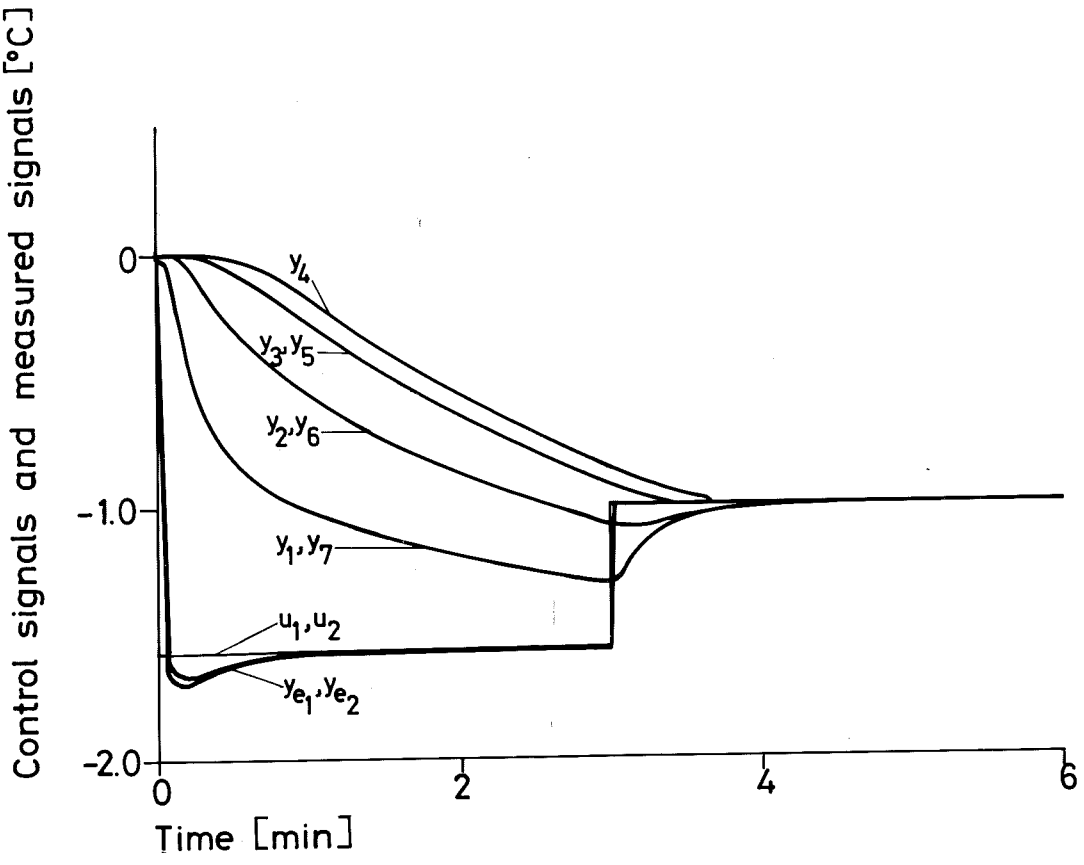

Fig. 4.2 - Dead-beat control experiment with the controller FTV23. The signals required to run the controller are measured directly. All temperatures are referred to T_0 = 25.0°C.

Initial control variables $u_1 = u_2 = 0.5^{\circ}C$

t min	u_1 °C	u_2 °C	y_1 °C	y_2 °C	y_3 °C	y_4 °C	y_5 °C	y_6 °C	y_7 °C	y_{e1} °C	y_{e2} °C
0	-1.315	-1.315	0.488	0.488	0.488	0.488	0.488	0.488	0.488	0.493	0.488
1	0.086	0.085	-0.674	-0.142	0.181	0.288	0.181	-0.142	-0.669	-1.338	-1.333
2	0.003	0.002	0.015	-0.010	-0.005	0.000	0.000	-0.010	0.015	0.073	0.078
3	0.000	0.000	0.000	0.000	0.000	0.000	0.000	0.000	0.000	0.000	0.000
4	0.000	0.000	0.000	0.000	0.000	0.000	0.000	0.000	0.000	0.000	0.000

Table 4.1 - Control signals u_1, u_2 and measured signals y_1, y_2, ..., y_7, y_{e1}, y_{e2} at the sampling instants for the control experiment with the regulator FTI21. The signals required to run the regulator are measured directly. All temperatures are referred to $T_0 = 25.0^{\circ}C$.

Initial control variables $u_1 = u_2 = 0.5^{\circ}C$

t min	u_1 °C	u_2 °C	y_1 °C	y_2 °C	y_3 °C	y_4 °C	y_5 °C	y_6 °C	y_7 °C	y_{e1} °C	y_{e2} °C
0	-1.317	-1.317	0.488	0.488	0.488	0.488	0.488	0.488	0.488	0.493	0.488
1	0.093	0.090	-0.679	-0.142	0.176	0.288	0.176	-0.142	-0.669	-1.338	-1.338
2	-0.001	-0.001	0.020	-0.005	-0.005	0.000	0.000	-0.010	0.020	0.088	0.078
3	0.000	0.000	0.000	0.000	0.000	0.000	0.000	0.000	0.000	0.000	0.000
4	0.000	0.000	0.000	0.000	0.000	0.000	0.000	0.000	0.000	0.000	0.000

Table 4.2 - Control signals u_1, u_2 and measured signals y_1, y_2, ..., y_7, y_{e1}, y_{e2} at the sampling instants for a control experiment with the regulator FTV21. The signals required to run the regulator are measured directly. All temperatures are referred to $T_0 = 25.0^{\circ}C$.

Initial control variables $u_1 = u_2 = 1.0^{\circ}C$

t min	u_1 °C	u_2 °C	y_1 °C	y_2 °C	y_3 °C	y_4 °C	y_5 °C	y_6 °C	y_7 °C	y_{e1} °C	y_{e2} °C
0	-0.562	-0.562	0.991	0.991	0.991	0.996	0.991	0.991	0.991	0.996	0.996
3	0.004	0.004	-0.298	-0.063	0.083	0.146	0.088	-0.063	-0.293	-0.566	-0.566
6	0.000	0.000	0.000	0.000	0.000	0.000	0.000	0.000	0.000	0.000	0.000

Table 4.3 - Control signals u_1, u_2 and measured signals y_1, y_2, ..., y_7, y_{e1}, y_{e2} at the sampling instants for the control experiment with the regulator FTV23. The signals required to run the regulator are measured directly. All temperatures are referred to $25.0^{\circ}C$.

Moreover, the results for the controller FTV41 are given. The signals required to run this controller cannot be measured and therefore a Kalman filter is used to estimate these signals. The employed filter is (FI4, GA4, TH42, AK42). The measured signals of the filter are y_{e1} and y_{e2}. The Kalman filter had become stationary before the control experiment was started. The experimental results are given in Table 4.5. A comparison with Table 4.2 shows that the performance of the system is almost identically to the one obtained when the controller and the filter are calculated from less accurate models of the diffusion process. This result is interesting since it shows that there is no need to use very elaborate models of the rod for control purposes.

Finally one experiment was performed where the profile of the rod was controlled between several stationary values. The employed controller was FTV23. The signals required to run the controller were measured directly. In the experiment the profile was initially at 0 (25.0°C). Then the profile was forced to a linear profile with the end temperatures 1 (26.0°C) and -1 (24.0°C). Thereafter, the profile was driven back to the value 0. This is illustrated in Fig. 4.3.

5. REFERENCE

[1]: Åström, K.J.: "Introduction to stochastic control theory", Academic Press, New York, 1970.

Initial control variables $u_1 = u_2 = 0.5^{\circ}C$

t min	u_1 °C	u_2 °C	y_1 °C	y_2 °C	y_3 °C	y_4 °C	y_5 °C	y_6 °C	y_7 °C	y_{e_1} °C	y_{e_2} °C
0	-1.328	-1.327	0.488	0.488	0.488	0.488	0.488	0.483	0.488	0.493	0.488
1	0.087	0.087	-0.688	-0.146	0.176	0.283	0.176	-0.142	-0.679	-1.348	-1.348
2	0.002	0.002	0.015	-0.010	-0.010	0.000	-0.010	-0.010	0.015	0.078	0.078
3	0.004	0.004	0.000	0.000	0.000	0.000	0.000	0.000	0.000	0.000	0.000
4	0.001	0.001	0.000	0.000	0.000	0.000	0.000	0.000	0.000	0.000	0.000

Table 4.4 - Control signals u_1, u_2 and measured signals y_1, y_2, ..., y_7, y_{e_1}, y_{e_2} at the sampling instants for the control experiment with the regulator FTV21. The signals required to run to regulator are reconstructed with the Kalman filter (FI2, GA2, TH22, AK22). All temperatures are referred to $T_0 = 25.0^{\circ}C$.

Initial control variables $u_1 = u_2 = 0.5^{\circ}C$

t min	u_1 °C	u_2 °C	y_1 °C	y_2 °C	y_3 °C	y_4 °C	y_5 °C	y_6 °C	y_7 °C	y_{e_1} °C	y_{e_2} °C
0	-1.308	-1.307	0.488	0.488	0.488	0.488	0.488	0.488	0.488	0.493	0.488
1	0.074	0.074	-0.669	-0.137	0.186	0.288	0.181	-0.137	-0.664	-1.328	-1.328
2	0.001	0.001	0.010	-0.010	-0.005	0.000	0.000	-0.010	0.010	0.068	0.068
3	0.004	0.004	0.000	0.000	0.000	0.000	0.000	0.000	0.000	0.000	0.000
4	0.001	0.001	0.000	0.000	0.000	0.000	0.000	0.000	0.000	0.000	0.000

Table 4.5 - Control signals u_1, u_2 and measured signals y_1, y_2, ..., y_7, y_{e_1}, y_{e_2} at the sampling instants for the control experiment with the regulator FTV41. The signals required to run the regulator are reconstructed with the Kalman filter (FI4, GA4, TH42, AK42). All temperatures are referred to $T_0 = 25.0^{\circ}C$.

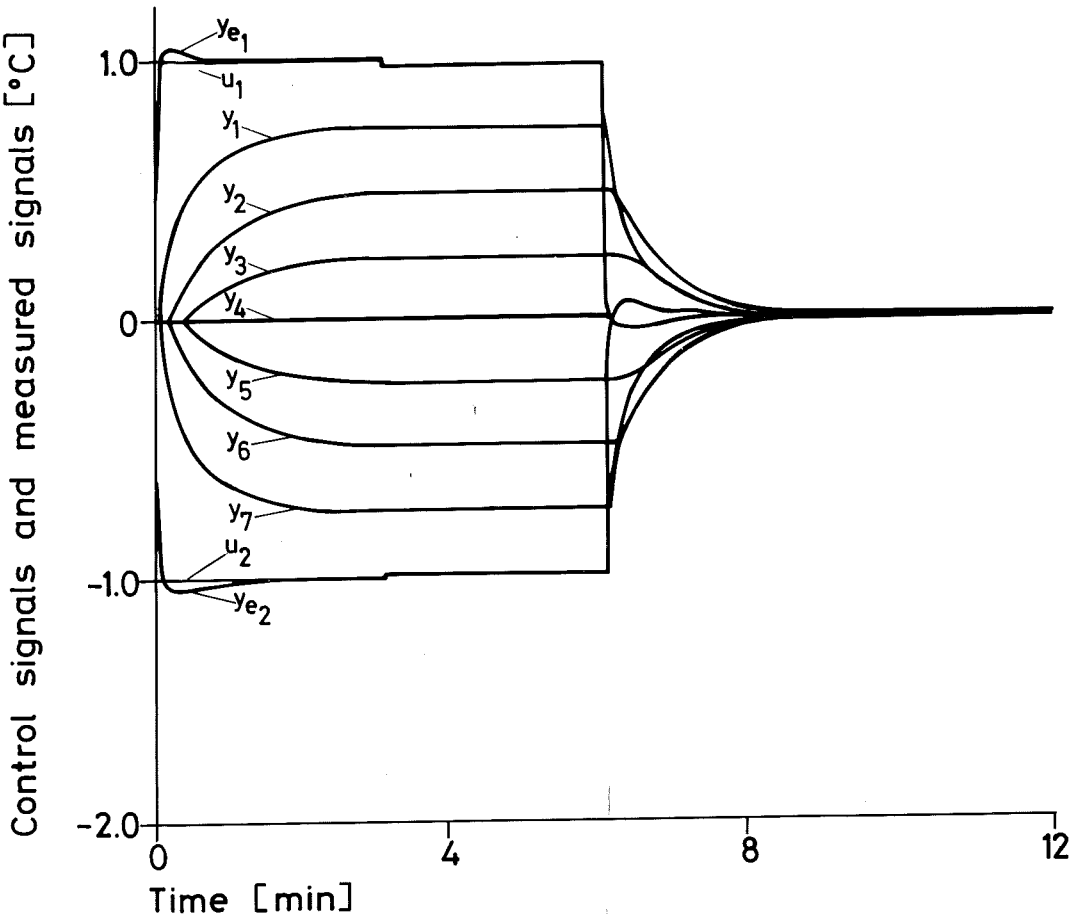

Fig. 4.3 - Dead-beat control experiment with the regulator FTV23. The signals required to run the controller are measured directly. All temperatures are referred to 25.0°C.

APPENDIX 7A

Gain K_∞:

$$\begin{bmatrix} -0.696360 \cdot 10^{-2} & 0.0 \\ -0.980206 \cdot 10^{-2} & 0.0 \\ 0.978711 \cdot 10^{-1} & -0.112541 \cdot 10^{-4} \\ 0.889481 \cdot 10^{-1} & 0.158369 \cdot 10^{-3} \\ 0.416401 \cdot 10^{-1} & 0.211934 \cdot 10^{-2} \\ 0.122026 \cdot 10^{-1} & 0.118669 \cdot 10^{-1} \\ 0.224704 \cdot 10^{-2} & 0.412806 \cdot 10^{-1} \\ 0.191904 \cdot 10^{-3} & 0.897022 \cdot 10^{-1} \\ -0.274344 \cdot 10^{-5} & 0.100340 \\ 0.0 & -0.102565 \cdot 10^{-1} \\ 0.0 & -0.567255 \cdot 10^{-2} \end{bmatrix}$$

Covariance matrix R_{ε_∞}:

$$\begin{bmatrix} 0.434107\ 10^{-4} & 0 \\ 0 & 0.437493\ 10^{-4} \end{bmatrix}$$

Eigenvalues of $\Phi - K_\infty C$ and diagonal elements of P_∞:

k	λ_k	$(P_\infty)_{kk}$
1	0.892663	$0.135805 \cdot 10^{-7}$
2	0.641095	$0.284107 \cdot 10^{-4}$
3	0.502173	$0.471670 \cdot 10^{-5}$
4	0.411453	$0.703249 \cdot 10^{-6}$
5	0.386205	$0.294280 \cdot 10^{-6}$
6	0.207240	$0.236862 \cdot 10^{-6}$
7	0.101152	$0.294158 \cdot 10^{-6}$
8	$0.473177 \cdot 10^{-1}$	$0.693014 \cdot 10^{-6}$
9	$0.255379 \cdot 10^{-1}$	$0.465014 \cdot 10^{-5}$
10	$0.532957 \cdot 10^{-5}$	$0.287493 \cdot 10^{-4}$
11	$0.227671 \cdot 10^{-6}$	$0.113562 \cdot 10^{-7}$

Table A.1 - Gain K_∞, covariance matrix R_{ε_∞}, eigenvalues of $\Phi - K_\infty C$ and diagonal elements of P_∞ for the Kalman filter (FI2, GA2, TH22, AK22).

Gain K_∞:

$$\begin{bmatrix} -0.696002\cdot10^{-2} & -0.400262\cdot10^{-3} & -0.121917\cdot10^{-3} & -0.829713\cdot10^{-7} \\ -0.979702\cdot10^{-2} & -0.563433\cdot10^{-3} & -0.171619\cdot10^{-3} & -0.116795\cdot10^{-6} \\ 0.977732\cdot10^{-1} & 0.110580\cdot10^{-1} & 0.615597\cdot10^{-2} & -0.826621\cdot10^{-5} \\ 0.888047\cdot10^{-1} & 0.162348\cdot10^{-1} & 0.104187\cdot10^{-1} & 0.163010\cdot10^{-3} \\ 0.414987\cdot10^{-1} & 0.160472\cdot10^{-1} & 0.124640\cdot10^{-1} & 0.212429\cdot10^{-2} \\ 0.120830\cdot10^{-1} & 0.135873\cdot10^{-1} & 0.130720\cdot10^{-1} & 0.118713\cdot10^{-1} \\ 0.215256\cdot10^{-2} & 0.107061\cdot10^{-1} & 0.126656\cdot10^{-1} & 0.412842\cdot10^{-1} \\ 0.124063\cdot10^{-3} & 0.765351\cdot10^{-2} & 0.107128\cdot10^{-1} & 0.897048\cdot10^{-1} \\ -0.389744\cdot10^{-4} & 0.406997\cdot10^{-2} & 0.634325\cdot10^{-2} & 0.100341 \\ 0.943303\cdot10^{-6} & -0.100698\cdot10^{-3} & -0.285403\cdot10^{-3} & -0.102565\cdot10^{-1} \\ 0.521201\cdot10^{-6} & -0.556385\cdot10^{-4} & -0.157699\cdot10^{-3} & -0.567256\cdot10^{-2} \end{bmatrix}$$

Covariance matrix R_{ε_∞}:

$$\begin{bmatrix} 0.434107\cdot10^{-4} & 0.390272\cdot10^{-6} & 0.943320\cdot10^{-8} & -0.207621\cdot10^{-11} \\ 0.390272\cdot10^{-6} & 0.152641\cdot10^{-4} & 0.205512\cdot10^{-6} & -0.897757\cdot10^{-8} \\ 0.943320\cdot10^{-8} & 0.205512\cdot10^{-6} & 0.152059\cdot10^{-4} & 0.467780\cdot10^{-8} \\ -0.207621\cdot10^{-11} & -0.897757\cdot10^{-8} & 0.467780\cdot10^{-8} & 0.437493\cdot10^{-4} \end{bmatrix}$$

Eigenvalues of $\Phi-K_\infty C$ and diagonal elements of P_∞:

k	λ_k	$(P_\infty)_{kk}$
1	0.864608	$0.135772\cdot10^{-7}$
2	0.637866	$0.284107\cdot10^{-4}$
3	0.502069	$0.470930\cdot10^{-5}$
4	0.410446	$0.682042\cdot10^{-6}$
5	0.388991	$0.264137\cdot10^{-6}$
6	0.207752	$0.205952\cdot10^{-6}$
7	0.101155	$0.269494\cdot10^{-6}$
8	$0.472932\cdot10^{-1}$	$0.678735\cdot10^{-6}$
9	$0.255323\cdot10^{-1}$	$0.464591\cdot10^{-5}$
10	$0.533126\cdot10^{-5}$	$0.287493\cdot10^{-4}$
11	$0.220095\cdot10^{-6}$	$0.113556\cdot10^{-7}$

Table A.2 - Gain K_∞, covariance matrix R_{ε_∞}, eigenvalues of $\Phi-K_\infty C$ and diagonal elements of P_∞ for the Kalman filter (FI2, GA2, TH24, AK24).

Gain K_∞:

$$\begin{bmatrix} -0.696360 \cdot 10^{-2} & 0.000000 \\ -0.980206 \cdot 10^{-2} & 0.000000 \\ 0.577590 \cdot 10^{-1} & -0.454750 \cdot 10^{-5} \\ 0.100771 & -0.556420 \cdot 10^{-5} \\ 0.110556 & 0.158121 \cdot 10^{-4} \\ 0.937885 \cdot 10^{-1} & 0.117587 \cdot 10^{-3} \\ 0.423085 \cdot 10^{-1} & 0.169345 \cdot 10^{-2} \\ 0.112720 \cdot 10^{-1} & 0.109084 \cdot 10^{-1} \\ 0.181077 \cdot 10^{-2} & 0.418592 \cdot 10^{-1} \\ 0.145580 \cdot 10^{-3} & 0.946522 \cdot 10^{-1} \\ 0.298411 \cdot 10^{-4} & 0.112694 \\ 0.157488 \cdot 10^{-5} & 0.103748 \\ -0.142180 \cdot 10^{-5} & 0.600137 \cdot 10^{-1} \\ 0.000000 & -0.102565 \cdot 10^{-1} \\ 0.000000 & -0.567255 \cdot 10^{-2} \end{bmatrix}$$

Covariance matrix R_{ε_∞}:

$$\begin{bmatrix} 0.434107\ 10^{-4} & 0 \\ 0 & 0.437493\ 10^{-4} \end{bmatrix}$$

Eigenvalues of $\Phi - K_\infty C$ and diagonal elements of P_∞:

k	λ_k	$(P_\infty)_{kk}$
1	0.892551	$0.135805 \cdot 10^{-7}$
2	0.637133	$0.284107 \cdot 10^{-4}$
3	0.502173	$0.128456 \cdot 10^{-4}$
4	0.411453	$0.475772 \cdot 10^{-5}$
5	0.366359	$0.163500 \cdot 10^{-5}$
6	0.171334	$0.686009 \cdot 10^{-6}$
7	$0.728442 \cdot 10^{-1}$	$0.297172 \cdot 10^{-6}$
8	$0.334716 \cdot 10^{-1}$	$0.238524 \cdot 10^{-6}$
9	$0.167406 \cdot 10^{-1}$	$0.297163 \cdot 10^{-6}$
10	$0.284685 \cdot 10^{-2}$	$0.676431 \cdot 10^{-6}$
11	$0.284685 \cdot 10^{-2}$	$0.159743 \cdot 10^{-5}$
12	$0.124558 \cdot 10^{-4}$	$0.467801 \cdot 10^{-5}$
13	$0.124593 \cdot 10^{-4}$	$0.128197 \cdot 10^{-4}$
14	$0.532866 \cdot 10^{-5}$	$0.287493 \cdot 10^{-4}$
15	$0.226479 \cdot 10^{-6}$	$0.113562 \cdot 10^{-7}$

Fig. A.3 - Gain K_∞, covariance matrix R_{ε_∞}, eigenvalues of $\Phi - K_\infty C$ and diagonal elements of P_∞ for the Kalman filter (FI4, GA4, TH42, AK42).

Eigenvalues of FI2:

k	λ_k
1	0.892663
2	0.641095
3	0.491906
4	0.401650
5	0.386205
6	0.207240
7	0.101152
8	$0.473177 \cdot 10^{-1}$
9	$0.255379 \cdot 10^{-1}$
10	$0.158682 \cdot 10^{-4}$
11	$0.665087 \cdot 10^{-6}$

Eigenvalues of FI4:

k	λ_k
1	0.892551
2	0.637133
3	0.491906
4	0.401650
5	0.366359
6	0.171334
7	$0.728443 \cdot 10^{-1}$
8	$0.334716 \cdot 10^{-1}$
9	$0.167406 \cdot 10^{-1}$
10	$0.284685 \cdot 10^{-2}$
11	$0.284685 \cdot 10^{-2}$
12	$0.158698 \cdot 10^{-4}$
13	$0.124546 \cdot 10^{-4}$
14	$0.124596 \cdot 10^{-4}$
15	$0.667195 \cdot 10^{-6}$

Table A.4 - Eigenvalues of the matrices FI2 and FI4.

k	$(S_{t_1-1})_{kk}$	$(S_{t_1-2})_{kk}$	$(S_{t_1-3})_{kk}$
1	$0.128238 \cdot 10^{-1}$	$0.113201 \cdot 10^{-4}$	$0.697599 \cdot 10^{-12}$
2	$0.329892 \cdot 10^{-1}$	$0.347300 \cdot 10^{-4}$	$0.214582 \cdot 10^{-11}$
3	$0.652552 \cdot 10^{-1}$	$0.776640 \cdot 10^{-4}$	$0.480771 \cdot 10^{-11}$
4	$0.788635 \cdot 10^{-1}$	$0.985260 \cdot 10^{-4}$	$0.610664 \cdot 10^{-11}$
5	$0.652552 \cdot 10^{-1}$	$0.776640 \cdot 10^{-4}$	$0.481675 \cdot 10^{-11}$
6	$0.329892 \cdot 10^{-1}$	$0.347300 \cdot 10^{-4}$	$0.215468 \cdot 10^{-11}$
7	$0.128238 \cdot 10^{-1}$	$0.113201 \cdot 10^{-4}$	$0.702408 \cdot 10^{-12}$

Table A.5 - Diagonal elements of the matrices S_{t_1-1}, S_{t_1-2} and S_{t_1-3} for the controller FIV21. The value of S_{t_1} is I.

k	$(S_{t_1-1})_{kk}$	$(S_{t_1-2})_{kk}$
1	$0.138664 \cdot 10^{-2}$	$0.894522 \cdot 10^{-11}$
2	$0.317127 \cdot 10^{-2}$	$0.205372 \cdot 10^{-10}$
3	$0.582516 \cdot 10^{-2}$	$0.378317 \cdot 10^{-10}$
4	$0.684740 \cdot 10^{-2}$	$0.445206 \cdot 10^{-10}$
5	$0.582516 \cdot 10^{-2}$	$0.378238 \cdot 10^{-10}$
6	$0.317127 \cdot 10^{-2}$	$0.205292 \cdot 10^{-10}$
7	$0.138646 \cdot 10^{-2}$	$0.894047 \cdot 10^{-11}$

Table A.6 - Diagonal elements of the matrices S_{t_1-1} and S_{t_1-2} for the controller FIV23. The value of S_{t_1} is I.

k	$(S_{t_1}-1)_{kk}$	$(S_{t_1}-2)_{kk}$	$(S_{t_1}-3)_{kk}$
1	$0.181529 \cdot 10^{-2}$	$0.242735 \cdot 10^{-5}$	$0.114769 \cdot 10^{-12}$
2	$0.385760 \cdot 10^{-2}$	$0.559085 \cdot 10^{-5}$	$0.264491 \cdot 10^{-12}$
3	$0.181529 \cdot 10^{-2}$	$0.242735 \cdot 10^{-5}$	$0.114771 \cdot 10^{-12}$
4	$0.529801 \cdot 10^{-1}$	$0.979611 \cdot 10^{-4}$	$0.464125 \cdot 10^{-11}$
5	$0.820816 \cdot 10^{-1}$	$0.191638 \cdot 10^{-3}$	$0.909650 \cdot 10^{-11}$
6	0.100253	$0.255120 \cdot 10^{-3}$	$0.121300 \cdot 10^{-10}$
7	$0.820816 \cdot 10^{-1}$	$0.191638 \cdot 10^{-4}$	$0.912562 \cdot 10^{-11}$
8	$0.529801 \cdot 10^{-1}$	$0.979611 \cdot 10^{-5}$	$0.467018 \cdot 10^{-11}$
9	$0.181529 \cdot 10^{-2}$	$0.242734 \cdot 10^{-5}$	$0.115812 \cdot 10^{-12}$
10	$0.385760 \cdot 10^{-2}$	$0.559085 \cdot 10^{-5}$	$0.266694 \cdot 10^{-12}$
11	$0.181529 \cdot 10^{-2}$	$0.242734 \cdot 10^{-5}$	$0.115810 \cdot 10^{-12}$

Table A.7 - Diagonal elements of the matrices $S_{t_1}-1$ and $S_{t_1}-2$ for the controller FIV23. The value of S_{t_1} is I.

ERRATA

B. LEDEN: IDENTIFICATION AND DEAD-BEAT CONTROL OF A HEAT DIFFUSION PROCESS

page	line		read
12	15+	$20<T<30$	$20\leq T\leq 30$
15	1+	compesator	compensator
25	5-	$(Fo_{r_4})_4$	$(Fo_{r_3})_4$
26	1-	α_{r_2}	α_{r_1}
40	6-	events s s	events s
44	5-	[	|
44	5-	]	|
67	8+	3.1 and 3.2	3.2 and 3.3
67	14+	3.3	3.4
71	2+	$\ell/4$	$\ell/2$
99	16-	$a=1.163\pm0.009$	$a=1.163\ 10^{-4}\pm0.009\ 10^{-4}\ m^2/s$
115	6+	$A:X\to Y$ be a linear map	A be a $\dim(Y)\times\dim(X)$ matrix
115	7+	linear map $A^+:Y\to X$	$\dim(X)\times\dim(Y)$ matrix A^+
115	4-	$Im(A')^{\perp}=Ker(A)$	$Im(A)^{\perp}=Ker(A')$
118	10-	S(A,B	S(A,B)
119	2+	$A^{-m}b_{i_m}$	$A^{-\nu}b_{i_m}$
120	5+	$B^{(1)}$	$B^{(i)}$
121	3+	0_r	0_{r_ν}
123	15-	]	$]x_t$
125	8+	+	$\oplus$
128	4-	$\hat{v}$	$\hat{V}$
177	2-	$[\xi_{A/D_i}(t)$	$[\xi_{A/D_i}(t)]$
185	12+	innovations ε_3	conversion errors e_3
185	13+	and ε_4	and e_4
187	16-	sis.	sis. The normality of the residuals is tested by a chi-square goodness-of-fit test. The number of degrees of freedom is 17. The test quantity is denoted by χ^2_n
187	10-	χ^2_{ac} 5.4 8.8 7.0 2.0	χ^2_n 12 31 13 19 χ^2_{ac} 5.4 8.8 7.0 2.0
187	4-	and $\chi^2_{cc}\leq 15.0$	$\chi^2_{cc}\leq 15.0$ and $\chi^2_n\leq 33$
198	1+	0	1.0
198	2+	-1.0	0
198	3+	-2.0	-1.0